Generation and characterisation of progenitor cell lines from human fetal kidneys

Chiara Mari

Student Number: 12086510

DEVELOPMENTAL BIOLOGY AND CANCER PROGRAMME

DEVELOPMENTAL BIOLOGY OF BIRTH DEFECTS SECTION

INSTITUTE OF CHILD HEALTH

UNIVERSITY COLLEGE LONDON

Supervisors: Prof. Paul J.D. Winyard
Dr. Karen L. Price

This dissertation is submitted for the degree of Doctor of Philosophy

June 2018

DECLARATION

I, Chiara Mari confirm that the work presented in this thesis is my own. Where information has been derived from other sources, I confirm that this has been indicated in the thesis.

Signed

Date: 19th June 2018

Chiara Mari

ABSTRACT

Kidney disease is a global public health burden. Chronic kidney disease, with an incidence increasing annually in the Western world, is a progressive kidney damage that can lead to end-stage renal failure (CKD5), in which kidney function is completely lost. CKD5 treatment options are dialysis, which is not a cure for kidney disease and kidney transplantation limited by the shortage of donor organs. Kidney disease new interventions have two aims:

1. preventing the progression to CKD5
2. creating a healthy organ *in vitro* with bioengineered scaffolds in order to permanently replace defective kidneys.

The first aim involves the utilisation of drug- and cellular- based therapies to delay or to stop the progression to CKD5. However, this aim is made problematic by the paucity of available primary human renal cell lines to be used for new drugs testing and the incapability to accurately assess the efficacy of cellular-based therapies in appropriate animal models.

The PhD Thesis illustrates the attempt in meeting this need. The thesis focuses on the generation and characterisation of human progenitor cell lines and further assessment of their potential to be used as cell-based therapy.

I have generated human fetal cell lines from healthy kidneys, based on the expression of known markers of renal progenitor cells, CD24 and CD133. I have characterised their gene expression profile over multiple passages, assessing the expression of progenitor and lineage markers and evaluated their capacity to differentiate towards multiple lineages (osteoblasts, adipocytes and renal epithelia).

Furthermore, the potential of these cells to be used as therapy has been assessed in mouse model of acute renal injury induced by folic acid after comparing the course of the folic acid-induced renal injury in immunocompetent and immunodeficient mice strains.

IMPACT STATEMENT

The research presented in this PhD thesis gives insights on a method that can be used to isolate specific progenitor cell populations from human fetal kidneys and the ways to test their potential as a cell-based therapy to cure injured kidneys.

Professionals within the same area of interest might benefit from the results discussed in this manuscript by choosing carefully the method of human fetal kidney cells *in vitro* isolation and maintenance. Multiple markers should be chosen to target progenitor cell lines from human fetal kidneys, and several factors should be placed in culture to mimic the environment in which these cells live. Only with the combination of these approaches such cells can be maintained long term and used for pre-clinical studies.

The pre-clinical experiments of human fetal kidney cells injection in murine models of kidney injury discussed in this study can be a first step to translate cell-based therapy into clinical trials. The administration of exogenous kidney progenitor cells should avoid the cell entrapment in the lungs, as this was a major issue encountered in a part of this study. When this pitfall is avoided, cell-based injection might represent a potential cure for patients suffering of Acute Kidney Injury (AKI), caused by the rapid loss of kidney function. This condition, nowadays, can only be resolved with dialysis or replacement of the kidney, however the therapeutic potential of fetal kidney progenitor cells could be evaluated in clinical trials as a possible therapy in the treatment of AKI.

TABLE OF CONTENTS

DECLARATION I
ABSTRACT 1
IMPACT STATEMENT 2
TABLE OF CONTENTS 3
LIST OF FIGURES 8
LIST OF TABLES 12

1 INTRODUCTION 16

1.1 ANATOMY OF THE KIDNEY AND FUNCTION 16
1.2 STEM AND PROGENITOR CELLS DEFINITION 20
1.3 KIDNEY DEVELOPMENT 23
1.3.1 Genes involved in nephron development 26
1.4 NEPHRON STEM/PROGENITOR CELLS AND NICHE SIGNALS: BALANCING SELF-RENEWAL AND DIFFERENTIATION 33
1.4.1 Application of stem cells niche signals on in vitro culture 37
1.5 CD24 AND CD133 41
1.5.1 CD24 41
1.5.2 CD133 42
1.5.3 CD24 and CD133 in the kidney 43
1.6 ACUTE KIDNEY INJURY AND CHRONIC KIDNEY DISEASE 44
1.7 STEM CELL THERAPIES FOR KIDNEY INJURY 49
1.7.1 Renal stem/progenitor cells from adult kidneys 49
1.7.2 Renal stem/progenitor cells from fetal kidneys 50
1.7.3 NCAM1⁺ cells 51
1.7.4 ALDH⁺ cells 51
1.7.5 Endogenous adult renal stem/progenitors or dedifferentiated cells? 51
1.7.6 Extra renal stem/progenitor cell lineages 53
1.8 PRE-CLINICAL STUDIES ON STEM CELLS THERAPEUTIC EFFECTS ON ACUTE AND CHRONIC KIDNEY INJURY 56
1.9 HYPOTHESIS AND AIMS 60

2 MATERIALS AND METHODS 61

2.1 KIDNEY HISTOLOGY 61
2.1.1 Human Fetal Kidney Collection *61*
2.1.2 Preparation of histological samples *61*
2.1.3 PAS staining *62*
2.1.4 Paraffin sections immunohistochemistry *62*
2.1.5 Enzymatic detection *63*
2.1.6 Fluorescent detection *64*
2.1.7 Frozen sections immunofluorescence *65*
2.1.8 Double labelling *65*
2.1.9 CD24 and CD133 staining optimisation *65*
2.1.10 Immunocytochemistry *67*
2.1.11 Negative controls *67*
2.1.12 Microscopy *67*
2.1.13 Secondary Antibodies *74*
2.2 IN-VITRO STUDIES 74
2.2.1 Isolation of human fetal kidney cells from 'fresh' kidney *74*
2.2.2 Isolation of human fetal kidney cells from explants *74*
2.2.3 Determination of cell number and viability *75*
2.2.4 Flow cytometry experimental conditions and gating strategy *76*
2.2.5 Analysis of CD24 and CD133 expression using flow cytometry *79*
2.2.6 Fluorescence activated cell sorting (FACS) *79*
2.2.7 $CD24^{+}CD133^{+}$ and $CD24^{-}CD133^{-}$ maintenance and passaging *80*
2.2.8 Population doubling *80*
2.2.9 Freezing and thawing *80*
2.2.10 Adipo-differentiation and Osteo-differentiation *81*
2.2.11 Oil Red Staining *83*
2.2.12 Alizarin red S staining *83*
2.2.13 Collagen coating *84*
2.2.14 Matrigel coating *84*
2.2.15 Lithium Chloride stimulation *84*
2.2.16 mRNA levels of progenitor genes and fibrosis markers *86*
2.2.17 Isolation and quantification of ribonucleic acid (RNA) *86*
2.2.18 RNA quantification *87*

2.2.19 Reverse transcription *87*
2.2.20 Primer design *88*
2.2.21 Gradient Polimerase chain reaction (PCR) *89*
2.2.22 Agarose gel electrophoresis *89*
2.2.23 Quantitative polymerase chain reaction (Q-PCR) *89*
2.2.24 Ex vivo studies: kidney rudiment assay *93*
2.2.25 CellTracker staining *93*
2.2.26 Chimeric pellet formation and culture *94*
2.2.27 Fixation and staining of pellets *94*
2.3 IN-VIVO STUDIES 95
2.3.1 Experimental models *95*
2.3.2 Folic acid injection *95*
2.3.3 Blood Urea Nitrogen (BUN) assay *98*
2.3.4 $CD24^{-}CD133^{-}$ and $CD24^{+}CD133^{+}$ effects on FA-induced renal injury in NOD-SCID mice *99*
2.3.5 Tracking Renal Cells with Bioluminescence *100*
2.3.6 pGL4.51[luc2/CMV/Neo] Vector *100*
2.3.7 Transformation of competent cells *101*
2.3.8 Analysis of transformants *102*
2.3.9 pGL4.51[luc2/CMV/Neo] transfection *103*
2.3.10 Cells transduction with lentiviral vector *104*
2.3.11 In vitro Bioluminescence assay *104*
2.3.12 Human Cell Tracing in mouse *105*
2.3.13 In vivo Bioluminescence assay *105*
2.3.14 Statistics *105*

3 CHARACTERISATION OF HUMAN FETAL KIDNEY DEVELOPMENT AND CD24/CD133 EXPRESSION 106

3.1 RESULTS 108
3.1.1 Histology of the developing kidney *108*
3.1.2 Expression of CD24 and CD133 ..... *111*
3.1.3 CD133 co-localisation with progenitor markers *116*
3.2 SUMMARY 118

4 ISOLATION OF CD24+CD133+ AND CD24-CD133- CELL POPULATIONS 121

4.1 RESULTS 124

4.1.1 Isolation of CD24⁺CD133⁺ and CD24⁻CD133⁻ cell populations 124

4.1.2 CD24, CD133 surface protein expression after FACS sorting 131

4.1.3 CD24⁺CD133⁺ and CD24⁻CD133⁻ phenotype in culture 133

4.1.4 CD24, CD133 mRNA expression in CD24⁻CD133⁻ and CD24⁺CD133⁺ 135

4.1.5 CD24, CD133 flow cytometric analysis on cultured renal cells 137

4.2 SUMMARY 139

5 CHARACTERISATION OF GENE EXPRESSION AND PROLIFERATION OF CD24⁺CD133⁺ AND CD24⁻CD133⁻ 141

5.1 RESULTS 142

5.1.1 Association of CD24, CD133 expression with proliferation (population doubling) 142

5.1.2 Molecular characterisation of isolated cell populations 143

5.2 SUMMARY 151

6 IN VITRO AND EX VIVO MULTI LINEAGE DIFFERENTIATION OF CD24⁺CD133⁺ AND CD24⁻CD133⁻ 153

6.1 RESULTS 154

6.1.1 OsteoDifferentiation 154

6.1.2 AdipoDifferentiation 159

6.1.3 Epithelial differentiation 163

6.1.4 Kidney rudiment assay 173

6.2 SUMMARY 179

7 PRE-CLINICAL EVALUATION OF CD24⁻CD133⁻ AND CD24⁺CD133⁺ CELLS EFFECTS ON FOLIC ACID- INDUCED KIDNEY INJURY 182

7.1 RESULTS 184

7.1.1 Evaluation of Folic acid-induced renal injury in BALB/C wild type 184

7.1.2 Evaluation and comparison of folic acid-induced renal injury in immunodeficient mice 193

7.1.3 Evaluation of therapeutic effects on Folic acid-induced injury by administration of CD24⁺CD133⁺ and CD24⁻CD133⁻ cells 201

7.1.4 Evaluation of biodistribution of CD24+CD133+ and CD24-CD133- cells upon administration in Folic acid-treated NOD-SCID mice 206
7.2 SUMMARY 210
8 GENERAL DISCUSSION 212
8.1 DISCUSSION 214
8.2 FUTURE DIRECTIONS 217
8.2.1 $CD24^+$ $CD133^+$ cells as source of progenitor cell lines 217
8.2.2 Evaluation of immunodeficient mouse strains for pre-clinical studies 219
8.3 CONCLUSIONS 220
9 REFERENCES 221

LIST OF FIGURES

FIGURE 1-1. SCHEMATIC FIGURE OF THE SURFACE OF A HUMAN KIDNEY DIVIDED IN TWO, REPRESENTING IMPORTANT ANATOMIC STRUCTURES. 19

FIGURE 1-2 SCHEMATIC ILLUSTRATION MODIFIED FROM MARI AND WINYARD, 2015..... 25

FIGURE 1-3 SCHEMATIC ILLUSTRATION REPRESENTING STAGES OF NEPHRON DEVELOPMENT. 39

FIGURE 2-1 HAEMOCYTOMETER GRIDLINES..... 76

FIGURE 2-2 GATING STRATEGY FOR FLOW CYTOMETRY ANALYSES. 78

FIGURE 2-3 ADIPO-DIFFERENTIATION EXPERIMENT TIMELINE. 82

FIGURE 2-4 OSTEO-DIFFERENTIATION EXPERIMENT TIMELINE..... 82

FIGURE 2-5 EXPERIMENTAL DETERMINATION OF OPTIMAL ANNEALING TEMPERATURE OF CD24 AND CD133. 89

FIGURE 2-6 FOLIC ACID PILOT STUDY GROUPS AND TIMELINE. 97

FIGURE 2-7 STUDY OF HUMAN RENAL CELL LINE EFFECTS ON FOLIC ACID-CAUSED INJURY IN NOD-SCID FEMALE AND MALE MICE. 100

FIGURE 2-8 PGL4.51 VECTOR CIRCLE MAP. 101

FIGURE 2-9 GEL ELECTROPHORESIS OF PGL4.51 PLASMID CLONES. 103

FIGURE 3-1 HUMAN FETAL KIDNEY SECTIONS OF 9 TO 20 WEEKS OF GESTATIONAL AGE STAINED WITH PAS..... 109

FIGURE 3-2 CD24 LOCALISATION ON 9 WEEKS KIDNEY. 113

FIGURE 3-3 CD133 LOCALISATION ON 9 WEEKS KIDNEY. 114

FIGURE 3-4 CD24 AND CD133 CO-LOCALISATION ON 9 WEEKS KIDNEY SECTIONS..... 115

FIGURE 3-5 CD133 STAINING WITH PAX2, SIX2 AND WT1 IN THE NEPHROGENIC ZONE OF HUMAN FETAL KIDNEY ON THE 9TH WEEK OF GESTATION. 117

FIGURE 4-1 ANALYSIS OF FACS SORTING EXPERIMENT PERFORMED ON FRESHLY COLLECTED 10 WEEKS HUMAN KIDNEY. 126

FIGURE 4-2 FACS SORTING ON FRESHLY COLLECTED 8 WEEKS KIDNEY. 128

FIGURE 4-3 FACS SORTING PERFORMED ON CULTURED FETAL KIDNEY CELLS. 129

FIGURE 4-4 CD24, CD133 SURFACE MARKERS EXPRESSION IN GENERATED CELL LINES AFTER 2 PASSAGES IN CULTURE. 132

FIGURE 4-5 MORPHOLOGY OF ISOLATED CELL LINES OBSERVED WITH LIGHT MICROSCOPY AT DIFFERENT PASSAGES. 134

FIGURE 4-6 DETERMINATION OF OPTIMAL ANNEALING TEMPERATURE, SPECIFICITY OF CD24 AND CD133 PRIMERS AND CD24, CD133 MRNA RELATIVE QUANTIFICATION. 136
FIGURE 5-1 POPULATION DOUBLING (PD) OF CD24-CD133- AND CD24+CD133+. 143
FIGURE 5-2 Q-PCR FOR PAX2. 146
FIGURE 5-3 Q-PCR FOR WT1 AND OSR1. 147
FIGURE 5-4 Q-PCR FOR SIX2, CITED1, EYA1. Q-PCR FOR SIX2. 148
FIGURE 5-5 QRT-PCR FOR OCT4. 149
FIGURE 5-6 Q-PCR FOR E-CADHERIN AND FOXD1. 150
FIGURE 6-1 CELL MORPHOLOGY DURING OSTEODIFFERENTIATION. 155
FIGURE 6-2 ALIZARIN RED STAINING IN CONTROLS AND OSTEODIFF TREATED CELL LINES AFTER 12 DAYS OF DIFFERENTIATION.....156
FIGURE 6-3 MRNA LEVELS OF OSTEOGENIC MARKERS IN TREATED CELL LINES. 157
FIGURE 6-4 MRNA LEVELS OF OSTEOGENIC MARKERS IN TREATED CELL LINES. 160
FIGURE 6-5 OIL RED O STAINING IN CONTROLS AND ADIPODIFF TREATED CELL LINES AFTER 21 DAYS OF DIFFERENTIATION.....161
FIGURE 6-6 MRNA LEVELS OF ADIPOGENIC MARKERS IN CD24-CD133- TREATED CELL LINES. 162
FIGURE 6-7 EPITHELIAL DIFFERENTIATION WITH LICL ON PLASTIC. 165
FIGURE 6-8 E-CADHERIN MRNA EXPRESSION ASSESSED WITH Q-PCR IN CD24-CD133- CELLS (SAMPLES 12141, 12391, 12637) TREATED WITH LICL ON PLASTIC PLATES VS CONTROL. 166
FIGURE 6-9 EPITHELIAL DIFFERENTIATION WITH LICL ON MATRIGEL COATED PLATES. 167
FIGURE 6-10 E-CADHERIN, FGF8 AND AMINOPEPTIDASE A MRNA EXPRESSION ASSESSED WITH Q-PCR IN CD24-CD133- AND CD24+CD133+ CELL LINES (ISOLATED FROM KIDNEY SAMPLE NUMBER 12391) TREATED WITH LICL ON MATRIGEL COATED PLATES FOR 7 DAYS. 169
FIGURE 6-11EPITHELIAL DIFFERENTIATION WITH TRANSIENT LICL (48H) ON MATRIGEL COATED PLATES.....170
FIGURE 6-12 Q-PCR CT VALUES OF THE EPITHELIAL DIFFERENTIATION ON MATRIGEL WITH TRANSIENT LICL ADDITION (48H). 172
FIGURE 6-13 CONFOCAL SECTIONS OF SELF-ORGANISED MOUSE EMBRYONIC KIDNEY RUDIMENTS.....176

FIGURE 6-14 CD24-CD133- AND CD24+CD133+ RE-AGGREGATION WITH OR WITHOUT MOUSE EMBRYONIC KIDNEY CELLS. 178
FIGURE 7-1 BUN MEASURES AT DIFFERENT TIMES IN CONTROL MICE (VEHICLE, PBS/$NaHCO_3$) AND IN FA MICE (FA/$NaHCO_3$). 187
FIGURE 7-2 BODY WEIGHT MEASUREMENTS AT DIFFERENT TIME POINTS IN CONTROL GROUP (VEHICLE, PBS/$NaHCO_3$) AND FA GROUP (FA/$NaHCO_3$). 188
FIGURE 7-3 PAS STAINING IN VEHICLE TREATED MICE (PBS/$NaHCO_3$, 42 DAYS POST INJECTION) AND IN FOLIC ACID TREATED MICE AT DIFFERENT TIME POINTS (FA/$NaHCO_3$, 2, 14,21 AND 42 DAYS). 189
FIGURE 7-4 F4/80 IMMUNOSTAINING OF MACROPHAGES IN VEHICLE MICE (PBS/$NaHCO_3$, 42 DAYS POST INJECTION) AND IN FA MICE AT DIFFERENT TIME POINTS (FA/$NaHCO_3$, 14, 21 AND 42 DAYS). 190
FIGURE 7-5 COLLAGEN I IMMUNOSTAINING OF FIBROSIS IN VEHICLE MICE (PBS/NAHCO3, 42 DAYS POST INJECTION) AND IN FA MICE AT DIFFERENT TIME POINTS (FA/NAHCO3, 14, 21 AND 42 DAYS). 191
FIGURE 7-6 COLLAGEN III IMMUNOSTAINING OF FIBROSIS IN VEHICLE MICE (PBS/NAHCO3, 42 DAYS POST INJECTION) AND IN FA MICE AT DIFFERENT TIME POINTS (FA/NAHCO3, 14, 21 AND 42 DAYS). 192
FIGURE 7-7 BUN AND BODY WEIGHT MEASUREMENTS AT DIFFERENT TIME POINTS IN NUDE, SCID (N=4 AND N=8 RESPECTIVELY) AND IN NOD-SCID MICE (N=4). 195
FIGURE 7-8 PAS STAINING PERFORMED ON KIDNEYS FROM NUDE, SCID AND NOD-SCID AFTER 21 DAYS (NUDE, SCID) AND 42 DAYS (NOD-SCID). 198
FIGURE 7-9 MACROPHAGES (F4/80), COLLAGEN I AND COLLAGEN III IMMUNOSTAINING ON KIDNEYS FROM NUDE, SCID AND NOD-SCID MICE AFTER 21 DAYS (NUDE, SCID) AND 42 DAYS (NOD-SCID). 199
FIGURE 7-10 COMPARISON OF BUN VALUES AMONG WILD TYPE, NUDE, SCID AND NOD-SCID MICE STRAINS AT DIFFERENT TIME POINTS. 200
FIGURE 7-11 ASSOCIATION BETWEEN PBS, CD24-CD133- OR CD24+CD133+ ADMINISTRATION AND NOD-SCID MICE OVERALL SURVIVAL. 204
FIGURE 7-12 BUN VALUES 21 DAYS POST FA OF PBS CONTROL GROUP (N=3) AND GROUP DELIVERED WITH $CD24^{-}CD133^{-}$ CELLS (N=4). BUN IN MICE THAT RECEIVED $CD24^{-}CD133^{-}$ CELLS INJECTION WAS SIGNIFICANTLY HIGHER THAN CONTROL WHEN ANALYSED WITH UNPAIRED T TEST. *P=0.0281. 205

FIGURE 7-13 MRNA EXPRESSION OF MACROPHAGES GENE CD68, COLLAGEN I AND COLLAGEN III. 205
FIGURE 7-14 BIOLUMINESCENCE IMAGING OF CD24-CD133- AND CD24+CD133+ CELLS TRANSFECTED WITH PGL4.51 VECTOR USING LIPOFECTAMINE 3000 AND GENEJUICE OR INFECTED WITH THE LENTIVIRUS VECTOR ENCODING A LUCIFERASE-GFP TRANSGENE. 208
FIGURE 7-15 BIOLUMINESCENCE IMAGING OF MICE INJECTED WITH $CD24^{-}CD133^{-}$ AND $CD24^{+}CD133^{+}$ CELL LINES TWO DAYS AFTER FA ADMINISTRATION.....209

LIST OF TABLES

TABLE 1-1. GENES KNOWN TO CONTRIBUTE TO CAP MESENCHYME FORMATION AND/OR SURVIVAL OF CAP MESENCHYMAL CELLS IN MICE 32

TABLE 1-2 GENES INVOLVED IN THE NEPHRON PROGENITORS NICHE MAINTENANCE IN RODENTS. 40

TABLE 1-3 DEFINITION AND STAGES OF ACUTE KIDNEY INJURY 47

TABLE 1-4. STAGES OF CHRONIC KIDNEY DISEASE 48

TABLE 2-1 PRIMARY ANTIBODIES USED IN THE PROJECT. 69

TABLE 2-2 LITHIUM CHLORIDE STIMULATION EXPERIMENTS SUMMARY 85

TABLE 2-3 HUMAN PRIMERS USED FOR PCR CHARACTERISATION OF CELL LINES. 91

TABLE 4-1 FACS ANALYSIS OF CD24, CD133 EXPRESSION (IN PERCENTAGE) IN FRESHLY SORTED FETAL KIDNEY CELLS 129

TABLE 4-2 FACS ANALYSIS OF CD24 AND CD133 CELL SURFACE PROTEIN EXPRESSION ON CELLS DERIVED FROM 8 TO 9 WEEKS HUMAN FETAL KIDNEYS (N=16) 130

TABLE 4-3 FLOW CYTOMETRY ANALYSIS OF CD24 AND CD133 CELL SURFACE PROTEINS EXPRESSION IN 13 HUMAN FETAL KIDNEY DERIVED CELLS. 138

TABLE 6-1 Q-PCR CT VALUES OF OSTEOGENIC GENES IN CONTROL AND OSTEODIFF TREATED CD24+CD133+ AND CD24-CD133- GENERATED FROM THREE DIFFERENT SAMPLES OF 9 WEEKS 158

TABLE 6-2 Q-PCR FOLD CHANGE VALUES OF ADIPOGENIC GENES IN CONTROL AND ADIPODIFF TREATED CD24-CD133- GENERATED FROM THREE DIFFERENT SAMPLES OF 9 WEEKS. 162

TABLE 6-3 Q-PCR CT VALUES OF THE EPITHELIAL DIFFERENTIATION ON MATRIGEL WITH LICL OF CD24-CD133- AND CD24+CD133+ GENERATED FROM A KIDNEY SAMPLE (12391). 168

TABLE 6-4 Q-PCR CT VALUES OF THE EPITHELIAL DIFFERENTIATION ON MATRIGEL WITH TRANSIENT LICL ADDITION (48H). 171

TABLE 7-1 BLOOD UREA NITROGEN VALUES IN NUDE, SCID AND NOD-SCID MICE AT DIFFERENT TIME POINTS. 196

TABLE 7-2 BODY WEIGHT MEASUREMENTS IN NUDE, SCID AND NOD-SCID MICE AT DIFFERENT TIME POINTS. 197

LIST OF ABBREVIATIONS AND ACRONYMS

2D: two-dimensional

3D: three-dimensional

APC: allophycocyanin

ANOVA: Analysis of variance

BMI1: B-cell-specific Moloney murine leukaemia virus insertion site 1BMP2: bone morphogenetic protein 2

BUN: blood urea nitrogen

C: comma-shaped body

cDNA: Complementary deoxyribonucleic acid

CFDA: 5-(and-6)-carboxyfluorescein diacetate

CITED1: Cbp/P300-Interacting transactivator with Glu/Asp-Rich carboxy-terminal domain,1

CM: cap/condensed mesenchyme

CMFDA: 5-chloromethylfluorescein diacetate

DNA: Deoxyribonucleic acid

DMEM: Dulbecco's modified Eagle medium

E: embryonic day

ECM: extracellular matrix

EGF: epidermal growth factor

EpCAM: Epithelial cell adhesion molecule

EYA1: EYA transcriptional coactivator and phosphatase 1

FA: folic acid

FACS: fluorescence activated cell sorting

FBS: fetal bovine serum

FC: flow cytometry

FITC: fluorescein isothiocyanate

FGF: fibroblast growth factor

FOXD1: forkhead box d1

FSC: forward scatter

GDNF: glial cell derived neurotrophic factor

HFK: human fetal kidney

HGF: hepatocyte growth factor

HOX: homeobox

HPRT: hypoxanthine guanine phosphoribosyl transferase

ICC: immunocytochemistry

IHC: immunohistochemistry

IP: intraperitoneal

iPSCs: induced pluripotent stem cells

IV: intravenous

JNK: c-Jun N-terminal Kinases

KDR: kinase insert domain receptor

LiCl: Lithium chloride

MSCs: mesenchymal stem cells

mAb: monoclonal antibody

mRNA: messenger ribonucleic acid

MEM: minimum essential medium

MET: mesenchymal to epithelial transition

mTOR: mechanistic target of Rapamycin

MUC18: melanoma cell adhesion molecule

NCAM1: neural cell adhesion molecule 1

NOD-SCID: non-obese diabetic-severe combined immunodeficiency

OCT4/POU5F1: octamer-binding transcription factor 4/ POU domain, class 5, transcription factor 1

OSR1: odd-skipped related 1

PA: pre-tubular aggregates

pAb: polyclonal antibody

PAS: periodic acid Schiff

PAX2: paired box 2

PBS: phosphate buffered saline

PCR: polymerase chain reaction

PD: population doubling

PDX: podocalyxin

PE: phycoerythrin

PRKDC: protein kinase DNA activated catalytic polypeptide

Q-PCR: quantitative reverse transcriptase- polymerase chain reaction

REGM: renal epithelial growth medium

RNA: ribonucleic acid

ROI: region of interest

RT-: reverse transcriptase minus

RT: room temperature

RUNX2: Runt-related transcription factor 2

RV: renal vesicle

SALL1: sal-like 1

SCID: Severe Combined Immune Deficiency

SIX2: sine oculis homeobox (Drosophila) homolog 2

SSC: side scatter

TGFβ: transforming growth factor

UB: ureteric bud

VEGF: vascular endothelial growth factor

WNT: Wingless-Type MMTV Integration Site Family

WT1: Wilms Tumour 1

1 INTRODUCTION

1.1 Anatomy of the kidney and function

The kidneys perform essential functions to life, these span from elimination of nitrogenous waste through maintenance of blood volume and composition, to preservation of bone density. The kidneys are two bean-shaped organs lying one on each side of the vertebral column. The right kidney is usually positioned slightly lower than the left. The weight of each kidney ranges from 125 g to 170 g in human adult males, being approximately 11cm to 12 cm in length (Maarten W. Taal, 2012).

The lateral surface of the kidney is convex, while the medial surface is concave. Here is located a slit, the 'hilum', through which the renal artery, the renal vein, the lymphatic vessels, a network of nerves and the renal pelvis pass into the sinus of the kidney. The kidney is a complex organ, likewise its architecture is extremely intricate. Kidney structure can be simplified as follows: the most external layer is the renal capsule, a fibrous membrane surrounding and protecting the kidney. Below the renal capsule, in the outer layer named 'cortex' lays the nephron. In particular, here are localised the Bowman's capsules and the glomeruli, the proximal and distal convoluted tubules and their associated blood supplies. The middle region 'medulla' is divided into 8 to 18 cone-shaped regions named 'pyramids'. Each pyramid base faces the renal cortex, whereas the apex points internally towards the renal pelvis forming the 'papilla'. The renal pyramid together with the cortex is called 'renal lobus'(Figure 1-1). For this particular feature, the human kidney differs to the mouse, rat and rabbit kidneys, where it is present only a single renal pyramid with the overlying cortex and is therefore named 'unipapillate' (Maarten W. Taal, 2012).

The papilla lies into a cavity called the minor calyx composed of collecting ducts. Multiple minor calyces merge to form a major calyx. The major calyces convey the urine through the renal pelvis into the ureter, which in turn propels it to the bladder.

Each kidney is supplied by a renal artery which enters through the hilar region and branches few times supplying all the regions of the kidney (Stein and Fadem, 1978).

The structural and functional unit of the kidney is the nephron. The human kidney is composed of approximately 200,000 to 1.8 million nephrons (Hughson et al., 2003) in contrast with the approximately 30,000 nephrons in each adult rat kidney (Nyengaard, 1993).

A nephron is essentially composed of blood vessels, a renal corpuscle, and a long renal tubule. The renal corpuscle consists of a capillary network lined by a thin layer of endothelial cells (glomerulus), a central zone of mesangial cells and extracellular matrix, all enclosed in a two-layered glomerular (Bowman's) capsule. At the vascular pole, where the afferent arteriole enters and the efferent arteriole exits the glomerulus, the visceral layer of the Bowman's capsule is composed of special cells, called podocytes, wrapped around the capillaries (Maarten W. Taal, 2012).

Continuous with the visceral layer, at the urinary pole, there is the parietal epithelium, the outer layer of Bowman. This is formed of squamous cells, which change morphology to taller cuboidal cells with brush borders towards the urinary pole. Evidences have shown that these cells can transdifferentiate into podocytes and eventually repopulate the glomerular tuft (Appel et al., 2009).

The glomerulus function is to produce an ultrafiltrate of plasma. The main players in the filtration process are three glomerular barriers: the fenestrated epithelium of the capillaries, the glomerular basement membrane and the slit pores between foot processes of the podocytes. The glomerular basement membrane is made of three different layers or 'lamina' that restrict the passage of molecules based on the size and charge (Brenner et al., 1977).

At the urinary pole of the glomerulus begins the proximal tubule. It comprehends of an initial convoluted portion and a straight portion. Length of proximal tubule in human is approximately 14 mm while is 5 mm in mouse (Zhai et al., 2003). On the apical basement membrane of proximal tubule cells the microvilli cover the surface forming the so-called 'brush border', this amplifies greatly the apical cell surface available for reabsorption (Welling and Welling, 1975). The proximal convoluted tubule plays an important role in the reabsorption into the blood two thirds to three quarters of the glomerular ultrafiltrate. This is composed of several ions: Na^+ , Cl^-, K^+ , PO_4, HCO_3 (Burg MB. Brenner BM, 1986). Tubular cells contain abundant mitochondria providing ATP for the active transport of Na^+ and Cl^- coupled to the water reabsorption, reabsorbing (Maarten W. Taal, 2012). $Ca2^+$ absorption is passive,

following the Na^+ and water reabsorption (Friedman, 1999). The proximal convoluted is also responsible of reabsorption of organic solutes such as vitamins, glucose, and amino acids and for the production of ammonia, produced from the mitochondria from the glutamine metabolism (Good and Burg, 1984).

The proximal tubule continues in the Loop of Henle. This is composed of a straight segment, the thin limb. The thin limb can be long and extend into an area of the medulla called 'inner medulla' or short bending within the 'outer medulla', usually the length of the loop of Henle is related to the localisation of its parent renal corpuscle in the cortex. Most nephrons originate from superficial locations and have shorter loops, other nephrons originating from the juxtamedullary region close to the corticomedullary margin, have long loops of Henle immersing far into the medulla (Pannabecker, 2012). Based on structural characteristics of the cells, four types of epithelia have been distinguished in the mouse thin limbs (Dieterich et al., 1975).Type I epithelium, found in nephron with short loop of Henle, is thin and with few surface specializations. Type II, found in long-looped nephrons, is more complex with extensive interdigitations of lateral and basal processes of adjacent cells. Type III epithelium is typical of inner medulla and is simpler than the type II epithelium, with less prominent interdigitations. Type IV epithelium bends to form the loop and the entire ascending thin limb to the transition into thick limb.

The thick ascending limb is the initial portion of the distal tubule and it is characterised by cells with extensive invaginations of the basolateral plasma membrane as well as several interdigitations (Maarten W. Taal, 2012). The epithelium is almost impermeable to water, also, the presence of Na^+- K^+-$2Cl^-$ cotransport mechanism drives the reabsorption of NaCl from the lumen to the surrounding interstitium. The active reabsorption of solutes contributes to the formation of a hypertonic interstitium and a more diluted tubular fluid flowing to the distal convoluted tubule (Greger et al., 2001).

The distal convoluted tubule is relatively impermeable to water and it is composed of tall and cuboidal cells lacking of well-developed brush borders (Madsen et al., 1988b). At the apical plasma membrane, these cells express the thiazide-sensitive Na^+Cl^- cotransporter, NCC, through which sodium and chloride are reabsorbed (Reilly and Ellison, 2000). The distal tubule also expresses the $Na^+/Ca2^+$ exchanger NCX1, the calcium-binding protein calbindin-D28K, and the $Ca2^+$ channel TRPV5 (transient

receptor potential cation channel subfamily V member 5) also seen in the connecting tubule (Hofmeister et al., 2009, Campean et al., 2001). $Ca2^{+}$ transporters and calbindin expression in the distal convoluted tubule are involved in the reabsorption of Ca2+.

The distal tubule continues into the collecting duct, which extends from the cortex, through the outer and inner medulla. Based on its location can be divided in three regions in cortical, outer medullary and inner medullary collecting duct. Two kinds of cells are present in collecting ducts: the intercalated cells and the principal cells (Madsen et al., 1988a). Intercalated cells have high levels of HCO_3 , possibly due to a role in the acidification of the fluid in the collecting duct (Kim et al., 1990). Principal cells are involved in sodium absorption, through an amiloride-sensitive sodium channel, ENaC (Hager et al., 2001). An important function of the cortical collecting duct is the secretion of K^{+}(O'Neil and Helman, 1977). The outer medullary collecting duct is involved in urine acidification (Lombard et al., 1983). The inner medullary collecting duct plays a role in the reabsorption of Na^{+},Cl^{-}, K^{+} , urea and water (Sands and Knepper, 1987).

The interstitium is another component of the kidney, it comprehends of interstitial cells and extracellular matrix consisting of sulfated and nonsulfated glucosaminoglycans (Lemley and Kriz, 1991). Other components include the lymphatic and nerve fibers.

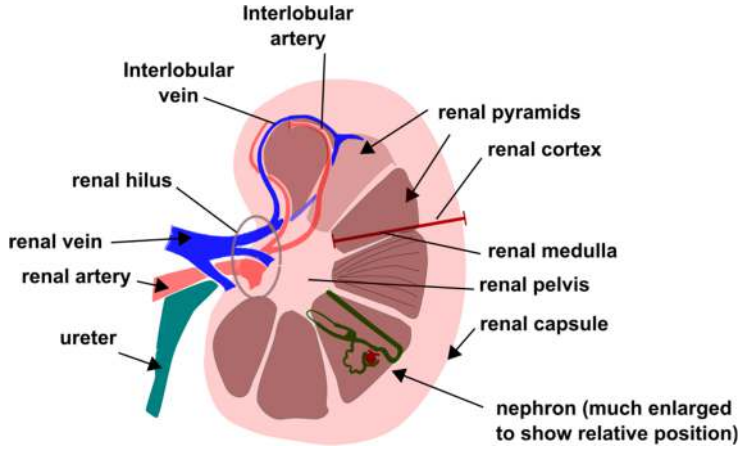

Figure 1-1. Schematic figure of the surface of a human kidney divided in two, representing important anatomic structures.

The most external kidney layer is the renal capsule, below the renal capsule is situated the renal cortex. The inner part of the kidney corresponds to the renal medulla. Renal medulla is divided into 8 to 18 pyramids containing collecting ducts and loop of Henle of juxtamedullary nephrons. The renal vessels, nerves and ureter pass through a central fissure named the 'renal hilum'. The renal artery divided into segmental arteries and interlobular arteries that reach the renal cortex. Here they branch several times forming afferent arterioles which serve the nephron.

1.2 Stem and progenitor cells definition

The definition of stem cells has historically been quite vague and many attempts have been made to define the term more clearly. However, even now the terminology often depends on the perspective of the viewer: for an embryologist, this term is very different compared to a haematologist, dermatologist or cancer. Hence, I will define the stem cells characteristics used here that I consider important in this project for the identification of kidney stem/progenitor cells: or a 'stem cell population', I refer to a cell population that is self-renewing, of variable potency (i.e. able to generate multiple but not necessarily all cell types) and usually clonal. This rather simplistic definition is not applicable in all instances and can be best utilised as a guide to help describe stem cell attributes.

1.2.1.1 Self-renewal

The most fundamental property of a stem cell is a cell capable of 'self-renewal', through which stem cells generate daughter cells identical to their mother, as well as other progeny with more restricted developmental potential. In stem cell self-renewal, symmetric cell division generates two identical daughter cells with the same properties of their mother cell whereas asymmetric division generates two daughter cells, one identical to the mother the other being more differentiated (Knoblich, 2010, Morrison and Kimble, 2006).

The extensive proliferation capability has been shown for embryonic stem cells cultured *in vitro*, where they display an apparently unlimited proliferative capacity maintaining a normal karyotype without oncogenic transformation. Most somatic cells *in vitro* undergo a limited number of population doublings (less than 80) prior to replicative arrest or senescence whereby embryonic stem cells can undergo more than twice this number (i.e. 160).

It is difficult to demonstrate infinite proliferative capacity of adult stem cells similarly to embryonic stem cells *in vitro*, due to the incomplete knowledge of the factors required for their long-term maintenance *ex vivo*. However, this property has been addressed *in vivo* by single or serial cell transfer into immunocompromised hosts. Hematopoietic stem cells serially transplanted into lethally irradiated mice increased in number repeatedly without evidence of exhaustion therefore demonstrating extensive self-renewal capacity (Iscove and Nawa, 1997).

1.2.1.2 Potency

Potency defines the ability of stem cells to differentiate into cells of various lineages and can be used to classify stem cells as pluripotent, multipotent, and unipotent (Singh et al., 2016).

Embryonic stem cells, either in mice or in humans, derived from the embryo at the stage of blastocyst, from the inner cell mass preimplantation, are pluripotent (Evans and Kaufman, 1981). These are able to generate all somatic lineages except for the extra-embryonic tissues (such as placenta) and they gradually become more restricted to different cell fates. Mouse embryonic stem cells, under well-defined conditions, proliferate in culture *in vitro* and can produce live-born chimeric mice when injected back into blastocyst, contributing to all somatic lineages also forming functional germ cells following their incorporation (Bradley et al., 1984).

Multipotent stem cells hold a more restricted differentiation potential, being committed to generate specific cell types of the tissue of origin. An example of multipotent stem cells are the adult hematopoietic stem cells residing in the bone marrow, a rare cell population able to give rise to all blood cell lineages (Spangrude et al., 1989). Another example of multipotent stem cells includes the neural stem cells, isolated from both the developing and the adult brain. These demonstrate multilineage differentiation into neurons, astrocytes and oligodendrocytes, the main CNS lineages (Gage, 2000). The best way to assess whether a purified cell line holds multipotent stem cells properties is with *in vivo* transplantation of a single cell into an acceptable host without prior *in vitro* culture, and observation whether this cell can reconstitute either a tissue, organ or cell lineage (Melton, 2014).

The descendants of multipotent stem cells are more constrained in their differentiation potential or self-renewal capacity, able to give rise to a more restricted subset of cell lineages or defined as ‘unipotent’ when capable to differentiate toward one cell type only. An example of this cell type is the blast forming unit-erythroid (BFU-E) that can only differentiate into erythrocytes (Lodish et al., 2010).

Progenitor cells have a limited self-renewal capacity and are often unipotent (Potten and Loeffler, 1990). This has been well demonstrated in neuroscience, where putative stem cells in the subgranular cell layer in the hippocampal dentate gyrus were shown to be progenitor cells when tested for extensive self-renewal capacity with the neurosphere assay (Reynolds and Weiss, 1992). These progenitors formed sphere

colonies, however after dissociation of a single, clonally derived neurosphere, single cells did not proliferate to form new neurospheres showing lack of self-renewal (Seaberg and van der Kooy, 2002).

1.2.1.3 Clonality

A clonal population is defined as homogenous cell line derived from a single stem cell. A way to show whether a cell is a stem cell is through the clonal analysis, intended as the tracking of a single cell over time to assess whether this cell can generate more stem cells equals to itself as well as differentiated cells. In this way, hematopoietic stem cells were identified. These generate clones *in vitro* by subcloning individual colonies and *in vivo* by transplantation of single stem cells into irradiated mice (Iscove and Nawa, 1997).

1.3 Kidney development

The kidney comprises of specialised cell types co-operating together to perform numerous roles essential for life. The development of the human kidney is a fascinating and complex process relying on the synergic interaction between epithelial and mesenchymal cells leading to the coordinated development of highly specialised stromal, vascular and epithelial cell types (Faa et al., 2012).

The kidney originates from the intermediate mesoderm through three stages, known as 'pronephros', 'mesonephros' and 'metanephros'. The pronephros forms 22 days post conception in humans and 8 days post coitum in mice. It consists of pronephric tubules and the pronephric duct, which is the precursor of the Wolffian duct. The mesonephros develops caudally to the pronephric tubules serving as the main excretory organ in lower vertebrates (Saxen and Sariola, 1987). In humans the majority of the mesonephros degenerates, however cells migrate from the mesonephros into the adregonadal primordia which will differentiate into the adrenal gland and gonads (Capel et al., 1999)

The third and final stage of kidney development, the metanephros, arises at the 5th week of gestation in humans and at embryonic day 10.5 in mice. The metanephros develops through interactions between two derivatives of the intermediate mesoderm, the ureteric bud, originated from the Wolffian duct, and the metanephric mesenchyme (Saxen and Sariola, 1987). The ureteric bud is an epithelial tube that gives rise to the collecting system, renal pelvis, ureter and bladder (Reidy and Rosenblum, 2009). The ureteric bud grows into the surrounding metanephric mesenchyme dividing into a T-shape, the tips of which branches into several ramifications (Reidy and Rosenblum, 2009).

During ureteric bud and metanephric mesenchyme interactions, the latter forms two portions with different cell lineages: the stromal mesenchyme and the cap mesenchyme.

Stromal mesenchyme is a cell population characterised by the expression of Forkhead box D1 (*Foxd1*) transcription factor, this will also give rise to the non-nephrogenic lineage (e.g. medullary interstitium, renal capsule, putative mesangium and pericytes). A subset of cells of the cap mesenchyme aggregates adjacent and inferior to the tips of the branching ureteric forming the pre-tubular aggregate, which, in their more

peripheral portion, undergo a regulated process of transformation from mesenchymal to epithelial cells called ‘mesenchymal to epithelial transition’ or ‘MET’ (Figure 1-3). As a result of MET, a single epithelial renal vesicle is formed (Hendry et al., 2011). The renal vesicle segments and proceeds through distinct morphologic stages to form the glomerulus and components of the tubular nephron from the proximal convoluted tubule to the distal tubule. These stages are known as ‘comma shaped bodies’, ‘S-shaped bodies’, ‘capillary loop’ and ‘mature’ stage. The S-shaped bodies elongate forming the proximal tubule and distal tubule separated by the loop of Henle. The proximal end of these tubules become vascularised to form the glomerulus while the other end fuses with the ureteric epithelium to form a contiguous uriniferous tubule (Saxen and Sariola, 1987, Mugford et al., 2009, Georgas et al., 2009, Davies and Bard, 1998, Little, 2006). The full complement of nephrons is formed via continuous ureteric epithelial branching and renal vesicles induction.

At a later stage, the renal vasculature matures and the glomerular capillary system appears while the main components of the renal corpuscle and the tubular segments terminally differentiate (Faa et al., 2012).

Kidney development is considered to cease after 32-36 weeks of gestation in humans and within a few days after birth in mice as a result of exhaustion of the condensed mesenchyme (Hartman et al., 2007, Tank, 2012). In mice, after birth, burst of differentiation of nephron progenitor cells occurs leading to the final production of multiple nephrons per ureteric bud tip (Rumballe et al., 2011). No *de novo* nephron formation has been observed in adult kidneys.

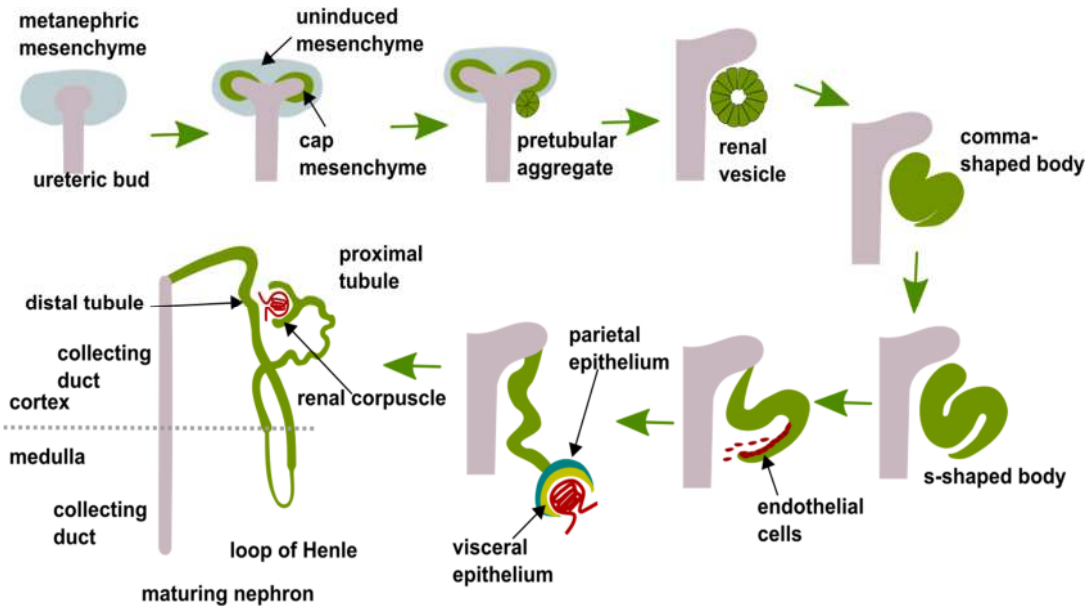

Figure 1-2 Schematic illustration modified from Mari and Winyard, 2015.

Schematic illustration modified from Mari and Winyard, 2015. Stages of nephron development: the ureteric bud invades the surrounding metanephric mesenchyme, meanwhile a subset of mesenchymal cells condense around the tips of the ureteric bud forming the cap mesenchyme. These cells form the pretubular aggregates first and after they undergo MET epithelialising to renal vesicles, which elongate to comma- and S-shaped bodies. S-shaped bodies further differentiate into distal tubules, proximal tubule, loop of Henle, glomerular Bowman's capsule (derived from parietal epithelium) and podocytes (derived from visceral epithelium).

1.3.1 *Genes involved in nephron development*

As mentioned before, the cap mesenchyme is the structure giving rise to the epithelial elements of the nephron except for the collecting ducts (Mugford et al., 2009). The cap mesenchyme is formed by a heterogeneous cell population that can self-renew and to differentiate into epithelium by undergoing MET (Hendry et al., 2011). There are several key transcription factors that coordinate cap mesenchymal cell specification, self-renewal, survival and differentiation.

These include Odd-Skipped Related 1 (*Osr1*), Paired box 2 (*Pax2*), sine oculis homeobox (Drosophila) homolog 2, (*Six2*), Wilms Tumour 1 (*WT1*), sal-like transcription factor 1(*Sall1*), eyes absent homolog 1 (*Eya1*) and Cbp/P300-Interacting transactivator with Glu/Asp-Rich carboxy-terminal domain,1 (*Cited1*), these are summarised in Table 1-1.

1.3.1.1 Osr1

Osr1 encodes a zinc-finger protein homologous to the Drosophila odd-skipped transcription factor (So and Danielian, 1999, Lan et al., 2001). *Osr1* is first expressed in the mesoderm, remaining upregulated throughout the intermediate mesoderm stage, being then restricted to the cap mesenchymal cells and downregulated upon differentiation to epithelial cells (Mugford et al., 2008, James et al., 2006). No expression of *Osr1* has been detected in ureteric bud (Xu et al., 2014). Targeted *Osr1* null mutations in mice cause aberrant intermediate mesoderm apoptosis starting at embryonic day 9.5, thus suggesting its early role in intermediate mesoderm survival (James et al., 2006).

Cap mesenchymal specific inactivation of *Osr1* determines a premature differentiation of progenitor cells resulting in renal hypoplasia, thus suggesting a role in cell survival also in the cap mesenchyme. *Osr1* maintenance of cap mesenchymal undifferentiated cells has been linked to *Six2* presence in these cells, in fact *Osr1* and *Six2* interact synergistically to maintain nephron progenitors during kidney organogenesis (Xu et al., 2014). In mice, *Osr1* acts upstream of *Eya1, Pax2, Six2* and *Sall1* pathways (James et al., 2006).

1.3.1.2 Pax2

The *Pax2* gene encodes for a transcription factor belonging to the paired box gene family, characterised by the conserved paired box domain, a 128-amino acid DNA-binding domain that binds specific sites on DNA to initiate gene regulation (Treisman et al., 1991). In mammals, nine *Pax* genes have been identified (*Pax 1 – 9*) controlling the specification of a variety of cells and tissues. Their deregulation has been linked to cancer and human congenital malformations (Chi and Epstein, 2002, Robson et al., 2006). In mice, *Pax2* and *Pax8* are expressed in developing kidneys having essential roles in its development (Torres et al., 1995).

Loss of PAX2 functional protein in PAX2 mutant mice causes severe defects to the urogenital systems, leading to death shortly after birth. These mice lack of kidneys, ureters, genital organs and have ophthalmologic and inner ear defects (Torres et al., 1995).On the contrary, *Pax8* only mutant embryos show normal kidney development (Mansouri et al., 1998). *Pax2* gene is not only expressed in the kidney but also during eye, ear, central nervous system and genital tract development (Dressler et al., 1990, Eccles et al., 1992).

In humans, PAX2 mutations are associated with renal-coloboma syndrome, an autosomal dominant condition in which renal and eye development are impaired. This causes hypoplastic kidneys and malformation of the optic nerve, often associated with a hole (coloboma) in the retina that can impair vision (Bower et al., 2012). Heterozygous Pax2 mutant mice show phenotype similar to the human syndrome, due to the same site of mutation in the exon 2 (Eccles, 1998).

Conversely, an overexpression of PAX2 is associated with developmental aberrations such as dysplastic kidneys and autosomal dominant polycystic kidneys and in adult renal cell carcinoma and Wilms tumour (Dressler and Douglass, 1992, Gnarra and Dressler, 1995, Winyard et al., 1996).

Pax2 expression is first seen in the intermediate mesoderm and continues as the intermediate mesoderm gives rise to the nephric duct, the ureteric bud, and the surrounding metanephric mesenchyme. When the ureteric bud invades the metanephric mesenchyme, both ureteric bud tips and condensed mesenchyme around them express *Pax2*. The cap mesenchymal cells undergo mesenchymal-to-epithelial transition and *Pax2* is yet again essential to start this conversion while its

downregulation occurs in the proximal loop of the S-shaped body and then in the mature epithelial cells of the nephron (Dressler, 2011, Ryan et al., 1995).
In addition, *Pax2* has a role in specifying and restricting the fate of progenitor cells through modification of their epigenetic state, it appears to commit undifferentiated cell types towards the epithelial lineage, this ability is performed through its recruitment of epigenetic regulators, such as activators of the Thrithorax family or repressors of the Polycomb family (Patel et al., 2014). Adult kidneys do not express *Pax2*, however it is reactivated in adult renal tissues upon injury, suggesting a role in epithelial regeneration (Kusaba et al., 2014, Humphreys et al., 2008).

1.3.1.3 Six2

Six2 is a crucial transcription factor expressed throughout the development of the excretory system. In mice, SIX2 protein localisation is observed in the metanephric mesenchyme before, during and after ureteric bud invasion when metanephric mesenchyme condenses around the tips of the ureteric bud. At the dorsal side of the ureteric bud tips SIX2 protein expression overlaps with PAX2, however cells after MET maintain PAX2 expression while downregulating SIX2 (Oliver et al., 1995).
This expression pattern suggests that SIX2 specifically address the early renal progenitor cells of the cap mesenchyme not yet differentiated towards epithelia. This is strongly corroborated by the phenotype of $Six2^{-/-}$ homozygous mice, that die soon after birth and show smaller kidneys with rapid loss of the cap mesenchymal cells pool due to premature differentiation into epithelia (Self et al., 2006). On the contrary, $Six2^{+/-}$ heterozygous mice do not exhibit any obvious abnormalities. The role of *Six2* in the cap mesenchymal progenitor cell population has been better elucidated with genetic cell fate analyses. In the interesting work from Kobayashi et al., in mouse, $Six2^{+}$ cells are seen to contribute to the whole segments of the nephrons except for the ureteric epithelium thus specifying cells with a great differentiation potential. In addition, *Six2* appears to have a central role in maintaining the progenitor cell self-renewal by acting cell-autonomously (Kobayashi et al., 2008). SIX2 expression is not detected in adult mouse kidneys (Humphreys et al., 2008).

1.3.1.4 WT1

WT1 gene encodes a zinc finger protein that acts both as a transcription factor and an RNA binding protein. These functions are accomplished by different isoforms of the same gene, which is very complex and characterised by at least 36 isoforms. Small differences in these isoforms, such as the presence of three amino acids between two domains, can determine different protein functions. *WT1* has a central role in the kidney development by regulating many genes (Kreidberg et al., 1993).

WT1 expression is observed in different stages of developing kidneys. It is first detected in the intermediate mesoderm and its expression continues at low levels in the metanephric mesenchyme, it is absent in the ureteric bud tissue (Pritchard-Jones et al., 1990). Within cap mesenchymal cells, its expression increases due to its central role during MET, in which it promotes expression of *Wnt4* (Sim et al., 2002). *In vitro* knockdown in murine kidneys culture of *WT1* at embryonic day (E) 11.5, leads to nephron blockage at a pre-MET stage (Davies et al., 2004). *WT1* expression continues in comma and S-shaped bodies and in the proximal part of the developing nephron where glomerulus forms. Also, adult kidneys show strong expression and an important role of *WT1* in podocytes (Chau et al., 2011). There is a close correlation between *WT1* expression in mouse (Armstrong et al., 1993) and human (Pritchard-Jones et al., 1990), for this reason, many *WT1* mutant murine models have been generated to study its role in development and disease in order to translate the findings in humans. Loss of *WT1*, by knockout of the exon 1 in mice, is embryo lethal and results in complete renal agenesis, with increased apoptosis in the metanephric mesenchyme and lack of the ureteric bud (Kreidberg, 2010). Other organs development is affected by *WT1* is absence, such as gonads and adrenal glands, heart, retina, olfactory epithelium and spleen (Herzer et al., 1999, Wagner et al., 2002). Heterozygous $WT1^{+/-}$ knockout mice show normal kidneys but are prone to develop glomerular sclerosis and interstitial fibrosis with severe proteinuria and albuminuria (Menke et al., 2003). In humans, mutations in *WT1* gene predispose to Wilms tumours, syndromic forms of childhood kidney disease and gonadal dysgenesis (Kreidberg, 2010). *WT1* mutations within exon 8 or 9 cause Denys-Drash syndrome in which *WT1* loss of function determines mesangial sclerosis, abnormalities in kidneys and genitalia and high risk of developing Wilms tumour (Pelletier et al., 1991). Rarely, a disruption in distribution of *WT1*

isoforms leads the Fraiser Syndrome, which is characterised by a pseudohermaphroditism and progressive glomerulopathy (Barbaux et al., 1997).

1.3.1.5 Eya1

Eya1 gene encodes a transcription coactivator whose expression in the developing kidney is restricted to the condensed mesenchyme surrounding the ureteric bud tips and it is excluded from the ureteric bud branches and the uninduced metanephric mesenchyme (Kalatzis et al., 1998). During kidney development, *Eya1* interacts with *Six1* and *Pax2* to upregulate *Six2* expression to induce glial cell derived neurotrophic factor (GDNF) expression, which in turn is required for the normal growth of the ureteric duct (Sajithlal et al., 2005, Gong et al., 2007).
EYA1 expression, when disrupted in humans causes the branchio-oto-renal syndrome, characterised by branchial, otic and renal anomalies (Schmidt et al., 2014). Both heterozygous and homozygous *Eya1*mutations in mice affect inner ear morphology and hearing, and result in dysmorphic or absent kidneys (Zou et al., 2008, Xu et al., 1999).

1.3.1.6 Sall1

Sall1 is an important transcription factor expressed in the cap mesenchyme. Its expression is also observed in the uncommitted mesenchyme and early epithelial structures derived from cap mesenchyme after MET (Nishinakamura et al., 2001).
In mice, heterozygous *Sall1* mutants show cystic kidneys, *Sall1*-null mice exhibit renal agenesis or dysgenesis and die after birth (Nishinakamura and Osafune, 2006).
Heterozygous mutations of *SALL1* in humans cause Townes-Brocks syndrome, determining facial and limb defects, renal and urinary tract abnormalities and anorectal malformations (Kohlhase et al., 1998).
Sall1 is required for the maintenance of cap mesenchymal cells as its deletion at E12.5 in mice results in loss of nephron progenitors and ectopic differentiation (Basta et al., 2014).

1.3.1.7 Cited1

Cited1 is a transcription factor expressed within the cap mesenchyme surrounding ureteric bud tips in mouse and rat developing kidney (Plisov et al., 2005). CITED1^{+} cells subset also expresses *Six2* and it is identified as the 'true' un-induced- self-renewing renal stem cell population. Whereas, when *Cited1* is downregulated, this population becomes induced to undergo MET and thus committed to the epithelia differentiation (Brown et al., 2013, Mugford et al., 2009). *Cited1* expression is absent in the adult kidney. Surprisingly its deletion does not impair kidney development suggesting potential compensatory mechanisms. No functional role for Cited1 has been described and it is often used only as a marker for the least differentiated cell compartment within the cap mesenchyme. (Boyle et al., 2008, Boyle et al., 2007).

Table 1-1. Genes known to contribute to cap mesenchyme formation and/or survival of cap mesenchymal cells in mice

Gene	Expression	Function	Kidney LOF phenotype	References
Cited1	CM	Uncommitted progenitors in the CM	No phenotype	(Brown et al., 2013, Boyle et al., 2008, Boyle et al., 2007)
WT1	CM, PTA. Increased in podocytes	Upstream of FGF, Sall1, Bmp7, Pax2,	Agenesis – CM apoptosis	(Kreidberg, 2010)
Pax2	IM, UB, CM, CSB and SSB, no in more developed tubules	Epigenetic regulation in the stem cells, upstream of Six2	Agenesis	(Dressler, 2006, Patel et al., 2014)
Eya1	CM	Regulates Six2	Agenesis	(Gong et al., 2007, Wellik et al., 2002, Xu et al., 1999, Kalatzis et al., 1998)
Osr1	IM, MM and CM	Upstream of Eya1, Pax2, Six2, Sall1, and GDNF	Agenesis	(Mugford et al., 2008, James et al., 2006)
Sall1	MM, CM	Stem cell maintenance	Agenesis, premature differentiation	(Nishinakamura et al., 2001)
Six2	CM	Stem cell maintenance	Excess nephrons induced, premature loss of CM	(Kobayashi et al., 2008)

CSB, Comma-shaped bodies; CM, cap mesenchyme; IM, intermediate mesoderm; LOF, loss of function; MM, metanephric mesenchyme; PT, proximal tubules; PTA, pre-tubular aggregates; RV, renal vesicles; SSB, S-shaped bodies; UB, ureteric bud.

1.4 Nephron stem/progenitor cells and niche signals: balancing self-renewal and differentiation

The cap mesenchyme can be considered as the fetal renal stem cell niche. As such, it provides a sheltering environment from differentiation stimuli, apoptotic stimuli, and other stimuli that would challenge stem cell reserves. Here, stem cells while retaining a pool of undifferentiated cells, replicate into progenitors more committed to produce mature cell lineages; it is therefore not a homogenous cell population but rather a heterogenic group where stem and progenitor cells coexist. The way cap mesenchymal cells are balanced between self-renewal and differentiation is of considerable interest and it comprises a fine regulation of various pathways. As a consequence, these signals deregulation determines the cap mesenchymal cells apoptosis. It has been shown that murine cap mesenchymal cells die within 48 hours when eradicated from their *in vivo* position (Perantoni et al., 1995).

Essential roles within the renal stem cell niche are played by members of the FGF family of proteins, such as FGF2, and BMP7; a combination of these molecules has been seen to promote survival and proliferation of isolated cap mesenchymal cells (Dudley et al., 1999). *Bmp7* is normally expressed in both cap mesenchyme and ureteric bud tips adjacent to this (Dudley et al., 1995).

Loss of *Bmp7 in vivo* leads to increased apoptosis of cap mesenchymal cells (Dudley et al., 1995). BMP7 protein affects cell proliferation or differentiation of nephron progenitors, this depends whether BMP7 binds to cell surface receptor serine/threonine kinases activating SMAD (R-SMAD) or mitogen-activated protein kinase/c-Jun N-terminal Kinase (MAPK/JNK) pathway (Shi and Massague, 2003). For this reason, BMP7 promotes proliferation through the MAPK/JNK pathway, also synergising with FGF factor (Blank et al., 2009, Brown et al., 2011b, Barak et al., 2012). Conversely, via phosphoSMAD1/5/8, BMP7 has a pro-differentiation role (Brown et al., 2013).

As mentioned before, the pool of cap mesenchymal cells is not a homogenous population and high-resolution mapping studies have suggested that different cell types coexist (Figure 1-3 A):

- cells co-expressing *Six2* and *Cited1*($CITED1^+SIX2^+$) are believed to have the greatest capacity in terms of self-renewal and differentiation. Early differentiation is prevented in this population by their incapacity to respond to differentiation signal (Brown et

al., 2013). Upon BMP7 mediated SMAD signalling activation, these refractory cells down-regulate *Cited1* and move towards the outer part of the cap mesenchyme, closer to the ureteric bud tip, becoming:

- cells CITED1^{-}SIX2^{+}, these acquire the potential to respond to differentiation signalling, mainly from Wingless-Type MMTV Integration Site Family members (WNT), they then downregulate *Six2* differentiating *in:*
- cells CITED1^{-}SIX2^{-}LEF1^{+}, they activate WNT differentiation gene targets via β-catenin interaction of T cell factor/lymphoid enhancer factor (Tcf/Lef1) starting the differentiation in pre-tubular aggregates and consequently the transition to epithelial cells (Brown et al., 2013, Mugford et al., 2009, Schmidt-Ott and Barasch, 2008, Boyle et al., 2008).

The cap mesenchyme organisation in different cell compartments might represent a mechanism to balance progenitor cell renewal and epithelial differentiation enabling multiple rounds of nephrogenesis without early exhaustion of stem cells.

Other factors mediate nephron progenitor cells maintenance, an essential role is played by fibroblast growth factor family members, indeed inactivation of FGF receptors 1 and 2 in the cap mesenchyme causes arrest in kidney development (Poladia et al., 2006, Sims-Lucas et al., 2011). FGF receptors are present with two splice variants, ‘b’ and ‘c’, generated via alternative splicing. These have distinctive tissue location, predominantly with the ‘b’ splice variant in epithelial cell types and ‘c’ in mesenchymal tissues (Itoh, 2007). Normally, FGF ligands secreted from epithelial cells signal to the isoform ‘c’ of the FGFR, whereas ligands originated from mesenchymal cells signal to the epithelial splice form ‘b’ of the FGFR (Zhang et al., 2006).

Ligand binding to FGF receptors is facilitated by the interaction with proteoglycan heparin and heparin sulphate. Accordingly, *in vitro* FGF addition to nephron progenitor culture may require heparin-like molecules to improve binding (Yayon et al., 1991).

FGF2 is usually expressed by the ureteric bud and it is able to maintain the cap mesenchymal cells in culture preventing their apoptosis (Dudley et al., 1999, Perantoni et al., 1995, Barasch et al., 1997, Brown et al., 2011a); *in vivo*, FGF2 acts redundantly with other FGFs to maintain nephron progenitors as FGF2 null mutant mice show relatively normal kidneys (Ortega et al., 1998, Dono et al., 1998).

Other FGFs involved in the maintenance of the niche are FGF9 and FGF20. The first is released by the ureteric bud, the second by the cap mesenchyme. When *in vitro* cultures

of murine metanephric mesenchymal cells (cap mesenchyme and stroma) and cap mesenchymal cells ($SIX2^+$ cells) are treated with FGF9 and FGF20, they not only survive but also actively respond to differentiation signals. However purified $SIX2^+$ cells cannot be maintained indefinitely in media even with the addition of FGF9 and are not detected after 7-8 days in culture (Brown et al., 2011a, Barak et al., 2012).

Differently from the $FGF2^{-/-}$ absence of phenotype, loss of both FGF9 and FGF20 in mice and FGF20 in humans causes impairment of kidney development (Barak et al., 2012).

Another FGF, FGF8, has been shown to be expressed during nephron development in renal vesicles and renal epithelia (Grieshammer et al., 2005, Perantoni et al., 2005). FGF8 mutation *in vivo* affects survival of nephron progenitors (Perantoni et al., 2005), *in vitro* FGF8 is not able to maintain this population, possibly due to its binding with a decoy receptor FGFR1 (expressed in cap mesenchyme) (Brown et al., 2011a). FGF7 and FGF10 expressed by cap mesenchymal cells are involved in the regulation of ureteric bud branching (Bates, 2011).

These considerations on factors affecting progenitor cell survival highlight an important role for BMP7 and FGFs to sustain its maintenance *in vitro*. Other factors signalling to nephron progenitors determine their differentiation; these can be simplified in ureteric bud-derived and stroma-derived factors.

1.4.1.1 Ureteric bud-derived factors

WNT factors, released by the ureteric bud, are involved in epithelialisation of cap mesenchyme (Table 1-2, Figure 1-3 B). The first evidence of this appeared in co-culture experiments, where isolated cap mesenchyme cultured with the embryonic spinal cord was induced to undergo MET. WNT1-secretion by spinal cord was found to be the signal responsible to trigger mesenchymal cells differentiation (Herzlinger et al., 1994). Although WNT1 is not expressed in the developing kidney, other WNTs, WNT9b and WNT4 are an essential component of the regulation of MET *in vivo*.

In mice, lack of *Wnt9b* causes major defects in ureteric bud branching resulting in kidney agenesis, whereas *Wnt4* null mutants show hypoplastic kidneys with undifferentiated mesenchyme and few epithelial tubules (Carroll et al., 2005, Stark et al., 1994). In humans, WNT4 mutation has renal dysgenesis as a consequence, suggestive of a clinical relevance of this factor (Mandel et al., 2008, Biason-Lauber et al., 2004).

WNT9b from the ureteric bud signals via βcatenin controlling either self-renewal or differentiation of nephron progenitors. WNT9b is able to maintain progenitors in an undifferentiated state through activation of target genes such as *Cited1* (Karner et al., 2011). These roles appear to be mediated by the co-operation with SIX2 although the exact mechanism is still unknown (Karner et al., 2011, Park et al., 2012). WNT9b/β-catenin can also induce expression of *Fgf8*, *Pax8* and *Wnt4* determining differentiation of nephron progenitors (Park et al., 2007, Carroll et al., 2005, Grieshammer et al., 2005).

In addition to WNT factors, other molecules influence the nephron progenitor niche. One of these is the Leukaemia Inhibitor Factor (LIF) secreted by the ureteric bud originally shown to trigger epithelialisation in isolated rat metanephric mesenchyme (Barasch et al., 1999, Plisov et al., 2001).
As well as WNTs, also LIF can have opposite actions on nephron progenitors depending on its concentration: higher LIF concentrations determine differentiation of isolated rat metanephric mesenchyme, while lower concentrations cause progenitor expansion (Tanigawa et al., 2015).

1.4.1.2 Stroma-derived factors

Other factors acting on the nephron progenitors are released by the surrounding stromal cells (Figure 1-3, B). This is a population of cells expressing the transcription factor *Foxd1* whose loss causes ureteric tree disruption and mislocalisation of pre-nephrogenic structures (such as pre-tubular aggregates and renal vesicles) leading to a striking reduction in nephron number (Levinson et al., 2005, Hatini et al., 1996).

Stromal cells modulate nephron progenitors differentiation through the release of the factor FAT4; this is an atypical cadherin in the Salvador-Warts-Hippo pathway (Harvey and Hariharan, 2012). FAT4 differentiation effects are carried out by inhibition of self-renewal genes such as *Cited1* and promotion of WNT9b/β-catenin differentiation genes such as *Pax8* and *Wnt4*. It has been found that combination of WNT9b (from the ureteric bud) and FAT4 (from the stroma) inactivates Yes-associated protein (YAP) and the transcriptional coactivator with PDZ-binding motif (TAZ) allowing the transcription of WNT9b/βcatenin differentiation target genes. Conversely, when FAT4 is absent YAP is active and localises to the nucleus where it drives the transcription of β-catenin pro-self-renewal target genes as summarised in Figure 1-3 (Das et al., 2013).

1.4.1 *Application of stem cells niche signals on in vitro culture*

The increased understanding of the signals inducing nephron progenitor amplification or differentiation has prompted the research towards optimisation of the in vitro culture conditions to maintain nephron progenitors. The achievement of long-term nephron propagation of progenitor cells might in fact contribute greatly to regenerative medicine approaches as well as to the integration of genomic and proteomic data (proteogenomics) to yield a more complete picture of nephron development.

Protocols for the generation of nephron progenitors from mouse embryonic stem cells (ESCs) and human induced pluripotent stem cells (iPSCs) have been established by different groups (Taguchi and Nishinakamura, 2014, Takasato et al., 2014, Takasato et al., 2015, Morizane et al., 2015). Recently, nephron progenitors derived by murine embryonic kidneys as well as ESCs and iPSCs were expanded *in vitro* with a method developed by Tanigawa et al.

In this study, the culture conditions used for the maintenance or rat metanephric mesenchyme were adopted and then better refined to be used for $SIX2^+$ cells isolated from

murine kidney embryos at E11.5, E15.5 and postnatal at P0 (Tanigawa et al., 2016, Tanigawa et al., 2015). The most promising results were obtained from E11.5 metanephric mesenchyme cells $SIX2^{-}GFP^{+}$ (green fluorescent protein expressed under the regulation of SIX2 promoter). Purified murine $SIX2^{+}$ cells were aggregated in clusters and cultured on dishes coated with iMatrix, a fibronectin with the E8 fragment of laminin. For up to 19 days, these cells were successfully expanded 1,800-fold while the 85% of the total population retained protein expression of SIX2, PAX2 and WT1. The protocol comprised a combination of low concentrations of LIF, Rho kinase inhibitor and NOTCH inhibitor to prevent premature progenitor differentiation. In addition, since experiments demonstrated that low concentration of WNT agonist and BMP7 could lead to expansion of $SIX2^{+}$ cells, while higher concentration would support the SIX2- negative cells, these were added to the mixture as well as FGF2, necessary for maintenance of nephron progenitors. Within this microenvironment $SIX2^{+}$ cells maintained their differentiation potential forming three-dimensional nephron structures when combined with embryonic spinal cord. The same combination applied on nephron progenitors derived from ESCs and iPSCs achieved similar results. This study was particularly encouraging because it showed that by manipulating the microenvironment of nephron progenitors it was possible to extend their lifespan to an extent never achieved before. However, in extended cultures cells lost their self-renewal, E 11.5 $SIX2^{+}$ cells cultured for 30 days were not able to form tubules or glomeruli and reduced the expression of markers of nephron progenitors.

Nevertheless, this research contributes to the understanding of how different factors contribute to nephron progenitor maintenance and differentiation suggesting an efficient combination of factors at concentrations able to maintain nephron progenitor cells *in vitro* cultures.

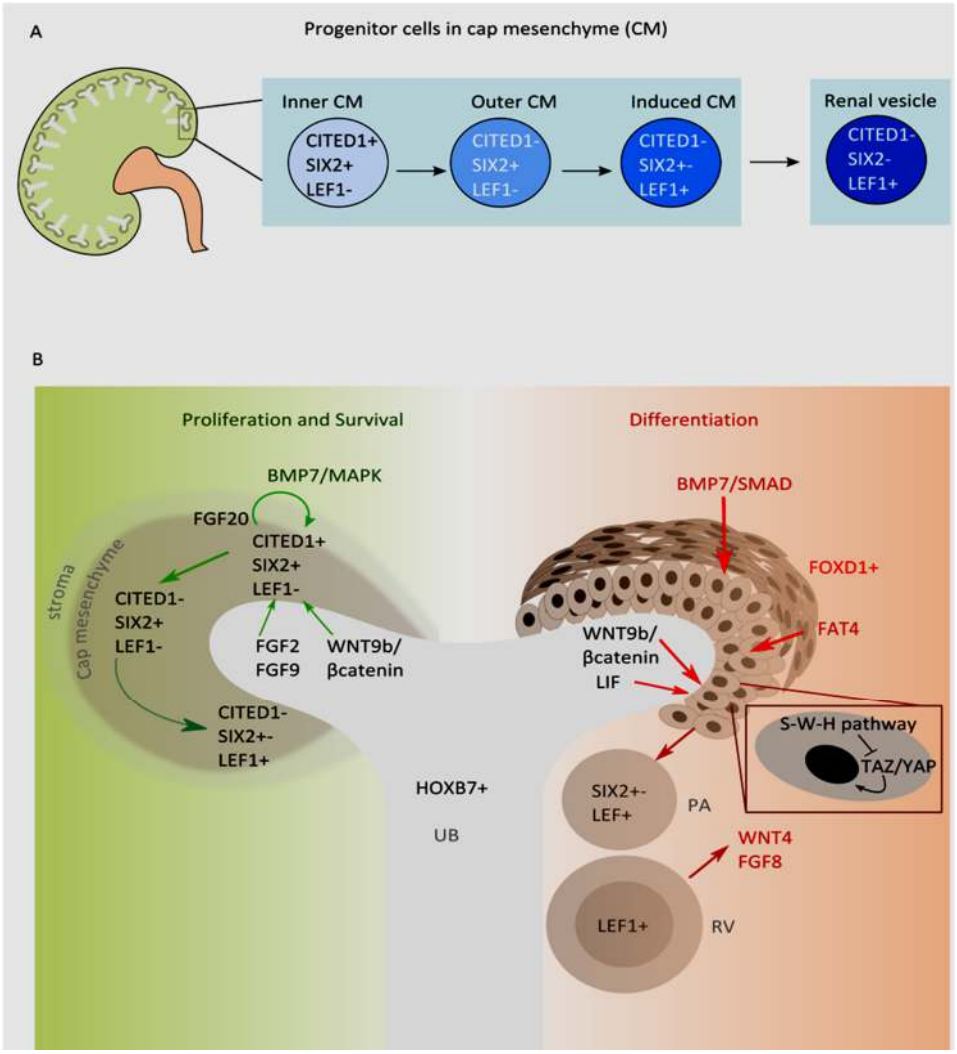

Figure 1-3 Schematic illustration representing stages of nephron development.

A) Scheme of CITED1, SIX2, LEF1 expression by renal progenitor cells in the compartments of the cap mesenchyme. B) Illustration of the signals within the nephron progenitor cells niche. The earliest stem/progenitor in the cap mesenchyme are CITED1^{+}SIX2^{+}LEF1^{-} cells, along with their commitment and differentiation in pre-tubular aggregates (PA) and renal vesicles (RV) they gradually lose expression of CITED1, SIX2 and acquire expression of LEF1. BMP7 expressed by cap mesenchyme cells promotes prolieferation through MAPK pathway, whereas it can also promote differentiation when acting through SMAD pathway. FGF2 is expressed by ureteric bud and it is able to maintain cap mesenchymal cells survival together with FGF9 and FDF20 expressed by CITED1^{+}SIX2^{+}LEF1^{-} cells. WNT9b/βcatenin and LIF signalling is required for differentiation of CITED1^{+}SIX2^{+} early stem/progenitor cells to CITED^{-}SIX2^{+}. Wnt9b/βcatenin induce expression of FGF8 and WNT4 determining differentiation towards renal vesicles (RV).Stromal cells modulate cap mesenchyme cells differentiation by releasing FAT4 an atypical cadherin in the Salvador-Warts-Hippo pathway (S-W-H) , which together with Wnt9b inactivates Yes-associated protein (YAP) and the transcriptional coactivator TAZ allowing the transcription of differentiation target genes. Stromal cells express FOXD1, important for ureteric bud branching. Ureteric bud cells express HOXB7 , important for the correct branching.

Table 1-2 Genes involved in the nephron progenitors niche maintenance in rodents.

Gene	Expression	Function	Kidney LOF phenotype	References
BMP7	UB, CM, PTA, podocytes	Progenitor cell maintenance or differentiation	Smaller kidneys	(Dudley et al., 1999, Brown et al., 2013)
FGFR 1 and 2	CM, UB	Reception of niche signals	Agenesis – small UB, no CM	(Poladia et al., 2006)
FGF2	UB	Progenitor maintenance	No phenotype	(Ortega et al., 1998, Dono et al., 1998)
FGF 8	PTA and proximal tubules	Nephron progenitor maintenance *in vivo*	No PTA, no progenitor cells	(Perantoni et al., 2005)
FGF 9	CM, UB	Progenitor maintenance	Agenesis with FGF20	(Barak et al., 2012)
FGF 20	CM	Progenitor maintenance	Agenesis with FGF 9	(Barak et al., 2012)
LIF	UB	Progenitor maintenance or differentiation	No phenotype	(Tanigawa et al., 2015, Yoshida et al., 1996)
NOTCH 1, NOTCH2	RV, CSB, SSB	Progenitor differentiation	No maturation of RV into CSB and SSB, no PT and glomeruli	(Surendran et al., 2010, Boyle et al., 2011)
Wnt4	PTA, CSB, SSB	Progenitor differentiation	Agenesis	(Stark et al., 1994)
Wnt9b	UB	Progenitor differentiation	Agenesis	(Carroll et al., 2005)

CSB, Comma-shaped bodies; CM, cap mesenchyme; IM, intermediate mesoderm; LOF, Loss of Function; MM, metanephric mesenchyme; PT, proximal tubules; PTA, pre-tubular aggregates; RV, renal vesicles; SSB, S-shaped bodies; UB, ureteric bud.

1.5 CD24 and CD133

1.5.1 *CD24*

CD24 and CD133 have been described as stem cell markers when previously identified in several human tissues.

CD24 is a sialoglycoprotein anchored to the cell membrane through a glycosyl phosphatidylinositol-linkage (Fischer et al., 1990). CD24 is strongly expressed on immature T and B cells, developing neurons, regenerating muscle and during the development of several kinds of epithelium (Allman et al., 1992, Shirasawa et al., 1993), while it is usually absent in differentiated cells.

A central role has been proposed for CD24 in maintaining cancer cell growth and anchorage-independent proliferation and survival (Smith et al., 2006). Many studies have correlated CD24 expression to clinicopathological parameters in multiple human cancers. CD24 is suggested as a marker of a more aggressive cancer biology in primary breast cancer (Kristiansen et al., 2003b), a predictor of shortened patient survival in non-small-cell lung cancer and poorer prognosis in prostate cancer (Kristiansen et al., 2003a, Kristiansen et al., 2004) and higher risk of urothelial carcinoma progression (Winkler et al., 2007).

In renal cell carcinoma high expression of CD24 is associated with large tumour size, and shorter progression-free survival, CD24 is therefore proposed as a novel prognostic marker for tumour recurrence or metastasis in renal carcinoma (Lee et al., 2008).

Little is known about CD24 molecular regulation and its biological effects. The transcriptional regulation of CD24 by the Wnt pathway has been suggested in a human mammary epithelial cell line (Shulewitz et al., 2006). It has been shown that, once translated, CD24 is transported to the cell membrane where its function is modulated through interaction with lipid rafts and β1-integrins (Suzuki et al., 2001, Runz et al., 2008). Once completed its function, CD24 is either endocytosed to the cell cytoplasm and then degraded, or incorporated into exosomes (Keller et al., 2007). It has also been hypothesised that nuclear translocation of CD24 may upregulate the epithelial transcriptome (e.g. expression of the epithelial marker E-cadherin) (Ye et al., 2006). CD24 is expressed in early human nephrogenesis, seen in renal vesicles, comma and S-shaped bodies. However it is downregulated during the second trimester of gestation,

persisting only in selected cells in the medullary interstitium by late gestation and postnatally (Ivanova et al., 2010).

1.5.2 *CD133*

CD133, also known as prominin-1, is a pentaspanning transmembrane glycoprotein localised to cellular protrusions (Miraglia et al., 1997). Although its biological function remains unknown, CD133 has been proposed as a stem cell marker for normal and cancerous tissues (Shmelkov et al., 2008).

In mouse, prominin-1 was shown to localise to microvilli and plasma membrane of the apical surface of neuroepithelial cells and other embryonic epithelia as well as on brush borders of adult kidney proximal tubules (Weigmann et al., 1997).

In humans, CD133 expression was studied with antibodies recognising a glycosylated epitope (AC133) identified on immature cells such as hematopoietic/progenitor cells and developing intestinal and neuronal cells (Corbeil et al., 2000, Ito et al., 2007, Richardson et al., 2004, Kemper et al., 2010, Yin et al., 1997). Immunoreactivity for AC133 was downregulated upon cell differentiation, showing that AC133 antigen was specifically located on immature cells whereas CD133 expression was retained upon differentiation (Corbeil et al., 2000).

AC133 is used as a surface marker to address haematopoietic stem/progenitor cells able to engraft and differentiate towards different lineages. Upon isolation from peripheral blood and *in vitro* manipulation to undergo myogenesis, $AC133^+$ cells contribute to muscular regeneration when transplanted into dystrophic mice (Torrente et al., 2004).

CD133 has also been used as stem cell marker in non-haematopoietic lineages. Uchida et al., isolated $CD133^+$ cells from human fetal brain. These are highly clonogenic and able to differentiate either towards neurons or glial cells, furthermore upon transplantation into brains of immunodeficient neonatal mice are capable of engraftment, proliferation, migration and differentiation towards neurones (Uchida et al., 2000).

$CD133^+$ cells appear to identify cancer initiating stem cells in various human tumours. $CD133^+$ isolated from prostate cancer samples can self-renew, proliferate, differentiate *in vitro* and to recapitulate the original tumour phenotype (Collins et al., 2005).

Furthermore, tumorigenic $CD133^+$ cells derived from human colon cancer and hepatocellular carcinomas demonstrate the ability to reform the original tumour when engrafted *in vivo* compared to $CD133^-$ counterpart (Ricci-Vitiani et al., 2007, Yin et al., 2007).

$CD133^+$ cells from medulloblastoma recapitulate the original tumour and are radioresistant (Blazek et al., 2007) as well as $CD133^+$ from anaplastic thyroid carcinoma cell lines (Zito et al., 2008).

These studies demonstrate that CD133 positivity identifies a tumour stem cell population involved in the proliferation and self-renewal of the tumour. In contrast to these data, $CD133^+$ population isolated from human renal cell carcinomas do not show features of tumour-initiating cells population being unable to induce tumours in immunodeficient mice (Bruno et al., 2006). It was hypothesised that these $CD133^+$ cells represent a resident renal stem cell population (Florek et al., 2005). $CD133^+$ cells, when co-transplanted with renal tumour cells significantly enhance tumour engraftment, growth, and vascularisation. Same results are obtained with normal renal-derived $CD133^+$ cells thus ruling out a tumorigenic nature of tumour-derived $CD133^+$. The same group showed that a population of $CD105^+$ stem cells with mesenchymal characteristics present characteristics of tumour initiating stem cells, being able to grow into a tumour mass when transplanted into immune-deficient mice (Bussolati et al., 2008).

1.5.3 *CD24 and CD133 in the kidney*

CD24 and CD133 roles in kidney development are currently unclear. Expression of CD24 and CD133 in human fetal kidneys is observed in epithelial structures derived from the cap mesenchyme, typically in renal vesicle, comma and S-shaped bodies. Kidney cells derived from human fetal kidneys of gestational age of 8.5 to 9 weeks, when analysed by flow cytometry, show numerous cells expressing both proteins (ranging from 35 to 50% of the total cell population analysed) (Ivanova et al., 2010, Lazzeri et al., 2007).

However, their presence gradually decreased during development, becoming only a 2% of the total population in adult kidneys.

CD24 and CD133 analysed in normal adult kidneys, show colocalisation in parietal epithelial cells of the Bowman's capsule and distribution within the proximal tubule, thick ascending limb, the distal convoluted tubule and the connecting segment (Angelotti et al., 2012, Lindgren et al., 2011).

CD133 localises within the Bowman's capsule, in proximal convoluted tubules, in some interstitial cells and in rare tubules (Bussolati et al., 2005, Sagrinati et al., 2006). CD24 is expressed in parietal epithelial cells of the Bowman's capsule, in the cells of the macula densa, adjacent to the juxtaglomerular cells of the glomerular vasculature and in a subset of distal tubule cells in the medulla (Ivanova et al., 2010, Sagrinati et al., 2006).

1.6 Acute kidney injury and chronic kidney disease

Acute kidney injury (AKI) refers to a heterogeneous clinical syndrome characterised by a rapid (hours to days) decrease in renal function resulting in the accumulation of products of nitrogen metabolism such as creatinine and urea with reduced urine output (Bellomo et al., 2012). The term 'acute kidney injury' substitutes the term 'acute renal failure' used previously to describe the same syndrome, and it is now used prevalently to the situations in which the organ damage requires renal replacement therapy (Maarten W. Taal, 2012). AKI includes a broad range of structural and functional kidney dysfunctions and different definitions and staging criteria have been proposed. In 2004, the Acute Dialysis Quality Initiative (ADQI) Group proposed the RIFLE classification (Risk, Injury, Failure, Loss and End-stage renal disease) in accordance to the increase in serum creatinine and duration of oliguria (Bellomo et al., 2004). Recently, the Acute Kidney Injury Network (AKIN) modified the RIFLE classification defining 3 stages according to abrupt increases in serum creatinine levels (Table 1-3) (Mehta et al., 2007). Although this classification facilitates the diagnosis, AKI staging does not solely relies on serum creatinine level and urine output but it also makes use of biomarkers for AKI including the kidney injury molecule 1 (KIM-1) (Coca et al., 2008).

The study of AKI in the population is relatively recent since the lack of a consensus definition of AKI has made difficult to compare the incidence of AKI among different studies.

The incidence of AKI has been estimated to have increased over the last fifteen years, and is predicted to double over the next decade (Silver et al., 2015). It varies between populations, occurring in one in five adults and one in three children hospitalised with acute illness in developed Countries (Rewa and Bagshaw, 2014). AKI is associated with a significant increase in hospital length of stay and mortality.

The aetiology of the AKI is often multifactorial, for brevity three major functional causes can be distinguished in prerenal, intrinsic and postrenal. Prerenal injury results from a reduced blood perfusion of the kidney due to decreased arterial blood volume. This can be caused by haemorrhage post traumatic events or by liver failure, gastrointestinal losses, septic shock or pancreatitis. Prerenal azotemia can be transient if the kidney is rapidly perfused or lead to acute tubular necrosis if this situation is prolonged in time (Blantz, 1998). Within the intrinsic acute kidney injury the most common causes are ischemic and septic acute tubular necrosis (Maarten W. Taal, 2012). Postrenal azotemia is a

consequence of either ureteric obstruction or bladder or urethral occlusion (Mustonen et al., 2001).

In pathological aspects, AKI shows tubular apoptosis and necrosis (Liu and Brakeman, 2008), glomerular misfiltration, tubular obstruction, interstitial nephritis and activation of proteolytic enzymes (L.C. Racusen, WB Saunders, Philadelphia, 2001).

The failure to replace the injured cells with functional tubular cells results in the progression towards tubule-interstitial fibrosis, scarring, often leading to chronic kidney injury.

Chronic kidney disease results when kidney damage (i.e., albuminuria) or decreased kidney function (i.e., glomerular filtration rate [GFR] <60 ml/min per 1·73 m²) occur for longer than 3 months irrespectively of clinical diagnosis (Foundation, 2002).

Five stages of CKD are described based on GFR measurements: more than 90 ml/min per 1·73 m²(stage 1), 60–89 ml/min per 1·73 m² (stage 2), 30–59 ml/min per 1·73 m² (stage 3), 15–29 ml/min per 1·73 m² (stage 4), and less than 15 ml/min per 1·73 m² (stage 5) (Table 1-3).

CKD can also result from focal causes (e.g. dysplasia) or from systemic disease (e.g. diabetes mellitus) (UK Renal Registry 14th Annual Report). The primary aetiology of CKD differs between children and adults. In the UK, CKD in children is predominantly caused by renal dysplasia and reflux nephropathy (32.6%) and by obstructive uropathy (17.3%) (Winyard and Price, 2013)

CKD is estimated to affect 11% of the adult population in Western countries (Szczech and Lazar, 2004). In the UK, 870 children under 18 years are affected by the most severe stage of chronic kidney disease, CKD5 (Winyard and Price, 2013).

Acute kidney injury and chronic kidney disease are closely interconnected being chronic kidney disease a risk factor for acute kidney injury and acute kidney injury a risk factor for chronic kidney disease development (Chawla et al., 2014).

Life-long dialysis is the only available treatment for AKI and CKD. although this replaces kidney filtration function by removing toxins from the blood circulation, it never fully replaces all the function of the organ, such as production of erythropoietin.

There is a urgent need to regenerate diseased kidneys in AKI and CKD with functional renal cells able to participate in the repair of renal tissue (Bussolati et al., 2009).

It has been proposed that cell-based approaches may represent a promising alternative to the current treatment options available.

When AKI and CKD develop into severe states, called end-stage renal disease (ESRD), the only treatment is the kidney transplant. However organ transplantation is also not without complication, requires life-long immunosuppression, and is restricted to the shortage of donor organs (Daar, 2006). The scarcity of donor kidneys is the most significant concern being their availability less than one-fifth of the demand (Benigni et al., 2010).

Tissue engineering and regenerative medicine are currently tackling this issue looking for the development of engineered functional kidneys, constructed with scaffolding systems made of biomaterials, living cells and growth factors/cytokines to direct cellular migration, proliferation, and differentiation, as well as to maintain specific cell-type phenotypes (Moon et al., 2016).

Table 1-3 Definition and stages of Acute Kidney Injury

RIFLE and Acute Kidney Injury Network (AKIN) **Definition and Staging of Acute Kidney Injury**				
RIFLE An increase in serum creatinine of ≥50% developing over <7 days or A urine output of <0.5 ml/kg/hr for >6 hr		AKIN An increase in serum creatinine of ≥0.3 mg/dl or ≥50% developing over <48 hr or A urine output of <0.5 ml/kg/hr for >6 hr		
Staging criteria				
RIFLE STAGE	INCREASE IN SERUM CREATININE	URINE OUTPUT CRITERIA	INCREASE IN SERUME CREATININE	AKIN STAGE
Risk	≥50%	<0.5 ml/kg/hr for >6 hr	≥0.3 mg/dl or ≥50%	Stage 1
Injury	≥100%	<0.5 ml/kg/hr for >12 hr	≥100%	Stage 2
Failure	≥200%	<0.5 ml/kg/hr for >24 hr or anuria for <12 hr	≥100%	Stage 3
Loss	Need for renal replacement therapy for >4 wk			
End Stage	Need for renal replacement therapy for >3 mo			

Table 1-4. Stages of Chronic Kidney Disease

Stage	Description	GFR (ml/min/1.73m^2)
1	Kidney damage with normal or increased GFR	≥90
2	Kidney damage with mild decreased of GFR	60-89
3	Moderate decrease in GFR	30-59
4	Severe decrease in GFR	15-29
5	Kidney failure (previously usually referred to as end-stage kidney disease)	<15 (or dialysis)

1.7 Stem cell therapies for kidney injury

The goal of regenerative medicine applied to nephrology, is to establish an effective cell-based therapy approach to support renal repair or to replenish a cell type in the damaged kidney, reducing the need for long term dialysis therapy or kidney replacement. In recent years, several stem cell-based approaches for regeneration have emerged. These approaches rely on stem cells of renal or not renal derivation.

1.7.1 *Renal stem/progenitor cells from adult kidneys*

CD24 and CD133 are among the surface markers utilised to sort out the stem/progenitor cell population in human kidneys,

$CD24^+CD133^+$ cells were isolated from normal adult human kidneys, these showed self-renewal potential and cloning efficiency and multi-differentiation potential, being able to express phenotypic characteristics of podocytes, proximal and distal tubule cells when treated in specific differentiation medium. The therapeutic effects of $CD24^+CD133^+$ have been tested in mouse model of rhabdomyolysis-induced acute renal failure by intramuscular injection with hypertonic glycerol. This cell population show significant improvement of the injury with engraftment into tubules thus participating at the regeneration of nephron compartments (Sagrinati et al., 2006, Ronconi et al., 2009a).

Supporting these studies, Bussolati et al. demonstrated that $CD133^+$ cells isolated from adult kidneys possess stem cells features, such as self-renewal and multi-lineage differentiation both *in vitro* and *in vivo*. Renoprotective effects upon injury were evaluated as following: $CD133^+$ renal progenitors isolated from the inner medullary papilla were tested in a model of acute kidney injury-induced by glycerol and their effects were also compared to mesenchymal stem cells (MSCs). The effects observed, in terms of renal function, were comparable among the two cell lines, whereas the biodistribution was different. Both cell lines were labelled and tracked upon injection in the tail vein using optical imaging. $CD133^+$ accumulated mainly within the renal interstitium of the kidney, whereas MSCs were detected not only in the kidney but also in extrarenal sites, such as lungs, spleen and liver. These observations were also confirmed with immunohistochemical data suggesting that $CD133^+$ from the inner medulla ameliorated the kidney function through the involvement of paracrine mechanisms, as already described for MSCs.

1.7.2 *Renal stem/progenitor cells from fetal kidneys*

Developing fetal kidneys are the site of active organogenesis, hence the presence of stem/progenitor cells is certain (Slack, 2008). Unfortunately, there are ethical concerns with sourcing human kidney stem/progenitor cells along with low availability of fetal organs. Moreover, another challenge arises when maintaining human nephron progenitor cells outside their niche; a well-defined culture medium is needed to enable cell expansion into clinically relevant numbers (Pleniceanu et al., 2010).

Recently, the increased research on the factors influencing nephron progenitors in the stem cells niche, has triggered the research on re-recreating an *in vitro* niche for nephron progenitors that is becoming possible in mouse cells (Brown et al., 2015, Tanigawa and Perantoni, 2016). However, the same results are difficult to be obtained with human nephron progenitors due to the difficulties in the isolation of the pure population of interest with the use of surface cell markers.

CD24 and CD133 markers can also be used to isolate fetal progenitor cells. Generated double positive cells were tested in mice after glycerol-induced acute renal failure, at the peak of blood urea nitrogen, which occur three days after glycerol injection. The mice group administered with the cells show significantly decrease of the blood urea nitrogen levels and less necrosis compared with the saline group (Lazzeri et al., 2007).

1.7.3 *NCAM1$^+$ cells*

By comparison of expression of human fetal kidney, the pediatric kidney cancer Wilms tumour, which is enriched for metanephric mesenchymal progenitors and adult kidneys, another surface marker, the neural cell adhesion molecule 1 (NCAM1) is observed to target normal and malignant renal progenitor cells (Metsuyanim et al., 2009, Pode-Shakked et al., 2009, Buzhor et al., 2013).

NCAM1 expression in human fetal kidneys was analysed and compared to CD133. While NCAM1 is seen in the cortical stroma, cap mesenchyme and early post-MET structures (comma and S-shaped bodies), as well as immature tubules and interstitium, CD133 expression is more specific to nephron related cells, seen in early post-MET structures and in more mature epithelial tubules, however it is excluded from the cap mesenchyme (Pode-Shakked et al., 2016). Co-localisation of NCAM1 and CD133 is observed in early epithelial structures derived from cap mesenchyme and in immature tubules.

1.7.4 *ALDH$^+$ cells*

Lindgren et al. used the high activity of aldehyde dehydrogenase (ALDH) as a marker for isolation of progenitor cells from adult human renal cortical tissue (Lindgren et al., 2011). ALDH$^+$ cells are scattered along the proximal tubules, express CD24 and CD133 and form long rows in tubules of kidneys regenerating from acute tubular necrosis. These and gene expression profile data led to the interpretation of this cell population as transit amplifying tubular progenitors.

1.7.5 *Endogenous adult renal stem/progenitors or dedifferentiated cells?*

Different groups have hypothesised that no progenitor cells exist in the renal tissue after birth and that any regeneration following mild to moderate kidney injury occurs from surviving tubular cells.

Smeets et al. observed that scattered tubular cell population CD24$^+$CD133$^+$ do not show expression of lineage markers and increase following injury in human acute tubular necrosis biopsies, the same cell population show upregulation of injury markers Kidney injury molecule-1 (KIM-1) and vimentin. In healthy rat kidneys, vimentin positive cells are addressed as the same proximal tubular cell population that in human is characterised by CD24$^+$CD133$^+$ expression. Since these only appear after kidney injury, it was

suggested that these cells reflect individual cells undergoing transient dedifferentiation after injury (Smeets et al., 2013).

To further challenge the existence of a residing progenitor cell population in adult kidneys, the Humphreys group used a genetically modified mouse in which differentiated proximal renal tubules were labelled in red colour because of the knock-in of a red fluorescence protein coding gene under the control of the sodium-phosphorus co-transporter (SLC34a1) locus, which is expressed on terminally differentiated proximal tubular epithelial cells only (Kusaba et al., 2014, Madjdpour et al., 2004). Upon injury labelled cells proliferated expressing dedifferentiation markers as well as CD24 and CD133. These findings imply that renal tubules dedifferentiated with consequent re-expression of stem cell markers during their proliferation and participation in the repair of renal tubules thus not supporting the evidence of intratubular stem/progenitor cell population (Kusaba et al., 2014).

In conclusion, there is a controversy whether stem/progenitor cells exist in adult kidneys. Some believe that there is no such thing as an adult renal stem cell population but only dedifferentiated renal cells that can re-enter cell cycle, proliferate, differentiate restoring the renal epithelium after injury. Others believe that stem cells residual of the embryonic population exist in adult kidneys, with their niche being present in parietal epithelium, scattered along tubules and even in the interstitium.

It is challenging to distinguish putative adult renal progenitor/stem cells from dedifferentiated renal epithelial cells as we lack knowledge on specific markers exclusively expressed in one of these populations, it is therefore a still unresolved matter whether human renal stem cells exist after birth.

1.7.6 *Extra renal stem/progenitor cell lineages*

1.7.6.1 Mesenchymal Stem Cells

Being bone marrow-derived mesenchymal stem cells a well-known cell type and the most advanced in clinical development, several studies tested these cells in murine models of acute and chronic kidney disease (Togel et al., 2005).

A meta-analysis of these studies demonstrated that MSCs administration significantly improve kidney function, however, when injected intravenously, few cells home to the kidneys, the majority being sequestered in the lungs (Wang et al., 2013).

MSCs protective effects could be attributed to non-cellular mechanisms, given that acute kidney injury decreases upon administration of MSCs conditioned medium or MSCs derived exosomes without the need of the whole cell (Milwid et al., 2012, Zhou et al., 2013). Factors released by MSCs could potentially work by reducing oxidative stress and cell apoptosis and by promoting survivor renal cells proliferation. Another mechanism proposed is the MSC-mediated modulation of the immune system, as it has been observed that MSCs are able to regulate T cells. In a study on ischemic acute kidney injury, MSCs attenuated renal injury by inducing regulatory T cells in the spleen and this effect was abrogated after splenectomy or depletion of regulatory T cells (Hu et al., 2013).

These and many more studies using MSCs in models of acute renal injury prompted the interest towards the clinical application of such cells, mainly for their immunomodulatory role, with the goal to use them to ameliorate treated graft-vs-host disease.

Autologous MSCs administered in a clinical trial to patients that had undergone renal transplantation (Tan et al., 2012), showed reduction of transplant rejection, improvement in renal function at 1 year and decrease risk of opportunistic infections, compared with conventional induction therapy with anti-IL-2 receptor antibody. Although these results are promising, it has to be demonstrated the long-term efficacy of MSCs infusion or any adverse side effect.

MSCs have been generally isolated from the bone marrow, however they reside in many adult tissues and their existence was also observed in the adult murine kidney where they showed gene and protein expression characteristic of MSCs (Pelekanos et al., 2012).

1.7.6.2 Renal progenitors from amniotic fluid

Another source of renal progenitor cells is the amniotic fluid. Cells isolated from the amniotic fluid collected between 12 and 18 weeks of gestation display long term self-renewal *in vitro* and integrate into mouse embryonic kidneys *in vivo* (Perin et al., 2007). Amniotic fluid stem cells are used in a model of human Alport syndrome, characterised by progressive glomerulonephritis with proteinuria leading to end stage renal disease. In this model, intracardiac administration of amniotic fluid stem cells before the onset of proteinuria significantly delay interstitial fibrosis prolonging animal survival (Sedrakyan et al., 2012). This type of cells may also represent a valuable source of progenitor cells with renal potential.

1.7.6.3 Renal progenitors from iPSC

In recent years regenerative medicine has been revolutionised by the generation of induced pluripotent stem cells. First in mouse and then in human, it was demonstrated that any somatic cells can be reverted to pluripotency, a condition equivalent to an embryonic stem cell (Takahashi et al., 2007, Takahashi and Yamanaka, 2006).
This is possible with induction of critical transcription factors, *OCT3/4, SOX2, c-MYC* and *KLF4.*The overexpression of these factors induces the formation of stem cell colonies that can be cultured and expanded. Being equals to embryonic stem cells, these cells have their same potential in terms of self-renewal and multilineage differentiation while overcoming ethical issues raised using embryonic stem cells. In addition, they offer the advantage of being an autologous source of cells.
Induced pluripotent stem cells have been generated from differentiated renal cells such as adult human proximal tubule cells (Montserrat et al., 2012) and renal cells excreted from urine (Zhou et al., 2012).
Different reprogramming factors are also used to generate iPSCs. Hendry *et al.,*(Hendry et al., 2013) generated nephron progenitor/stem cells from adult human proximal tubule cell lines (HK2) through overexpression of *SIX1, SIX2, OSR1, HOXA11, EYA1, SNAI2* with lentiviruses. This results in up-regulation of cap mesenchyme markers such as *CITED1* and down-regulation of epithelial markers such as *E-Cadherin*; moreover, the cells contribute to the cap mesenchyme in a reconstitution organoid assay (Chang and Davies, 2012, Xinaris et al., 2012).
A problem that might arise with generating iPSC is the necessity to use lenti- or retro-virus vectors to transfect the cells with each gene of interest. Unwanted effects can include

non-specific integration with potential oncogenic consequences. In addition, problems might arise when differentiation into unwanted lineages of pluripotent stem cells take place.

Studies to overcome these drawbacks focused on the use of alternative non-integration methods that but, thus far, these show a very low reprogramming efficiency (Morales and Wingert, 2014).

1.8 Pre-clinical studies on stem cells therapeutic effects on acute and chronic kidney injury

The translation on the clinical practice of stem cells based therapies requires pre-clinical studies to examine the feasibility, efficacy and safety of this possible therapy. Different animal models have therefore been used to test the potential of renal progenitor cells.

$CD133^+$ cells isolated from adult human kidneys were evaluated for their ability to localise to injured kidneys in a model of acute tubular injury caused by intramuscular injection of glycerol in SCID mice. A million of cells were injected intravenously in untreated or treated animals at the peak of renal injury, generally three days after glycerol injection. Human cells, expressing the human HLA class I protein were observed in proximal and distal tubules of the injured kidneys three days after cells injection, whereas control SCID mice without renal injury showed only a minimal cell localisation (Bussolati et al., 2005). Similar results were obtained with the same injury model by Romagnani's group, which tested the potential of fetal $CD24^+CD133^+$ in the acute renal injury, showing the ability of this population to improve altered renal function, assessed by BUN measurement, and to integrate in the regenerated tubules. Other experiments of progenitor cells homing to diseased kidneys were performed by the group of Prof. Dekel (Buzhor et al., 2013). Also in this work, glycerol was used to induce the acute renal injury in NOD-SCID mice. $NCAM1^+$ cells injected in the tail vein 2 hours after glycerol administration were detected in the kidney within the first 24 hours but decreased by day 3. Moreover, these cells did not show exclusive tropism for injured kidneys since they were also observed at high amounts in the lungs. However. BUN and creatinine levels, chosen to assess renal injury progression, were reduced in treated animals compared to saline-treated controls. The same group sought to test the therapeutic effects of such progenitor cells in the 5/6 kidney nephrectomy model of chronic renal injury (Harari-Steinberg et al., 2013). Half a million of cells were directly injected in the parenchyma of the remnant kidney a week after the nephrectomy for 3 weeks. At 12 weeks, a significant improvement in renal function was assessed in the treated group. Moreover, progenitor cells appeared to have integrated, to a certain extent, into the endogenous mouse tissue, thus suggesting a regeneration capacity of injured kidney.

To study therapeutic effects of human progenitor cells, I have used a model of acute kidney injury (AKI) caused by folic acid.

Folate is a component of the vitamin B complex playing essential roles in several metabolic processes such as DNA synthesis, repair and methylation (Nazki et al., 2014). It is known that high concentrations of folic acid (FA), i.e. > 100 mg/kg lead to transient acute nephrotoxicity with morphological and functional abnormalities proportional to the dose administered in murine models (Long et al., 2008, Schmidt et al., 1973, Klingler et al., 1980) while an association between folic acid and AKI in human diseases has not been observed. High doses of folic acid damage renal tubular epithelium in particular the proximal tubule with accumulation of folic acid crystals in the tubular lumen resulting in interstitial connective tissue proliferation, increased kidney weight and oliguria (Fink et al., 1987, Klingler et al., 1980, Witzgall et al., 1994). FA crystals obstruct renal tubules leading to tubular necrosis (Bosch et al., 1993, Byrnes et al., 1972, Schmidt et al., 1973). Tubular epithelium rapidly regenerates after FA induced injury but some atrophic and fibrotic areas persist after tubular regeneration has occurred (Long et al., 2001). The pathogenesis of AKI in this model is complex involving an intricate interplay of factors and is not merely attributed to the FA crystal accumulation. This was first observed by Fink et al., who demonstrated that decreased folic acid tubular deposition secondary to FA co-administration with $NaHCO_3$ leads to a less severe nephrotoxic phenotype but interestingly lesions still occur in proximal tubule cells (Fink et al., 1987). Many studies sought to characterise the features and molecular mechanisms involved in FA-dependent renal injury demonstrating a sequence of events, comprising an acute phase, usually occurring 1 or 2 days after administration rapidly followed by tubular cell regeneration and functional recovery that is incomplete and results in a chronic phase characterised by mild fibrosis. Soon after its administration, folic acid enhanced tubular cell apoptosis is observed by modulation of Bcl2 members expression, release of lethal factors such as tumour necrosis factor-α (TNF-α) and expression of genes promoting cell-death such as c-Myc (Ortiz et al., 2000). Mitochondrial biogenesis is down regulated by day 2 and can be seen until day 14. Increased expression of early fibrosis markers such as TGF-β_1 and α-SMA is observed from day 6 onwards (Stallons et al., 2014). Inflammatory injury is evident with infiltration of ROS-producing neutrophils around damaged tubules and consequent macrophage infiltration and interstitial fibrosis (Doi et al., 2006). Morphological and functional recovery observed in kidney after FA-induced injury arises from surviving renal epithelial cells that de-differentiate to an immature state, migrate to the site of cell loss and differentiate (Humphreys et al., 2008). FA is chosen as a good model to investigate the molecular mechanisms involved in renal regeneration. Several

studies have shown that FA dependent kidney damage occurs with transient up-regulation of *Pax2*, *vimentin* and *NCAM*, genes usually involved in the embryonic development and downregulated in mature kidneys (Imgrund et al., 1999, He et al., 2013) It has also been shown that renal tubule cells dedifferentiation and proliferation requires epidermal growth factor receptor (EGFR) and is impaired by its inhibition (He et al., 2013). A recent study suggests also a role for histone deacetylases (HDACs) activation in renal regeneration. It is demonstrated that renal epithelial cells require HDACs to proliferate after AKI induced by either folic acid or rhabdomyolysis, indeed class I HDACs inhibition increases tubular damage, cell apoptosis and impair tubular cell dedifferentiation and proliferation (Tang et al., 2014).

Considering that both acute and chronic injuries occur in the FA model, and that characteristics of FA-induced AKI resemble human AKI, this model can be used to study both AKI and CKD mechanisms and regenerative approaches including stem cell-based therapies. Different studies have tested the capacity of non-renal stem cells to improve renal function in this murine model of acute injury.

Human umbilical cord-derived mesenchymal stem cells (hUC-MSCs) has been proposed as a source of stem cells and their capacity of improving renal function in non-obese diabetic-severe combined immune deficiency (NOD-SCID) mice suffering from acute kidney injury has been tested (Fang et al., 2012). Injection of folic acid (250 mg/kg body weight) causes renal tubule damage, as expected, and this is observed after 24 hours from folic acid administration. Serum urea nitrogen (SUN), serum creatinine (SCr) and tubular injury scores, measured at different time points, show increased levels after 24 hours with peaks at day 3, decrease after 7 days and return to baseline levels by day 14. In the study is shown that hUC-MSCs injections improve renal function assessed by tubular injury score and reduced levels of BUN and SCr. These beneficial effects seem to be exerted not by engrafted and differentiated hUC-MSCs but rather by hUC-MSCs secretion of factors that increase proliferation and decrease apoptosis of renal tubular (Fang et al., 2012). Another study exploited the capacity of human adipose tissue-derived stromal cells (hASCs) cultured in low serum (2%) to improve AKI induced in immunodeficient rats by intravenous injection of folic acid at the dose of 200mg/kg. After administration of hASCs into the renal subcapsule, renal damage provoked by folic acid is significantly decreased. Renal function, measured with BUN and serum creatinine is markedly lower in rats that received administration of hASCs compared to the controls. Also, tubular injury, macrophage infiltration and fibrosis are improved after hASCs administration.

Intravenous injection of the same cells or subcapsular injection of human bone marrow derived stromal cells does not improve acute renal damage. This renoprotective capacity is seen to reside in paracrine effects, in the secretion of HGF from hLASC.

As suggested by these studies, extra renal stem cells can improve renal function in AKI induced by folic acid by paracrine effects rather than engraftment and trans-differentiation in renal cells. The folic acid model represents a good model to exploit the tubular regeneration mechanisms following AKI and the factors involved in this process.

1.9 Hypothesis and aims

Fetal kidney hosts a heterogeneous population of stem/progenitor cells within the cap mesenchyme. Many of the transcription factors specifying these cells are known, however approaches aiming at the isolation of these cells alive and their subsequent *in vitro* culture require the targeting of molecules expressed on the cell surface.

The research for such molecules brought us to detection of CD24 and CD133, two surface markers found to be expressed by putative kidney stem/progenitor cells in adult and fetal kidneys.

I hypothesised that early stages of fetal kidneys contained a stem/progenitor cell population that could be isolated by CD24 and CD133 markers. The aims of my work were the following:

- the assessment of CD24 and CD133 protein localisation in sections of human fetal kidneys.
- the isolation of $CD24^{+}CD133^{+}$ cells from human fetal kidneys. Differently from published data, the goal was not to obtain these cells from freshly collected kidneys of different gestational age pooled together. Progenitor cells were isolated from kidneys of 9 weeks of gestation after culture. FACS sorting was used for the isolation of $CD24^{+}CD133^{+}$ cells, differently from previous experiments that used Magnetic Activated Cell Sorting.
- the accurate characterisation of $CD24^{+}CD133^{+}$ in terms of:
    - RNA expression profile of generated cell lines at different passages in culture: for the first time, the expression of general developmental markers was not limited to the freshly isolated cells but was determined over different passages in culture.
    - Capacity to differentiate towards renal epithelium lineages and extra-renal lineages (osteocytes and adipocytes), as well as assessment of nephrogenic potential with the use of a novel *ex vivo* assay.
    - Evaluation of renal regenerative potential in a murine model of Folic acid-induced kidney failure, localising the intravenously-injected cell lines upon kidney injury with the use of bioluminescence imaging *in vivo.*

2 MATERIALS AND METHODS

2.1 Kidney Histology

2.1.1 *Human Fetal Kidney Collection*

Fetal kidneys were collected from the MRC-Wellcome Trust Human Developmental Biology Resource (HDBR) based at the UCL Institute of Child Health, London, and *the Ins*titute of Human Genetics, Newcastle Upon Tyne. Tissues were donated entirely voluntarily through written consent forms by women undergoing termination of pregnancy. The type of termination of pregnancy depended on patient choice. This project was registered with HDBR which is a licensed tissue bank by the Human Tissue Authority. Material collected ranged from 7 to 20 weeks of gestation.

2.1.2 *Preparation of histological samples*

Intact human fetal kidneys were fixed in a solution of 4% paraformaldehyde in phosphate buffer saline (4% PFA in 1x PBS, Sigma-Aldrich, Dorset, UK) at room temperature. Kidneys of 9 to 11 weeks of gestation were fixed for up to 2 hours while samples ranging from 12 to 20 weeks of gestation were fixed for 3 to 4 hours.

BALB/c wild type, nudes, SCID and NOD-SCID mice were euthanised by Schedule 1 methods. Following washes with PBS, kidneys were cut in half longitudinally and fixed in 4% PFA in PBS for up to 2 hours at room temperature or overnight at 4°C.

For paraffin embedding, samples were placed in a series of solutions for one hour each. First, they were dehydrated through increasing ethanol concentration (70%, 80%, 90% and twice in 100% ethanol) then cleared twice in Histoclear (Histolcear II, National Diagnostics, Atlanta, GA), and immersed in a 1:1 solution of Histoclear and paraffin wax and finally twice in paraffin only. When kidneys were fully wax-permeated, they were embedded in wax blocks. 5 μm sections were cut using a microtome, transferred to a heated water bath to stretch and straighten the section before being transferred onto glass microscope slides (SuperFrost Plus microscope slides, VWR, Leicestershire, UK).

For frozen embedding, samples were placed into a 30% sucrose solution in 1x PBS overnight at 4°C allowed to be completely infiltrated. This displaced some of the water content to help protect the tissue morphology during freezing.
Excess of sucrose was cleansed by pressing the kidney on a piece of absorbent paper. Sample was placed on dry ice in a cryomold covered with O.C.T. (VWR, Leicestershire, UK) 5 μm sections were cut using a cryostat at -20°C and picked up using a warm microscope slide Slides were stored in the -20°C freezer.

2.1.3 *PAS staining*

In this thesis, histology using the periodic acid Schiff (PAS) stain with haematoxylin was used for the following purposes:

- to characterise the developing renal structures in the human fetal kidney
- to highlight folic-acid induced renal damage in the murine kidney.

PAS is a method used to highlights carbohydrates. When treated with periodic acid, glucose is oxidized to aldehydes, which are then stained magenta in a second reaction with Schiff reagent. PAS highlights basement membrane of glomeruli and the brush borders of the proximal tubules which are high in carbohydrates, these appear bright pink under the light microscope (Longley and Fisher, 1954).
5 μm sections cut from paraffin-embedded kidneys were deparaffinised by heating at 70°C for 10 minutes. Wax was cleared through two 5-minute immersions in Histoclear. The tissue was then rehydrated by submerging in graded series of alcohol starting with 100% ethanol twice, followed by 90%, 80% and 70% for one minute, finishing in running tap water. Rehydrated slides were placed in Periodic acid (Sigma) for five minutes, then incubated in Schiff reagent for fifteen minutes with five-minute running water washes after each step. Slides were then counterstained with hematoxylin, dehydrated by reversing the alcohol graduation above, cleared in Histoclear and mounted with 22x22 glass coverslips in Histomount (National Diagnostics, Atlanta, GA). The Histomount was allowed to set before slides were visualised under a light microscope or stored at room temperature.

2.1.4 *Paraffin sections immunohistochemistry*

5 μm slides cut from paraffin embedded kidneys were de-paraffinised and re-hydrated through Histoclear and dilutions of alcohol as described above for PAS, ending in running

water. Antigen retrieval was then performed to allow access to the antigen. Three methods were used:

- Microwave with citric acid. Citric acid (Sigma-Aldrich, Dorset, UK) was prepared by dissolving citric acid powder to a concentration of 10 mM in 1 litre of deionised water adding 22 ml of 0.2 M hydrochloric acid. The buffer was brought up to boil in a microwave for 10 minutes before the slides were added for a further 15 minutes. After cooling at room temperature for 20 minutes, the slides were washed in running water.
- Digestion with Trypsin. A 1 mg/ml solution of trypsin (Sigma-Aldrich, Dorset, UK) prepared from tablet was added onto the slides and incubated for 15 minutes at 37°C. Then washed away with running water.
- Digestion with proteinase K. Proteinase K solution of 20 µg/ml (Sigma-Aldrich, Dorset, UK) was prepared by dissolving 1 ml of 20x of proteinase K stock solution in 20 ml of TE Buffer (50mM Tris Base, 1mM EDTA, 0.5% Triton X-100, pH 8.0) Sections were incubated 10 minutes at 37°C in humidified chamber.

To quench any endogenous peroxidase present in the tissue and thus preventing background staining, slides were incubated in 1.6% hydrogen peroxide in 1x PBS for 15 minutes and rinsed in PBS-Tween 20 (0.1%). To prevent primary or secondary antibodies binding to non-specific sites the tissue was blocked in a protein solution for 1 hour. Block solution was made of 10% FCS, 2% BSA and 0.1% Tween-20 in 1x PBS. This block was made in advance and stored in the -20°C freezer and then defrosted when required. The primary antibodies, diluted in block, were applied and incubated at 4°C overnight in a humidified chamber. Preliminary experiments were performed to identify the ideal antibody dilution.

The next day, primary antibody was washed away with PBS-Tween-20 (0.1%) three times for five minutes each. The appropriate secondary antibody was added to the section for one hour at room temperature usually diluted in block (1:250). The secondary antibodies were either conjugated to HRP or to fluorochromes, a complete list of primary antibodies can be found in Table 2-1.

2.1.5 *Enzymatic detection*

For enzymatic detection, secondary antibodies were conjugated with HRP. DAB (SIGMAFAST™ 3,3′-Diaminobenzidine tablets, Sigma-Aldrich) was prepared from tablets and applied to the tissue. Colour development was detected by light microscopy

and terminated by placing the slides in distilled water when a brown colour developed. Sections were counterstained so that cellular structures of the kidney could be seen. Haematoxylin, which stains the nuclei dark purple, was used as the counterstain. This was achieved by incubating with haematoxylin for 2 minutes before washing under running water. Slides were dehydrated from water to 70% ethanol, and sequentially through to 100% ethanol. Slides finally underwent two 5-minute washes in Histoclear, before being mounted in Histomount and covered in glass cover slips. Once the mount had dried, slides were stored at room temperature before observation under light microscopy.

2.1.6 *Fluorescent detection*

Immunofluorescence staining was performed with the same antigen retrieval as for enzymatic detection. However, peroxidase blocking was omitted and sections were permeabilised with PBS-0.1% Triton X-100 for 10 minutes before blocking 10% BSA and 0.1% Tween-20 in 1xPBS for 1 hour and incubating with the appropriate primary antibody. If a second step was required, a secondary antibody conjugated to a fluorophore was added.

The secondary antibody was diluted to the concentration recommended by the manufacturer in block solution and applied to the slides for 1 hour in a humidified chamber. Autofluorescence was quenched by incubating slides in Sudan Black dissolved in 70% ethanol for 10 minutes. This helped to reduce the natural background fluorescence of the tissue. Nuclei were counterstained with 15 µg/ml Hoechst (Hoechst 33342, trihydrochloride, trihydrate, Thermo Fisher Scientific. UK) diluted in 1x PBS.

Glass cover slips were sealed to the slide using Cytoseal-60 and stored at 4°C and imaged using fluorescent microscopy.

2.1.7 *Frozen sections immunofluorescence*

Frozen tissue slides were placed into PBS-Triton X100 (0.3%) for 2 hours to permeabilise the tissue. Antibodies were then diluted in block solution composed of 0.3% Triton X-100, 0.2% BSA and 0.1% sodium azide dissolved in 1x PBS, and incubated for two hours in a humidified chamber at room temperature, 10% normal serum of the species in which the secondary antibodies were raised, was added to the block prior to use. Slides were then washed in PBS-Triton X-100 (0.3%) three times for ten minutes each. To better preserve the fluorophores, the slides were fixed in 1% PFA for five minutes followed by more washes in 1x PBS. Autofluorescence was quenched using 0.1% Sudan black dissolved in 70% ethanol. Sections were then counterstained with Hoechst.

2.1.8 *Double labelling*

Double labelling was used to visualise two antibodies on the same section. I made sure that the species of the antibodies did not clash. For example, when co-staining CD24 and CD133, CD133/2 antibody was made in mouse and the CD24 was made in rabbit, with the secondary antibodies made in goat and donkey respectively, allowing for double labelling. Preliminary experiments were performed to determine the optimal concentration of each antibody before sections were stained using the frozen section immunohistochemistry method described above.

2.1.9 *CD24 and CD133 staining optimisation*

For CD24 immunostaining, an anti-human CD24 rabbit polyclonal (Abcam, ref. ab110448) was tested.

CD24 expression was analysed by immunohistochemistry on paraffin embedded kidney sections of 11 and 20 weeks of gestation. Antigen retrieval method consisted of microwaving in citric acid. The staining was visualised with DAB.

Various antibody dilutions were tested. Since CD24 immunostaining, compared to negative control, appeared always dimly positive, also immunofluorescence staining was performed. Paraffin or frozen embedded sections were tested, however the staining observed was in all cases faint.

Published work from Lazzeri et al., showed specific staining of CD24 marker on fetal kidneys using a CD24-FITC conjugated (SN3) from Santa Cruz Biotechnology (Lazzeri et al., 2007).

Hence, CD24-FITC staining was tested and optimised by immunofluorescence on frozen embedded sections yielding positive results.

Immunodetection of CD133 was performed on frozen sections using the antibody against the epitope CD133/2 expressed only in immature cells. Immunodetection of CD133, as for CD24, was particularly challenging. Indeed, immunostaining was performed, according to manufacturer's suggestions, on wax embedded sections, boiling slides for 15 minutes in 0.01M sodium citrate buffer using a microwave oven to retrieve the antigen however the resulting staining was inefficient. Literature data (Bussolati et al., 2005) suggested that CD133 is positively detected on frozen sections. As all the samples collected before and at the beginning of my PhD project were embedded on wax, I waited for new human fetal kidneys collections from HDBR, fixed and embedded kidneys for frozen sections. I then proceed with CD133 immunostaining. When tested on frozen sections, the dilution 1:10 of the antibody produced positive results.

2.1.10 *Immunocytochemistry*

$2x10^4$ cells were usually plated in 4-well chamber slides (Millipore, UK) one day prior to staining. Cells were then fixed with 4% PFA dissolved in 1x PBS for 15 minutes at room temperature. After gently washes in PBS for three times, wells were covered in blocking solution as described for immunohistochemistry procedure on paraffin embedded sections. Cell were incubated in a humidified chamber, 1 hour at room temperature. After that, cells were gently washed three times with PBS and the diluted primary antibody was added overnight at 4°C.

The following day, washes were performed to remove the unbound primary antibody. Secondary fluorophore-conjugated antibody was applied and incubated in the dark for one hour at room temperature. After this time, unbound secondary antibody was washed and nuclei were counterstained using Hoechst (Life Technologies, UK). Coverslips were mounted using anti-fade mounting (SlowFade Gold, Life Technologies, UK). The edges of the coverglass were sealed with nail polish. Slides were allowed to dry for 2 hours before visualising. If not visualised on the same day, slides were stored at 4°C protected from light.

2.1.11 *Negative controls*

Negative controls were used to ensure that the positive staining observed was attributed to the specific antibody binding. In my thesis, negative controls were performed by omitting the primary antibody and substituting for the same volume of block.

2.1.12 *Microscopy*

I used several microscopes to observe and photograph my samples. For light microscopy, an Axiophot 2 upright microscope (Carl Zeiss, Oberkochen, Germany) was used. This was useful to visualise histology by PAS but also for immunohistochemistry on paraffin-embedded sections using the enzymatic method as a way to detect antigen location. Pictures were taken using a Axiocam HRc mounted on the microscope (Carl Zeiss). The Axiophot 2 has objective lenses at 5x, 10x, 20, 40, magnification as well as oil immersion lenses at 40x and 63x magnification. Photos were taken using AxioVision Rel. 4.8 software (Carl Zeiss) and exported as TIFF files.

For pictures taken under the fluorescent microscope, an IMAGER Z1 fluorescent microscope with ApoTome attachment (Carl Zeiss was used with a mounted AxioCam

MRm camera (Carl Zeiss). The IMAGER Z1 has objective lenses at 5x, 10x, 20x magnification as well as oil immersion lenses at 40x, 63x and 100x magnification. The fluorescent microscope has lasers for detection of DAPI, FITC and Alexa Fluor 568. Photos were taken using AxioVision Rel.4.8 software (Carl Zeiss) and exported as TIFF files.

Table 2-1 Primary antibodies used in the project.

Antibody name	Clone	Company	Reactivity and cross-reactivity	Application and working dilution	Immunogen	References
CD24	32D12	Miltenyi Biotec, PE conjugated. 130-095-953	Mouse monoclonal anti-human	FC (1:100)	Generated using the human pre-B lymphoblastic leukaemia cell line Reh.	(Gao et al., 2010)
CD24-FITC	SN3	Santa Cruz Biotechnology	Mouse monoclonal anti-human	IF on frozen sections, ICC (1:10)	Raised against NALM-1 human pre-B leukaemia cell line.	(Angelotti et al., 2012)
CD133/1 pure and APC conjugated	AC133	Miltenyi Biotec APC conjugated 130-090-826	Mouse monoclonal anti-human	FC (1:10)	Generated against the epitope 1 of the CD133 antigen	(Yin et al., 1997)
CD133/2-PE	293C3	Miltenyi Biotec, PE conjugated 130-098-046	Mouse monoclonal anti-human	IF on frozen sections ICC (1:10)	Generated against the epitope 2 of the CD133 antigen	(Yin et al., 1997)
calbindin-D-28K	CB-955	Sigma-Aldrich	Mouse monoclonal anti-human (cross reacts with mouse)	ICC (1:100)	Derived from the CB-955 hybridoma produced by the fusion of mouse myeloma cells and splenocytes from	(Rumballe et al., 2011)

					BALB/c mice immunized with a purified bovine kidney calbindin-D-28K	
CITED1	5H6	Abnova	Mouse monoclonal anti-human	ICC (1:200)	Raised against a partial recombinant CITED1 corresponding to amino acids 94 to 194	(Murphy et al., 2012)
Collagen I		Southern Biotech	Goat polyclonal anti-human type I collagen (cross reacts with murine collagen I)	IHC (1:20) on paraffin sections (proteinase K)	Raised against collagen I	(Long et al., 2001)
Collagen III		SouthernBiotech,	Goat polyclonal anti-human type III collagen (cross reacts with murine collagen III)	IHC (1:20) on paraffin sections (proteinase K)	Raised against collagen III	(Long et al., 2001, Aggarwal et al., 2013)
E-cadherin	36/E-Cadherin	BD Biosciences,	Mouse anti-human and mouse	IC (1:100)	Raised against the peptide immunogen generated from human	(Weng et al., 2002)

					E-Cadherin aa. 735-883.	
F4/80	Cl:A3-1	AbD Serotec	Rat anti-mouse	IHC (1:1000) on paraffin sections (proteinase K)	Raised against Thioglycollate stimulated peritoneal macrophages from C57BL/6 mice	(Kihira et al., 2014)
IgG1-PE, IgG1-APC	IS5-21F5	Miltenyi Biotec	Mouse Isotype antibody	FC	Used as negative control. Specific for KLH (keyhole limpet hemocyanin). Protein not expressed on human cells.	
IgG-FITC		Santa Cruz Biotech,	Mouse anti- mouse IgG	IF (1:10)		(Landsverk et al., 2012)
Lamin A + C	EPR4100	Abcam	Rabbit monoclonal anti-human	IHC on paraffin sections (citric buffer, 1:250)	Raised against a peptide corresponding to amino acids 500 – 600 of human Lamin A + C.	(Roy et al., 2013)

Laminin		Sigma-Aldrich	Rabbit polyclonal anti-mouse (cross reacts with human)	IC (1:1000)	Produced using laminin purified from the basement membrane of Englebreth Holm-Swarm (EHS) mouse sarcoma as the immunogen	(Siegel et al., 2010)
Mitochondria	MTC02	Abcam	Mouse monoclonal anti-human	IF on paraffin sections (citric buffer,1:50)	Recognises a 60 kDa non glycosilated protein component of mitochondria found in human cells	(Kanojia et al., 2013)
PAX2		Zymed Laboratories	Rabbit polyclonal anti-mouse (cross reacts with human)	IC, IF (1:100. Paraffin sections (citric acid) and frozen sections	A GST-Pax-2 fusion protein derived from the C-terminal domain (aa188-385) of the murine Pax-2 protein	(Dressler et al., 1993)
SIX2		Proteintech	Rabbit polyclonal anti-mouse (cross reacts with human)	IC (1:400), IF (1:100) on paraffin sections (citric acid) and frozen	Raised against full length SIX2 of human origin	(Song et al., 2016)

WT1		Acris	Rabbit polyclonal anti-human (cross reacts with mouse)	IC, IF (1:100) on paraffin sections (citric acid) and frozen	Raised against a synthetic peptide derived from the C-terminus of Human Wilm's Tumour protein.	(Yates et al., 2010)

2.1.13 *Secondary Antibodies*

Secondary antibodies were conjugated with HRP or with a fluorochrome. For DAB visualisation on paraffin sections of collagen I, collagen III and F4/80, rabbit anti-goat HRP and rabbit anti-rat HRP (Dako, Cambridgeshire, UK) were added prior to use of Envision+ Kit (Dako, Cambridgeshire, UK). For the other primary antibodies raised in rabbit or mouse, Envision+ Kit was used without an intermediary step.

For fluorescent visualisation, the following secondary antibodies, all purchased from Invitrogen, were used: Alexa Fluor 488 donkey anti-rabbit IgG, Alexa Fluor 488 goat anti-mouse IgG, Alexa Fluor 594 donkey anti-rabbit IgG, Alexa Fluor 594 goat anti-mouse IgG, Alexa Fluor 594 chicken anti-rabbit.

2.2 In-vitro studies

In vitro studies consisted of isolation, maintenance and characterisation of human fetal kidney derived cell lines.

2.2.1 *Isolation of human fetal kidney cells from 'fresh' kidney*

Kidneys collected from HDBR were dissected under sterile conditions. Kidneys were transferred into a 60 mm^2 tissue culture dish (Corning, UK), minced into small pieces, transferred to 1.5 ml tube and digested up to single cell suspension by addition of Trypsin-EDTA 0.25% (2.5 g/L Trypsin and 0.38 g/L EDTA, Gibco, UK) for up to 5 minutes in the incubator at 37°C. After this time, growth medium with FBS was added to neutralise the enzyme digestion and cells were passed in a 15 ml tube through a 70-μm cell strainer. The filtered cell fraction was allowed to go through a new cell strainer, this time a 40-μm. The cell suspension was then centrifuged at 300 x g for 5 minutes. The supernatant was discarded and the cell pellet was resuspended in 1 ml of 1x PBS prior to counting and staining.

2.2.2 *Isolation of human fetal kidney cells from explants*

Fetal kidneys were diced using sterile needles under a cell culture hood. Tissue was cultured in growth medium composed of Dulbecco's modified eagle medium/Hams F12 (1:1) mix (Invitrogen, UK) supplemented with 5% fetal bovine serum (FBS, Gibco, UK),

3′,5-Triiodo-l-thyronine sodium salt, 20 μg/μl (Sigma-Aldrich), insulin-transferrin-selenium liquid medium supplement (insulin 25mg, transferrin 25 mg, sodium selenite 25 μg Sigma-Aldrich), 50 μg/ml prostaglandin E1, Dexamethasone 20 μg/ml (Sigma-Aldrich), Holo-Transferrin 10μg/μl (Sigma-Aldrich), penicillin 1000 units/ml (Sigma-Aldrich), streptomycin (1 mg/ml) at 37°C in a 5% CO_2 incubator. When 70% confluent, cells were detached and stained with CD24 and CD133 antibodies prior to flow cytometry analysis or cell sorting.

2.2.3 *Determination of cell number and viability*

Cell number and viability were determined using a haemocytometer Figure 2-1) with Trypan Blue Solution, 0.4% (Thermo Fisher Scientific, UK). This dye does not stain viable cells, while non-viable cells take up the dye appearing dark blue under the microscope light. This is therefore considered a simple method to count live cells. Usually, a 1:2, 1:5 or 1:10 dilution of the cell suspension using and 0.4% Trypan Blue solution was prepared. The suspension was left to stand for 1 minute and 10 μl of Trypan blue-cells were transferred to the haemocytometer.

Using a microscope with a x10 objective, the cells contained in the 4 sets of 16 corner squares were counted. The average cell count from each of the sets was multiplied by 10,000 and by 2, 5 or 10 to correct for the 1:2, 1:5 or 1:0 dilution. The final value obtained was the number of viable cells/ml in the original cell suspension. To calculate viability, also dead cells were counted and added to the live to obtain a total cell count. The live cell count was then divided by the total cell count to calculate the percentage viability.

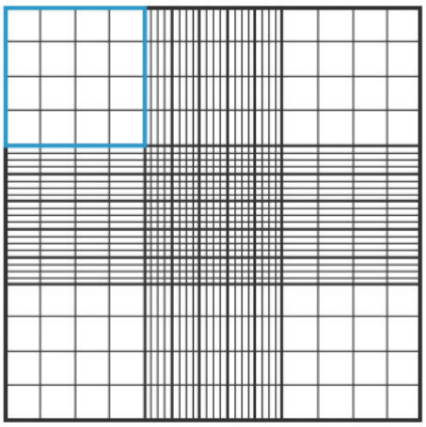

Figure 2-1 Haemocytometer gridlines.

Haemocytometer chamber is composed of nine 1.0 mm x 1.0 mm large squares distinguished from one another by dense triple lines. Each of the larger corner 1mm^2 squares are composed of 16 smaller squares. The central 1mm^2 area is divided into 25 small squares and each of these is furtherly marked into 16 smaller squares.

2.2.4 *Flow cytometry experimental conditions and gating strategy*

Conditions for flow cytometry experiments were tested and proved prior to cell sorting on human fetal kidney cells using previously derived kidney cells stored in liquid nitrogen. These consisted of: choice of primary labelled antibody, antibody staining dilution and cell number, staining buffer, incubation time and temperature and gating strategy to analyse and sort cells both on flow cytometer and off-line on analysis software. To identify CD24 expression I used a mouse IgG1anti-human CD24 antibody (32D12) conjugated to Phycoerythrin (PE), while CD133 was detected with mouse IgG1 anti-human CD133/1 antibody (AC133) conjugated to Allophycocyanin (APC). These were all purchased from Miltenyi Biotec (Germany) and are listed in Table 2-1. PE and APC are fluorochromes that offer good resolution of dim to medium expressed targets.

The optimal antibody dilution was detected testing different dilutions (1:10, 1:50, 1:100 and 1: 200). CD24-PE was used with a dilution of 1:100, while CD133-APC dilution was set to 1:10. Gating strategy for FACS analysis was developed as it follows: a gate was drawn around the whole cell population based on forward-scattered light (FSC) and side scattered light (SSC). Light scattering occurs when a cell deflects incident laser light, the extension of this depends on the physical properties of the cell such as size and internal complexity (e.g. granules inside the cell). Forward-scattered light (FSC) is proportional

to cell-surface area or size while Side-scattered light (SSC) is proportional to cell granularity or internal complexity.

Then, I aimed to exclude cell doublets from the analysis. These may either be the consequence of two cells becoming physically attached to each other or because two cells have passed through the laser beam so close to each other that they have been 'seen' as a single event. Such an occurrence could lead to 'false positive' cells. Doublets can be distinguished on the flow cytometer with the SSC peak width against SSC peak height. When cells pass through the laser beam evoke a SSC signal that is different from single cells to doublets, doublets have a signal that lasts twice as long as single cells. This is reflected in the width of the signal peak. Therefore, I excluded doublets that displayed high width signal by drawing a gate on single cells displaying lower width signal. Also, dead or dying cells were excluded from analysis by staining with the fluorescent DNA binding dye 4', 6-diamidine-2-phenylindole (DAPI) that can enter only dead cells. Alive cells can pump out the dye while dead cells passively uptake the dye and fluorescent brightly. Finally, cells were gated based on their CD24-PE and CD133-APC expression. Gates were drawn around CD24-PE single positive cells, CD24-PE and CD133-APC double positive cells and CD133-APC single positive.

For each antibody, isotype control was used as a negative control. The isotype of an immunoglobulin (antibody) is determined by the differences of amino acid sequences in the constant region (FC region) of antibody heavy chains. A conjugated primary antibody is composed of a FC region that belongs to the host species where the primary antibody has been raised. So, the isotype of a primary antibody is determined by the host species. This leads to a flurochrome conjugated non-specific antibody, which is consisted of FC region of the host species. The level of fluorescence resulting from staining with the isotype control reveals the non-specific bindings or the background fluorescence that must be excluded in analysis (see Figure 2-2).

Unstained controls (with the omission of antibody and replacement with wash buffer), and isotype matched controls, using monoclonal Mouse IgG1 antibody conjugated to APC and PE (mouse IgG1-PE, IS5-21F5; mouse IgG1-APC, IS5-21F5, Miltenyi Biotec) were performed in every flow cytometry experiment

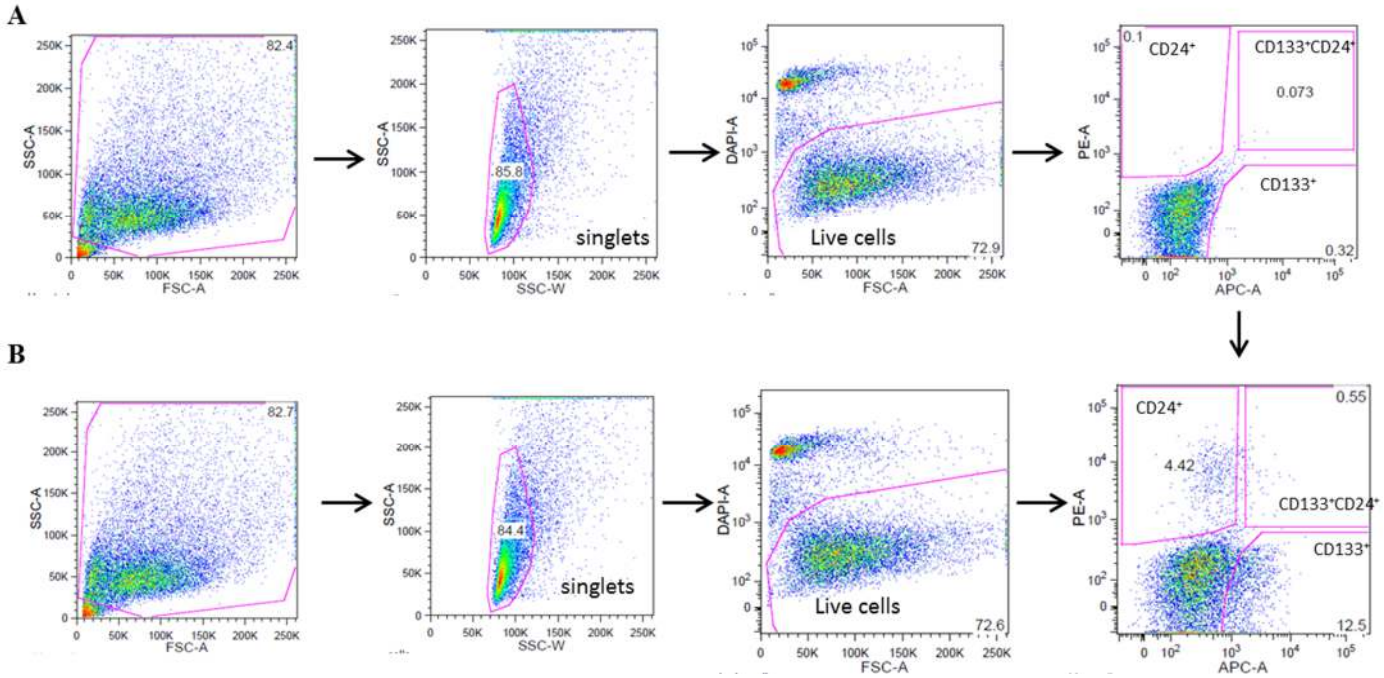

Figure 2-2 Gating strategy for flow cytometry analyses.

The figures show the gating strategy for the correct visualisation and analysis of live $CD24^{+}CD133^{+}$ cells using the Flow cytometer. The total cell population is gated according to its side- and forward-scatter area (SSC-A vs FSC-A). The gated cell population is then furtherly analysed for its side-scatter area against side-scatter width. A circle is drawn around the single cells, which are then divided into live and dead cells according to the viability die stain (DAPI-A vs FSC-A). Cells negative for DAPI compose the live cell fraction, gates are placed around this population to investigate CD24 and CD133 expression (PE-A vs APC-A). (A) Isotype control. (B) sample stained with CD24-PE and CD133-APC).

2.2.5 *Analysis of CD24 and CD133 expression using flow cytometry*

CD24 and CD133 protein expression in human fetal kidneys derived cells was analysed using flow cytometry using the following protocol.

Cultured cells in monolayer were rinsed with sterile 1x PBS (Gibco, UK) and then detached using enzymatic solution of Trypsin-EDTA 0.25% (Gibco). After neutralisation of trypsin with serum containing medium, cells were filtered through cell strainer caps (40 μm mesh). The live cell fraction was counted by Trypan Blue exclusion on a haemocytometer chamber. The strained cell suspension was washed by addition of 2 ml of medium and then spun at 300 x g for 5 minutes. The supernatant was discarded and cell pellet washed a second time with 2 ml of PBS supplemented with 1% FBS (Gibco), then again centrifuged at 300 x g for 5 minutes.

Up to $0.5x10^6$ of total cells were resuspended in a final volume of 100 μl including the primary antibodies CD133-APC and CD24-PE. 20 μl of FcR Blocking Reagent (Miltenyi Biotec) were added before the antibodies and incubated for 5-10 minutes. After this time 80 μl of antibodies diluted in PBS/FBS 1% were added. Sample was incubated for 15 minutes on ice in the dark. Unbound antibody was washed by the addition of 2 ml of and centrifuged at 300 x g for 5 minutes. Labelled cells were resuspended in 200 μl of PBS/FBS 1% prior to analysis.

Negative control and isotype matched control were performed following the same staining procedures.

Flow cytometric analysis was accomplished using a BD LSRII Flow cytometer (BD Biosciences). Data was analysed by collecting a minimum of 10,000 events and using the FlowJo software. Gating parameters between positive and negative populations were established based on cells labelled with IgG isotype control.

2.2.6 *Fluorescence activated cell sorting (FACS)*

Cells were stained using the previous staining protocol. Incubation time was for 30 minutes, agitating the tube every 10 minutes to avoid cells settling at the bottom of the tube. To insure the purity of the sorted cells, the gating was stringently conducted to include the highly expressing cells and the lowest negative ones. To check the purity of the sorted populations, the sorted cells were re-analysed again by flow cytometry.

Samples were sorted on MoFlo XDP or FACS Aria when MoFlo was not available (Beckman Coulter, California) cell sorters. During sort, cells were harvested in 1.5 ml tubes and with a small initial amount of culture medium (300 µl) in the tubes. Samples were then spun at 300 x g for 5 minutes and plated. Each cell population was plated in 24, 12 or 6 well plates.

2.2.7 *$CD24^+CD133^+$ and $CD24^-CD133^-$ maintenance and passaging*

After FACS sorting, cells were plated in 24, 12 or 6 well plates according to the number of cells obtained after sorting. Then they were gradually amplified and transferred in 10 cm^2 tissue culture dishes (BD Falcon). Medium was changed every two days. $CD24^+CD133^+$ cells were passaged 1:2 when they reached 70% of confluence, while $CD24^-CD133^-$ cells were passaged 1:3 when they reached 70% of confluence. When confluent, the medium (1 ml/24 well plates, 2 ml/6 well plates, and 10 ml/10 cm^2 dish) was aspirated and the cells were rinsed with sterile PBS. Cells were detached enzymatically by addition of Trypsin-EDTA 0.25% (Gibco). Trypsin-EDTA was neutralised with growth medium, cells were divided into dishes and volume of medium per dish was made up to 1 ml/24 well plates, 2 ml/6 well plates and 10 ml/10 cm^2 dish with fresh medium.

2.2.8 *Population doubling*

The number of population doublings (PD) is a measure of proliferation.
The PD was calculated at every passage (n=3 per time point) on generated cell lines by solving the following equation: PD = logN/log2, where N is determined as a ratio of the number of cells yielded (N_t) and the number of cells plated (N_0).
From passage 2 upwards 30,000 cells were seeded in 24 well plates in triplicates and separated into different tissue culture vessels when 70% confluent.

2.2.9 *Freezing and thawing*

Following trypsinisation, cells were neutralised and spun at 300 x g for 5 minutes. The supernatant was aspirated and discarded. The pellet was resuspended in 1 ml of the cold freezing solution consisting of 10% dimethyl sulfoxide (DMSO, Sigma-Aldrich), 20% growth medium, 70% heat-inactivated FBS, transferred to a cryovial (Nunc, Thermo

Fisher Scientific) and frozen slowly at -80° C freezer. Cells were stored at -80° C for up to 2 months before being transferred to liquid nitrogen container for long term storage. Cells were thawed by warming the cryo vial in a 37°C water bath upon continuous gentle agitation until the suspension was liquid. Cell suspension was then transferred into 15ml Falcon tube. 9 ml of prewarmed growth medium were added drop-wise. The suspension was then centrifuged at 800 g for 5 minutes. Pellet was resuspended in 1ml of pre-warmed growth medium and transferred to culture dishes. Cells were seeded onto the same sized dishes that they were frozen down from and allowed to adhere overnight at 37° C and 5% CO_2.

2.2.10 *Adipo-differentiation and Osteo-differentiation*

StemMACS AdipoDiff Media (Miltenyi Biotec) was used to promote differentiation of progenitor cells into adipocytes according to manufacturer's indications. The StemMACS OsteoDiff Media (Miltenyi Biotec) was used to promote differentiation of progenitor cells into osteoblasts.

When used for the first time, StemMACS Adipo- or OsteoDiff Media was thawed completely, mixed thoroughly and aliquot to a sample size of 25 ml. Aliquots were stored at -20°C until use. Before use, aliquots were warmed to 37°C in a water bath, 1% penicillin-streptomycin was added to prevent bacterial contamination of the cell culture and throughout the duration of the experiment the aliquots were stored at 4° C.

For Adipo-differentiation, progenitor cells at passage 4, were plated in growth medium, in triplicates, in 24-multiwell plates (BD Biosciences) at a density of 12,000 cells/well. When cells were 80-90% confluent, the growth medium was replaced with control and AdipoDiff medium and the culture was further incubated until day 21 with 3 media changing every 6 days during the differentiation time (see Figure 2-3)

For Osteo-differentiation, progenitor cells at passage 4, were plated in growth medium, in triplicates, in 24-multiwell plates (BD Biosciences') at a density of 7,000-8,000 cells/well. When cells were 70% confluent, the growth medium was replaced with control and OsteoDiff medium and the culture was further incubated until day 12 with 2 media changing every 5 days during the differentiation time (see Figure 2-4).

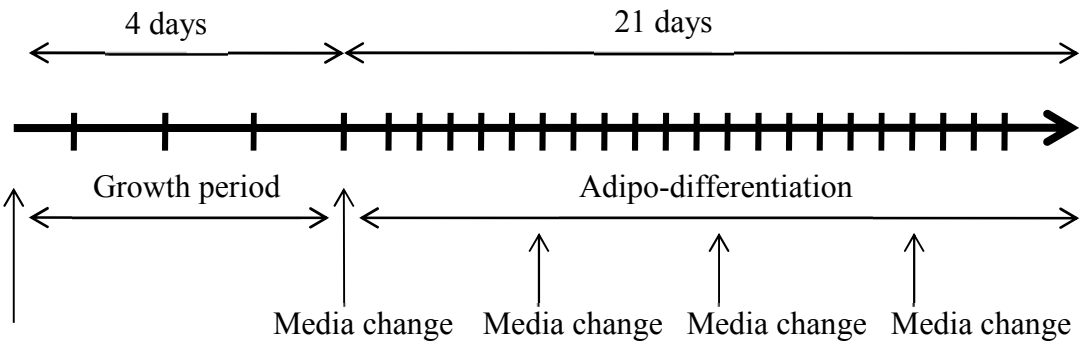

Figure 2-3 Adipo-differentiation experiment timeline.

Progenitor cells were plated in growth medium for four days. Growth medium was then replaced with AdipoDiff medium and the culture was further incubated until day 21 with 3 media changing every six days during the differentiation time.

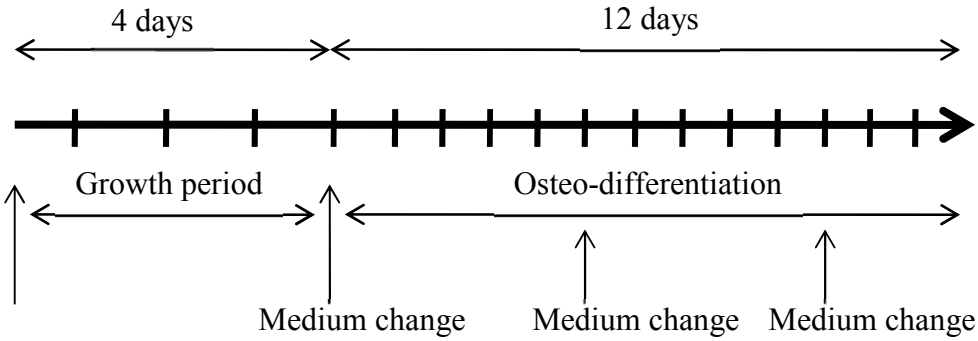

Figure 2-4 Osteo-differentiation experiment timeline.

Progenitor cells were plated in growth medium for four days. Growth medium was then replaced with OsteoDiff medium and the culture was further incubated until day 21 with 3 media changing every four days during the differentiation time.

2.2.11 *Oil Red Staining*

Oil Red O solution is a lysochrome (fat-soluble dye) diazo dye used for positive staining of neutral triglycerides and lipids in fresh and frozen tissue sections.

On day 21, a plate of cells containing 3 wells cultured in growth medium (control) and 3 wells in differentiation medium was removed from incubator and placed in fume hood. All the media was removed and the plate was gently rinse with 500 µl of PBS. PBS was then removed and cells were fixed in 4% PFA in 1x PBS for 15 minutes. Prior to staining, 3 parts of Oil Red O solution in 0.5% isopropanol stock solution (Sigma-Aldrich) were diluted with 2 parts of distilled water and allowed to sit at room temperature for 10 minutes. After 15 minutes, all the PFA was removed and each well was rinsed gently with 500 µl of sterile water. Water was removed and 500 µl of 60% isopropanol was placed in each well for 2 minutes. Isopropanol was then removed and 500 µl of the working solution of oil red O staining was added and kept for 15 minutes. After this time, the solution was removed and wells were thoroughly rinsed 3 times with tap water prior to plate inspection on the phase contrast microscope (Pittenger et al., 1999).Alizarin red staining of osteoblasts

2.2.12 *Alizarin red S staining*

Alizarin red S is an anthraquinone derivative usually used to identify calcium in tissue sections (Owen et al., 1987).

Calcium reacts with alizarin red S forming a complex in a chelation process and the product is birefringent. Two grams of alizarin red S powder (Sigma Aldrich) were resuspended in 100 ml of distilled water. The solution was mixed well and the pH was adjusted to 4.1~4.3 with 10% ammonium hydroxide. Since pH is critical, before any use, alizarin red solution pH was measured. Usually, over time the solution became more basic with pH around 4.6, therefore pH was adjusted by addition drop by drop of HCl 0.1 M.

On day 12, a plate of cells containing 3 wells cultured in growth medium (control) and 3 wells in differentiation medium (treated) was removed from incubator and placed in fume hood. All the media was removed and the plate was gently rinse with 500 µl of PBS. PBS was then removed and cells were fixed in 4% PFA for 15 minutes. After 15 minutes, PFA was removed, wells rinsed gently with PBS and incubated with 500 µl of alizarin red for

10 minutes. After this time, wells were thoroughly rinsed three times with tap water prior to plate inspection on the phase contrast microscope.
Medium was changed twice and cells were processed for RNA or immunocytochemistry after 7 days.

2.2.13 *Collagen coating*

Collagen I solution (Collagen I from rat tail, Sigma-Aldrich) was diluted 10-fold in sterile water to obtain a working concentration of 0.01%. Dishes were coated 1 hour at 37°C, or overnight at 4°C. After this time, the excess fluid was removed from the coated surface, and allowed it to dry. The coated dish was then rinsed with PBS prior to cells seeding.

2.2.14 *Matrigel coating*

Matrigel (BD Biosciences) is composed of extracellular matrix proteins derived from Engelbreth-Holm-Swarm (EHS) mouse tumour cells. The exact composition is batch-dependent, however the predominant component is laminin, but fibronectin, collagen and other proteins are also present.
500 µl of Matrigel were distributed in 1.5 ml Eppendorf on arrival and stored at -20°C. Matrigel aliquots were thawed either on ice or overnight at 4°C. Aliquot of Matrigel was added to appropriate volume of cold DMEM/F12 (diluted 100-fold). Immediately, the diluted Matrigel solution was distributed to the tissue culture vessel. Matrigel coated dishes were incubated one hour in a 37°C incubator before use.

2.2.15 *Lithium Chloride stimulation*

Lithium Chloride (Sigma) was used to induce mesenchymal to epithelial transition and thus to differentiate the cells towards epithelia. The concentration used was the result of preliminary experiments performed by my Supervisors Dr. Karen Price. 20mM was found to be a concentration able to induce morphological and gene expression changes towards epithelia.
The experiment was repeated several times, setting up the protocol in different ways to achieve a successful differentiation. These are summarised in the Table 2-2 Lithium Chloride stimulation experiments summary In all cases LiCl was always used at the same concentration.

Table 2-2 Lithium Chloride stimulation experiments summary

	Cell lines	Cell density	Coating	Experiment description
I	CD24-CD133- (n=3, p4)	40,000/well in a 12 well plate	None	Cells stimulated with LiCl 20mM 24 hours post seeding for 7 days without media changing.
II	CD24+CD133+ (n=1, p4) CD24-CD133- (n=1, p4)	40,000/well in a 12 well plate	Matrigel coated plates	
III	CD24-CD133- (n=2, p4) CD24+CD133+ (n=2, p4)	40,000/well in a 12 well plate	Matrigel coated plates	Cells stimulated with LiCl 20mM 24 hours post seeding. After 48 hours LiCl containing medium was replaced by normal growth medium. Experiment was stopped after further 48 hours

P, passage number.

2.2.16 *mRNA levels of progenitor genes and fibrosis markers*

mRNA levels of progenitor genes were assessed in $CD24^{+}CD133^{+}$ and $CD24^{-}CD133^{-}$ at different passages to assess their expression after FACS sorting and the changes in culture. Changes observed were compared against the expression of the same genes in a suitable positive control, consisting of the whole human fetal kidney of 9 weeks of gestation. Moreover, mRNA was useful to quantify the levels of fibrosis in the folic acid model by measuring the expression of collagen I, collagen III and the macrophage marker CD68 of folic acid treated animals against controls.

2.2.17 *Isolation and quantification of ribonucleic acid (RNA)*

RNA was extracted using Tri Reagent (Sigma-Aldrich) according to the manufacturer's recommendations.

When kidneys were isolated at the end of folic acid-induced nephrotoxicity studies, mice were euthanised using Schedule 1 method, kidneys were collected in sterile conditions and washed twice with sterile cold PBS. PBS was then removed completely and kidneys were frozen in -80°C.

When needed for RNA extraction, kidneys were thawed in ice, minced in small pieces and transferred to tubes (BD Falcon). 1 ml of Tri Reagent was added every 50-100 mg of tissue and tissue was processed using a homogenizer.

When monolayer of cells was used as starting material for total RNA isolation, cells were rinsed twice in cold PBS, 1 ml of Tri Reagent was added to 10 cm^2 culture dish and left for 2 minutes before scraping off the cells (cell scrapers, Greiner, Germany) and transferring the lysate into a 1.5 ml microcentrifuge tube (VWR, UK). If RNA extraction was not carried out on the same day, cell lysate was stored at -80°C. On the day of extraction, samples were thawed and allowed to stand for 10 minutes at room temperature for complete dissociation of nucleoprotein complexes. 0.2 ml of chloroform were added (Sigma) the sample was vortexed for 1 minute and allowed to stand for 10 minutes at room temperature. The resulting mixture was centrifuged at 13,000 g for 30 minutes at 4°C. This separated the mixture into 3 phases: a red organic phase (protein) in the bottom, an interphase pellet (DNA) in the middle, and a colourless aqueous phase (RNA) at the top. The top aqueous phase was transferred to a new autoclaved microcentrifuge tube and 0.5 ml of isopropanol was added (Sigma-Aldrich). After mixing well, sample was

centrifuged at 12,000 g for 30 minutes. The RNA formed a pellet at the bottom of the tube. After removing the isopropanol, it was washed with 70% ethanol and centrifuged at 7,500 g for 7 minutes. Ethanol was then removed and the pellet was air-dried and then resuspended in 15 µl of distilled water (DEPC-Treated Water, Invitrogen). RNA was stored at -80°C.

2.2.18 *RNA quantification*

RNA was tested for both concentration and quality. 2 µl of RNA was loaded into a well of a 96-well UV star plate (Greiner), and diluted with 98 µl distilled water (1:50 dilution). A control sample (100 µL distilled water) was loaded into one well. Absorbance at 260 and 280 nm was measured using a spectrophotometer (Bio-Tek), and the mean control absorbance was subtracted from each sample. Ideal 260:280 ratio is between 1.6 and 1.8, signifying little to no protein or DNA contamination. The 260:280 ratio of samples analysed was between 1.5 and 1.7 and it was considered good enough to proceed with the reverse transcription. To assess the physical quality of the RNA, 1 µL of each sample was added to 1 µl loading dye (Promega) and 7 µl distilled water. Solution was run on a 2% agarose gel in Tris Borate EDTA buffer containing SybrSafe (ethidium bromide homolog) at 80 V for 20 minutes. Gels were visualised using a transilluminator on a Bio-Rad ChemiDoc.

2.2.19 *Reverse transcription*

Total RNA isolated from cell monolayer or tissue was reverse transcribed into complementary cDNA with the use of reverse transcriptase. The cDNA is then used as a template to amplify specific genes of interest detected using appropriate primers, this process in called ‘Q-PCR’.

The first step was the reverse transcription of total RNA into cDNA. In my thesis, this step was carried out with the help of a kit (iScript cDNA synthesis, Bio-Rad, CA, USA). This kit makes use of a modified Moloney Murine Leukaemia Virus Reverse Transcriptase which has a Ribonuclease H activity (RNAse H+ M-MLV RT, Bio-Rad). This enzyme is a DNA polymerase that synthesises a complementary DNA strand from single-stranded RNA as well as cleaving, with its RNase H activity, the RNA strand in RNA-DNA hybrids. The buffer provided with it is constituted of a mixture of deoxy-

thymine nucleotides (oligo-dT) and random hexamer primers that can be extended by the reverse-transcriptase.
cDNA was made from 500 ng of mRNA. Each reaction contained volume equivalent of 500 ng RNA, 4 µl of 5x iScript reaction mix, 1 µl of iScript reverse transcriptase, and topped to 20 µl with nuclease-free water. The reaction was run on program: 5 minutes at 25°C, 30 minutes at 42°C, 5 minutes at 85°C, and hold at 4°C.

2.2.20 *Primer design*

The target sequence was obtained either as a sequence in FASTA format, an NCBI accession or RefSeq accession (National Center of Biotechnology Information, US National Institute of Health, http://www.ncbi.nlm.nih.gov/). The sequence obtained was copied in the Primer-BLAST, an open source program of the National Center of Biotechnology Information, US National Institute of Health (http://www.ncbi.nlm.nih.gov/tools/primer-blast).
On Primer-BLAST interface, the option to design primers to span exon/exon junction was ticked to exclude genomic DNA. Once obtained a suitable set of primers, the likelihood of formation of primer secondary structures or primer dimmers was checked using the Custom DNA Oligo Tool available on the Sigma-Aldrich website (http://www.oligoevaluator.com/Login.jsp). Often set of primers were found in publishes papers. In that case, primers were checked by entering the sequences in the 'Primer Parameters' section of the Primer-BLAST interface.

CD24 and CD133 primers design

Eight mRNA splicing variants of CD24 are known. Of these, only four encode for a functional protein. Splice variants 1 to 3 encode for CD24 isoform a, while transcript 4 encodes for isoform b. Since I did not know which transcript was going to be expressed in human fetal kidneys, I designed a pair of primers that covered all the 4 splice variants. CD133 gene produces different isoforms by alternative splicing. Isoform 1 was found to be expressed in hematopoietic stem and progenitor cells found in different lymphoid tissues, as well as other organs such as kidney (Yu et al., 2002). Isoform 2 was found in fetal liver, skeletal muscle, kidney, heart and adult pancreas, kidney, liver, lung and placenta (Yu et al., 2002). For CD133, primers covering all the isoforms were also chosen.

2.2.21 *Gradient Polimerase chain reaction (PCR)*

Gradient PCR was used to determine primers optimal annealing temperature. Using the gradient function of the Mastercycler thermal cycler (Eppendorf), different annealing temperatures were tested.

2.2.22 *Agarose gel electrophoresis*

PCR products were resolved on 2% (w/v) agarose gel in TBE containing SybrSafe at 80 V for 20 minutes. DNA ladders were run alongside the products. Gels were visualised using a transilluminator on a Bio-Rad ChemiDoc.

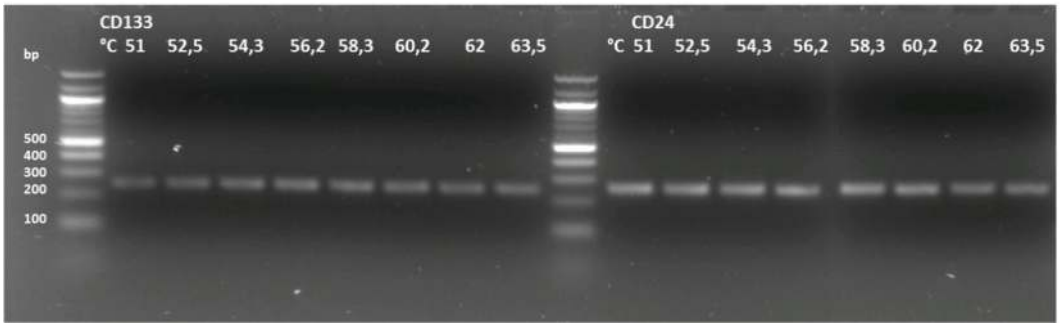

Figure 2-5 Experimental determination of optimal annealing temperature of CD24 and CD133.
Gel electrophoresis of PCR products (CD24 and CD133) run on 2% agarose gel. No obvious differences in the intensities of desired product bands were observed. The annealing temperature does not appear as a critical factor for the PCR amplification, based on these results the annealing temperature of 60°C was selected.

2.2.23 *Quantitative polymerase chain reaction (Q-PCR)*

After cDNA synthesis, gene of interest was quantified using Q-PCR. This is based on the PCR method that comprises of several cycles of denaturing, annealing and extension. The first step occurs at 94°C where DNA is denatured in single strands, following denaturation there is a step of annealing in which the primers bind the appropriate complementary strand. The last step of extension at 72°C the DNA synthesis between forward and reverse primers occurs. I used the fluorescent dye SYBR Green (Bio-Rad) to detect the PCR products, SYBR green binds to double strand DNA and when excited with blue lights, it emits green light. During the PCR reaction, the target sequence is amplified and SYBR green binds to the new copies of the gene of interest resulting in an increase in the level

of fluorescence over time that reflects the amount of PCR product. The Real-time PCR software calculates the baseline and the threshold value (C_t value) which is the number of cycles after which the fluorescent signal exceeds the background level. Therefore, the lower the C_t value, the greater the number of target nucleic acid in the sample.

To determine the level of expression of the genes of interest, I used the ΔΔct method (Livak and Schmittgen, 2001). This involves comparing the Ct values of the samples of interest to a control or calibrator. Controls were a non-treated sample or RNA extracted from total kidney, the different choice of controls is explained in Results Chapters according to the experiments performed. The Ct values of both the control and the samples of interest were normalised to an appropriate endogenous housekeeping gene.

ΔΔct method is also known as the $2^{-\Delta\Delta Ct}$ method, where: $\Delta\Delta Ct = \Delta Ct_{sample} - \Delta Ct_{control}$, where ΔCt sample is the Ct value for any sample normalised to the endogenous housekeeping gene and ΔCt control is the Ct value for the calibrator also normalised to the endogenous housekeeping gene.

Q-PCR was performed on CFX96 Touch Real-Time PCR Detection System (Bio-Rad Laboratories, Hertfordshire). Each reaction contained 1 µl of cDNA product, 10 µl of Sso Advanced SYBR Green supermix (Biorad) and 100 nM of forward and reverse primers.

Table 2-3 Human primers used for PCR characterisation of cell lines.

Gene	Forward primer 5' to 3'	Reverse primer 5' to 3'	Bp	Annealing T.(°C)
CD24	GACTTCCAGACGCCATTTGGATT	CCCACGCAGATTTATTCCAG	255	60
CD133	CAGAGTACAACGCCAAACCA	AAATCACGATGAGGGTCAGC	245	60
CITED1	AGGATGCCAACCAAGAGATG	CTGCAGCTGCATACTAGCCA	236	58
E-Cadherin	GGTGGGTGACTACAAAATCAATCT	TTCTCCGCCTCCTTCTTCATCATA	310	60
EYA1	CCC CCAGATTCTGATCTTGA	GGTGGATCCCTCCCATATCT	113	58
FOXD1	TGGGGACTCTGCACCAAGGGACT	TGGGGACTCTGCACCAAG GGACT	169	62
NCAM1	GACTCTGGATGGGCACATGG	GATCGTGGCACTGGGATAGG	250	64
OCT4	AGTGAGAGGCAACCTGGAGA	AGTGCAGTGAAGTGAGGGCT	279	65
OSR1	TTCGTCTGCAAGTTCTGTGG	TGTAGCGTCTTGTGGACAGC	236	64
PAX2	TTTGTGAACGGCCGGCCCCTA	CATTGTCACAGATGCCCTCGG	301	61
SALL1	TGATGTTTGAGCCAGCATGT	TGTGTTCTGAAAGGTCGCTG	365	60
SIX2	TGTTGGTTCTTGTTTGGGATTT	TTCCCTTCTGTGGTTCAAGACT	89	56
WT1	GATAACCACACAACGCCCATC	CACACGTCGCACATCCTGAAT	90	61
β-Actin	ATCTGGCACCACACCTTCTACAATGAG	CGTCATACTCCTGCTTGCTGATCCACA	837	60

Table 2-1 Primers used in multi-differentiation experiments

Gene	Forward primer 5' to 3'	Reverse primer 5' to 3'	Bp	Annealing T.(°C)
ADIPONECTIN	GGCCCGGAGTCCTGCTTCCCC	GACCTGGATCTCCTTTCTCAC	147	56
BMP2	TCAAGCCAAACACAAACAGC	ACGTCTGAACAATGGCATGA	197	62.5
MATRIX GLA PROTEIN	CCCTCAGCAGAGATGGAGAG	CGCTTCCTGAAGTAGCGATT	162	62.5
OSTEOPONTIN	AGCTGGATGACCAGAGTGCT	TGAAATTCATGGCTGTGGAA	151	62.5
PPARγ	TCCATGCTGTTATGGGTGAAACT	GTGTCAACCATGGTCATTTCTTGT	112	62
RUNX2	CCTTGACCATAACCGTCTTCAC	GGACACCTACTCTCATACTGGG	275	62.5

Table 2-5 Primers used for in vivo experiments

Gene	Forward primer 5' to 3'	Reverse primer 5' to 3'	Bp	Annealing T. (°C)
COLLAGEN I	GAGCGGAGAGTACTGGATCG	TACTCGAACGGGAATCCATC	204	62
COLLAGEN III	TGGTCCTCAGGGTGTAAAGG	GTCCAGCATCACCTTTTGGT	221	61
CD68	GGGGCTCTTGGGAACTACAC	GTACCGTCACAACCTCCCTG	167	60
HPRT	TGCTCGAGATGTCATGAAGC	TATGTCCCCGTTGACTGAT	195	60

2.2.24 *Ex vivo studies: kidney rudiment assay*

Kidney rudiments were dissected from E12.5 embryos of pregnant CD-1 mice sacrificed following schedule 1 methods. Kidneys were quickly rinsed with sterile PBS to remove excess media and transferred to 15 ml Falcon tube. Kidneys were then incubated with one ml of 5x Trypsin-EDTA (Sigma-Aldrich) made up in 1x PBS at 37°C for 5 minutes. After this time, disaggregating tissue was gently resuspended by mechanical pipetting. Trypsinisation was followed by incubation in complete culture medium composed of Eagle's Minimum Essential Medium supplemented with 10% FCS, 2 mM L-glutamine and 1% penicillin/streptomycin (Gibco). The resulting suspension was filtered through 40 μm cell strainer and collected by centrifugation of two minutes at 800 x g. Supernatant was then removed and cells were resuspended in one ml of medium. 100,000 or 180,000 cells were placed into distinct 1.5 ml tubes.

After centrifugation of each cell suspension a pellet was obtained. Pellet was flushed away from the side of the tube and transferred onto pre-cut Millipore Isopore Membrane Filter (Millipore, Billerica, MA, USA,) placed on top of a metal grid in a 6 well plate.

Both intact and reformed embryonic kidneys were cultured in complete culture medium (2 ml in a well of 6 well plates) at the gas/medium interface in 37°C, 5% CO_2 humidified incubator. In the first 24 h of culture, medium was supplemented with 5 mM Y-27632 Rho kinase inhibitor (ROCK inhibitor, Sigma-Aldrich) to promote the survival of the reformed kidneys.

2.2.25 *CellTracker staining*

Human cells were labelled before mixing with murine embryonic kidney cells suspension. Cells were harvested and labelled with 5 μM of Cell Tracker Green CMFDA dye working solution (5-chloromethylfluorescein diacetate, Thermo Fisher Scientific) as following: cells were incubated for 30 minutes at 37°C and 5% CO_2. After this time, the CellTracker working solution was removed and normal culture media was added.

2.2.26 *Chimeric pellet formation and culture*

$1x10^4$ human CMFDA-labelled cells were mixed with 9×10^4 mouse embryonic kidney cells (1:10) in a 500 µl tube. The cell mixture was then spun at 800 x g for three minutes. The resulting pellet was detached from the bottom of the tube and placed gently onto a 5 µm pore polycarbonate filter using a glass pasteur pipette. The filter was supported by a metal grid. The culture medium was composed of human fetal kidney cells complete culture medium. The pellets were cultured for 5 days at 37°C, 5% CO_2. For the first 24 hours of culture, the medium was supplemented with the ROCK-Inhibitor.

2.2.27 *Fixation and staining of pellets*

Whole mount immunofluorescence of kidney rudiments and chimeras were fixed with cold methanol for 10 minutes at room temperature. Specimens were subsequently washed and blocked for one hour with blocking solution composed of 10% goat serum (Sigma) and 1% Triton X-100 in PBS. This was followed by incubation overnight at 4°C in primary antibody solution. The following primary antibodies were used: mouse anti-Wt1 1:500 (DAKO), rabbit anti-laminin1 1:1000 (Sigma), mouse anticalbindin 1:500 (Abcam). Following 3 washes with PBS, the appropriate secondary antibodies were applied for 1 hour at room temperature. Samples were analysed using a fluorescent microscope.

2.3 *In-vivo studies*

2.3.1 *Experimental models*

The renal response to a high dose of folic acid (FA) was assessed in four mice strains with increased genetic immunodeficiency. Procedures were approved by the UCL local ethics committee and the UK Home Office (project licence PPL70/6627). I was trained to collect blood from the lateral saphenous vein and this procedure was carried out by myself, whilst the intraperitoneal (IP) and intravenous (IV) injections were performed by experienced researchers in my laboratory group. In details, IP injections were performed either by Dr Hortensja Brzóska or Dr Elisavet Vasipoulou, whereas IV injections were performed by Dr Elisavet Vasipoulou only.

BALB/c wild type, nude (BALB/cOlaHsd-Foxn1^{nu}), SCID (BALB/cJHanHsd-Prkdc^{scid}) and NOD-SCID (NOD.CB17-Prkdc^{scid}/NCrHsd) mice were purchased from Harlan (Bicester, UK). BALB/c wild type mice have a functional immune system; BALB/c nude have a mutation in the *Foxn1* gene that is important for development of the thymus, its lack causes a consequent deficiency in the T cells maturation and mediated response (Corbeaux et al., 2010). BALB/c SCID mice (Severe Combined Immune Deficiency) carry a mutation in the gene encoding for the enzyme involved in DNA repair (protein kinase DNA activated catalytic polypeptide or 'PRKDC')(Blunt et al., 1995). This determines a defective rearrangement of genes encoding for antigen-specific receptors on B and T lymphocytes. Therefore, the mice present with impaired ability to make T or B lymphocytes. NOD-SCID mice carry the SCID mutation transferred onto a non-obese diabetic background (NOD). As a result, they lack in mature T and B cells and circulating complement. They also show the presence of a functionally less mature macrophage population defective in the lipopolysaccharide-stimulated Interleukin-1 secretion (Shultz et al., 1995).

2.3.2 *Folic acid injection*

Previous published experiments in C57Bl/6J mice performed in my laboratory (Kolatsi-Joannou et al., 2011, Long et al., 2001) showed that FA at the dose of 240 μg/g of body weight was sufficient to cause an acute renal injury with loss of epithelial cell integrity and a low mortality rate (less than 5%). Following the FA insult, the regeneration of the

renal epithelium occurred over the subsequent two weeks, however the healing process was incomplete with patchy fibrotic areas in the kidneys. We therefore tested this dose in the different murine strains on the same BALB/c background.

FA (Sigma-Aldrich) was dissolved in the vehicle of 0.3 M sodium bicarbonate, ($NaHCO_3$, Sigma-Aldrich) and 240 μg/g body weight was injected intraperitoneally in BALB/c mice using 25 g needles (surguard safety hypodermic needle, VWR).

Seven- to eight-week-old male BALB/c wild type (n=18), nude (n=5), SCID (n=8) and NOD-SCID (n=5) mice were injected with FA. BALB/c wild type control group was composed of mice injected with sodium bicarbonate (n=4). To observe the early development of kidney damage, BALB/c wild type mice administered at day 0 with FA were sacrificed at day 2, whereas to examine the regenerated epithelium after the injury and the eventual occurrence of fibrosis, mice were sacrificed at day 14, day 21 or day 42. The number of animals used and sacrificed was reduced to the minimum, according to this, nude and SCID mice were euthanised at day 21 and the progression of the acute injury was evaluated by measurements of renal function without the need to sacrifice animals at day 2; histology after 21 days was utilised to evaluate the occurrence of fibrosis. Differently from the other strains, NOD-SCID mice were sacrificed at day 42 to examine for a longer time this strain in order to gain further information on the development of FA-induced acute renal failure in NOD-SCID animals.

Body weight was monitored during FA-induced nephropathy. When loss of body weight exceeded the 20% mice were euthanised according to Project Licence requirements.

Kidneys were collected after euthanasia. Both kidneys were weighed to determine the kidney/body weight ratio. The left kidney was used for immunohistochemical analyses whilst the right kidney was frozen for RNA/protein extraction. In the case of the NOD-SCID mice, both kidneys were used for immunohistochemical analyses and both for RNA extraction, half of each kidney was embedded for immunohistochemistry or processed for RNA extraction. The different groups are summarised in Figure 2-6**Error! Reference source not found.**. Folic acid induced acute renal injury was monitored over time by checking body weight loss and measuring renal function by testing urea nitrogen in serum. For this reason, at day 2 and every week until the end of the experiment, mice body weight was measured and blood was collected from the saphenous vein to assess renal function.

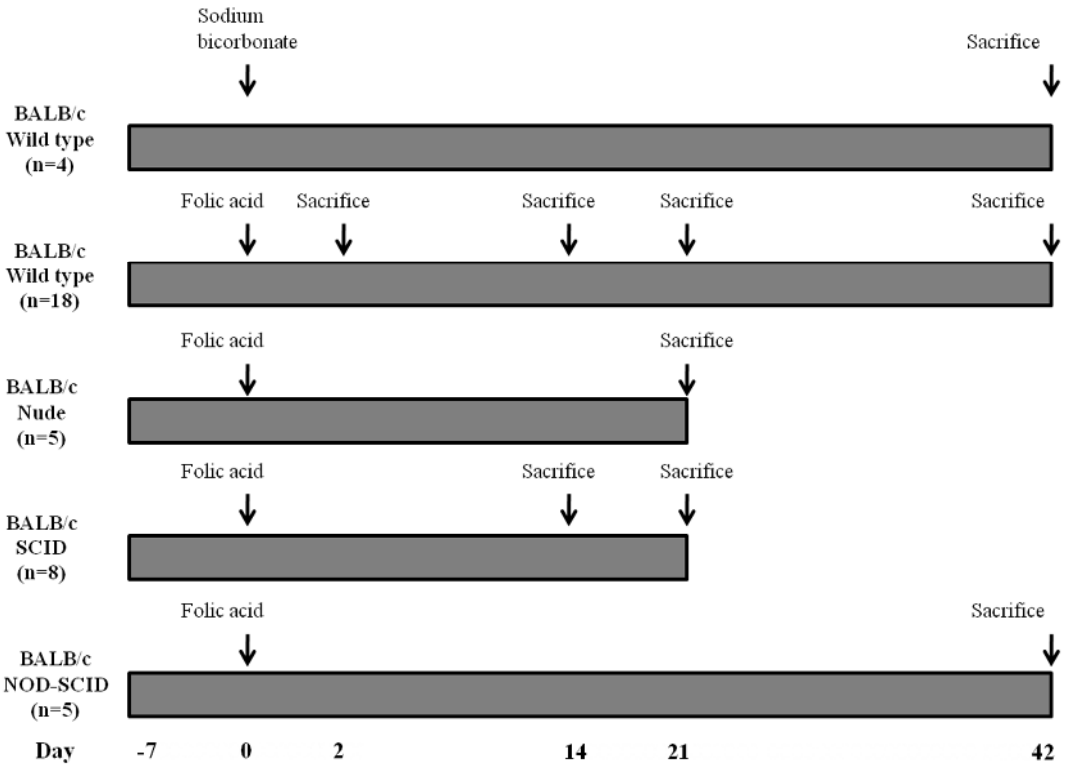

Figure 2-6 Folic acid pilot study groups and timeline.

Figure shows the experimental design of the *in vivo* experiments. Seven days prior to folic acid injection, baseline measurements were taken (BUN and body weight). On day 0, folic acid (240 μg/g of body weight) was injected intraperitoneally into adult male BALB/c wild type mice (n=18), nude (n=5), SCID (n=8) and NOD-SCID (n=5). Four BALB/c wild type mice composed the control group in which sodium bicarbonate was injected instead of folic acid. To examine the early effects of folic acid in BALB/c wild type, these were euthanised after 2 days, whereas to investigate the long-term effects of folic acid-induced kidney injury, mice were sacrificed at day 14, day 21 or day 42. Renal function (BUN) and body weight were assessed at day 2 and every 7 days.

2.3.3 *Blood Urea Nitrogen (BUN) assay*

Blood was collected from the saphenous vein. Serum was prepared by centrifuging at 800 g for 15 minutes. Cells and clotting factors were discarded. BUN concentration was determined using the QuantiChrom Urea Assay Kit (BioAssay Systems, Hayward, CA). This kit uses a chromogenic reagent that reacts with urea producing a colour change, whose intensity, measured at 520 nm, was directly proportional to the urea concentration in the sample (Jung et al., 1975). This kit has been validated in mice in previous experiments in our laboratory(Kolatsi-Joannou et al., 2011). The urea standard provided in the kit contained 50 mg/dl urea. To perform the assay, 5 µl of water (blank), 5 µl of the standard, and 5 µl of sample were transferred into separate wells of a clear flat-bottom 96-well plate. Then to each well, 200 µl of freshly prepared working reagent was added and mixed quickly by gently rocking the plate. The reaction was incubated for 20 minutes at room temperature. The optical density (OD) at 520 nm was then measured placing the plate in a spectrophotometer. Urea was then calculated according to manufacturer's instructions:

$$\text{Urea} = \frac{OD_{SAMPLE} - OD_{BLANK}}{OD_{STANDARD} - OD_{BLANK}} \text{ x } 50(\text{mg/dl})$$

BUN was then calculated as: BUN = Urea (mg/dl) x 2.14

(2.14 conversion factor was derived as follows: MW of urea = 60, MW of urea nitrogen = 28, then 60/28 = 2.14).

2.3.4 *$CD24^{-}CD133^{-}$ and $CD24^{+}CD133^{+}$ effects on FA-induced renal injury in NOD-SCID mice*

We tested the effects of human fetal cell lines administration on FA nephropathy in the NOD-SCID strain. $CD24^{+}CD133^{+}$ and $CD24^{-}CD133^{-}$ obtained from four fetal kidneys of 8-9 weeks of gestation were amplified in culture for 3 passages prior to injection in mice. Two hours before injection in mice, cell lines were detached from tissue culture vessels, filtered using 40-μm cell strainers (BD Falcon), counted and collected by centrifugation at 300 x g for 5 minutes. The supernatant was discarded and cells were resuspended in sterile PBS at room temperature before the injection.

The study involved eight-week old females (n=12) and males (n=16, Figure 2-8).

Females were included in the experiment for two reasons: to enlarge the number of the mice population treated and to observe any difference with males in the development of the renal injury and response to human renal progenitor cells. Gender differences in renal disease progression have been previously shown, these were attributed to the renal protection function of the female sex hormone estrogen exploited by its interaction with endogenous vasoactive molecules such as endothelial nitric oxide synthase (eNOS) and vascular endothelial growth factor (VEGF) (Stringer et al., 2005)

A week before FA injection, blood was collected to determine the baseline levels of BUN. FA injection was performed at the same dose as for the comparison among mice strains (paragraph 2.3.2). Surprisingly, after 48 hours there was a high degree of mortality in this experiment and 2 females and 7 males were sick and consequently euthanised. Blood was collected from the remaining mice and BUN was measured. Mice with similar BUN levels were divided into 3 groups which received the following interventions:

- Group I (n= 5, 2 males and 3 females) received intravenous injection in the tail vein of 80 μl of PBS.
- Group II (n=5, 3 males and 2 females) received injection of $0.4x10^{6}$ of $CD24^{-}CD133^{-}$ in 80 μl of PBS.
- Group III (n=6, 3 males and 3 females) was injected with $0.4x10^{6}$ of $CD24^{+}CD133^{+}$ in 80 μl of PBS.

Blood was collected at day 7 and day 14 after FA injection and the experiment completed at day 21. The experiment was designed as a therapeutic intervention to apply to individuals with acute kidney injury.

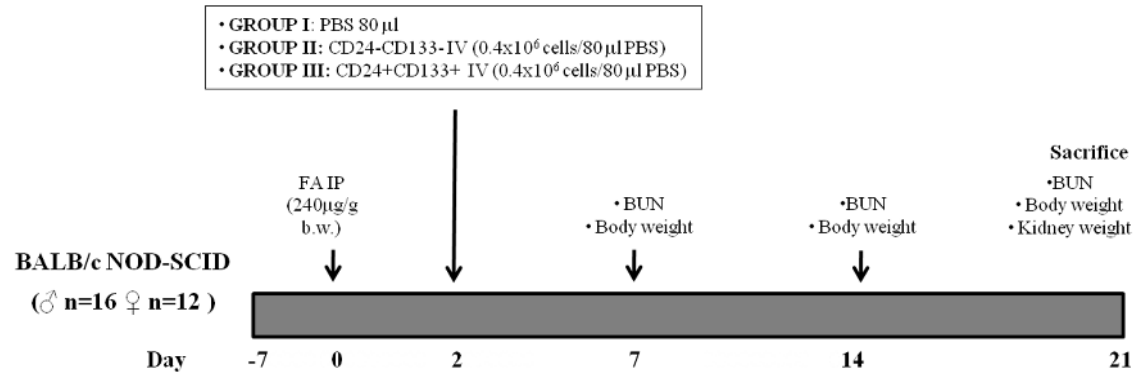

Figure 2-7 Study of human renal cell line effects on folic acid-caused injury in NOD-SCID female and male mice.

Twenty-eight adult BALB/c NOD-SCID mice (16 female and 12 male) were divided into three groups: Group I received IV injection of 80 µl of PBS; group II received IV injection of $0.4x10^6$ of $CD24^-CD133^-$ in 80 µl of PBS; group III was IV injected with $0.4x10^6$ of $CD24^+CD133^+$ in 80 µl of PBS. All the groups received IP injection of folic acid at day 0 and the IV injection after 2 days from folic acid. Baseline measurements were taken 7 days before folic acid. BUN and body weight were measured at day 7, day 14 and day 21 after folic acid injection. Mice were euthanised at day 21.

2.3.5 *Tracking Renal Cells with Bioluminescence*

Bioluminescence imaging was used to track the human renal cell lines injected IV in mice with FA-induced nephropathy. These experiments were performed in the UCL Centre for Advanced Biomedical Imaging (CABI) in collaboration with Dr Tammy Kalber and Dr Stephen Patrick. Tammy performed IP injections of FA and IV injections of human cells as well as bioluminescence imaging post-cells injection, Patrick performed lentiviral infection of the human cells and bioluminescence imaging and measurements. Initially, transfected human cells with a reporter vector strongly expressing the firefly luciferase luc2 gene (*luc2*). However, I found that the transfected cells expressed luciferase transiently and dimly, therefore a viral method to introduce of *luc2* was subsequently adopted.

2.3.6 *pGL4.51[luc2/CMV/Neo] Vector*

pGL4.51 (Promega, Southampton, UK) is a reporter vector expressing the luciferase gene luc2, under the control of the strong constitutive CMV (cytomegalovirus) promoter. The vector possesses a series of features which make it suitable for expression in mammalian cells and *in vivo* tracking. Firstly, the vector encodes the luciferase reporter

gene luc2 (Photinus pyralis), which has been codon optimised for mammalian expression. Secondly, fewer consensus regulatory sequences are present thus reducing background and decreasing the risk of anomalous transcription. This vector includes late Simian virus 40 PolyA (SV40 PolyA) sequence, which is a 240 bp DNA sequence that possesses the activity of transcription termination and can add PolyA tail to mRNA. This signal sequence is positioned downstream of luc2 to provide efficient transcription termination and mRNA polyadenylation.

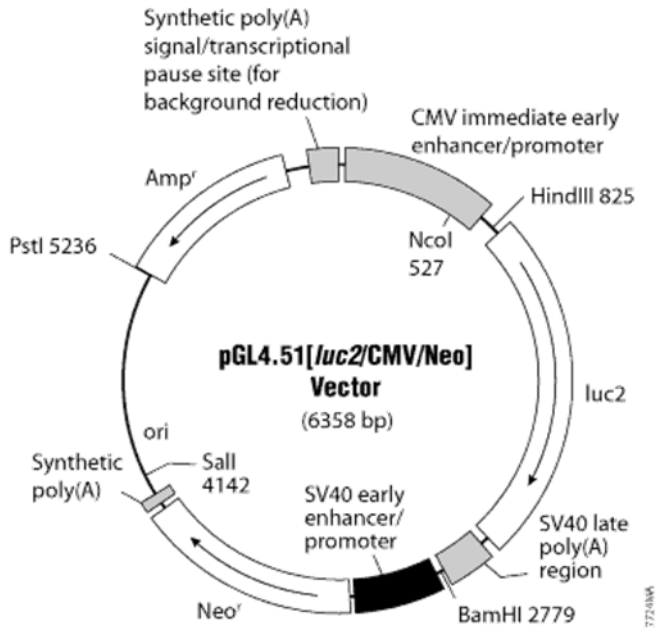

Figure 2-8 pGL4.51 vector circle map.

pGL4.51 is a reporter vector expressing the luciferase gene *luc2*, under the control of the strong constitutive CMV (cytomegalovirus) promoter. This vector includes late Simian virus 40 PolyA (SV40 PolyA) sequence, a signal sequence positioned downstream of luc2 to provide transcription termination and mRNA polyadenylation. Synthetic poly(A) signal/transcription start site; synthetic Neomycin-resistance gene for mammalian cell selection of the plasmid; plasmid replication origin; Amp^r gene for bacterial selection for vector amplification.

2.3.7 *Transformation of competent cells*

DH5α E. Coli competent cells (Invitrogen) stored in -80°C freezer were thawed. Cells were gently mixed and 100 µl were transferred to polypropylene tube (BD Biosciences) on ice. 100 ng of pGL4.51 vector was mixed with the competent cells and the mixture was first incubated on ice for 30 minutes, then cells were heat-shocked for 45 seconds in a 42°C water bath before being transferred to ice for a further 2 minutes. SOC (Super Optimal broth with Catabolic repressor) medium was added to the tube, tightly closed

and placed at 37°C on a shaking incubator at 225 rpm for 1 hour. After this time, the transformation mix was diluted 1:100 in Luria Broth (Sigma-Aldrich) and 100 µl was spread on Luria Broth agar plates with 100 µg/ml ampicillin (Invitrogen) as a selection antibiotic to allow growth of bacteria containing the plasmid; the plate was incubated at 37°C.

2.3.8 *Analysis of transformants*

Five colonies were picked and cultured overnight in Luria Broth medium (Sigma-Aldrich) with 100 µg/ml ampicillin for 12-16 hours at 37°C on a shaking incubator. Then, plasmid DNA was isolated using QIAprep Spin Miniprep Kit (Qiagen, Manchester, UK) following the manufacturer's instructions. Briefly, one ml of the recombinant *E.coli* was centrifuged at 6800 x g for 3 minute and then resuspended in the Buffer P1 (supplied with the kit). Cells were lysed by adding lysis solution-Buffer P2 (supplied with the kit) and mixed gently followed by addition of neutralization/binding solution (Buffer N3, provided) in order to precipitate the cell debris. The supernatant, composed of the lysate was added to a QIAprep spin column after 10 minutes centrifugation at 17,900 g. All the following centrifugation steps were performed using the same speed. The flow-through was then discarded, pellet was washed with Buffer PB. Plasmid DNA was eluted by addition of Buffer PE to the column and further centrifugation for another minute. The quantity and purity of the eluted plasmid were assessed by using NanoDrop ND-1000 UV-Vis Spectrophotometer (LabTech International Ltd, Ringmer, UK). A 260/280 ratio of 1.8- 2.0 was considered an indication of relative purity.

The plasmid DNA was analysed by restriction enzyme analysis method to confirm the presence of the pGL4.51 plasmid vector. *BamHI* enzyme (New England Biolabs, Hitchin, UK) was used for the restriction digestion analysis. In a sterile 1.5 ml tube, the reaction mix was prepared in a final volume of 50 µl as follow: 1 unit of *BamHI*, 1 µg of DNA, NEB buffer concentration of 1X (New England Biolabs). PGL4.51 Plasmidic DNA was analysed by gel electrophoresis. The reaction was incubated for 1 hour at 37°C. Gel electrophoresis was done by using 1 % agarose gel and 1 Kb ladder (New England Biolabs) to visualise the results of restriction analysis.

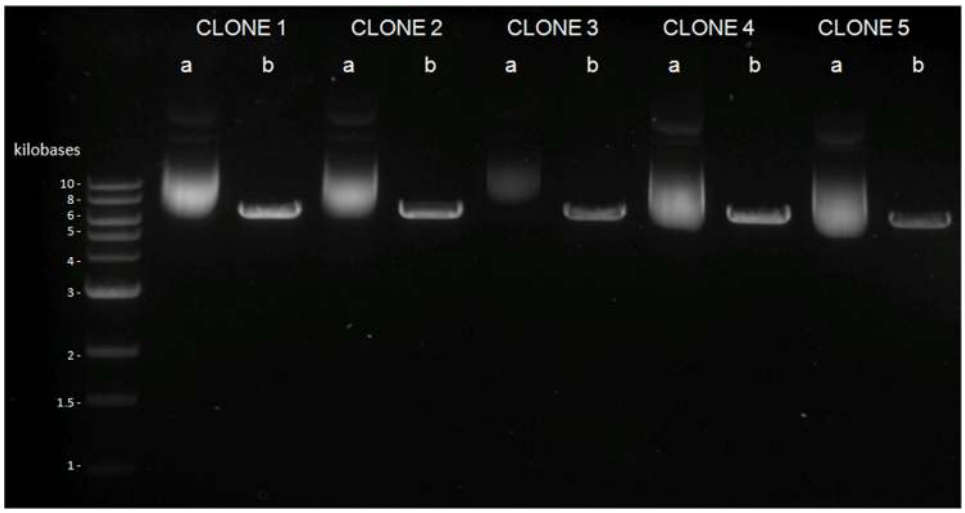

Figure 2-9 Gel electrophoresis of pGL4.51 plasmid clones.

Plasmid DNA isolated from 5 colonies (CLONE 1 to 5) was digested by restriction enzyme *BamHI* to confirm the presence of the pGL4.51 plasmid vector. Uncut DNA (a) and cut DNA (b) were analysed by gel electrophoresis using 1 % agarose gel. The uncut DNA (a) showed extra bands because of its non-linear conformations. Cut DNA showed a single band of approximately 6.3 kb (based on 1kb ladder) representing the full size of the plasmid. The result on the gel corresponded to the predicted size.

2.3.9 *pGL4.51[luc2/CMV/Neo] transfection*

For plasmid DNA transfection, Lipofectamine 3000 transfection reagent (Life technologies) and Genejuice transfection reagent (Novagen, Darmstadt, Germany) were used following the manufacturer's protocol. For Lipofectamine 3000 the following protocol was used: one day before transfection, the cells were seeded in 2 ml of complete growth medium in a 6 well plate to achieve 70%-90% of confluence. On the day of transfection medium was aspirated, cells were washed with PBS, and then 2 ml of complete growth medium supplemented with 250 µl of DNA/lipid complex was added. For each transfection reaction complexes were prepared as follow. Firstly, a 5 µg plasmid DNA was diluted in 250 µl of Opti-MEM Reduced Serum Medium (Gibco) with 10 µl of P3000 Reagent (provided with the kit) and mixed gently. Then, diluted DNA was combined 1:1 to either 3.75 µl and 7.5 µl Lipofectamine 3000 diluted in 250 µl of Opti-MEM and incubated for 5 minutes. After the incubation, the complexes were added to the wells and mixed gently. After 24 or 48 hours incubation at 37°C in 5% CO_2 atmosphere, the medium was changed and cells were ready for luciferase detection.

The transfection procedure using Genejuice Transfection Reagent was performed as follows: cells were either incubated with a mixture containing 1μg DNA and 3 μl of Genejuice or with 1μg DNA and 6 μl of Genejuice at 37°C in 5% CO_2 atmosphere for 24 or 48 hours, after that the medium was changed and cells were ready for luciferase detection.

2.3.10 *Cells transduction with lentiviral vector*

Lentiviral vector preparation and cells transduction was carried out by Dr Patrick Stephen in CABI. Lentivirus encoding a luciferase-GFP transgene was prepared using a 2nd generation packaging system. HEK 293T cells were transfected with the EGFP-Luciferase transfer plasmid (pSEW-Flagx3-FLuc-2A-GFP, gift from Dr Martin Pule at UCL), Gag-pol (pCMV-DR8.74) and VSV-G (pMD2.G) packaging plasmids, using the $CaPO_4$ precipitation method (Tiscornia et al., 2006). For every plate of HEK 293T cells at 60% confluence, plasmid DNA (10 μg transfer vector, 6 μg pCMV-DR8.74, 4 μg pMD2.G) was diluted to 1ml in 0.25M $CaCl_2$ solution. This was added dropwise to 1 ml of 2x HBSS (HEPES buffered saline solution, pH6.95), while vortexing, and then added to the plated HEK 293T cells. Successful transfection was assessed using fluorescence microscopy the next day to confirm GFP expression. Media was changed 24 hours after $CaPO_4$ transfection for DMEM F12 media for the transduction of $CD24^-CD133^-$ and $CD24^+CD133^+$ cell lines. Sodium butyrate was added to the media at a final concentration of 1mM, 24 hours prior to lentiviral harvest, to improve viral titres (Cribbs et al., 2013). This media was stored at -20ºC or used immediately to transduce the target cells, by replacing their normal DMEM F12 media with the virus-containing media for a period of 24 hours. Successful transduction at > 90% was confirmed using fluorescence microscopy to detect GFP expression at 48 hours post transduction. Stably-transduced cell lines were expanded and used for all subsequent experiments.

2.3.11 *In vitro Bioluminescence assay*

D-Luciferin (Beetle Luciferin, Potassium Salt, Promega) was made to 30 mg/ml in sterile water and then filtered using 0.45-μm syringe filter. It was then used immediately or frozen at -20 °C. A working solution of 150 μg/ml of D-Luciferin in prewarmed tissue

culture medium was prepared and the luciferin solution was applied to cells before imaging.

2.3.12 *Human Cell Tracing in mouse*

$CD24^{+}CD133^{+}$ and $CD24^{-}CD133^{-}$ cells stably expressing the luciferase gene, were injected IV into NOD-SCID mice via the tail vein 48 hours after induction of FA nephropathy. Mice were monitored after injection of the cells. Both kidneys were surgically removed and processed for histology.

2.3.13 *In vivo Bioluminescence assay*

For *in vivo* imaging, D-Luciferin (Beetle Luciferin, Potassium Salt, Promega) was made up to 15 mg/ml in sterile PBS and then filtered.
Mice were anesthetised using 2 % isoflurane in 75 % air/25 % O_2 (flow rate 2 L/min) and injected intraperitoneally with 150 mg/kg of D-luciferin. 10 minutes post injection mice were imaged using an AMI-X bioluminescence imaging device (Spectral Instruments, Tucson USA), with exposure time between 60 and 120 s. Image analysis was done using AMI-view software (Spectral Instruments). On completion of the imaging, mice were placed back in the cage and monitored for recovery which usually occurred within few minutes.

Image analysis

To quantify luminescence intensity, light radiance was measured. Regions of interest (ROI) were selected on the surface with the automatic ROI tool and the bioluminescence was measured quantitatively by the AMI-view software.

2.3.14 *Statistics*

Statistical analyses are outlined in each individual Chapter.

3 CHARACTERISATION OF HUMAN FETAL KIDNEY DEVELOPMENT AND CD24/CD133 EXPRESSION

Few studies exist that describe the normal morphological structure of the human fetal kidney at early- and mid- gestation. It is known that the definitive human kidney is formed by reciprocal interactions between two mesoderm derivatives: the epithelial ureteric bud and the metanephric mesenchyme.

The ureteric bud in the first stages invades the metanephric mesenchyme. The cap mesenchyme, a subpopulation of the metanephric mesenchyme, adjacent to the ureteric bud tips, differentiates towards epithelia through the mesenchymal to epithelial transition (MET). The cap mesenchyme is formed by a heterogeneous cell population that can self-renew and differentiate into renal epithelium, which express transcription factors such as *PAX2*, *SIX2* and *WT1* (Kreidberg, 2010, Self et al., 2006, Dressler, 2011).

These cells form pre-tubular aggregates first and renal vesicles after, which elongate to form a comma-shaped body and then reorganise into a S shaped body. The distal portion of the S shape forms the proximal convoluted tubule, the descending and ascending limbs of the loop of Henle, and the distal convoluted tubule, which fuses with the adjacent branch of the ureteric bud to form a continuous functional unit. The proximal S shape differentiates into the glomerular epithelium, the cleft is invaded by capillaries which form the mesangial region. The first fully developed and vascularised glomeruli are formed around 8 to 9 weeks of human gestation, and new nephron formation stops around 34 weeks of gestation (Woolf, 2003).

Several fate mapping studies have identified transcription factors expressed in cap mesenchymal cells and their derivatives.

Inconsistent data was reported in previously published work regarding CD24 and CD133 expression in the developing human fetal kidney (Lazzeri et al., 2007, Ivanova et al., 2010). Ivanova *et al*. showed CD24 and CD133 co-expression in condensed mesenchyme epithelial derivatives and ureteric bud, whereas CD133 expression was also observed in uninduced mesenchyme. Lazzeri *et al.,* confirmed co-expression of these markers on cap

mesenchyme epithelial derivatives while not observing CD133 immunoreactivity within the ureteric bud. These works did not specifically observe these markers expression by the cap mesenchymal cells. While addressing $CD24^{+}CD133^{+}$ as a self-renewing population derived from cap mesenchyme these reports did not show co-expression of CD24 and CD133 with *WT1*, *PAX2* and *SIX2*, known transcription factors characterising the self-renewing cell population in the fetal kidney.

Hypothesis and aims

My hypothesis was that CD24 and CD133 are expressed in the fetal kidney, particularly in the subset of self-renewing cells expressing *PAX2*, *SIX2* and *WT1*.

The first aim was to define the morphology of human kidney, as complexity increases through successive gestational stages.

This was performed with Periodic Acid Schiff (PAS) staining, a routine stain in use in our laboratory to define anatomy, it offers the advantage over the haematoxylin and eosin staining to highlight the basement membranes of all epithelial lined structures allowing proximal tubules to be identified by their brush border staining. PAS staining clearly demarcates the architecture of the kidney and the renal corpuscle.

My second aim was to assess CD24 and CD133 localisation, using human fetal kidney sections from different gestations.

The last aim was to better clarify CD133 expression in relation to potential progenitor cell pools using co-localisation experiments with anti- WT1, anti-SIX2 and anti-PAX2 antibodies.

3.1 RESULTS

3.1.1 *Histology of the developing kidney*

Development of early- and mid-gestation human fetal kidneys was carried out on 14 formalin fixed human kidneys, eight first trimester (week 8 to week 12) and six second trimester (week 13 to week 20) of known gestational age. Samples of different ages ranging from the 8^{th} to the 20^{th} week of gestation were collected from HDBR and processed for PAS staining.

Kidney sections of the first trimester of gestation, from 8 to 12 weeks were observed under low and high magnification and displayed a wide zone containing clusters of mesenchymal cells around the tips of the ureteric bud. In addition, early epithelial structures such as renal vesicles, comma and S-shaped bodies could be distinguished. At 9 weeks, deeper towards the medulla of the kidney, developing glomeruli with a network of capillaries were detected. Various immature tubules were observable lined by simple layer of cells without any surface modifications. In the kidney medulla were seen tubules with cuboidal cells without any distinct blood vessels.
From 13 weeks to 19 weeks, the wider nephrogenic cortex and thinner medulla were differentiated by a distinct cortico-medullary junction. At 20 weeks (Figure 3-1 I and J), when nephron formation moved forward, developing and mature glomeruli were widely diffused in the renal cortex. Mature renal corpuscles were observed with well differentiated Bowman's capsule and tuft of glomeruli within it.

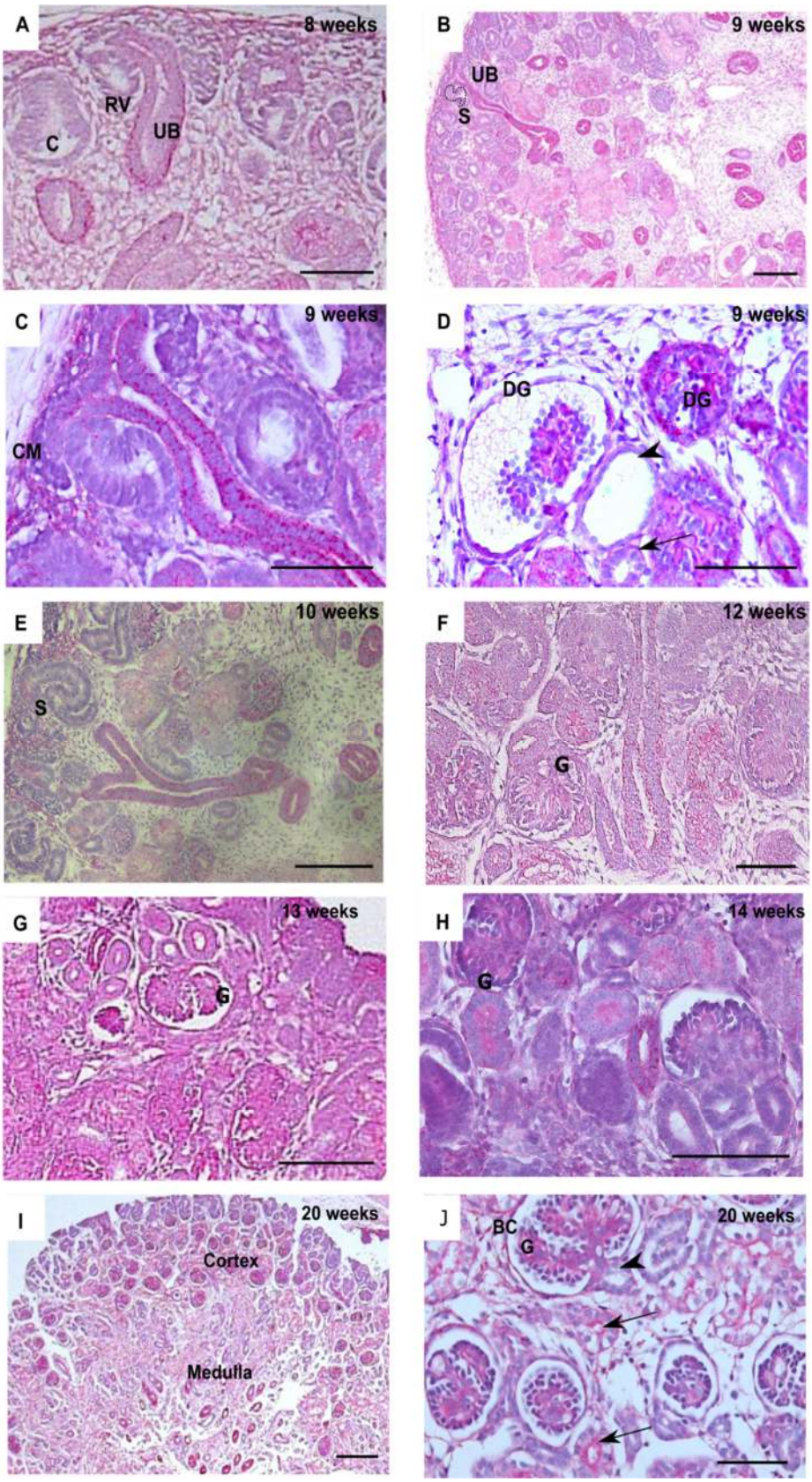

Figure 3-1 Human Fetal kidney sections of 9 to 20 weeks of gestational age stained with PAS.

(A) Eight weeks kidney section representative of 25 sections examined showing a wide nephrogenic zone at the edge, with early epithelial structures such as renal vesicle (RV) and comma-shaped body (C) close to the ureteric bud (UB). (B) Kidney development at 9 weeks showing developing ureteric bud (UB) and S-shaped body (S)(figure representative of 34 sections examined). (C) Higher magnification of 9 weeks kidney where cap mesenchyme can be better appreciated (CM). (D) Higher magnification of 9 weeks kidney showing developing glomeruli (DG), immature tubules, probably distal tubules (arrowhead) and proximal tubules without the specialised brush borders (arrow). (E) 10 weeks kidney section. S-shaped body (S) developed after several rounds of mitosis from the cap mesenchyme. (F) 12 weeks kidney. Glomeruli (G) visible within kidney cortex. Representative pictures of respectively 14 and 22 sections examined.(G) and (H) 13 and 14 weeks kidney sections showing early epithelial structures at the periphery of the kidney and several layers of developed glomeruli (G) (representative of 14 and 6 sections examined of each age). (I) and (J) at 20 weeks there is a clear distinction among cortex and medulla. Mature renal corpuscles with differentiated Bowman's capsule (BC), developed glomeruli (G) with capillaries network, proximal tubules with brush borders (brush borders in pink, arrow) and distal tubules (arrowhead). Figure representative of 12 sections examined. A, C, D, F, G, H scale bar= 100 μm. B,E, I scale bar= 200 μm J scale bar= 50 μm

3.1.2 *Expression of CD24 and CD133*

To distinguish the localisation of each marker, I used immunofluorescence on kidney section with primary antibodies directly conjugated to different fluorophores. Compared to immunohistochemistry with 3,3'-Diaminobenzidine (DAB), immunofluorescence gives the possibility to distinguish on the same section, markers with the same sub-cellular location, as CD24 and CD133, both surface markers.

Anti-CD133/2-PE and anti-CD24-FITC antibodies were used in direct immunofluorescence experiments, antibodies used are listed in Table 2-1. Direct immunofluorescence compared to indirect-immunofluorescence has the disadvantage of producing a lower signal, missing the step of incubation with secondary antibodies that can greatly amplify the signal (as more than one secondary antibody can attach to each primary antibody).

CD24 expression was assessed in 9 weeks kidney sections (Figure 3-2). CD24 staining was detected at the tips of the ureteric bud and in epithelial derivatives of the condensed mesenchyme.

Weak CD133 staining could be detected, at 9 weeks, in the apical membrane of the ureteric bud (UB, Figure 3-2) while stronger staining was observed in the proximal tubule (PT). CD133 immunoreactivity was also seen in the comma (C) and S-shaped body (S) derived from the condensed mesenchyme as well as the Bowman's capsule of forming glomeruli (BC).

A very faint staining was observed in the cap mesenchyme around the ureteric bud tip. To confirm this data, I performed CD133 double labelling with cap mesenchymal markers such as SIX2, WT1 and PAX2.

At 9 weeks, key nephrogenesis steps are occurring in the developing kidney, which is enriched in stem/progenitor cells residing in the cap mesenchyme and in the early epithelial derivatives formed after MET. At this age, we have the great advantage of being able to target progenitors and to confirm whether isolation of CD24 and CD133 expressing cell population effectively targets a stem/progenitor cell population.

The co-localisation of CD24 and CD133 was therefore analysed by immunohistochemistry on 8-9 weeks gestation kidney sections. CD24 and CD133 co-localised in the early epithelial structures derived from the cap mesenchyme such as renal vesicle and comma-shaped body as shown in Figure 3-4. In addition, co-staining was observed in forming epithelial tubules. CD133 was dimly expressed in the ureteric bud,

while CD24 showed stronger expression at the tips of the ureteric bud. These observations were in accordance with Ivanova et al. study whereas they were in contrast with Lazzeri et al., observation that CD133 only targets cap mesenchyme-derived early progenitor epithelial cells.

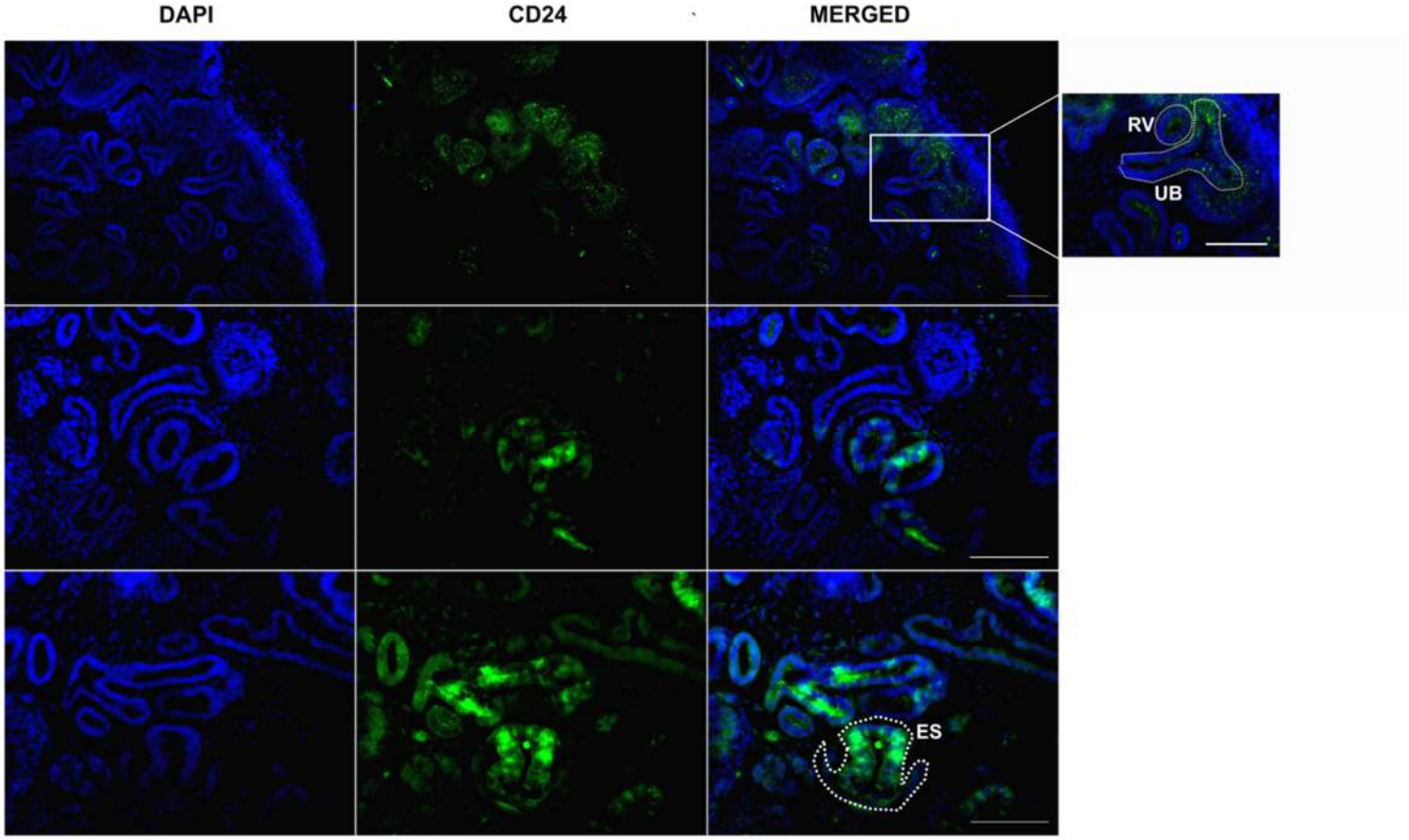

Figure 3-2 CD24 localisation on 9 weeks kidney.

Anti-CD24 antibody appeared to stain faintly early developing ureteric bud (UB), renal vesicles (RV) and epithelial structures (ES), whereas CD24 expression was not detected within cap mesenchyme. According to staining in 9 weeks kidney, CD24 expression observed in epithelial derivatives of the cap mesenchymal self-renewing cells and the developing ureteric bud, suggested that this protein targets cells committed towards epithelial lineage and is not specific to an early progenitor cell population derived from cap mesenchymal cells. Top right panel is a high-power magnification of ureteric bud. Scale bars are 100 μm.

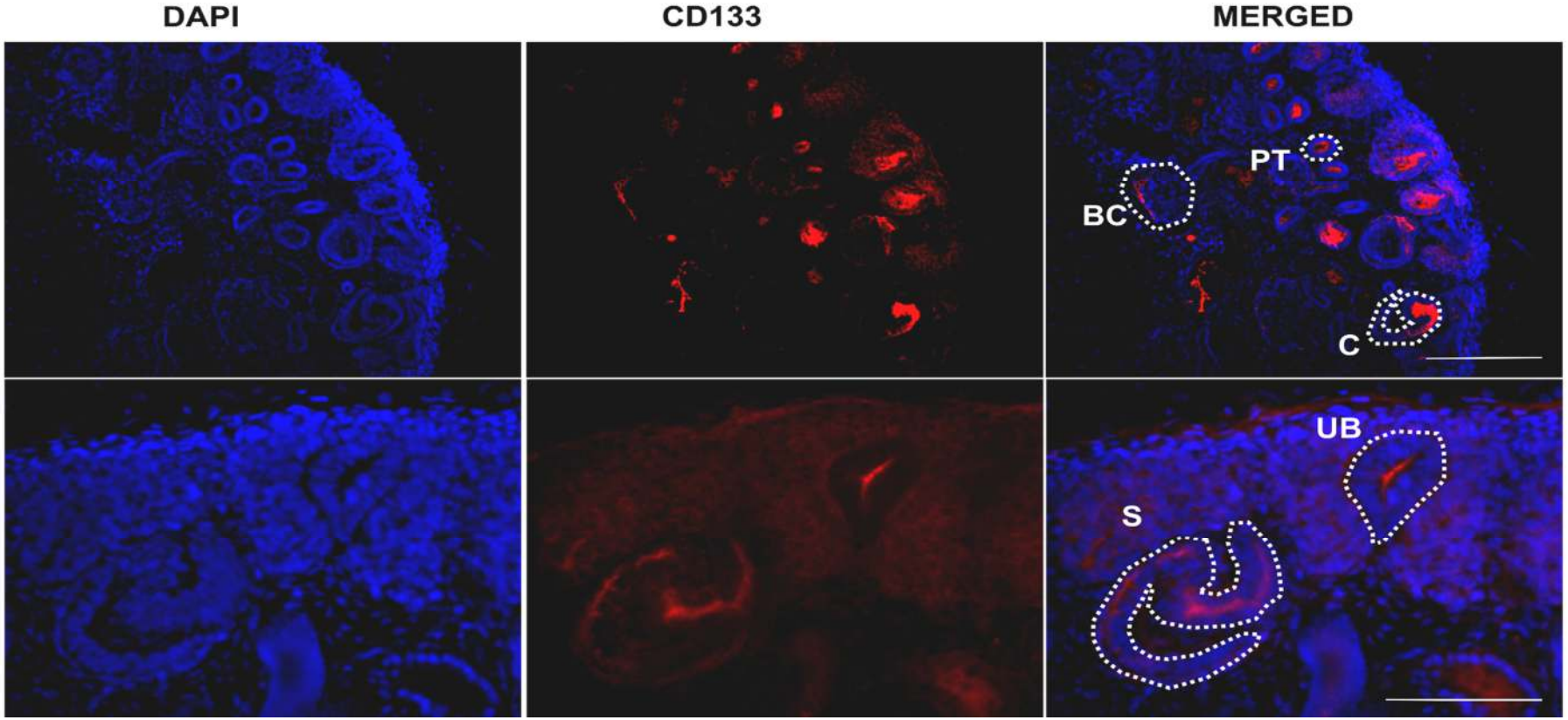

Figure 3-3 CD133 localisation on 9 weeks kidney.

Representative figure of CD133 staining on kidney sections of 9 weeks of gestation. In the upper panel merged picture, positive staining was observed in developing proximal tubules (PT), comma shaped body (C) and in the Bowman's capsule (BC). The lower panel shows higher power views with CD133 immunoreactivity detected in the ureteric bud lumen (UB) and S-shaped body (S). CD133 staining, similarly to CD24 staining, suggested that this marker expression was not restricted to the cap mesenchyme-derived cells, but it also targeted ureteric bus cells, which will form the collecting ducts of the nephron. Scale bas are 100 µm (upper right panel) and 200 µm (bottom right panel).

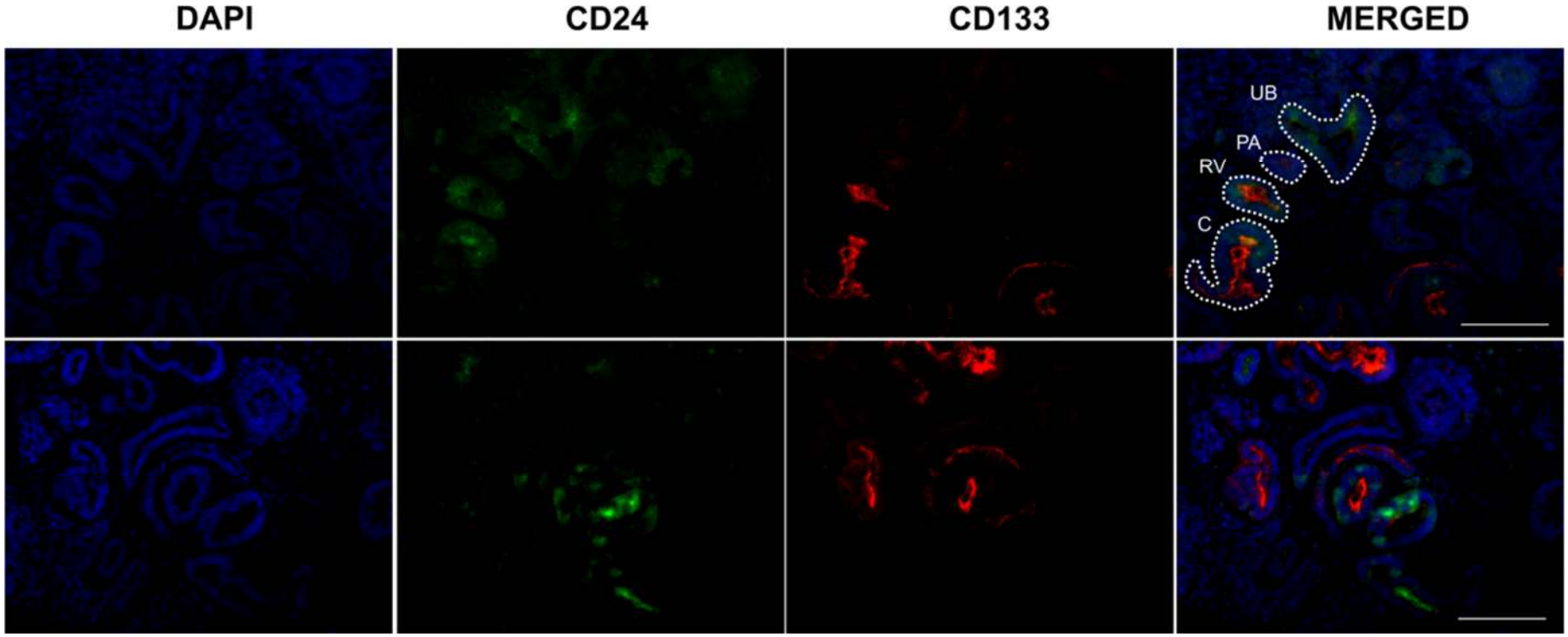

Figure 3-4 CD24 and CD133 co-localisation on 9 weeks kidney sections.

CD24 and CD133 co-localised in the early epithelial structures derived from the condensed mesenchyme such as renal vesicle (RV) and comma-shape body (C), weak expression of both proteins was observed in the pre-tubular aggregates (PA), composed of cells committed to undergo mesenchymal to epithelial transition. Tips of the ureteric bud (UB) appeared to be positive for CD24 whereas weak expression of CD133 at the apical side of ureteric bud was observed. Bottom panels show CD24 and CD133 localisation in forming epithelial tubules. Co-localisation stainings suggested that CD24 and CD133 targets epithelial cells both from cap mesenchyme and ureteric bud, these are therefore not restricted to one of these mesoderm derivatives but generally targeting an epithelial cell line. Bars are 100 μm.

3.1.3 *CD133 co-localisation with progenitor markers*

Double staining of CD133 with PAX2, SIX2 and WT1 was performed to better characterise CD133 localisation in the nephrogenic zone in order to examine whether this marker was linked to the self-renewing cap mesenchyme cell lines expressing these factors.

These transcription factors specify the stem/progenitor cell population within the cap mesenchyme. It was thus novel and interesting to understand whether CD133 would also address the same population or it would only be found in epithelial cells derived from cap mesenchyme and already committed to differentiate towards the tubular compartment of the nephron.

For this reason, 9 weeks of gestation human kidney frozen sections were stained with antibodies against the stem cell transcription factors PAX2, SIX2 and WT1 in association with the antibody against CD133/1 (AC133/1).

Anti-PAX2 antibody positively stained the nuclei of cap mesenchyme and its epithelial derivatives as well as the ureteric bud cells (Figure 3-5 top panel).

CD133 was observed apically on the cell membrane of the early epithelial structures derived from the cap mesenchyme and within some ureteric buds always in the same location (apical membrane). CD133 and PAX2 appeared to specify the ureteric bud cells and other epithelial cells, with CD133 expressed on cell surface, particularly apically on cell protrusions and PAX2 being expressed within the nucleus. However, It was not possible to clearly ascertain whether PAX2 and CD133 co-localised in the same cell type due to low resolution of the fluorescence microscope. To confirm this data, confocal microscopy should be used.

As shown before, SIX2 specifies renal progenitors and its expression was seen specifically in the cap mesenchyme (‘CM’, Figure 3-5). CD133 appeared to be not expressed in the cap mesenchymal cells, while its expression was restricted to the ureteric bud and to epithelial structures.

As observed in previous studies, WT1 was expressed in the cap mesenchymal cells (Fanni et al., 2011) when cells were undergoing mesenchymal to epithelial transition (Figure 3-5 arrows). Contrary to CD133, WT1 localisation was not observed in the ureteric bud. CD133 and WT1 appeared to co-localise in the proximal loop of the S-shaped body.

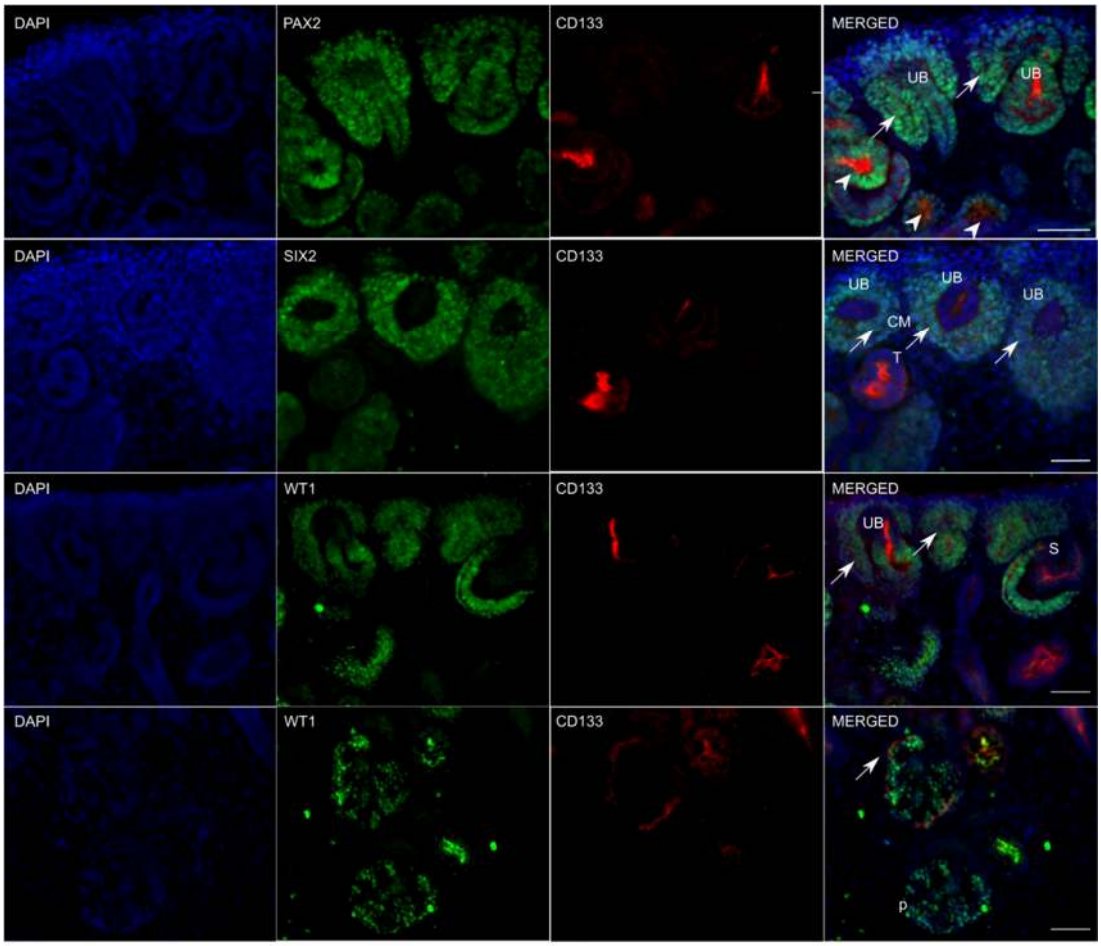

Figure 3-5 CD133 staining with PAX2, SIX2 and WT1 in the nephrogenic zone of human fetal kidney on the 9th week of gestation.

First row from the top shows DAPI staining (blue), PAX2 staining (green) and CD133 staining (red). The last panel is the merged figure. PAX2 was observed in both ureteric bud (UB) and cap mesenchyme cells (CM). CD133 staining was only seen in ureteric bud. In the merged figure, PAX2 and CD133 co-localised to the ureteric bud (UB) and to the early epithelial derivatives of the condensed mesenchyme (arrowheads), whereas PAX2 expression was also observed in the condensed mesenchyme (arrows). Second row from the top show DAPI in blue, SIX2 in green and CD133 in red. SIX2 was expressed by cap mesenchymal cells, whereas CD133 appeared in the lumen of ureteric bud. Merged figure showed expression of SIX2 in the cap mesenchymal cells (CM and arrows in the merged figure) whereas CD133 antibody strongly stained the ureteric bud (UB). Third and fourth row from the top shows DAPI staining (blue), WT1 staining (green) and CD133 (red). When co-labelled with CD133 and WT1, fetal kidney sections showed co-staining in the proximal side of the S-shaped body (S). WT1 expression characterised condensed mesenchyme (arrows) and podocytes (p) in mature glomeruli, while CD133 was expressed in parietal epithelial cells (arrow). Staining of CD133 with progenitor markers WT1, SIX2 and PAX2 showed that CD133 is not expressed within cap mesenchyme and it is expressed in epithelial structures from both mesodermal derivatives. Scale bars =50 μm.

3.2 SUMMARY

Kidney histology was examined with PAS staining in early and late gestation kidneys (8 to 20 weeks). In early gestation samples, ureteric bud and cap mesenchyme were evident, as well as the epithelial cell populations differentiated from those constituting structures such as renal vesicles, comma and S-shaped bodies, developing glomeruli and immature proximal and distal tubules. Later gestation kidneys (from 13 to 20 weeks) showed a thinner layer of nephrogenic zone compared to early gestation kidneys, more layers of completed structures such as glomeruli with their tubular compartment extended across the kidney. Glomeruli also comprised of a well-developed capillary network and proximal tubules epithelium acquired the typical microvilli-covered surface called 'brush borders'.

CD24, CD133 expression in fetal kidneys was assessed by immunofluorescence on frozen sections. For these experiments, CD24 and CD133 mouse monoclonal antibodies were used. CD24 antibody was raised against NALM-1 human pre-B leukemia cell line and extensive literature reports showed specificity to kidney parietal epithelial cells in the Bowman's capsule of human adult kidneys, podocyte progenitors, proximal tubule, distal tubule and both cap mesenchyme and ureteric bud derivatives (Sagrinati et al., 2006, Lazzeri et al., 2007, Ronconi et al., 2009b, Lasagni et al., 2010, Angelotti et al., 2012). Anti-CD133 monoclonal antibodies recognizing CD133/1 (clone AC133) epitope was used. This was previously reported to selectively stain condensed mesenchyme-derived structures and, in maturing glomeruli, the urinary pole of the Bowman's capsule (Angelotti et al., 2010).

These antibodies were thus chosen as there was evidence in the literature of their tissue selectivity. However, a limitation of these experiments consisted in a thorough antibody validation. In fact, CD24 and CD133 should also have been tested in cells/tissues that expressed such proteins (positive controls) as well as cells/tissues that did not express the aforementioned proteins as a proper negative staining control.

Expression of CD24, CD133 surface markers was observed in the early gestation kidneys of 9 weeks, as at this age the majority of nephron structures were still immature constituting a reservoir for progenitor cell populations.

CD24 localised on the surface of the epithelium layer composing the ureteric bud, in particular its tips, suggesting a possible role of this protein towards the neighbour mesenchymal cells. Moreover, CD24 was not observed in cap mesenchyme itself,

however positive stain was restricted to cap mesenchymal derivatives such as renal vesicle, comma and S-shaped bodies.

CD133 localised to the apical side of the epithelium of ureteric bud and immature structures derived from the cap mesenchyme. When kidney sections were co-stained for CD24 and CD133, these proteins appeared to co-localise to ureteric bud epithelium, early epithelial structures cap mesenchyme derived and tubules.

CD133 localisation was compared to the expression of PAX2, SIX2 and WT1. As expected, PAX2 localised in the cap mesenchyme and ureteric bud, while SIX2 was specifically expressed by cap mesenchymal cells and WT1 was expressed by cap mesenchymal cell population, its derivatives committed to become podocytes (proximal part only of the S-shaped body) and the podocytes of maturing and differentiated glomeruli. CD133 only appeared to co-localise with PAX2 in the ureteric bud epithelium and with WT1 in the proximal lumen of the S-shaped bodies. However, when WT1 brightly stained differentiated podocytes in glomeruli, CD133 expression appeared to be restricted to subset of Bowman's capsule cells.

In summary, the data reported here suggested the following:

- According to published reports, CD24 and CD133 localised in condensed mesenchyme derived structures
- Differently from Lazzeri *et al.* study, CD24 and CD133 were both expressed by the ureteric bud cells, thus suggesting that these markers are not specific to epithelial cells derived from the cap mesenchyme.

Furthermore, co-staining of CD133 with PAX2, WT1 and SIX2 indicated no evidence of CD133 expression by the cap mesenchymal cell compartment itself.

The data I reported regarding CD133 expression went beyond Lazzeri *et al.* study because I additionally showed reactivity of CD133 antibody also in the ureteric bud epithelium. This may relate to unknown variation between laboratories or perhaps to differences between the antibody, although I tried to reduce variability by using the same antibody reported in Lazzeri's paper (clone AC133), sections from similar gestational ages and the same technique of fluorescence microscopy on frozen sections. Nevertheless, I am confident that my results were reproducible and that CD133 in the ureteric bud epithelium is real expression. Co-staining with epithelial markers, such as E-cadherin, would be helpful in the future.

Although these findings should be taken with caution, they suggested that CD24 and CD133 are markers expressed by epithelial cells, being observed only in epithelial derivatives (renal vesicle, comma bodies, S-shaped bodies, tubular compartment, ureteric bud) and being absent in mesenchymal cells (condensed mesenchyme). The advantage of my study over published report is that it suggests that CD24 and CD133 appear to target epithelial cell lines in general, thus not a specific cell line derived from cap mesenchyme. For this reason, targeting $CD24^{+}CD133^{+}$ cells in 9-weeks old fetal kidneys might isolate cells composing the following structures:

- ureteric bud
- pre-tubular aggregates
- renal vesicles
- comma-shaped bodies
- S-shaped bodies
- Bowman's capsule
- proximal and distal tubules
- collecting ducts

Being epithelial committed cells, it suggested that such cells would be progenitor cells with a limited self-renewal capacity and therefore not a renal stem cell population. However, they could be precious for tissue regeneration of the tubular compartment of damaged kidneys if proved of being able to have such capacity.

4 ISOLATION OF CD24+CD133+ AND CD24-CD133- CELL POPULATIONS

In the previous chapter, I have shown co-localisation of surface proteins CD24 and CD133 in early epithelial structures derived from the cap mesenchyme and in immature tubules in human fetal kidneys of 9 weeks of gestation.

Hypothesis and aims

Having localised these markers in the kidneys, I hypothesised that CD24 and CD133 markers could be used to isolate an epithelial progenitor cell line from human fetal kidneys.

Isolation of progenitor cells from fetal as well as adult kidneys has been previously performed targeting CD24 and CD133. Lazzeri *et al*., obtained total cell suspensions from embryonic kidneys with gestational age of 8.5 to 9 weeks and checked CD24 and CD133 markers expression by flow cytometric analysis, observing that the $CD24^{+}CD133^{+}$ cells are between 35% to 50% of the total cell population (Lazzeri et al., 2007). This number decreased in later gestational ages and in adult kidneys. This led to the hypothesis that the older the kidney gets, the less immature stem/progenitor CD24/CD133 expressing cells, are present.

Ivanova *et al*. analysed the same population with a slightly different approach, 48 hours *in vitro* culture of renal cortical cells from fetal kidneys of 14 to 18 weeks was performed prior to analysis and sorting, showing that the 13% of the total cell population was $CD24^{+}CD133^{+}$, the 16% was $CD24^{+}CD133^{-}$, the 43% was $CD24^{-}CD133^{-}$ and the 2% was $CD24^{-}CD133^{+}$ (Ivanova et al., 2010). These results similarly to Lazzeri *et al*. showed that mid-gestation fetal kidney cells even when cultured for 48 hours had similar pattern to not cultured kidney cells of the same age (Lazzeri et al., 2007).

Differently from Romagnani's group, Dekel's group found that CD24 and CD133 cells are high in percentage also in later gestational ages: Metsuyanim *et al*, analysed human fetal kidneys of 15 to 19 weeks and adult kidney derived cells for CD24 and C133 expression (Metsuyanim et al., 2009). Fetal kidneys cells were cultured and at low passage (passage 0 and passage 1), CD24 and CD133 FACS analysis was performed. In

these samples 56.9±15.8% and 73.6±20.6% of cells were represented by $CD133^+$ and $CD24^+$ cells respectively. In addition, the same subpopulation composed the 64.26±10% in adult kidneys. The same authors analysed $CD24^+$, $CD133^+$ cells present in the epithelial cell adhesion molecule (EpCAM) positive population. EpCAM is a marker expressed highly by the ureteric bud and weakly by comma and S- shaped bodies of early gestation kidneys (Trzpis et al., 2008). Thus, EpCAM expression correlates with the degree of epithelial differentiation, where dim EpCAM is associated with less mature epithelial structure and bright EpCAM with differentiated epithelia. When CD24 and CD133 were analysed in regard with EpCAM sub-population, the $CD24^+$ cells constituted approximately the 80% of EpCAM bright cells and similarly the largest fraction of CD133 expressing cells was contained in EpCAM bright cells.

Romagnani's group addressed CD24 and CD133 as markers specifying a 'stem/progenitor cell population, whereas Dekel's group suggested that CD24 and CD133 cells are expressed by differentiated epithelial cells.

Furthermore, a lack of congruence was observed among literature data showing a high percentage of cells CD24 and CD133 double positive and the apparent CD24/CD133 staining on human fetal kidney sections I analysed. My immunostaining data on 9 weeks fetal kidney sections, suggested that CD24 and CD133 double expressing cells are a low percentage of the total cell population within 9 weeks human fetal kidneys.

For this reason, I aimed to demonstrate whether any of my findings supported one or the other side of the previous findings, also adding a novel contribution by investigating the influence of *in vitro* culture to the generation and maintenance of $CD24^+CD133^+$ cell population.

To achieve this, I proceeded with the isolation of CD24 and CD133 co-expressing cells from early gestation kidneys (8 to 10 weeks).

Compared to published data, my study was different for:

- The cell populations sorted: fetal renal cells outgrown from kidney specimens were first cultured *in vitro* before sorting. In addition, it was sorted not only the CD24, CD133 double positive cell population, but also the heterogenous double negative cells of the same sample.

-The sorting technique used: I have used FACS and not the Magnetic Activated cell sorting used in Romagnani's paper. Furthermore, I have assessed the isolation quality by confirmation of CD24 and CD133 expression from isolated double positive cells and lack of expression in double negative cells after sorting.

- The study of *in vitro* culture effects on the above-mentioned cell populations. For each cell line, I have assessed at distinct cell passages, changes in cell morphology with light microscopy and CD24 and CD133 mRNA expression by Q-PCR.

4.1 RESULTS

4.1.1 *Isolation of $CD24^+CD133^+$ and $CD24^-CD133^-$ cell populations*

Isolation from fresh collected kidney samples

Total cell suspension was obtained from fetal kidneys with gestational age of 8 and 10 weeks (n=3, two 8 weeks and one 10 weeks). These were collected and immediately processed for FACS sorting. Total cell suspensions obtained from fetal kidneys labelled with CD24-PE and CD133-APC was run through the FACS sorter machine.

The gating strategy is shown in Figure 4-1. Cell population was first gated according to its light scatter properties. Dead cells that tend to have lower forward scatter and higher side scatter than living cells were distinguished. The resulting cell subpopulation was then further gated to exclude doublets by using side scatter area against side scatter width. Subpopulations were then analysed for the expression of CD24-PE and CD133-APC. These final gates were positioned by comparison with gates drawn from appropriate controls. Controls consisted of isotypes of the antibodies conjugated to the same fluorochromes, and fluorescence minus one control, consisting of CD24-PE or CD133-APC single controls.

Sorting experiments were analysed off-line with the use of the software Flowjo. Samples exhibited a range of 4% to 7% of cells co-expressing both CD24 and CD133, 34% to 60% not expressing these proteins, 35% to 61% expressing CD24 only and 0.1%-0.3% expressing only CD133 (Table 4-1).

As observed before by Romagnani's group, in fresh human fetal kidneys 99.7%-99-9% of the cells positive for CD133 were also positive for CD24 (Lazzeri et al., 2007).

After FACS sorting, $CD24^+CD133^+$ and $CD24^-CD133^-$ were assessed for their purity. $CD24^-CD133^-$ showed a good level of purity (90% of total cell population was $CD24^-CD133^-$), the $CD24^+CD133^+$ were 20% of the total cell population isolated, with the rest expressing only CD24 but not CD133 (Figure 4-2).

Isolated cell populations were then placed in culture, however, the subpopulation isolated from the 10 weeks kidney recovered well in culture, reaching enough confluence to be further amplified, whereas the 8 wk samples did not recover post sorting and did not attach to culture vessel. The following experiments were performed on human fetal renal cells cultured prior to FACS.

This was the result of mainly two considerations:

- Kidney samples collected from HDBR both in London and Newcastle were delivered to the laboratory 24 hours to 48 hours after the collection, being stored at 4°C during transport. I reasoned that this period could affect cell vigour/robustness/health. Consequently, I was worried that an immediate FACS sorting experiment straight after delivery might increase the risk of cell mortality, and there was no way to know if different cell types might be more or less prone to such a fate.
- Supply of fetal material was often patchy and always unpredictable, hence planning the sorting experiment was very complicated since I could not book the FACS sorter until samples were confirmed on the day of collection.

To avoid these issues with cells mortality and to facilitate the experiment planning, cells were cultured *in vitro* before FACS sorting.

Isolation from cultured renal cells

Kidneys collected from HDBR ranging from 8 to 9 weeks of gestation (n=16) were diced and placed in culture. Cells migrating from kidney specimens were cultured until 70 % of confluence and then processed for flow cytometry cell sorting. $CD24^{+}CD133^{+}$ and $CD24^{-}CD133^{-}$ cell subpopulations were isolated. $CD24^{-}CD133^{-}$ cells represented, on average the 46.2 % ± 5.7 (mean ± SEM) of the total cell population when analysed after sorting, while the double negative for CD24 and CD133 were 20.8% ± 4.2 (mean ± SEM). After FACS cells were seeded in sterile tissue culture dishes.

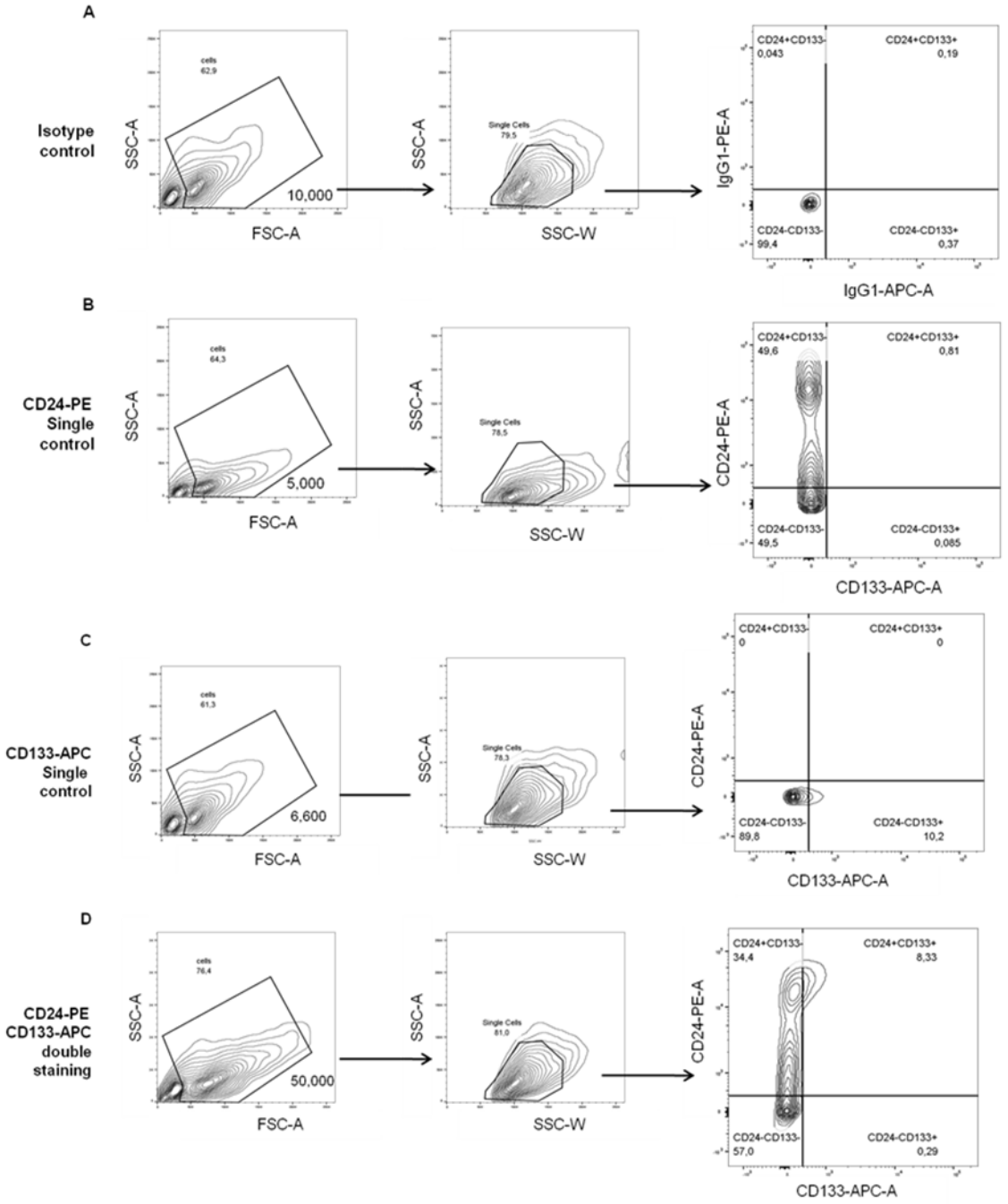

Figure 4-1 Analysis of FACS sorting experiment performed on freshly collected 10 weeks human kidney.

Cell suspension obtained from 10 weeks kidney (n=1) stained with CD24-PE and CD133-APC. Controls consisted of IgG1 isotype antibodies conjugated to PE or APC and single CD24-PE or CD133-APC labelled cell samples. Flow cytometric cell sorting for $CD24^{+}CD133^{+}$ and $CD24^{-}CD133^{-}$ was performed using the BD FACS Aria cell sorter. Events acquired in each sample are displayed as contour plots. A progressive gating scheme was used to identify and sort out CD24, CD133 expressing renal cells. Live cells were first gated according to forward and side scatter (left panels), from this subpopulation, doublets were excluded using side scatter area against width (middle panels). This subpopulation was then grouped into four quadrants (right panels): bottom left $CD24^{-}CD133^{-}$, upper left $CD24^{+}CD133^{-}$, upper right $CD24^{+}CD133^{+}$ and $CD24^{-}CD133^{+}$ bottom right. In each plot, the fraction of cells in the gate is shown as a percentage on the parental population. In these graph a logical scaling was applied. The number of events acquired is reported in the left panels. Gates were first drawn according to the isotype controls (A) and with the PE and APC single controls (B, C). (B) $CD24^{+}$ single positive cells were 49.6% of the parental population, $CD24^{-}$ composed the 49.5% of the gated population (C) $CD133^{+}$ positive cells were 10.2%. (D) When double labelled for CD24 and CD133, 57.0% were $CD24^{-}CD133^{-}$, 34.4% $CD24^{+}CD133^{-}$, 0.29% $CD24^{-}CD133^{+}$ and 8.33 $CD24^{+}CD133^{+}$%. When fresh human fetal kidney cells were analysed at FACS, only a small percentage showed positivity for both markers, moreover it was observed that the small percentage of CD133+ cells were also positive for CD24. These results suggested that only a small subset of the total cell population expressed both markers, being the 49.5% represented by $CD24^{+}$ cells negative for CD133.

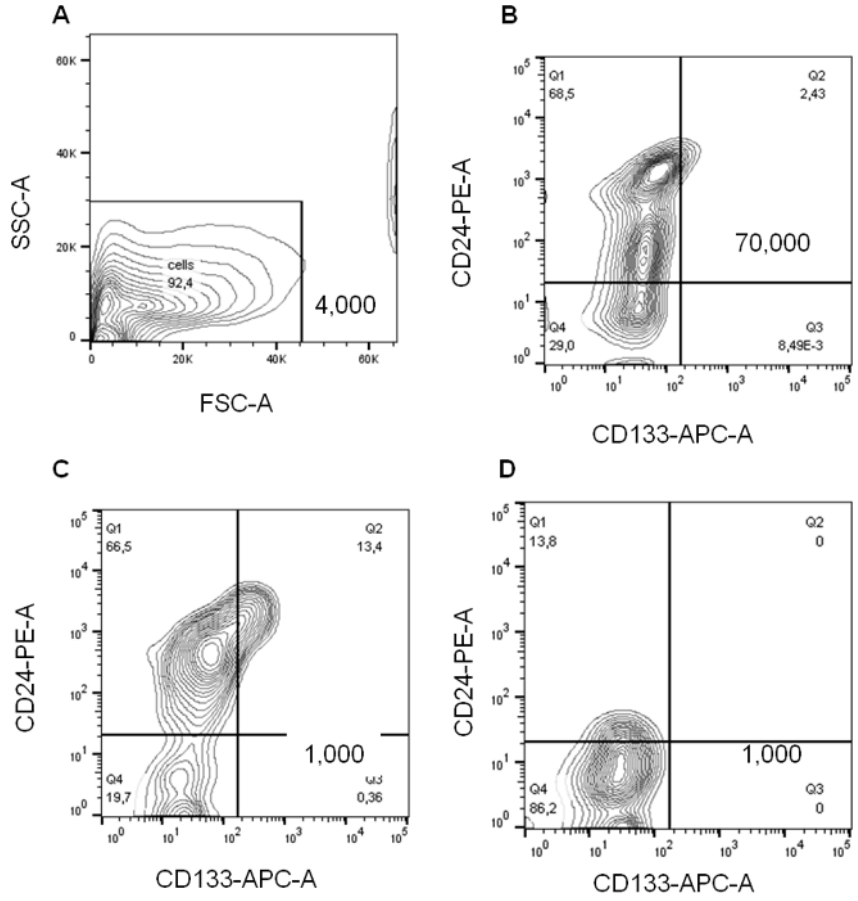

Figure 4-2 FACS sorting on freshly collected 8 weeks kidney.

FACS sorting on freshly collected 8 weeks kidney. FACS sorting on freshly collected 8 weeks kidney. FACS gating strategy was applied as explained in Figure 4-1. (A) Contour plots of the negative isotype controls IgG1-APC and IgG1-PE. (B) Sample labelled with CD24-PE and CD133-APC. (C) Purity check of sorted $CD24^{+}CD133^{+}$cells showed low purity. (D) Purity check of $CD24^{-}CD133^{-}$ after sorting showed almost 90% of $CD24^{-}CD133^{-}$ with 11.9% of $CD24^{+}$ contamination. Figures representative of experiments on 8 weeks kidneys (n=2).FACS analysis showed that $CD24^{+}CD133^{+}$ constituted only the 2% of the total human fetal kidney cells at early stage of 8 weeks, the percentage was even lower than the 10 weeks kidney suggesting that double positive cells might increase in number with the increment in kidney gestational age. Furthermore, as noticed previously, the CD133+ cells were also positive for CD24.However, when CD24, CD133 cells were isolated and then re-analysed with FACS (C), they showed a low percentage of double positive cells, therefore it appeared that the isolation did not achieve a good purity and the populations isolated might have been contaminated with single positive or double negative cells.

Table 4-1 FACS analysis of CD24, CD133 expression (in percentage) in freshly sorted fetal kidney cells

Sample gestational age	Cell surface protein expression (%)			
	$CD24^{-}CD133^{-}$	$CD24^{+}CD133^{-}$	$CD24^{-}CD133^{+}$	$CD24^{+}CD133^{+}$
10 wks	57.0	34.4	0.29	8.3
8 wks +	29.0	68.5	0	2.43
8 wks +	35.1	62.1	0.03	2.74

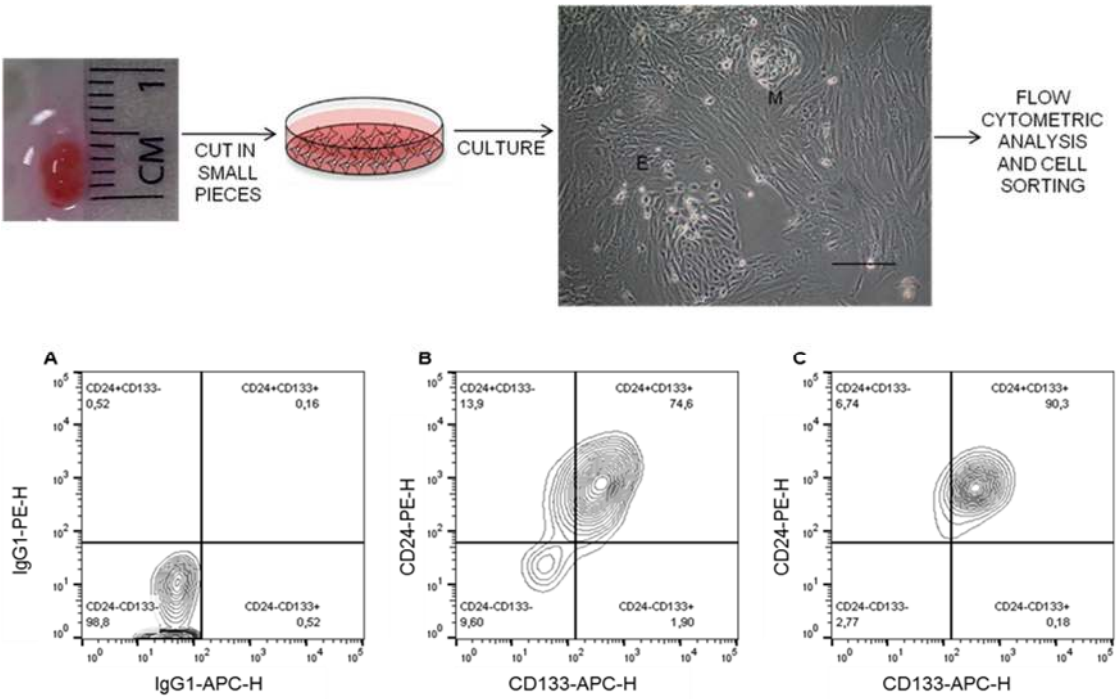

Figure 4-3 FACS sorting performed on cultured fetal kidney cells.

Upper panel summarises the steps prior to cell sorting from cultured renal cells. Kidneys of 8 to 9 weeks (n=16) were collected and cut into small pieces. These were transferred into plastic tissue culture dishes and cultured until 70% confluent. Cells outgrown from kidney specimens showed mixed morphology with appearance of mesenchymal (M) and epithelial-like cells (E). Cells were then trypsinised and processed for FACS sorting. Lower panel (A) contour graph of isotype controls. (B) Contour graphs depicting CD24-PE and CD133-APC stained cells. (C) Post-isolation purity control. Cultured renal fetal cells expressed a evidently higher CD24,CD133 double positive cells compared to the uncultured renal cells sorted straight after collection. Furthermore, these were easier to isolate as purity check run on isolated double positive cells revealed 90%of purity of the isolated cell population.

Table 4-2 FACS analysis of CD24 and CD133 cell surface protein expression on cells derived from 8 to 9 weeks human fetal kidneys (n=16)

Sample gestational age	**Cell surface protein expression (%)**			
	$CD24^{-}CD133^{-}$	$CD24^{+}CD133^{-}$	$CD24^{-}CD133^{+}$	$CD24^{+}CD133^{+}$
9 WKS	7.8	42.7	1.8	47.8
8 WKS+	17.6	36.8	1	44.6
8 WKS+	3.9	44.5	2.5	49.1
8 WKS+	2.2	16.6	3.7	77.5
9 WKS	8	34.1	2.8	55.1
9 WKS	2	11.5	1.4	85.1
9 WKS	39.6	31.5	5.82	23.1
9 WKS	13	16.9	1.3	68.7
9 WKS	34.6	44.2	9.5	11.7
9 WKS	30.8	27	14	27
9 WKS	14.3	35.8	2.6	47.3
8 WKS+	11.6	41.6	0.9	45.9
8 WKS+	45.0	8	3.9	42
8 WKS+	24.6	27.2	18.1	30
8 WKS+	19.7	8.7	8.1	76.4
WKS +	58	18.2	14.5	8.5
Mean ± SEM	20.8± 4.2	27.8 ± 3.2	5.7 ±1.4	46.2 ± 5.7

4.1.2 *CD24, CD133 surface protein expression after FACS sorting*

After cell sorting was performed, $CD24^+CD133^+$ cells purity was evaluated by re-running a small aliquot of isolated cells. Analysis showed that $CD24^+CD133^+$ were 95% ± 1.0 (mean ± SEM) pure.

Isolated cell populations were also analysed for the expression of CD24 and CD133 surface proteins by immunocytochemistry after 2 passages in culture. $CD24^+CD133^+$ and $CD24^-CD133^-$ cells were seeded onto chamber slides coated with fibronectin, fixed after one day and observed at the fluorescence microscope to detect CD24-FITC and CD133-PE fluorescence. As expected, both CD24-FITC and CD133-PE fluorescence signal was detected from $CD24^+CD133^+$ cells, while $CD24^-CD133^-$ appeared as negative for both markers.

Cells after sorting were re-analysed at the flow cytometer to evaluate the surface markers expression. $CD24^+CD133^+$ after 2 passages showed an average expression of CD24 and CD133 of 79.3% ± 6.7 (mean ± SEM) and 67.6% ± 13 (mean ± SEM) respectively (3 cell lines analysed), while only the 0.7% ± 0.4 (mean ± SEM) and 7% ± 6 (mean ± SEM) of the $CD24^-CD133^-$ cells analysed expressed CD24 and CD133 (Figure 4-4).

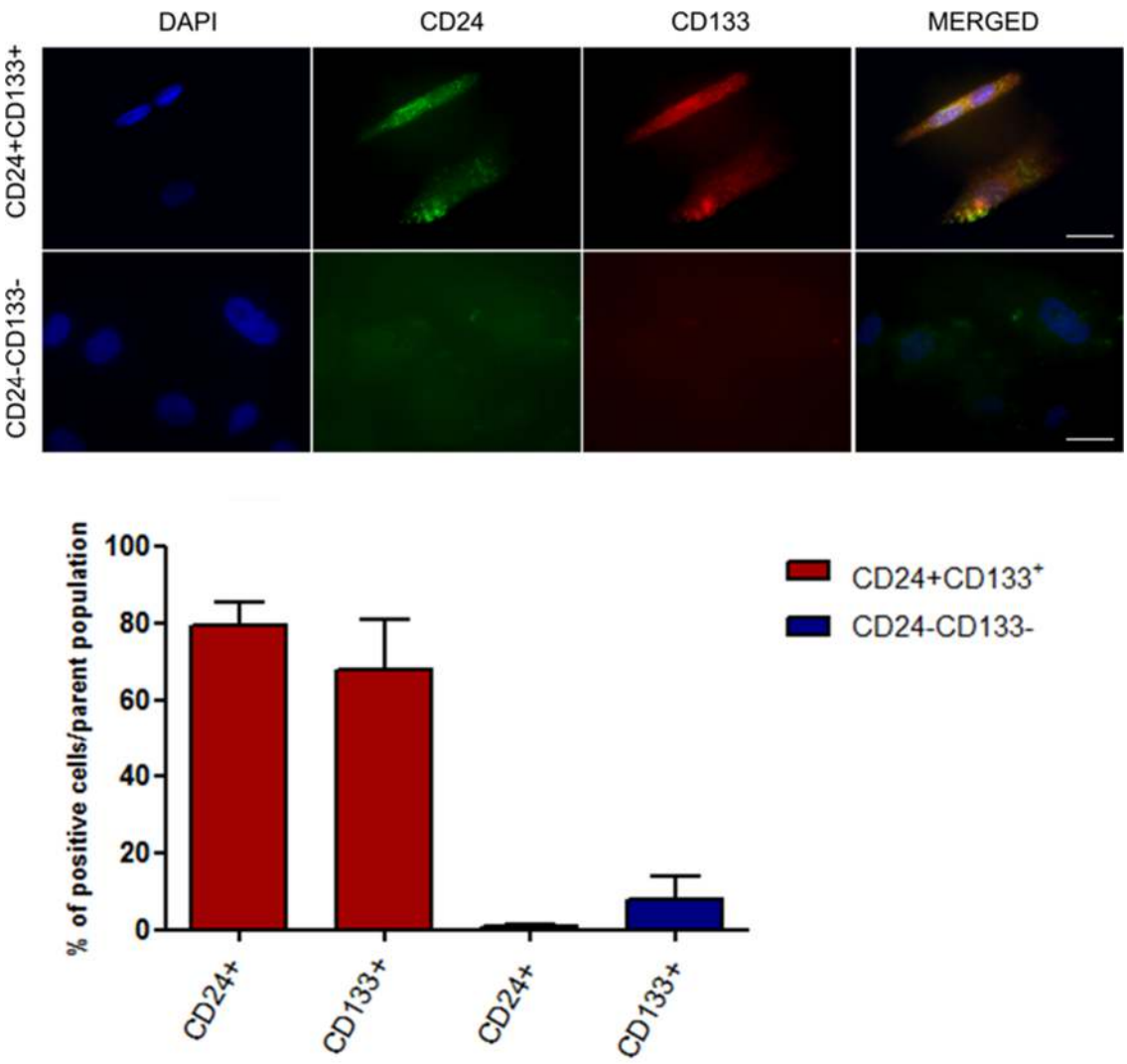

Figure 4-4 CD24, CD133 surface markers expression by FACS in generated cell lines after 2 passages in culture.

Upper panel shows staining of isolated $CD24^{+}CD133^{+}$ and $CD24^{-}CD133^{-}$ with $CD24^{-}$FITC and CD133-PE. Positive staining, as expected, was detected on $CD24^{+}CD133^{+}$ while $CD24^{-}CD133^{-}$ did not express the surface markers. Bar is 25 μm. Lower graph shows percentage of CD24 and CD133 expressing cells in the generated cell lines evaluated by flow cytometry analysis. $CD24^{+}CD133^{+}$ as expected highly expressed the markers after two passages in culture while cell subpopulations expressing these proteins in $CD24^{-}CD133^{-}$ were very few.

4.1.3 *$CD24^+CD133^+$ and $CD24^-CD133^-$ phenotype in culture*

After flow cytometric sorting, generated cell lines were seeded *in vitro* on plastic tissue culture dishes. Cell medium consisted of a mixture used previously in my laboratory to culture human fetal renal cells (Price et al., 2007). It was composed of Dulbecco's modified eagle medium/Hams F12 (1:1) mix supplemented with 5% fetal calf serum, antibiotics and growth factors. Growth factors added were prostaglandin E_1, able to stimulate both growth and ion transport in renal cell lines (Herman et al., 2010), insulin-transferrin-selenium, holotransferrin, triiodothyronine and dexamethasone used to stimulate cell growth (Chuman et al., 1982). A similar medium composition was previously used to maintain murine metanephric mesenchymal cells in culture (Oliver et al., 2002), medium was also supplemented with 50 ng/ml basic FGF and 10 ng/ml transforming growth factor-α (TGF-α). Passage number was assigned to zero when cell subpopulations where placed in *vitro* culture straight after cell sorting, passage numbers were increased every time cells were trypsinised. Generated cell lines grew in monolayer and morphology was observed over time (Figure 4-5).

$CD24^-CD133^-$ showed a mesenchymal-like aspect characterised by spindle shaped appearance. Over passages they appeared with a more circinate orientation and an elongated cell body.

$CD24^+CD133^+$ at early passages (p0 to p3) appeared as a mix population composed of smaller cells with an elongated shape and patches of epithelial-like cells with a polygonal rounded morphology. Morphological changes from a cobblestone- to a spindle-like morphology were seen after few passages.

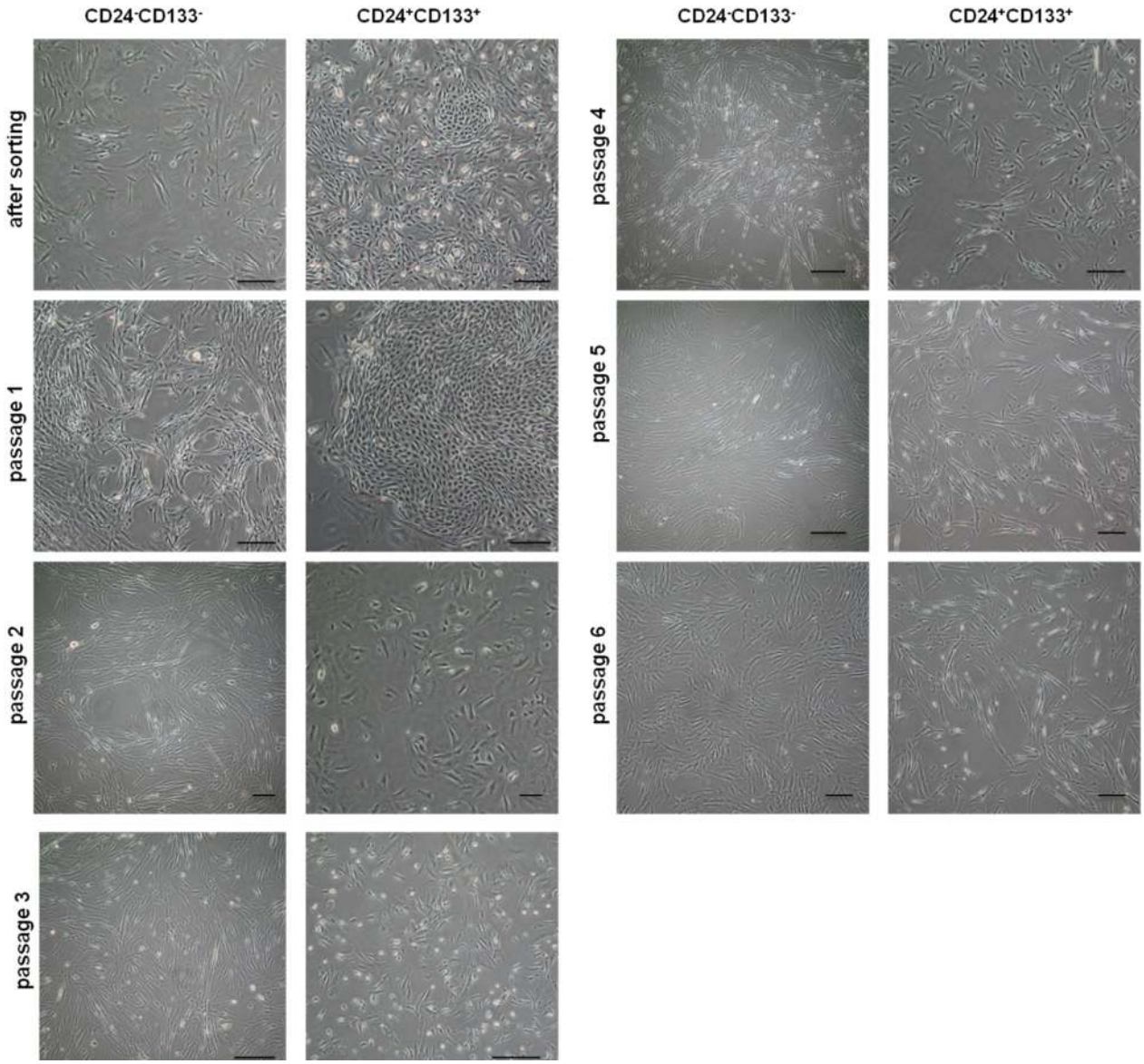

Figure 4-5 Morphology of isolated cell lines observed with light microscopy at different passages. **After cell sorting, generated cell lines were maintained *in vitro* on plastic tissue culture dishes. Prior to the first passaging, $CD24^{+}CD133^{+}$ and $CD24^{-}CD133^{-}$ showed a different morphology, with CD24, CD133 double negative cells showing a spindle-like appearance, whereas in double positive cells plates a mixture of distinct cell types could be distinguished: patches of cobblestone-like cells, showing an epithelial- like morphology interspersed to mesenchymal-like cells. Over cell passages mesenchymal morphology was accentuated with elongated cells having a circinate orientation. Interestingly, double positive cells over passages appeared more mesenchymal-like, suggesting either a de-differentiation of epithelial cells or a faster proliferation of mesenchymal-like cells over the epithelial population. Bars are 250 μm.**

4.1.4 *CD24, CD133 mRNA expression in $CD24^{-}CD133^{-}$ and $CD24^{+}CD133^{+}$*

The expression of CD24, CD133 at the mRNA level was scrutinised with RT-PCR (Q-PCR or Real Time PCR). Prior to PCR, annealing curves were optimised using the gradient function of the Mastercycler thermal cycler, different annealing temperatures were tested. The annealing temperature chosen was 60°C. For PCR, primers annealing temperature was optimised by using a wide range of annealing temperatures, from 51°C to 63.5°C to obtain the PCR products. The PCR products were then subjected to 2% agarose gel electrophoresis to analyse the effects of the distinct annealing temperatures and to further validate primers specificity by checking if the PCR product size matched the expected size and whether not specific co-products were detected

Moreover, when Q-PCR was performed, the melting curve was checked to have only a single peak indicating one PCR product. In my experiments, to evaluate CD24 and CD133 gene expression between cell lines, I used the relative quantification method. In this way, I compared the genes of interest mRNA expression to an endogenous control, a constant expressed reference gene, in my case β-actin. B-actin is an housekeeping gene and works over a range of temperatures (Price et al., 2007).

To determine the level of expression of the genes of interest, I used the ΔΔct method (Livak and Schmittgen, 2001) as it is explained in paragraph 2.2.23. I first calculated the relative expression of the genes of interest in relation to the housekeeping gene β-actin and in a further step I compared the gene of interest expression levels normalised for the housekeeping gene to a control. In these experiments, I used as a control cDNA derived from total RNA extracted from a human fetal kidney of 9 weeks of gestational age.

cDNA of $CD24^{+}CD133^{+}$ and $CD24^{-}CD133^{-}$, as well as the mixed unsorted cell population, all derived from 3 different human fetal kidney cells were screened for mRNA levels of CD24 and CD133. As expected CD24 and CD133 were expressed at low levels in $CD24^{-}CD133^{-}$ cells. CD24 and CD133 fold changes were 0.1 in $CD24^{-}CD133^{-}$ after two passages in culture, compared to the fetal kidney control.

$CD24^{+}CD133^{+}$ on average showed 2 times increase in CD24 expression at passage 2 and 2.7 increase in CD133 at the same passage, the mRNA expression of CD24 and CD133 was variable between the cell lines. In all the cases, CD24 and CD133 mRNA expression decreased progressively in culture, reaching levels lower than the control at passage four (Figure 4.6).

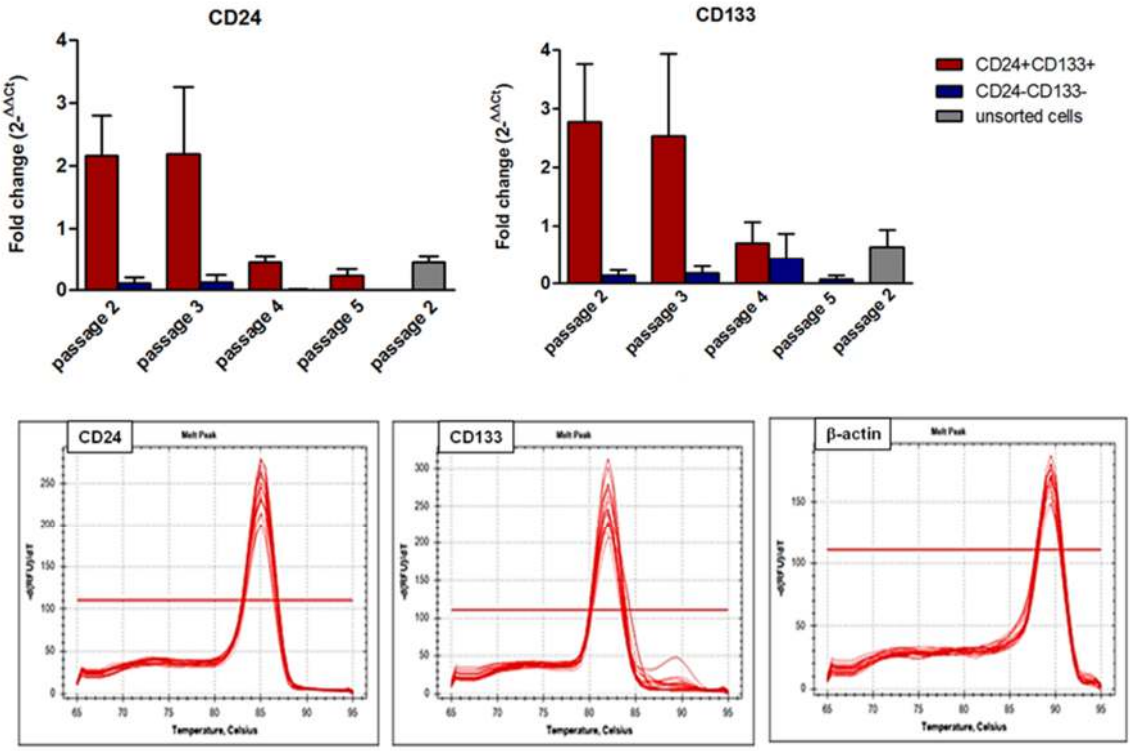

Figure 4-6 Determination of optimal annealing temperature, specificity of CD24 and CD133 primers and CD24, CD133 mRNA relative quantification.

Upper panel: CD24 and CD133 mRNA expression in $CD24^{+}CD133^{+}$ and $CD24^{-}CD133^{-}$ at different passages compared to cDNA obtained from human fetal kidney of same gestational ages. Graphs show fold change mean ± SEM. : Lower panel: melting curve peaks of CD24, CD133 and β-actin primers. CD24 and CD133 were expressed at lower levels in $CD24^{-}CD133^{-}$ cells compared to unsorted cells confirming that these cells. CD24 and CD133 expression in double positive cells decreased rapidly after passage 3 indicaitng the gradual loss of these genes expression in culture conditions.

4.1.5 *CD24, CD133 flow cytometric analysis on cultured renal cells*

Explants culture was set up from human fetal kidneys collected from HDBR by cutting fetal kidneys into small fragments and transferring these on plastic tissue culture plates with growth medium. After two days, tissue pieces attached to culture plates and cells started proliferating and migrating out from kidney specimens Cells showed heterogenic morphology. Many presented a polygonal shape and regular dimensions characteristic of epithelial cells, some cells appeared elongated and thin in shape with a mesenchymal like aspect. When cells confluency reached 70%, these were processed for CD24, CD133 flow cytometric analysis or sorting.

I first compared the surface expression of CD24 and CD133 on a 10 wk sample after culture. When kidney was collected, processed and analysed on the same day, only a few percentage of the total population was $CD24^{+}CD133^{+}$, while the majority of the cells were $CD24^{+}CD133^{-}$ and $CD24^{-}CD133^{-}$(Figure 4-3). After culture, the $CD24^{+}CD133^{+}$ subpopulation expanded becoming the 74.6% of the total cell population, while $CD24^{+}CD133^{-}$ and $CD24^{-}CD133^{-}$ constituted the 13.9% and the 9.6% respectively.

I then decided to analyse the expression of CD24 and CD133 by flow cytometry on cells derived from human fetal kidney explants of different gestational ages assuming they might display variable patterns of cell surface CD24 and CD133 protein expression.

I therefore analysed 13 samples, 5 of early gestation (from 9 to 10 weeks) and 8 of mid gestation (from 14 to 20 weeks). These were cultured as explained before and processed for flow cytometry analysis. The analysis did not show any significant variation among the cells subpopulation expressing or not expressing the surface markers CD24 and CD133. As observed for the 10 weeks kidney sample, the majority of the cells became CD24+CD133+ after culture, while CD24 single positive and $CD24^{-}CD133^{-}$ decreased conspicuously (Table 4-3).

Table 4-3 Flow cytometry analysis of CD24 and CD133 cell surface proteins expression in 13 human fetal kidney derived cells.

Sample gestational age		Cell surface protein expression (%)			
		$CD24^{-}CD133^{-}$	$CD24^{+}CD133^{-}$	$CD24^{-}CD133^{+}$	$CD24^{+}CD133^{+}$
Early gestation	(54 days) 7 wks plus	3.2	7.9	3.7	86.2
	8 wks	3.6	5.9	15.5	75
	9 wks	8.2	7.6	3.4	80.8
	10 wks	9.6	6.7	0.18	74.6
	10 wks	10.4	16.3	9.60	63.7
	Mean ± SEM	**6.9 ± 1.5**	**8.9 ± 1.9**	**6.5 ± 2.7**	**76.1 ± 3.8**
Mid gestation	14 wks	4	5.5	1.7	88.9
	14 wks	30.5	13.7	9.4	46.6
	14 wks	23.2	9.5	1.5	65.7
	16 wks	37.2	7.6	2.3	52.9
	19 wks	6.5	7.2	4.2	82.1
	19 wks	4.4	10.2	0.4	85
	20 wks	0.5	0.7	0.0	98.2
	20 wks	0.53	0.2	0.9	98.4
	Mean ± SEM	**13.4 ± 5.2**	**6.8 ± 1.6**	**2.5 ± 1.1**	**77.2 ± 7**

4.2 SUMMARY

$CD24^+CD133^+$ and $CD24^-CD133^-$ were first isolated by FACS from freshly collected human fetal kidneys (n=3, 8/10 weeks of gestation). However, performing cell sorting on the same day of sample collection encountered different issues, among these, the difficulty of the experiment planning, for instance the organisation between sample collection and same day FACS sorting. For this reason, fetal renal cells explants were set up prior to sorting.

The percentage of CD24, CD133 expression was analysed on 3 samples sorted on the same day of collection and compared with sorted renal cells outgrown from fetal kidney explants after *in vitro* culture.

CD24, CD133 double positive cells were 4.5% of the total cell population in the fresh sorted kidneys and 46.2% after culture. $CD24^-CD133^-$ represented the 40.3% in the fresh kidney and the 20.8% after culture. The lower percentage of CD24, CD133 double positive cells in freshly analysed fetal kidney cells was in line with the low co-expression of these markers observed in my immunostaining experiments on 9 weeks human fetal kidneys. However, this data was different from the one published by Lazzeri *et al*.,which showed an high expression by flow cytometric analysis of $CD24^+CD133^+$ cells (between 35% to 50% of the total cell population). The discrepancy between my data and the published ones could be due to several factors, ranging from sample processing, sorting conditions and antibody used and to address the factors of the discrepancy would require further comparative studies.

Percentage of CD24 and CD133 positive cells changed markedly following *in vitro* culture. Several explanations could be assumed on the influence of *in vitro* culture on double positive cells, however, to be directed towards a possible answer, further experiments would be needed. Possible factors to be accounted for would be the culture medium, which may promote changes in cell phenotype, the tissue culture plastic material or the high O_2 levels in culture compared to the levels *in vivo*. Furthermore, the lack of specific surrounding cells or soluble factors, the lack of a 3-dimensional organisation or different paracrine factors might have an effect.

$CD24^+CD133^+$ and $CD24^-CD133^-$ cells were then sorted after *in vitro* cultivation from 16 samples of 8 to 9 weeks of gestation. Sorted cells were placed in culture and examined in terms of morphology, retention of CD24 and CD133 proteins (n=3, at passage 2) and CD24, CD133 mRNA expression (n=3, at passage 2,3,4,5).

$CD24^-CD133^-$ showed a more mesenchymal-like morphology after sorting, which appeared even more evident after few passages in culture. As expected these cells did not express CD24 and CD133 markers both at the mRNA and protein level. $CD24^+CD133^+$ expressed mRNA of CD24 and CD133 at a higher level when compared with control RNA extracted by total human fetal kidneys of 9 weeks. However, after passage 3, CD24 and CD133 mRNA levels decreased reaching values lower than the control. Also, morphology of these cells changed in culture conditions. From an epithelial-like appearance to a more mesenchymal-like aspect. There might be two reasons why these changes occurred:

- The CD24+CD133+ cells might be de-differentiating with such culture conditions to a double negative population.
- Subculture might selectively expand a population negative for these markers which possesses characteristics in terms of proliferation rate that confer an advantage over the double positive population.

As a further investigation, CD24 and CD133 changes in cell populations percentage was examined in cells derived by kidney explants at different gestational ages. CD24 and CD133 expression was assessed by FACS analysis in renal cells cultured from 13 samples of early (7 to 10 weeks) and mid gestational age (14 to 20 weeks), however not significant differences were observed in the pattern of expression of these markers at different gestational ages after culture.

5 CHARACTERISATION OF GENE EXPRESSION AND PROLIFERATION OF $CD24^+CD133^+$ AND $CD24^-CD133^-$

Stem cells can be identified and characterised with features such as self-renewal and a specific molecular signature.

A way to examine whether cell populations can self-renew is to determine their population doublings (PDs) over time (Hayflick et al., 1973). Stem cells should in fact display a higher number of population doublings compared to somatic cells. $CD24^+CD133^+$ cells were previously associated with capacity to grow for 60 to 80 population doublings (Lazzeri et al., 2007). However, the studies were limited to the analysis of the $CD24^+CD133^+$ cell population without comparing these cells to the other cell populations derived from fetal kidneys.

Furthermore, stem cells should also express genes often down-regulated during differentiation and should lack expression of lineage markers. A transcription factor involved in maintenance of self-renewal in vitro is OCT4, which has been shown as an essential self-renewal master gene in mouse embryonic stem cells (Scholer et al.,1989). OCT4 has also been shown to be critical for somatic cell re-programming (Takahashi et al., 2007).

Hypothesis and aims

Assuming that CD24 and CD133 mark epithelial-committed fetal renal cells. $CD24^+CD133^+$, compared to double negative cells, should show a lower expression of known transcription factors found in renal cap mesenchymal cells (*PAX2, OSR1*, *WT1, SIX2, EYA1, CITED1*) and embryonic cells (*OCT4*), expressing higher levels of epithelial markers such as *E-cadherin*, lower levels of stromal marker *FOXD1*. Furthermore, hypothesising that these cells are able of limited self-renewal, the number of population doubling of double positive cells should be less than the population doubling in double negative cells.

The aims of this study were to characterise the generated cell lines in terms of population doubling, to compare mRNA expression of renal progenitor genes *PAX2*, *OSR1*, *WT1*,

SIX2, *EYA1*, *CITED1* and the pluripotency gene *OCT4* at different passages. Compare mRNA expression of the lineage markers *FOXD1*(stroma) and *E-cadherin* (epithelium) over *in vitro* culture cell passages.

5.1 RESULTS

5.1.1 *Association of CD24, CD133 expression with proliferation (population doubling)*

The association between CD24 and CD133 expression and proliferation rate was assessed with the population doubling (PD), which expresses the number of times a cell population can divide and thus its proliferation potential (Hayflick, 1973).

PD was evaluated from passage 2 onwards in cell lines generated from one kidney sample of 9 weeks of gestation. Cells were passaged for a period of 2 months. Both cell lines proliferation decreased when cells were split after 4 days, however while the $CD24^-$ $CD133^-$ (Figure 5-1, blue line) showed an increase in proliferation, the $CD24^+CD133^+$ appeared had a fluctuating trend and the growth arrested after 40 days in culture (Fig.5-1, red line). After 50 days, $CD24^-CD133^-$ PD was 8.96 ± 0.31 (mean ± SEM) compared to $CD24^+CD133^+$ PD at the same time of -0.4 2± 0.17 (mean ± SEM). An illustration of the entire time of evaluation is presented in Figure 5-1. The $CD24^+CD133^+$ cells proliferation rate fluctuated decreasing or increasing over the time and underwent senescence after day 40 (red line). $CD24^-CD133^-$ cells showed after 13 days in culture an increase in proliferation over the entire time (blue dashed line).

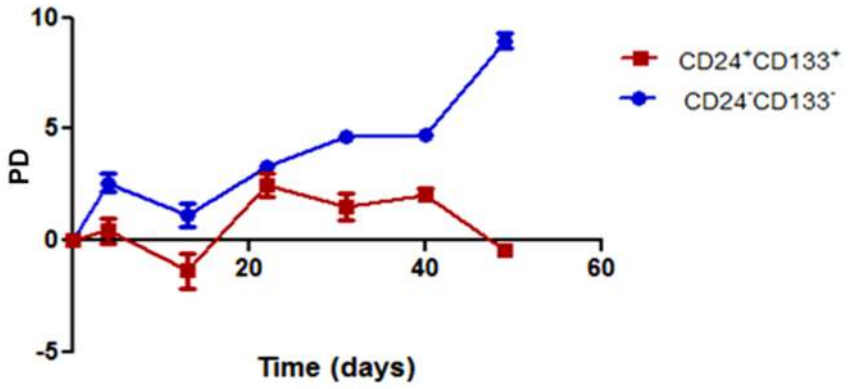

Figure 5-1 Population doubling (PD) of CD24-CD133- and CD24+CD133+.
$CD24^{-}CD133^{-}$ cells (blue line) appeared to increase in proliferation over time, whereas $CD24^{+}CD133^{+}$ showed growth arrested after 6 passages/40 days in culture (red line).

5.1.2 *Molecular characterisation of isolated cell populations*

Gene expression was evaluated by Q-PCR with the ΔΔCt method, calculated as following: $\Delta\Delta Ct = \Delta Ct_{sample} - \Delta Ct_{control}$, Ct values were normalised to the endogenous housekeeping gene *βactin*. 'Sample' refers to cDNA derived from $CD24^{+}CD133^{+}$ and $CD24^{-}CD133^{-}$ isolated from three samples of same gestational age (9 weeks) and cDNA from bulk unsorted fetal renal cells of 9 weeks of gestation ('unsorted'). 'Control' refers to cDNA from human fetal kidneys of 9 weeks of gestation (HFK). Since the data obtained did not follow a normal distribution, in order to proceed to a correct statistical analysis, the results were log transformed. Analysis was carried out with repeated measures one-way analysis of variance (ANOVA) and Bonferroni's post-test.

5.1.2.1 PAX2 expression

PAX2 expression, on average, was downregulated in cultured cells, in both unsorted/ $CD24^{+}CD133^{+}$ and $CD24^{-}CD133^{-}$ in comparison with the HFK control (HFK Log Fold change equals zero, HFK bar not shown on the graph, Figure 5-2).

$CD24^{-}CD133^{-}$ showed significant less expression of *PAX2* compared with HFK, decreasing over passages. Although, on average, unsorted population and $CD24^{+}CD133^{+}$ cells expressed less *PAX2* than the HFK control, this did not give evidence of statistically significance. The explanation might be attributed to the variability of the fold change in

each sample and the low N number. Double negative $CD24^{-}CD133^{-}$ cells showed less *PAX2* expression compared to CD24+CD133+ at passage 2 ($P \leq 0.05$).

5.1.2.2 WT1 and OSR1 expression

WT1 expression was significantly downregulated in cultured cells of all passages compared with HFK with no significantly differences between double positive and double negative cells (Figure 5-2). *OSR1* on average was downregulated in all cultured cells, however whereas $CD24^{+}CD133^{+}$ significantly showed less expression of *OSR1,* at all passages compared to HFK, $CD24^{-}CD133^{-}$ expression of *OSR1* was not significantly different from HFK and did not appear to change over passages.

5.1.2.3 SIX2, EYA1 and CITED1 expression

SIX2 showed a significant less expression in $CD24^{+}CD133^{+}$ cells at passage two and three compared with HFK, while difference in *SIX2* expression between HFK and $CD24^{-}CD133^{-}$ was not significant (Figure 5-4, A). *CITED1* (Figure 5-4, C) and *EYA1* (Figure 5-4, E) were less expressed in unsorted cell populations and generated cell lines compared to HFK. *CITED1* was significantly downregulated in $CD24^{+}CD133^{+}$ passage 2 and 3 and $CD24^{-}CD133^{-}$ passage 4. Whereas EYA1 significantly showed less expression of this progenitor gene in unsorted cells, $CD24^{+}CD133^{+}$ passage two and three and $CD24^{-}CD133^{-}$ passage three and four. $CD24^{-}CD133^{-}$ at early passage 2, appeared to express more *EYA* and *CITED1*, however this difference was not statistically significance.

5.1.2.4 OCT4 expression

OCT4 has been previously found in CD133-expressing cells in developing kidneys (Lazzeri et al., 2007). When analysed in isolated cell lines, significant less expression of *OCT4* was observed compared with HFK. When the $CD24^{+}CD133^{+}$ cells were compared to $CD24^{-}CD133^{-}$, the expression of the double positive cells was significantly higher than $CD24^{-}CD133^{-}$ (Figure 5-5).

5.1.2.5 E-cadherin and FOXD1 expression

E-cadherin expression was higher in $CD24^{+}CD133^{+}$ compared with $CD24^{-}CD133^{-}$ suggesting the epithelial nature of this cell line, however it was downregulated over passages. $CD24^{+}CD133^{+}$ *E-cadherin* log fold changes were analysed with repeated measures ANOVA with post-test for linear trend showing a significant downregulation with culture passaging ($P = 0.033$). Hence, this trend might suggest that a de-

differentiation process occurs over passages with these culture conditions (Figure 5.6 A)**.** *FOXD1* expression did not differ between HFK control, unsorted cells and generated cell lines. This may be due to the fact that FOXD1+ cells, which are a renal stromal progenitor population, could be present in similar amount in all these cell types, Figure 5.6 C.

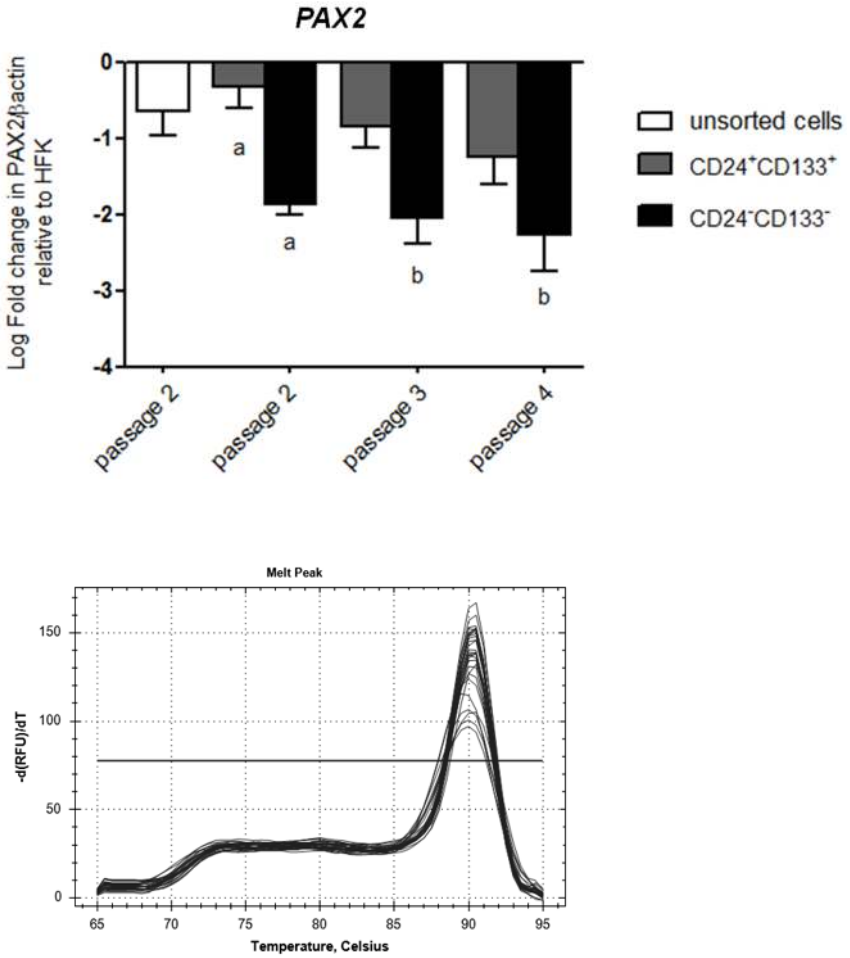

Figure 5-2 Q-PCR for PAX2.

Upper panel shows real-time quantitative transcriptase-PCR for *PAX2*. *B-actin* was used as a housekeeping gene and fetal kidney (HFK) of 9 weeks was used as calibrator. Fold changes values were log transformed and presented as (mean ± SEM) and then analysed by one-way ANOVA with Bonferroni's post test. *PAX2* expression was downregulated in cultured cells (unsorted/ $CD24^{+}CD133^{+}$ and $CD24^{-}CD133^{-}$) compared to HFK unsorted cells. $CD24^{-}CD133^{-}$ showed significant less expression of *PAX2* compared with HFK, decreasing over passages (b=$P \leq 0.01$ at p3 and p4). At p2 these cells significantly expressed less PAX2 compared to the double positive ($P \leq 0.05$). a=$P \leq 0.05$ compared with double negative cells. b=$P \leq 0.01$ compared with HFK. Lower panel: *PAX2* Q-PCR melting curve.

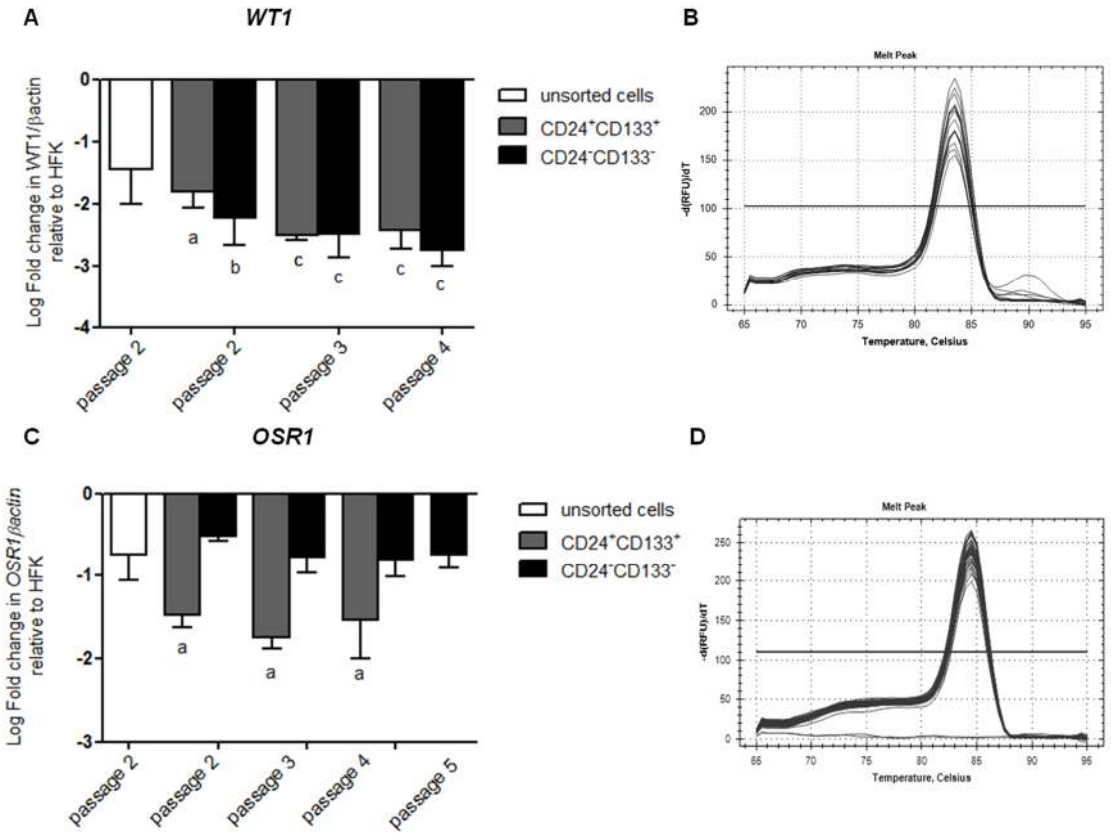

Figure 5-3 Q-PCR for WT1 and OSR1.

Real-time quantitative -PCR for *WT1* showing significant *WT1* downregulation in cultured cells of all passages compared with HFK (a=*P*≤0.05, b=*P*≤0.01,c=*P*≤0.001). (B) *WT1* melting curve (C) *OSR1* was downregulated in all cultured cells compared to HFK (a=*P*≤0.01 compared with HFK). $CD24^{-}CD133^{-}$ did not significantly differ to HFK in *OSR1* expression.. (D) OSR1 melting curve.

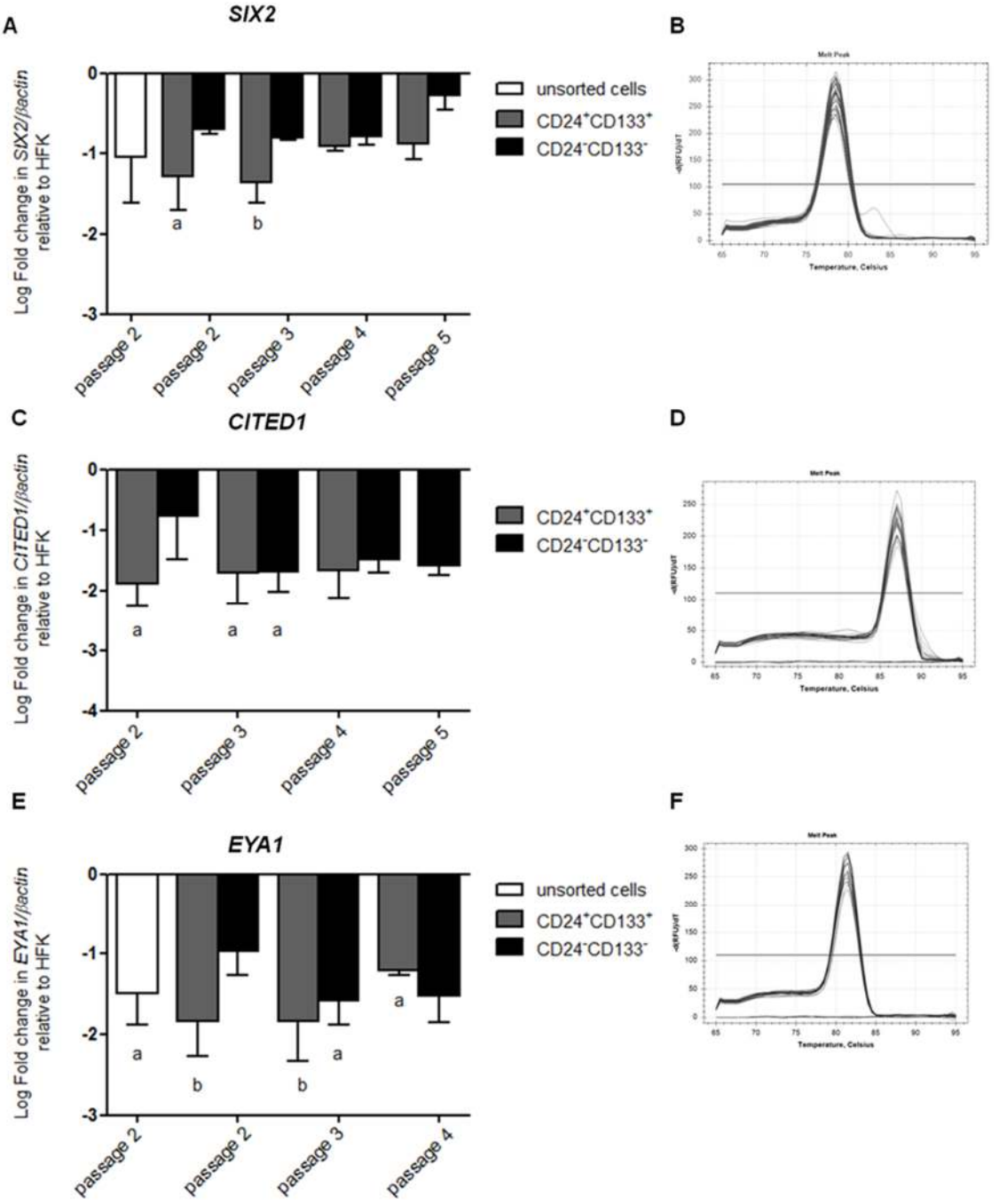

Figure 5-4 Q-PCR for SIX2, CITED1, EYA1. Q-PCR for SIX2.

(A) SIX2 expression analysis. CD24^{+}CD133^{+} cells had a significant less *SIX2* expression at p2 and p3 compared with HFK (a=*P*≤0.05; b=P≤0.01).No significant *SIX2* expression between HFK and CD24^{-} CD133^{-} was evident. (B) *SIX2* melting curve (C) *CITED1* expression was significantly downregulated in CD24^{+}CD133^{+} p2 and 3 and CD24^{-}CD133^{-} p4 (a =*P*≤0.05 compared with HFK). (D) *CITED1* melting curve. (E) *EYA1* was downregulated in all cultured cells, however double negative CD24^{-} CD133^{-} at p2, displayed an higher expression compared to double positive cells, this difference was however not significant. a=*P*≤0.05 compared with HFK; b=*P*≤0.01 compared with HFK (F) *EYA1* melting curve.

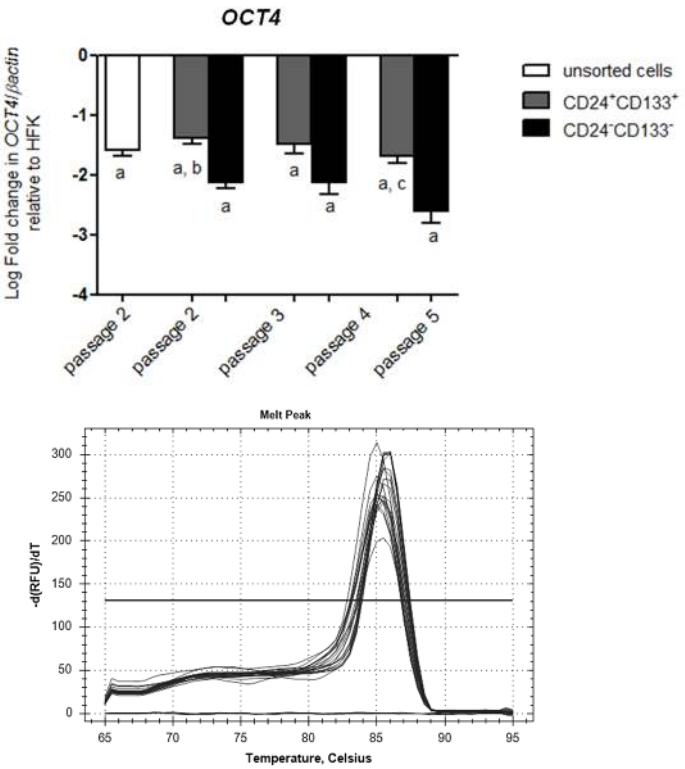

Figure 5-5 QRT-PCR for OCT4.

OCT4 expression was significantly downregulated in all cultured cells, on average $CD24^{-}CD133^{-}$ cells exhibited lower OCT4 compared with HFK (a=$P \leq 0.001$); b=$P \leq 0.01$ compared with $CD24^{-}CD13^{-}$ p2. c=$P \leq 0.05$ compared with $CD24^{-}CD133^{-}$ p5. Lower panel, melting curve.

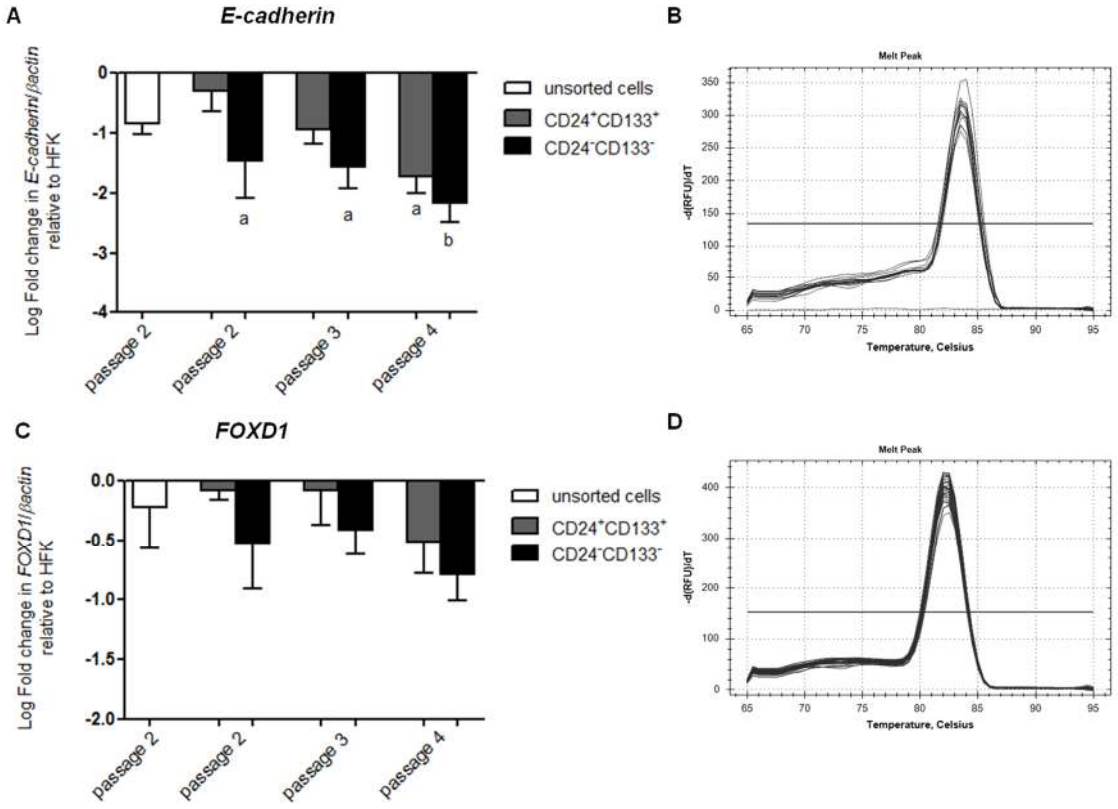

Figure 5-6 Q-PCR for E-cadherin and FOXD1.

(A) *E-cadherin* expression was higher in double positive $CD24^{+}CD133^{+}$ cells, a=$P \leq 0.05$ compared with HFK; b=$P \leq 0.01$ compared with HFK. (B) E-cadherin melting curve. (C) *FOXD1* expression did not significantly differ among cultured cells and the HFK unsorted control. (D) FOXD1 melting curve.

5.2 SUMMARY

$CD24^+CD133^+$ and $CD24^-CD133^-$ had a different proliferation rate when their population doubling was assessed and compared. The double positive cells showed a fluctuating growth rate, arresting growth after 6 passages *in vitro*. The double negatives were cultured up to passage 11 without fall off in proliferation or differences in morphology.

Progenitor gene expression was assessed in unsorted, double positive and double negative cells against RNA extracted from total human fetal kidney of 9 weeks of gestation. All the cultured cells showed downregulation of the progenitor genes with some differences:

PAX2 expression data showed that although this gene was downregulated in all the cultured cells, double negative cells compared to double positive cells showed even more decrease over passages. *PAX2* is a progenitor gene expressed in the condensed mesenchyme as well as ureteric bud. Therefore double negative cells might express less *PAX2* compared to double positive due to the presence of ureteric bud cells within the $CD24^+CD133^+$ subpopulation. *WT1* expression was significantly different from HFK in unsorted cells and generated cell lines.

SIX2 was expressed more highly in $CD24^-CD133^-$ than $CD24^+CD133^+$ and was not significantly different in levels compared with HFK.

OSR1 and *EYA1* expression was significantly lower in $CD24^+CD133^+$ compared with HFK. $CD24^-CD133^-$ expression of *OSR1* was not different from HFK, while *EYA1* decreased over passages.

CITED1 was less expressed in $CD24^+CD133^+$ compared with HFK, however, also $CD24^-CD133^-$ expression appeared to decrease over passages.

The embryonic gene *OCT4* was higher in $CD24^+CD133^+$ at all passages analysed. *OCT4* has been associated with renal development and in particular within some CD133 expressing cells, this might be the reason for increased expression in $CD24^+CD133^+$ cell lines.

E-cadherin, an epithelial marker, was more expressed by the epithelial –like $CD24^+CD133^+$ cells than mesenchymal like $CD24^-CD133^-$ cells, however its expression decreased over passages, suggesting that these cells might de-differentiate in culture.

FOXD1, a marker specifying stromal progenitor cells, was differently expressed between samples, these differences did not make possible any conclusion from *FOXD1* expression data.

In conclusion, these results suggest that the expansion of both cell lines in culture does alter the expression of genes associated with progenitor state. Isolated cell lines at early passages, showed a distinct molecular signature, with $CD24^{-}CD133^{-}$ expressing some progenitor genes, such as *EYA1, SIX2* and *OSR1*, and $CD24^{+}CD133^{+}$ expressing more *PAX2* and *OCT4*. The more epithelial-like phenotype of $CD24^{+}CD133^{+}$ cells was further confirmed by expression of *E-cadherin*; however the interpretation of the results could become more solid by increasing the number of $CD24^{+}CD133^{+}$ cell lines analysed and by improving culture conditions, which substantially influence the maintenance of these cells over passages.

6 *IN VITRO* AND *EX VIVO* MULTI LINEAGE DIFFERENTIATION OF $CD24^+CD133^+$ AND $CD24^-CD133^-$

Multipotent stem cells can generate multiple differentiated cell types. Examples of multipotent stem cells include the ones isolated from bone marrow, which can form blood cells and endothelial cells and stem cells isolated from brain, able to form neural cells and glia. Stem cell plasticity refers to 'the ability of some stem cells to give rise to cell types, formerly considered outside their normal repertoire of differentiation for the location where they are found' (Alison, 2017). As an example, circulating bone marrow derived cells can contribute to the repair of damaged non-hematopoietic tissues. Multipotency and plasticity of cell lines can be investigated to estimate cells potential to be used in regenerative medicine and tissue engineering.

Hypothesis and aims

The aim of this part of the study was to investigate $CD24^-CD133^-$ and $CD24^+CD133^+$ multi-differentiation potential and plasticity, hypothesising that these cell lines might display a difference in their differentiation ability.

The objectives of this part of the study were the following:

- To test differentiation ability towards non-renal lineages by directing *in vitro* differentiation toward the osteo- and adipo-lineages with the use of commercially available medium.
- To test cell differentiation towards renal epithelium, through the administration of the Wnt pathway inducer Lithium Chloride stimulation.
- To test the potential of isolated cells to undergo renal differentiation through kidney rudiment assay by mixing human fetal kidney cells with dissociated embryonic mouse kidney cells followed by re-aggregation to form a chimeric rudiment.

6.1 RESULTS

6.1.1 *OsteoDifferentiation*

OsteoDifferentiation was induced, $CD24^{-}CD133^{-}$ and $CD24^{+}CD133^{+}$ cell lines isolated from fetal kidneys at 9 weeks of gestation (n=3). These were treated with the commercially available OsteoDiff medium, commonly used for mesenchymal stem cells differentiation towards osteoblast.

Differentiation was performed in triplicates by treatment with OsteoDiff for 12 days. As an untreated control, human fetal kidney (HFK) complete growth medium was used.

Cells were evaluated under light microscopy at the beginning of the protocol, at day 0, and at intermediate time points of 4 and 7 days (Figure 6-1). At day 4, extracellular deposits were observed in treated $CD24^{+}CD133^{+}$ whereas $CD24^{-}CD133^{-}$ accumulated few deposits starting from day 7 These suggested that double positives could respond to the differentiation medium earlier than double negative cells. At day 12, the experiment was terminated and, as an indication of calcium deposits, alizarin red staining was performed. Bright red calcium deposits were observed in both cell lines treated with OsteoDiff (Figure 6-2).

To evaluate the degree of differentiation towards osteoblasts, total RNA was extracted from both untreated control and treated/differentiated cells at day 12. Bone morphogenetic protein 2 (*BMP2*), *Osteopontin* and *RUNX2* were chosen as osteogenic markers to assess the changes in fold expression analysed with the unpaired t test (Figure 6-3).

Double positive cells showed a significant increase in *Osteopontin* expression in treated cells compared with the untreated control (P=0.0324), whereas *BMP2* and *RUNX2* did not change in expression. *Osteopontin* in $CD24^{-}CD133^{-}$ did not appear to change in control and treated samples, whereas *BMP2* expression appeared to increase by an average of 2 times in two out of three samples.

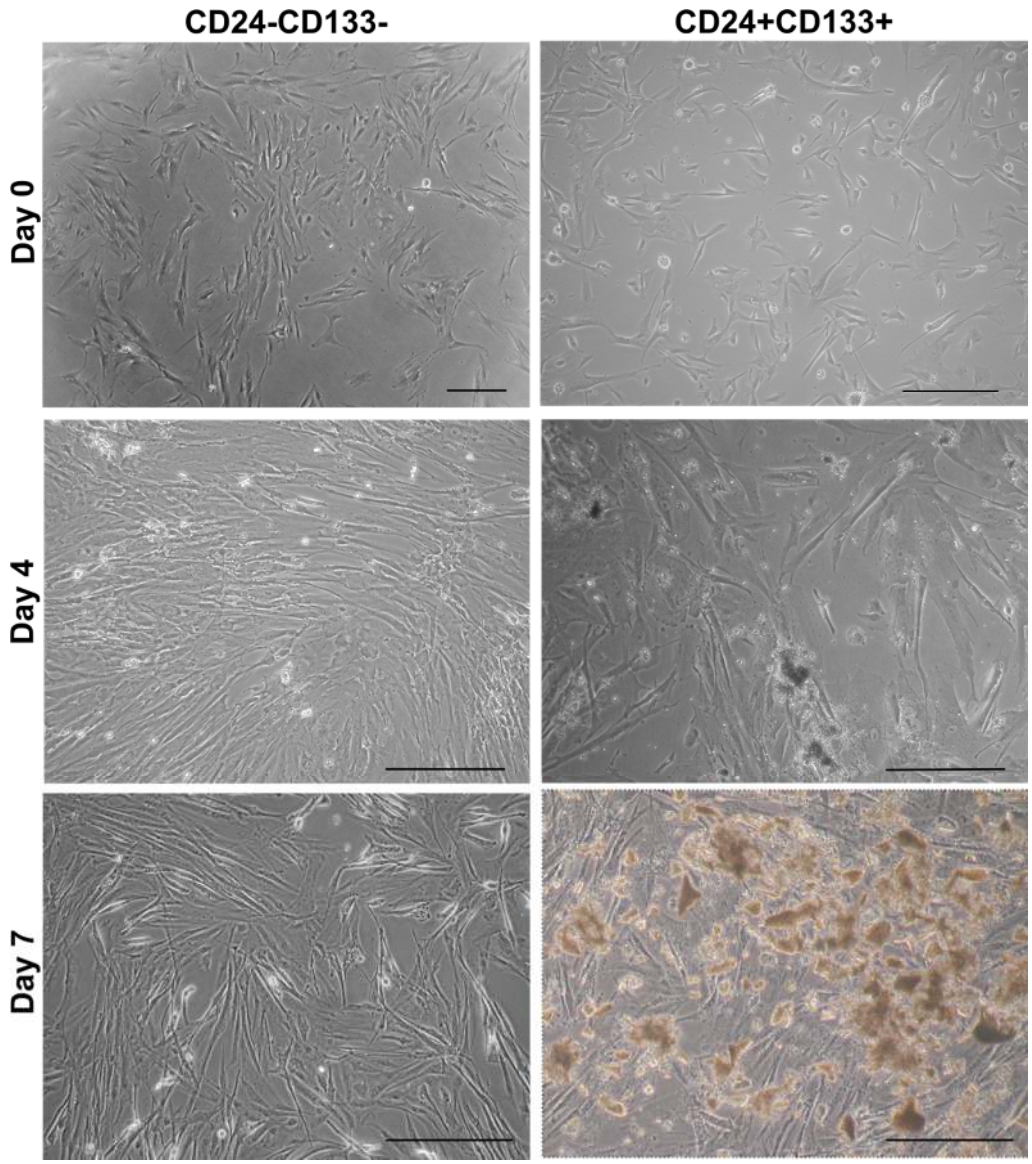

Figure 6-1 Cell morphology during OsteoDifferentiation.

Light microscopy pictures during OsteoDifferentiation of $CD24^{-}CD133^{-}$ and $CD24^{+}CD133^{+}$ at day 0, 4 and 7. Pictures are representative of experiments performed in triplicates on cell lines isolated from three different kidney samples of 9 weeks of gestation. Pictures were taken from the cells not treated and treated with OsteoDiff; these panels show only treated cells. At day 4 and day 7 calcium deposits were observed only in $CD24^{+}CD133^{+}$ cells suggesting this cell line was early responsive to induction towards osteocytes. Scale = 250µm.

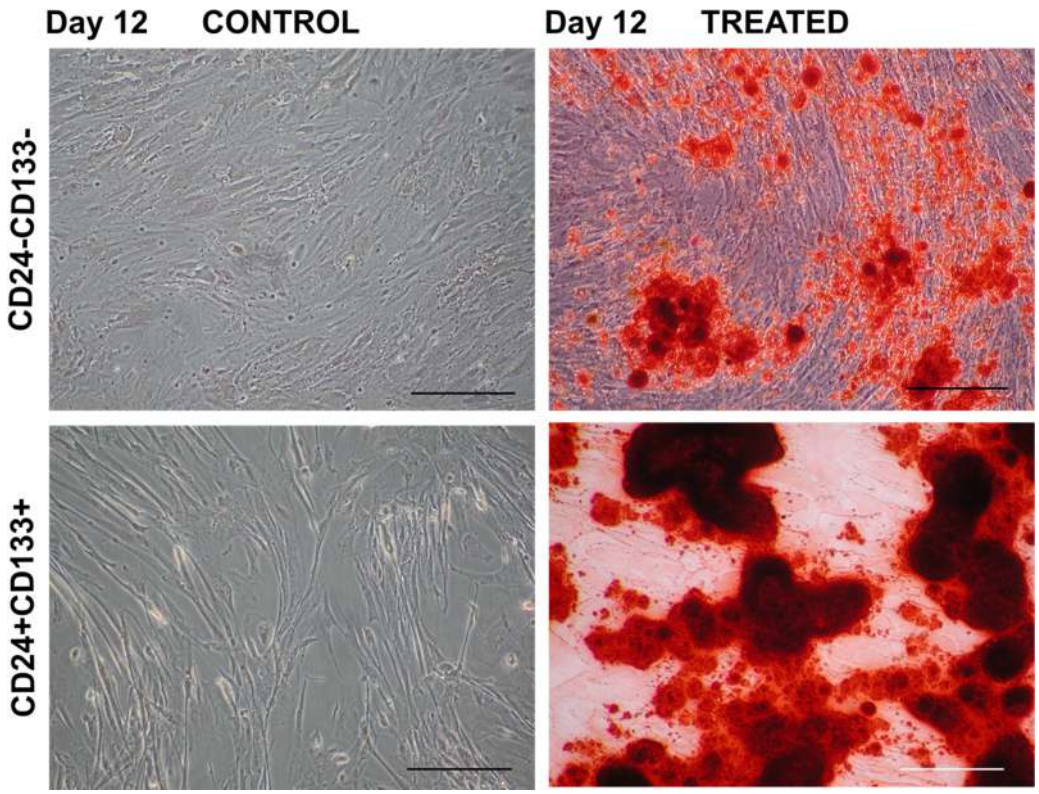

Figure 6-2 Alizarin Red staining in controls and OsteoDiff treated cell lines after 12 days of differentiation.

Alizarin red staining of $CD24^{-}CD133^{-}$ and $CD24^{+}CD133^{+}$ at the end of the differentiation experiment, day 12, normal complete growth medium (control) and treated with OsteoDiff medium. Alizarin red bound to calcium-rich regions, resulting in a strong dark-red staining in treated cell lines but not in controls. Both cell lines showed accumulation of calcium, initially suggesting that both cell lines might have responded to induction medium by differentiating towards osteoblasts. Pictures are representative of experiments performed in triplicates on 3 different samples of 9 weeks of gestation. Scale = 250µm.

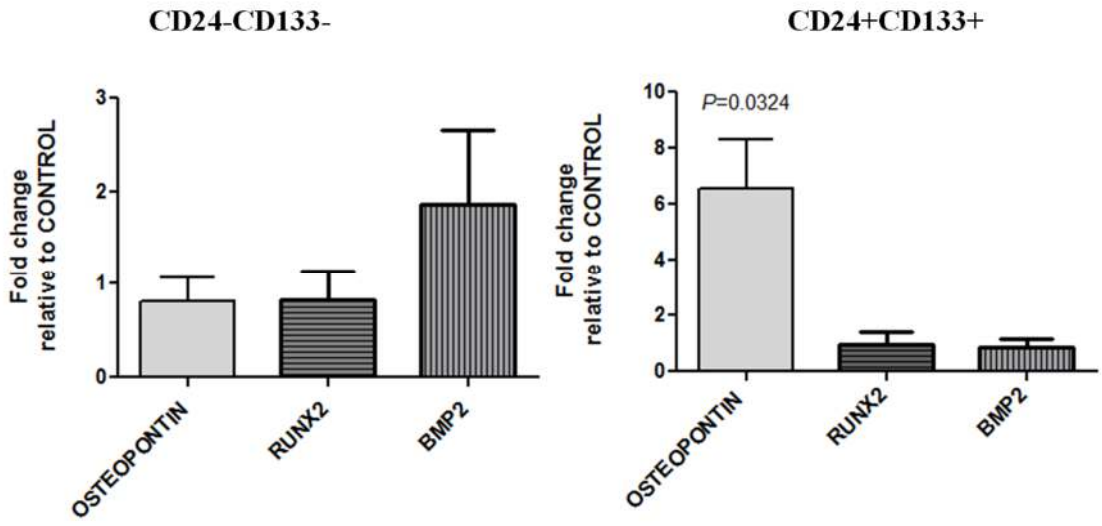

Figure 6-3 mRNA levels of osteogenic markers in treated cell lines.

Gene expression analysis by Q-PCR of osteogenic markers *Osteopontin*, *RUNX2* and *BMP2*, after 12 days of osteogenic differentiation of three different cell lines performed in triplicates. Relative expression: fold change normalised to the housekeeping gene β-actin and compared with the control, columns represent mean ± SEM. *Osteopontin* mRNA expression was significantly higher in $CD24^{+}CD133^{+}$ treated cells compared to control (analysed with unpaired t test, *P*=0.0324).

Table 6-1 Q-PCR Ct values of osteogenic genes in control and OsteoDiff treated CD24+CD133+ and CD24-CD133- generated from three different samples of 9 weeks.

$CD24^{+}CD133^{+}$						
Gene	Control			Treated		
	Mean Ct ±SEM	Mean Ct ±SEM	Mean Ct ±SEM	Mean Ct ±SEM	Mean Ct ±SEM	Mean Ct ±SEM
β-actin	18.63±0.13	18.60±0.17	16.90±0.11	18.40±0.09	18.96±0.13	16.91±0.09
BMP2	29.64±0.24	29.07±0.15	28.04±0.06	27.70±0.16	28.44±0.18	29.36±0.25
Osteopontin	27.47±0.08	29.02±0.12	24.50±0.40	28.34±0.23	29.09±0.07	26.78±0.15
RUNX2	25.96±0.43	26.70±0.133	25.10±0.10	25.56±0.05	26.53±0.09	26.07±0.15

$CD24^{-}CD133^{-}$						
Gene	Control			Treated		
	Mean Ct ±SEM	Mean Ct ±SEM	Mean Ct ±SEM	Mean Ct ±SEM	Mean Ct ±SEM	Mean Ct ±SEM
β -actin	21.78±0.07	17.72±0.26	17.12±0.33	16.90±0.18	18.03±0.19	17.01±0.46
BMP2	27.90±0.45	30.00±0.09	30.00±0.32	29.02±0.18	31.69±0.17	28.72±0.04
Osteopontin	22.69±0.13	28.65±0.08	27.32±0.39	21.88±0.06	25.75±0.14	22.90±0.27
RUNX2	22.56±0.16	26.16±0.27	27.24±0.56	25.15±0.11	26.72±0.06	26.19±0.08

6.1.2 *AdipoDifferentiation*

In order to induce the differentiation towards adipocytes, $CD24^{-}CD133^{-}$ and $CD24^{+}CD133^{+}$ cell lines, isolated from 3 kidney samples of 9 weeks of gestation, were treated with the commercially available AdipoDiff medium. The protocol is summarised in paragraph 2.2.10.

Differentiation was observed at day 0, 7, 14 through to day 21, end of the differentiation experiment (Figure 6-4). At day 7 and 14, $CD24^{-}CD133^{-}$ cells showed no macroscopic changes in morphology between control and treated cells. At day 21, vacuoles could be observed in the cytoplasm; when Oil Red O staining was performed to stain lipid deposition, treated $CD24^{-}CD133^{-}$ showed vacuoles positively stained with Oil Red O with red bright colour, as shown in Figure 6-5.

AdipoDiff treated $CD24^{+}CD133^{+}$, when observed at day 7, showed a stop in proliferation and an increase in cell death , morphology changed to a thinner spindle-shape and many cells lifted off the plate. These observations suggested that the inductive medium had a negative effect on this cell type.

mRNA expression of *Adiponectin* and *PPARγ* was assessed in $CD24^{-}CD133^{-}$only; $CD24^{+}CD133^{+}$ were not analysed for mRNA expression because few cells survived at day 21 and they did not appear to have changed in morphology, this suggested that these cell lines did not show adipo-differentiation potential under these culture conditions. $CD24^{-}CD133^{-}$ treated cells showed an increase in the expression of the adipogenes, however this did not appear as statistically significant (P=0.122 for *Adiponectin*; P=0.311 for *PPARγ*), because of the low number of the cell lines analysed (n=3) and the variability in terms of fold changes between those samples (Table 6-2 and Figure 6-6).

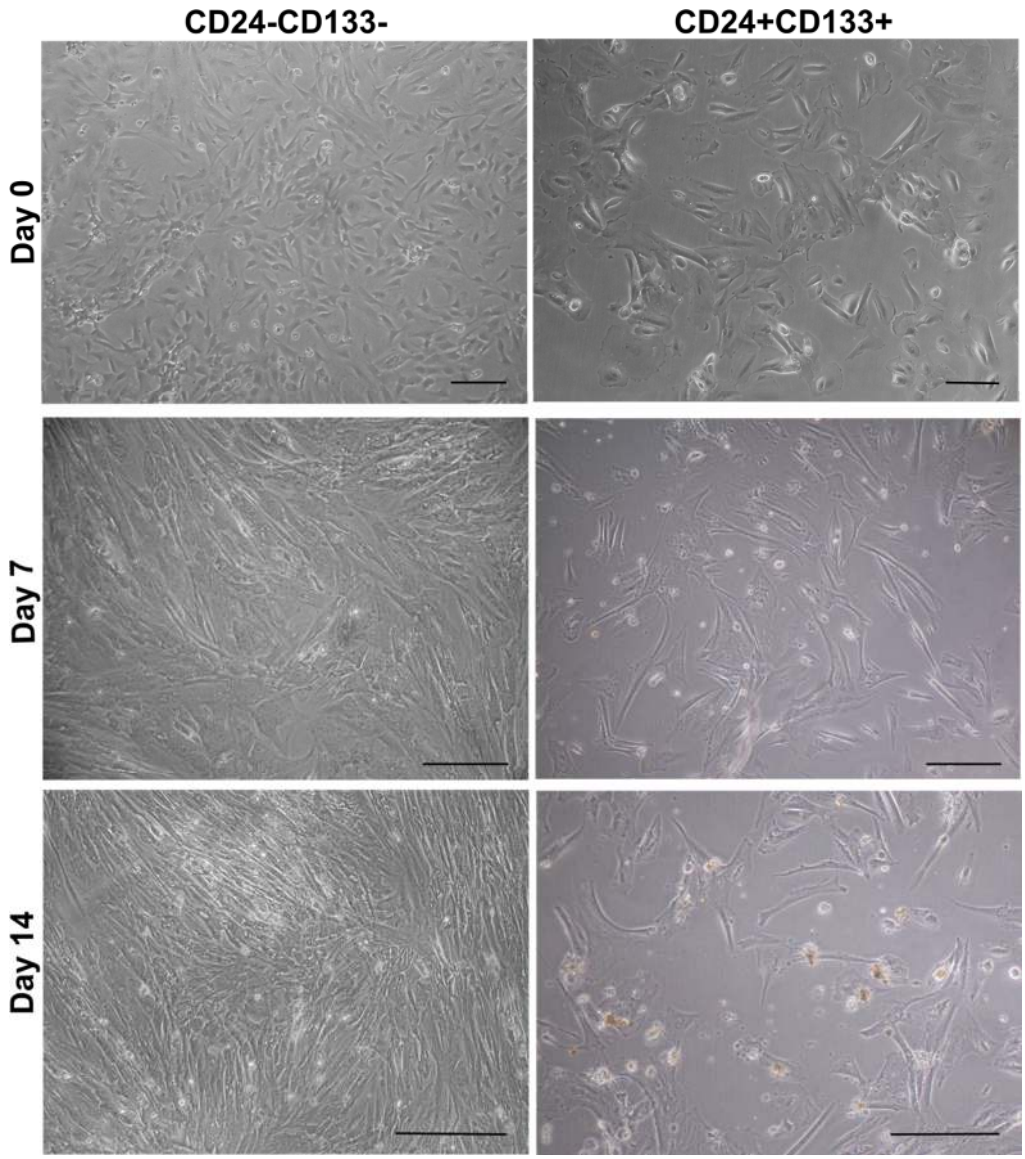

Figure 6-4 mRNA levels of osteogenic markers in treated cell lines.

Cell morphology during AdipoDifferentiation. Light microscopy pictures during AdipoDifferentiation of $CD24^{-}CD133^{-}$ and $CD24^{+}CD133^{+}$ at day 0, 7 and 14. Pictures are representative of experiments performed in triplicates on three different samples. Pictures were taken from the control cells in normal growth complete medium and cells treated with AdipoDiff; panels show only treated cells. $CD24^{-}CD133^{-}$ did not appear to change in morphology over days, whereas $CD24^{+}CD133^{+}$ showed a thinner shape, proliferated less than in control wells, suggesting that the AdipoDiff medium might have had a negative impact on these cells. Scale = 250µm.

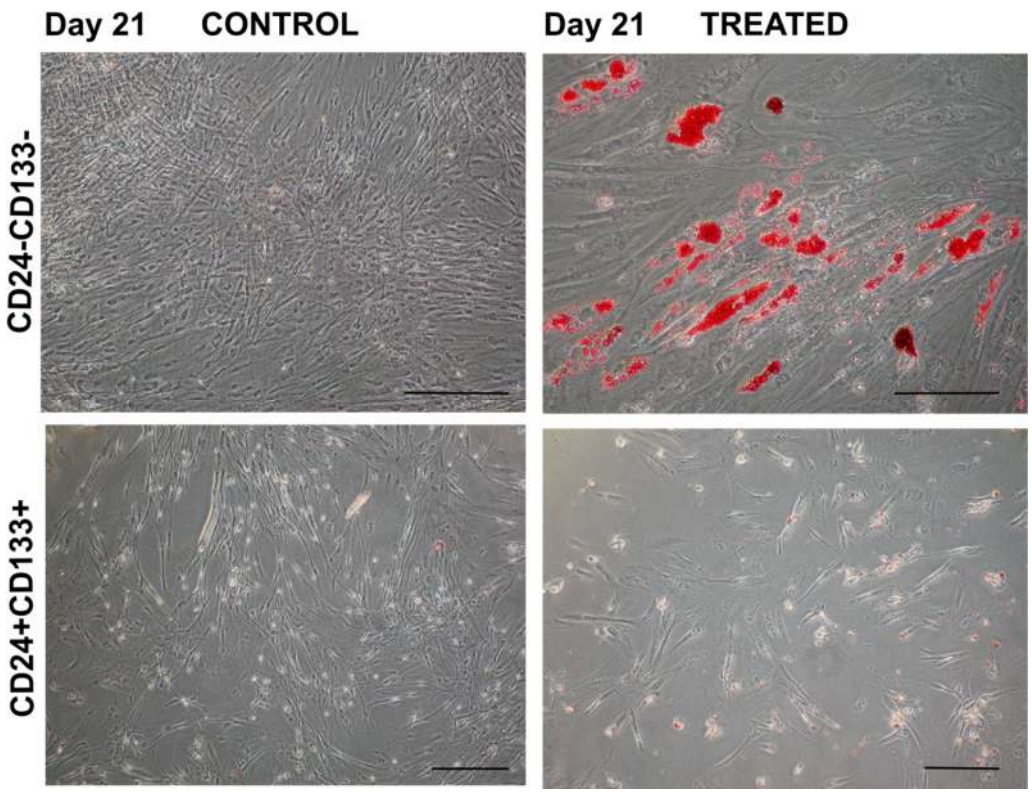

Figure 6-5 Oil Red O staining in controls and AdipoDiff treated cell lines after 21 days of differentiation.

Representative pictures of Oil Red O staining of $CD24^{-}CD133^{-}$ and $CD24^{+}CD133^{+}$ control and AdipoDiff medium (treated). Only $CD24^{-}CD133^{-}$ accumulated lipids in the cytoplasm positively stained with Oil Red O, while $CD24^{+}CD133^{+}$ did not show any differentiation, suggesting that compared to double positive clels, double negative cells might be induced to differentiate to adipocytes. Scale = 250µm.

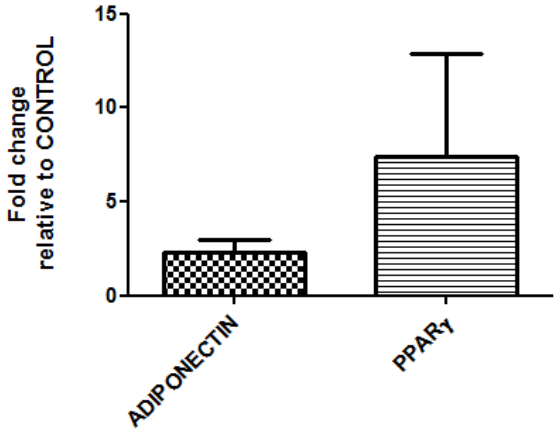

Figure 6-6 mRNA levels of adipogenic markers in CD24-CD133- treated cell lines.

Q-PCR analysis of adipogenic genes (*Adiponectin* and *PPARγ*) expression in CD24$^-$CD133$^-$ cells after 21 days in AdipoDiff medium. Columns depicting the fold change values (means) normalised to the housekeeping gene *β-actin* and compared with the control ± SEM. Expression of the adipogenes was higher in treated samples although value was not statistically significant when analysed with unpaired t test.

Table 6-2 Q-PCR fold change values of adipogenic genes in control and AdipoDiff treated CD24-CD133- generated from three different samples of 9 weeks.

CD24$^-$CD133$^-$	Mean ± SEM	Mean ± SEM
Adiponectin	1.0 ± 0.04	2.2± 0.40
PPARγ	1.0 ± 0.10	7.3± 2.70

6.1.3 *Epithelial differentiation*

Epithelial differentiation was performed by using Lithium Chloride at a concentration of 20 mM for 7 days. This was set as the best dose able to trigger a response towards the epithelial lineage with the minimal cell death (data not published).

In the first experiment, three $CD24^{-}CD133^{-}$ cell lines were seeded onto plastic culture plates and treated with LiCl for 7 days. After this time cells were evaluated for changes in cell morphology and expression of epithelial gene *E-cadherin*. $CD24^{-}CD133^{-}$ isolated from one sample (number 12141) and treated with LiCl showed formation of epithelial-like islands, while the treatment with LiCl in the other two cell lines showed an arrest in proliferation and no distinct changes in morphology (Figure 6-7). When *E-cadherin* mRNA was evaluated in control (HFK complete growth medium) and treated cell lines (HFK complete growth medium with 20 mM LiCl), a significant downregulation in its expression with LiCl treatment was observed (P=0.001, Figure 6-8). The data suggested that CD24, CD133 double negative cells treated for 7 days, not only did not response to epithelial differentiation induction but also appeared to significantly downregulate basal *E-cadherin* expression.

In the second experiment, it was tested whether growing cells on Matrigel could improve the outcome of the differentiation, since Matrigel has been previously shown to support differentiation of epithelial cells. $CD24^{-}CD133^{-}$ and $CD24^{+}CD133^{+}$ generated from one sample (number 12391), were treated with LiCl 20 mM for 7 days. $CD24^{-}CD133^{-}$ treated with LiCl showed a mixed phenotype with spindle like cells and smaller cuboidal cells (Figure 6-9). Interestingly $CD24^{+}CD133^{+}$ appeared more epithelial-like compared to the untreated control cells. Stimulated $CD24^{+}CD133^{+}$ showed a significant increase in *E-cadherin* expression (P=0.0061), whereas $CD24^{-}CD133^{-}$ significantly downregulated *E-cadherin* upon LiCl administration (P=0.0003,Table 6-3, Figure 6-10). In addition, the pre-tubular aggregates gene *FGF8* and the proximal tubule gene *Aminopeptidase A* gene expression was examined. *FGF8* mRNA expression increased in all the replicates in $CD24^{-}CD133^{-}$ cells, however this was no statistical significant (P=0.100). $CD24^{+}CD133^{+}$ expression of *FGF8* did not statistically change after LiCl treatment (Table 6-3, Figure 6-10). *Aminopeptidase A* mRNA expression was also evaluated as a marker of epithelial differentiation. *Aminopeptidase A* is a metalloprotease expressed from the stage of comma shaped bodies, then it is predominately observed in developing podocytes and brush borders of proximal tubular cells (Dijkman et al., 2006). *Aminopeptidase A* mRNA

expression, increased in both treated cells, however this was not significant when analysed with unpaired t test (*P*=0.20, Table 6-3, Figure 6-10).

This set of data suggested that $CD24^{+}CD133^{+}$ were able to upregulate the epithelial marker *E-cadherin* upon treatment with LiCl, however $CD24^{-}CD133^{-}$ appeared to respond in opposite way when given the same stimulus.

In the third experiment, another approach was used for the epithelial differentiation of double negative cells. This, considered a study, which observed that isolated nephrogenic cells fail to differentiate when the timing of the stimulus received is deregulated. These cells, when treated with a continuous stimulus that activate the canonical Wnt pathway, express *FGF8* retaining a mesenchymal phenotype and failed to differentiate towards an epithelial *E-cadherin*-expressing lineage. However, a transient stimulus, such as temporary activation of the canonical Wnt pathway through suppression of glycogen synthase kinase-3 (GSK3) with BIO, successfully stimulates the full epithelial transition (Kuure et al., 2007, Park et al., 2007).

I therefore planned a further experiment where the LiCl stimulation was not performed continuously for 7 days but transiently for 48 hours. Cells were grown on Matrigel coated plates, induced with LiCl for 48 hours and maintained for other 48 hours in normal complete growth medium.

When assessed for *E-cadherin* expression, $CD24^{-}CD133^{-}$ upregulated *E-cadherin* expression, however this was statistical significant only in cells isolated from one sample (number 13234) (*P*=0.0350, Figure 6-12, Table 6-4). As expected $CD24^{+}CD133^{+}$ significantly upregulated E-*cadherin* showing that also transient expression of LiCl could trigger epithelialisation in this cell population (*P*=0.0182). When evaluated for *Aminopeptidase A* expression, $CD24^{+}CD133^{+}$ upregulated this proximal tubule marker whereas $CD24^{-}CD133^{-}$ generated from 12141 downregulated *Aminopeptidase A*. $CD24^{-}CD133^{-}$ isolated from 13234 did not show any change after LiCl stimulation, the difference among the way $CD24^{-}CD133^{-}$ isolated from two different samples responded to the same stimulus from LiCl could be addressed to the 'freshness' of the cell line. In fact, $CD24^{-}CD133^{-}$ generated from 12141 were frozen and thawed before the experiment, while $CD24^{-}CD133^{-}$ from 13234 had never been frozen before the experiment. Cycles of freezing and thawing may indeed affect the plasticity of the cells causing a different behaviour when subjected to a stimulus (Figure 6-12, Table 6-4).

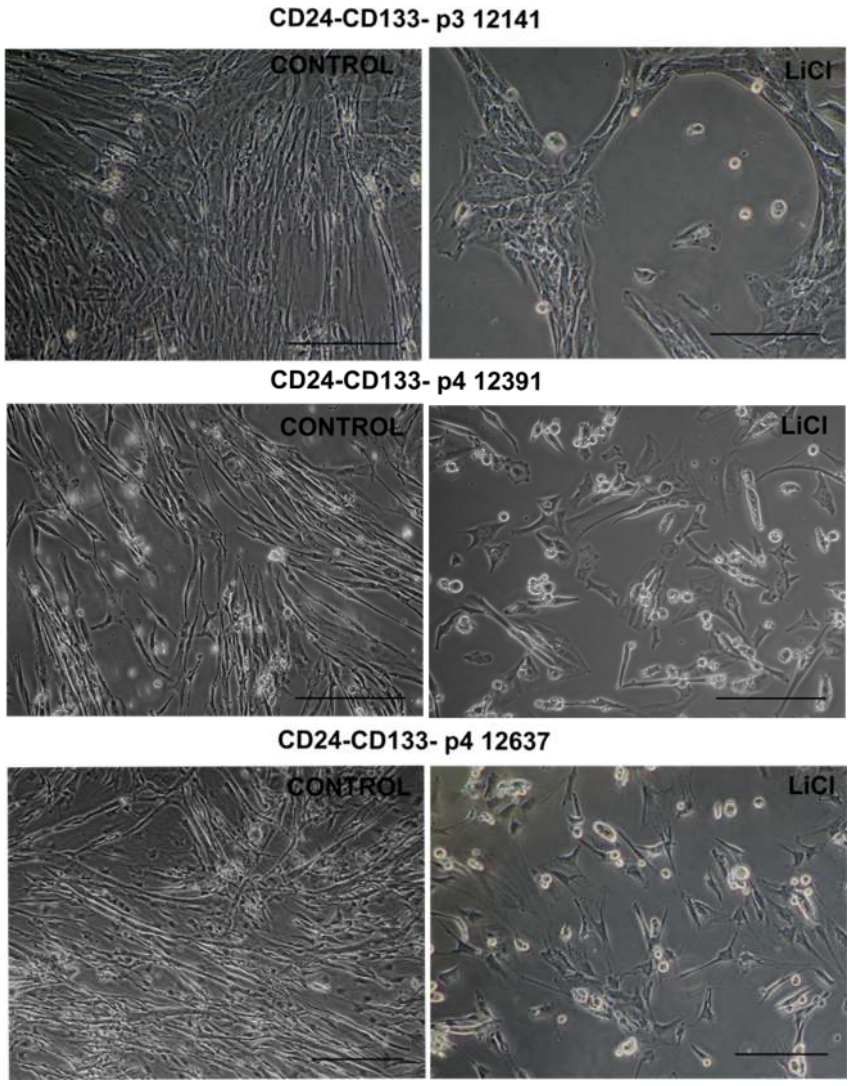

Figure 6-7 Epithelial differentiation with LiCl on plastic.

Pictures are representative of experiments performed in triplicates on $CD24^{-}CD133^{-}$ isolated from samples 12141, 12391, 12637, grown for 7 days in HFK medium (CONTROL) and in HFK medium supplemented with LiCl 20mM (LiCl). Epithelial-like patches were visible in only one of the cell lines treated (number 12141) while treatment in the other two cell lines appeared to be associated with decrease in cell proliferation compared to the untreated control. Scale = 250µm.

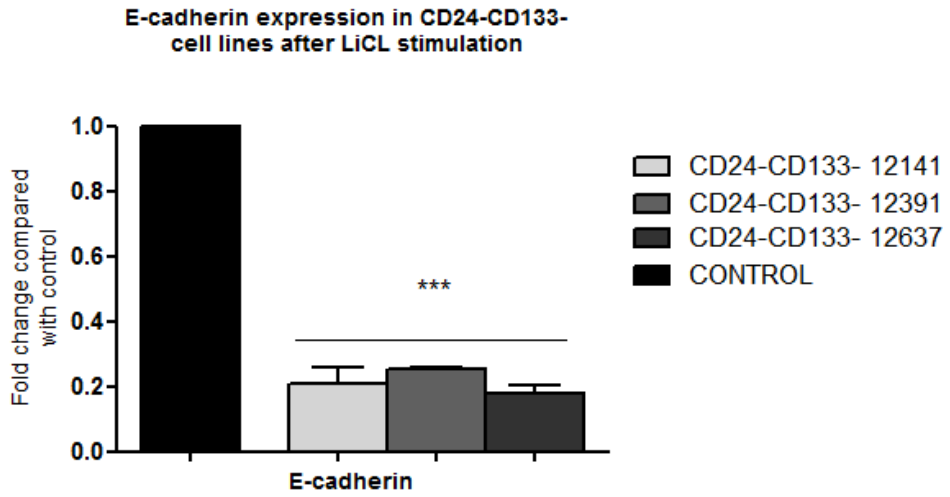

Figure 6-8 E-cadherin mRNA expression assessed with Q-PCR in CD24-CD133- cells (samples 12141, 12391, 12637) treated with LiCl on plastic plates vs control.

Unpaired t test was used to evaluate changes between control and treated cell lines. Double negative cell lines treated with LiCl appeared to significantly downregulate *E-cadherin* expression, suggesting that the continuous LiCL stimulation might hamper epithelial differentiation in these cell population. Values are ± SEM. * *P*=0.001.**

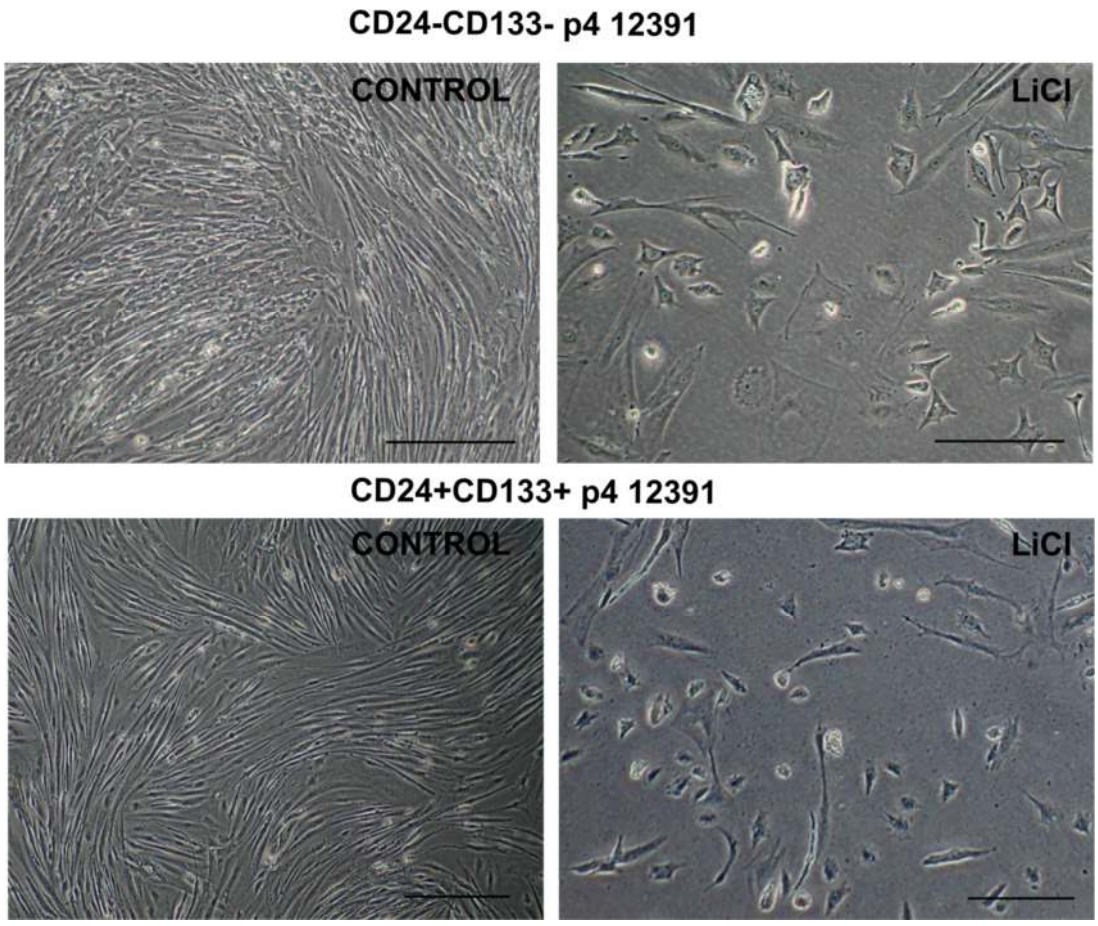

Figure 6-9 Epithelial differentiation with LiCl on Matrigel coated plates.

Pictures are representative of experiments performed in triplicates on $CD24^{-}CD133^{-}$ and $CD24^{+}CD133^{+}$ isolated from sample 12391 grown for 7 days in HFK medium (CONTROL) and in HFK medium supplemented with LiCl 20mM (LiCl). Treated cells of both cell lines showed changes in morphology as well as a decreased growth compared to untreated control. Scale = 250µm.

Table 6-3 Q-PCR Ct values of the Epithelial differentiation on Matrigel with LiCl of CD24-CD133- and CD24+CD133+ generated from a kidney sample (12391).

Gene	Control		Treated	
	CD24-CD133-12391	CD24+CD133 12391	CD24-CD133-12391	CD24+CD133+ 12391
	Mean Ct ±SEM	Mean Ct ±SEM	Mean Ct ±SEM	Mean Ct ±SEM
β-actin	15.77±0.05	15.14±0.13	15.96±0.19	15.99±0.08
E-cadherin	28.11±0.05	29.35±0.08	30.22±0.06	27.55±0.18
FGF8	32.14±0.05	31.57±0.15	31.39±0.09	32.12±0.11
β-actin	16.44±0.17	16.98±0.29	15.44±0.17	16.30±0.15
Aminopeptidase A	31.24±0.11	29.66±0.15	30.02±0.12	28.23±0.13

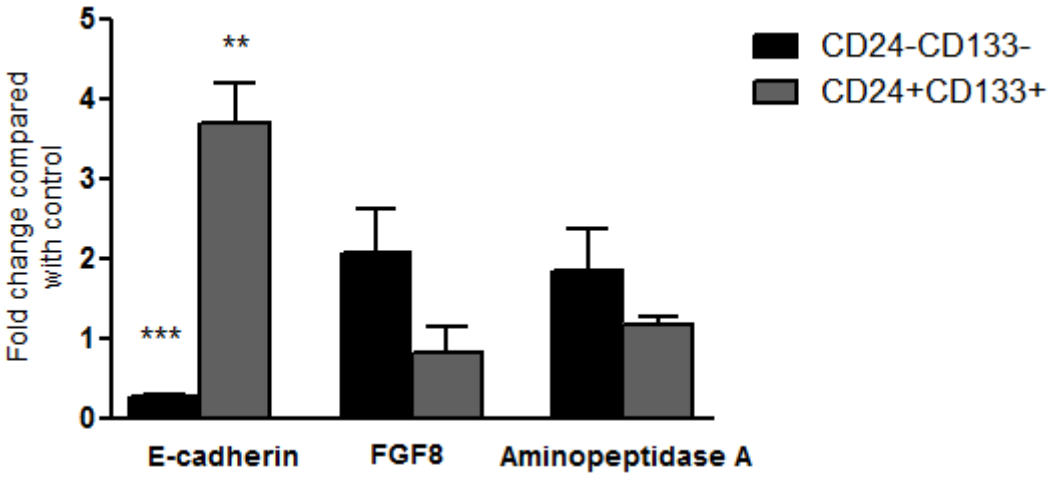

Figure 6-10 E-cadherin, FGF8 and Aminopeptidase A mRNA expression assessed with Q-PCR in CD24-CD133- and CD24+CD133+ cell lines (isolated from kidney sample number 12391) treated with LiCl on Matrigel coated plates for 7 days.

E-cadherin **expression was significantly upregulated by double positive cells suggesting that epithelial differentiation was induced in this cell line. Interstingly, LiCl treatment on double negative cells triggered a significant downregulation in this gene expression.** ***FGF8*** **expression did not change in treated double positive cell lines whereas increased in double negative cells.** ***Aminopeptidase A*** **was upregulated in both treated cell lines, although these changes were not statistically significant. Expression is indicated as fold change in gene/βactin compared with control. Unpaired t test was used to evaluate changes between control and treated cell lines. Values are ± SEM. *** *P*=0.0003, ** *P*=0.0061.**

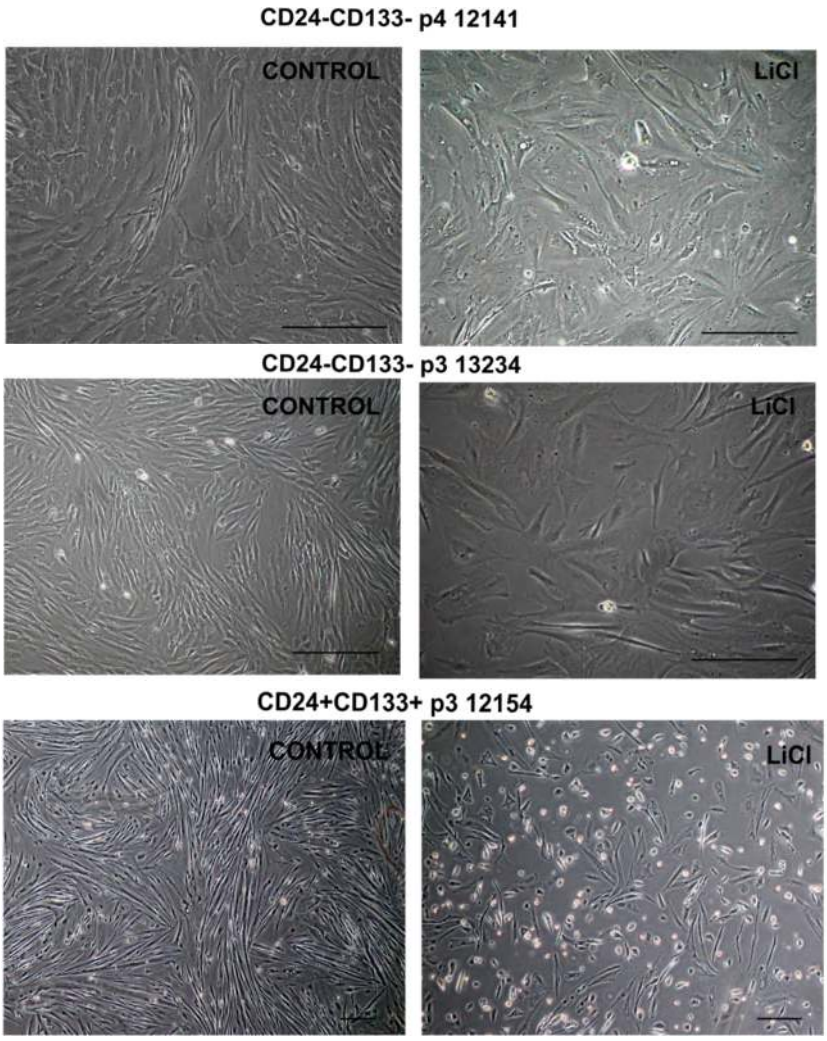

Figure 6-11Epithelial differentiation with transient LiCl (48h) on Matrigel coated plates.

Pictures are representative of experiments performed in triplicates on $CD24^{-}CD133^{-}$ (isolated from kidney samples number 12141, 13234) and $CD24^{+}CD133^{+}$ (isolated from kidney samples number 12141 and 12154) for 7 days in HFK medium supplemented with LiCl 20mM for 48 hours (LiCl) and replaced with HFK medium without LiCl for other 48 hours. Control triplicates were cultured for 4 days in HFK medium without LiCl. Both CD24, CD133 double positive and double negative cells transiently treated with LiCl appeared as more epithelial-like in morphology indicating that epithelial differentiation might have ooccurred in both cell lines with LiCl transient treatment. Scale = 250µm.

Table 6-4 Q-PCR Ct values of the Epithelial differentiation on Matrigel with transient LiCl addition (48h).

Gene	Control			Treated		
	CD24- CD133- 12141	CD24- CD133- 13234	CD24+ CD133+ 12154	CD24- CD133- 12141	CD24- CD133- 13234	CD24+ CD133+ 12154
	Mean Ct ±SEM	Mean Ct ±SEM	Mean Ct ±SEM	Mean Ct ±SEM	Mean Ct ±SEM	Mean Ct ±SEM
β-actin	16.98± 0.29	16.53± 0.19	17.84± 0.49	16.40± 0.12	16.31± 0.16	20.49± 0.46
E-cadherin	36.44± 0.75	33.85± 0.18	31.53± 0.50	34.91± 0.19	30.85± 0.18	31.78± 0.36
Aminopeptidase A	30.26± 0.22	29.52± 0.51	29.65± 0.47	30.78± 0.24	29.60± 0.47	31.07± 0.54

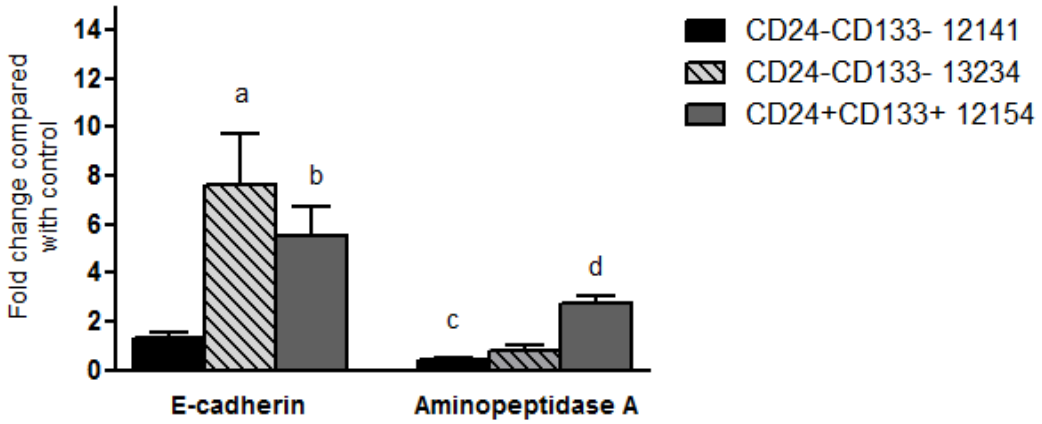

Figure 6-12 Q-PCR Ct values of the Epithelial differentiation on Matrigel with transient LiCl addition (48h).

E-cadherin **and** ***Aminopeptidase*** **A mRNA expression assessed with Q-PCR in $CD24^{-}CD133^{-}$ cell line (isolated from kidney samples number 12141 and 13234) and $CD24^{+}CD133^{+}$ (isolated from 12154) transiently treated with LiCl on Matrigel coated plates. Double negative cells, under transient LiCl stimulation, showed upregulation of** ***E-cadherin*** **expression as well as double positive cell line.** ***Aminopeptidase A*** **increased in expression in the double positive cell line only suggesting that double negative cells are not able to fully differentiate towards proximal tubule cells. Expression is indicated as fold change in gene expression compared with untreated control. Unpaired t test was used to evaluate changes between control and treated cell lines. Values are ± SEM. a=*P*=0.035, b=*P*=0.0182, c=*P*=0.0041, d=*P*=0.0086.**

6.1.4 *Kidney rudiment assay*

The kidney rudiment assay was used to evaluate the nephrogenic potential of $CD24^{-}$ $CD133^{-}$ and $CD24^{+}CD133^{+}$cell lines.

This technique was not in routine use in the research group of Prof. Winyard, I went to the University of Liverpool and learned it from the group of Dr. Murray at the Institute of Translational Medicine. Here I performed the technique on renal cells isolated from E13.5 mouse kidneys to learn and practice it while observing the capacity of these cells to form kidney-like structures *in vitro*. Aggregates were formed from a suspension of single cells obtained by enzymatic dissociation. The average cell viability, assessed by Trypan Blue staining, after dissociation into single cells was 90%. Suspensions containing 180,000 cells were subjected to mild centrifugation, and the pellets were cultured on filters membrane in minimum essential medium (MEM) supplemented with 10% serum with ROCK inhibitor, which was removed after 24 hours.

Aggregates were fixed and stained after 4, 5 and 7 days. I did not appreciate any substantial difference among these time points. Staining was always carried out with the antibody against the basal lamina protein, laminin, to distinguish any (re-) formed epithelial structure. After 4 days, renal cells formed short tubules not connected to each other and positively stained for the proximal tubule marker megalin. This indicated that embryonic renal cells could differentiate in culture and to have, to a certain extent, the capacity to form a proximal tubule- like system as seen *in vivo*. We also investigated whether embryonic cells arranged in glomerular-like structures. At day 5, the endothelial marker CD31 was detected, aggregates showed the presence of capillaries not organised in a defined network. Moreover, clumps of cells expressing WT1 were visible, their organisation resembled glomerular like structures with WT1 positive podocytes, limited by a basement membrane. These were more visible at day 7 where clearly WT1-positive aggregates of cells were delimited by laminin positive membrane (Figure 6-13).

Once learned this technique, the aim was to use this protocol to investigate the ability of human cell lines to contribute to renal tissues when mixed with embryonic cells isolated from murine kidneys. I therefore used this disaggregation-reaggregation approach to produce chimeric renal tissues that were composed of unlabelled murine embryonic kidney cells and of labelled $CD24^{-}CD133^{-}$ and $CD24^{+}CD133^{+}$. The protocol was modified using murine kidneys from embryonic day E12.5 instead of E13.5; other groups have used E11.5 – E12.5 murine kidneys in reaggregation experiments because earlier

renal cells are thought to have the greatest potential self-reorganisation (Hendry et al., 2013, Davies et al., 2012).

Human cells were labelled with the CellTracker CMFDA (green). Hence, before performing the reaggregation experiment, it was established whether CMFDA had any toxic effects on the cells. It was observed that CMFDA did not affect viability and cell proliferation when cells were labelled with CMFDA and cultured over 4 days.

Labelled human cells suspension was mixed with the embryonic murine kidney cell suspension in a ratio of 1:10 to reach 100,000 cells in total. After gentle centrifugation, the pellet was placed on the membrane filter supported by a metal grid. Controls consisted of reaggregated murine kidneys without human cells and intact embryonic kidneys. Moreover, reaggregation of only labelled human cells was performed to further evaluate any self-organisation potential present within these cell lines.

After 24 hours of treatment with ROCK inhibitor pellets were cultured for further 4 days in MEM. After this time reaggregates were fixed and stained with the general membrane basement marker laminin. As observed previously, aggregates formed by mouse embryonic cells showed capacity of self-organisation by arranging in tubule-like structures resembling the forming tubules during nephron development (Figure 6-14, A) however when compared to E 12.5 intact kidney cultured for 5 days in the same conditions (Figure 6-14, B), it was clear that these aggregates lacked the central organisation of the collecting duct tree. Furthermore, when mixed with $CD24^{-}CD133^{-}$ cells, these seemed, in one experiment, to have a detrimental action on the self-organisation of embryonic cells from mouse kidneys, with fewer epithelial structures developing and resembling more cysts than tubules (Figure 6-14, C), however this was not confirmed in other experiments set up with the same conditions. When $CD24^{-}CD133^{-}$ were aggregated by themselves, it was very difficult to transfer the pellet on the membrane filter as this was easily breakable. The only aggregate I was able to seed broke once in culture. Therefore, I was not able to show any data on the capability of this cell line to self-reorganise (Figure 6-14, D).

$CD24^{+}CD133^{+}$ on the other hand, when mixed with murine embryonic cells, appeared to be left outside the reforming murine structures and to not be able to participate to the reorganisation of such cells (Figure 6-14, E). When aggregated by themselves they did not show any self-organisation capacity Figure 6-14, F).

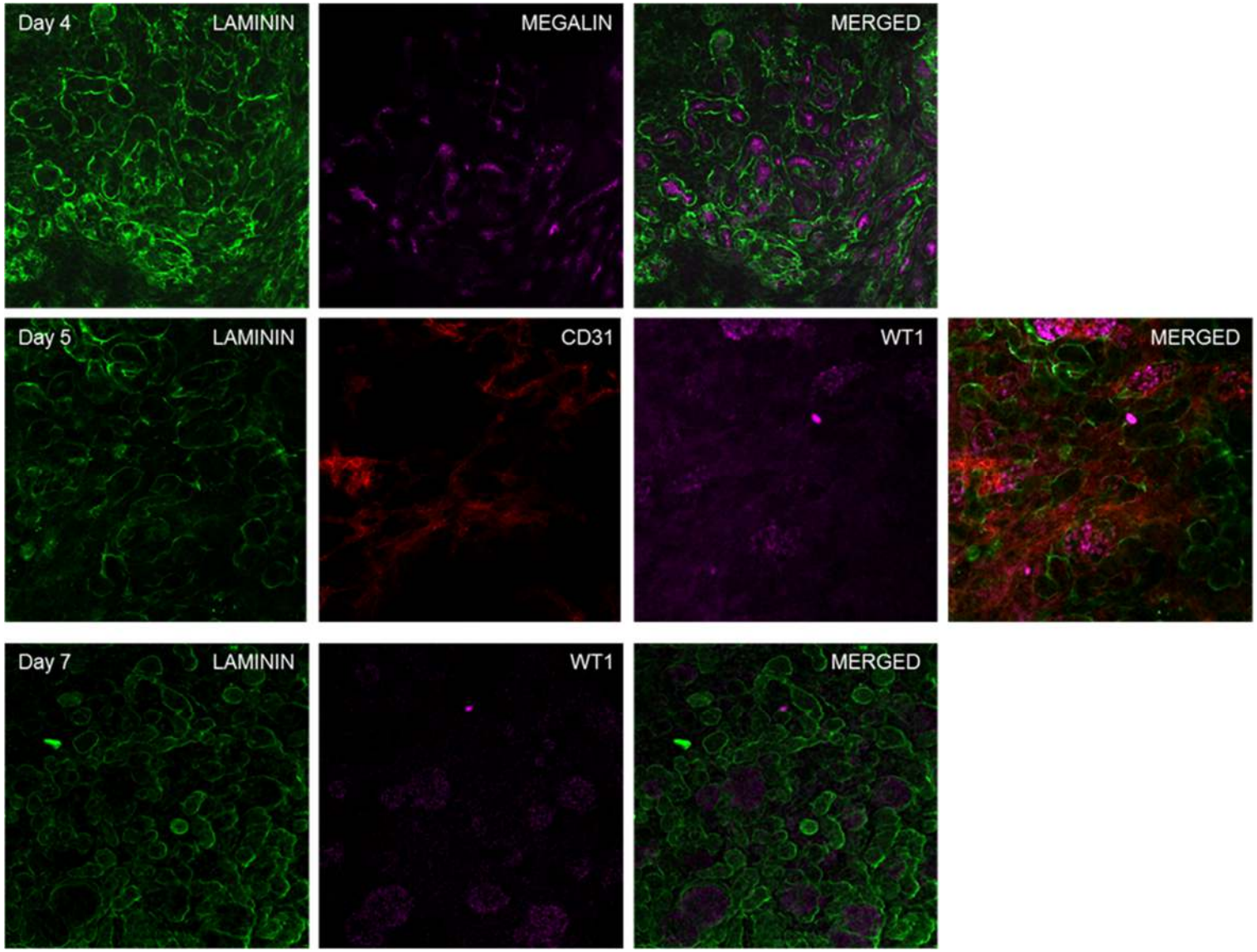
Day 4
LAMININ
MEGALIN
MERGED
Day 5
LAMININ
CD31
WT1
MERGED
Day 7
LAMININ
WT1
MERGED

Figure 6-13 Confocal sections of self-organised mouse embryonic kidney rudiments.

Kidney rudiments re-organised from suspension of separated embryonic kidney cells. Mouse embryonic kidney cells were disaggregated enzymatically, reaggregated and cultured for 4 (upper panel, day 4), 5 (middle panel, day 5) and 7 days in culture (day 7, bottom panel). When reaggregated, the cell re-formed epithelial structured that exhibited a laminin-rich basement membrane (green) and expressed the proximal tubule marker megalin (purple), and glomerular WT1 (Day 5, purple). Furthermore, at day 5, pellets showed presence of capillaries stained with CD31 (Day 5, red). Scale bars= 250 µm.

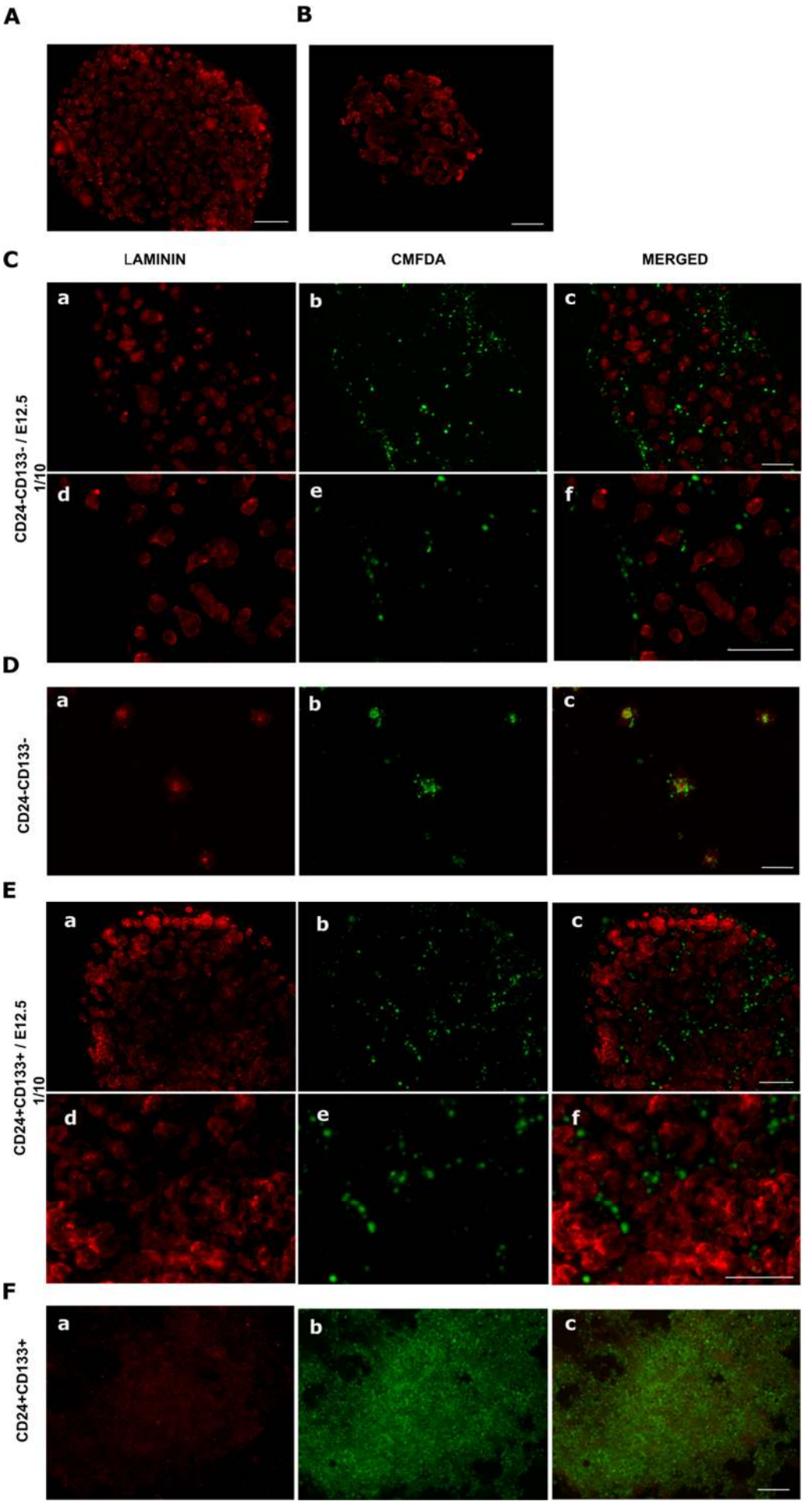
A
B
C
LAMININ
CMFDA
MERGED
a
b
c
d
e
f
CD24-CD133- / E12.5
1/10
D
CD24-CD133-
E
CD24+CD133+ / E12.5
1/10
F
CD24+CD133+

Figure 6-14 CD24-CD133- and CD24+CD133+ re-aggregation with or without mouse embryonic kidney cells.

(A) Laminin staining of aggregates obtained from suspension of embryonic murine kidneys. (B) As a control, intact murine embryonic kidneys were cultured in the same conditions and stained for laminin. (C) CMFDA-labelled $CD24^{-}CD133^{-}$ cell suspension (b, green) was mixed with embryonic kidney cell suspension in a ratio of 1:10 ratio and stained for laminin after 5 days culture (a, red). (D) $CD24^{-}CD133^{-}$ cells re-aggregated without murine cells and stained for laminin. (E) CMFDA-labelled $CD24^{+}CD133^{+}$ cell suspension (b, green) mixed with embryonic kidney cell suspension in a ratio of 1:10 ratio. Pellet was stained for laminin after 5 days culture. (F) $CD24^{+}CD133^{+}$ cells reaggregated without murine cells and stained for laminin. Neither $CD24^{+}CD133^{+}$ nor $CD24^{-}CD133^{-}$ had the potential to integrate into embryonic kidney rudiments and contribute to developing nephron structures and glomeruli. Scale bars = 50 µm.

6.2 SUMMARY

This part of the study was designed to examine and compare multi-differentiation and plasticity of the generated cell lines. Osteo-differentiation was evaluated by accumulation of extracellular calcium-deposits and upregulation of osteoblasts-related genes. In both cell lines calcium deposition was noticeable after 12 days of induction, appearing earlier in $CD24^{+}CD133^{+}$ compared to $CD24^{-}CD133^{-}$. When assessed for gene expression, only $CD24^{+}CD133^{+}$ significantly upregulated the osteo-gene *Osteopontin* whereas *RUNX2* and *BMP2* expression did not change.

Osteopontin is a late osteoblast marker, being expressed later in osteoblast differentiation, its expression is induced by BMP signalling pathway (Rahman et al., 2015). It therefore appeared that $CD24^{+}CD133^{+}$ might have differentiated towards osteo-lineage, as they expressed this late differentiation marker. On the contrary, $CD24^{-}CD133^{-}$, although accumulating calcium deposits, failed to fully differentiate. Adipo-differentiation on the other hand was only achieved by $CD24^{-}CD133^{-}$ cell lines isolated from 3 different samples of the same gestational age. Upon stimulation for 21 days with AdipoDiff, cells upregulated adipocytes markers *Adiponectin* and *PPARγ* and accumulated lipids positively stained with Oil Red O solution.

These results, although interesting in the demonstration of some sort of plasticity of isolated cell lines were limited by the following considerations:

- A more appropriate negative control should have been used. In this set of experiments, the negative control was composed of the same cell line but grown in normal growth medium. To better assess the effects of the induction and to avoid *in vitro* culture artefact, this should have been tested on a terminally differentiated cell line, which does not show plasticity potential.
- A positive control should have been added to the experiment setting. This could be a mesenchymal stem cell line which is known to be able to undergo osteogenesis and adipogenesis.
- A combination of various techniques, involving co-culture with fetal osteoblasts and introduction of appropriate ECM substratum within *in vitro* culture should have been used to better mimic the environment involved in the natural milieu of differentiation of stem cells.

Another part of the study aimed at evaluating whether generated cell lines are multipotential and can produce a limited range of differentiated cell lineages appropriate

to their location. This was investigated through stimulation with the MET inducer LiCl for 7 days. This resulted in upregulation of epithelial differentiation marker *E-cadherin* and proximal tubule protein *Aminopeptidase A* in $CD24^{+}CD133^{+}$ cell lines, whereas $CD24^{-}CD133^{-}$ upregulated *E-cadherin* only if treated transiently (48 hours) with LiCl.
The following considerations were drawn upon these results:

- The effect of transient LiCl induction in double negative cells as well as the effects on double positive cells should have been studied on a larger number of cell lines to improve reliability of the data presented.
- A more extensive study should be performed on the effects of LiCl treatment, in particular multiple markers should be used to highlight the different cell types formed upon LiCl induction of double positive and double negative cell lines (proximal tubule cells, distal tubule cells, collecting ducts cells and so on).
- Appropriate positive and negative controls should have been included in the experiment planning.

The last part of this study evaluated the nephrogenic potential of isolated cell lines with the use of the kidney rudiment assay. This experiment resulted in incapacity of labelled human cells to integrate in reformed renal structures constituted by murine embryonic cells only.
The lack of ability of human cells to contribute to differentiated murine renal tubules, could be due to unfavourable culture conditions and to species-specific differences. Embryonic murine cells might have faster proliferation rate dependent on species or embryonic age factors, compared to human cell lines. Human renal fetal-derived cells might be slower cycling thus being not able to compete with murine cells to form/be part of the epithelial aggregates.
Other factors may be represented by the different cell size between murine and human cells impairing the inclusion of human cells in the reforming renal-like structure due to their large size, or to the difference in cell signalling and microenvironment in which nephrogenesis takes place. Price *et al*. showed that human fetal kidneys display a different expression of growth factor receptors compared to mouse. In the study published in 2007, LIF receptors were detected in human stroma, mesenchyme and ureteric bud of fetal kidneys whereas LIF receptors in mice are only expressed by mesenchyme (Price et al., 2007).

To better examine the capacity of human cells to form kidney structures, these were re-aggregated without murine cells. Also in these conditions, human cells did not show ability to form any structure. These data showed that $CD24^{-}CD133^{-}$ and $CD24^{+}CD133^{+}$ when cultured in the same conditions displayed a different plasticity. In general, better results could be achieved with a clonal cell population rather than a mixed one, because in this case some cells might have contributed to the differentiation better than others and the other way around. Moreover, other two variables need to be considered: samples were frozen and thawed before differentiation. I did not assess whether this factor could have affected the differentiation ability of the cell lines. Moreover, I performed all the experiments with the lowest passage number possible, however as seen by the gene expression analyses, cell lines after few passages in culture change gene expression, this may result in loss of their 'stemness' properties decreasing the capacity to differentiate.

7 PRE-CLINICAL EVALUATION OF $CD24^{-}CD133^{-}$ AND $CD24^{+}CD133^{+}$ CELLS EFFECTS ON FOLIC ACID- INDUCED KIDNEY INJURY

Stem/progenitor cells can be proposed as a promising resource for regenerative medicine to treat renal disorders by replacing lost nephrons, or as a source of trophic support, as a therapeutic vehicle or as a tool for *in vitro* modeling to better study specific diseases and possibly to personalise specific treatments.

The translation on the clinical practice of stem cells based therapies requires preclinical studies in order to examine the feasibility, efficacy and safety of this possible therapy.

Hypothesis and aims

In this part of my study, I hypothesised that isolated cell lines might be able to localise to injured kidneys and to improve altered renal function in a mouse model with immunosuppressed immune system and acute tubular injury.

The aims were the following:

- Test in wild type mice with BALB/c genetic background the Folic Acid (FA)-induced nephrotoxicity, model previously established in my laboratory in eight-week-old, male, wild type CD1 mice (Long et al., 2001). 7 weeks old male BALB/c wild type mice were chosen as this is the common genetic background of different immunosuppressed mice strains in which the cell lines would be injected; FA-induced nephropathy was first tested and analysed in this strain to gain insights on the progression of the renal injury.
- Establish the best model of FA-induced nephrotoxicity in immunosuppressed mice with increasing degree of genetic immunodeficiency. FA-induced kidney injury was tested in:
    - 7 weeks old male BALB/c nude (BALB/c-$Foxn1^{nu}$), lacking the T-cell response
    - 7 weeks old male BALB/c SCID (BALB/c-$Prkdc^{scid}$) lacking a functional T- and B-cell response

    - 7 weeks old male NOD-SCID (NOD.CB17-Prkdc^{scid}) with reduced natural killer cells activity, presence of functionally less mature macrophages and lack of serum haemolytic complement activity (Shultz et al., 1995).
- Test whether human renal cell lines administered in immunodeficient mice at the peak of the renal injury caused by FA determined any amelioration of renal damage provoked by folic acid.
- Observe human renal cell lines body-distribution over time with *in vivo* bioluminescence imaging.

7.1 RESULTS

7.1.1 *Evaluation of Folic acid-induced renal injury in BALB/C wild type*

Seven-week-old male BALB/c mice were randomly assigned into two groups, those to be injected with folic acid (n=18) and those to be injected with sodium bicarbonate (n=4) as a vehicle control group. Kidneys, from the FA group, were collected after 2, 14, 21 and 42 days post injection with four animals at each time point.

In the FA group 17 animals started showing signs of sickness such as bristling of the coat, hunched posture and reduced alertness 24 hours after FA injection. One mouse did not show these signs, this mouse did not receive any injury post folic acid administration when assessed for renal function (BUN). These signs were absent in the vehicle group.

BUN and Body weight

Renal function changes were examined by assessing BUN. Three main questions were addressed in the planning and analysis of this set of data:

- Does the BUN in FA injected group change over time compared with the baseline value?
- Does the BUN in the control/vehicle group change over time compared with the baseline value?
- Do the FA and control groups differ in terms of BUN at specific time points?

We answered these questions graphing the BUN values obtained and by analysing the data with non-parametric test. The non-parametric test was chosen because the distribution of the data did not follow a normal/Gaussian distribution when tested with the 'D'Agostino-Pearson' normality test on the software GraphPad Prism. As BUN was measured repeatedly over time, the test used for statistical analysis was a 'repeated measures one-way ANOVA with multiple post-tests to compare specific groups.

To address the first question, I determined BUN in FA group before FA injection and after 2, 7, 14, 21, 28 and 42 days.

Two days post FA injection, BUN showed over 3-fold significant increase when compared with baseline values ($P \leq 0.001$, 83.57±2.63 mg/dl at day 2 compared with baseline 25.61±0.23 mg/dl).

After 7 days BUN was still high (64.32±6.73 mg/dl) and not significantly different to day 2.

By 14 days BUN started decreasing reaching lower levels (49.80±4.10 mg/dl) without any difference compared with day 7.

42 days after FA, BUN had further decreased although still significantly different compared with the baseline (32.50±2.49 mg/dl, $P \leq 0.01$) but not significantly different to day 28.

To address the second question, I measured BUN in the control group over time, BUN did not show any significant changes at day 2, 7, 14, 21, 28 and 42 compared with the baseline (Figure 7-1, Table 7-1).

To respond to the last question, I compared the BUN of the FA group against the control group. No differences in BUN were observed at baseline. At day 2, BUN in FA group was significantly higher than BUN in the control ($P \leq 0.01$). At day 7, BUN in FA group showed significant difference with the control ($P \leq 0.01$). At day 14, BUN in FA group was still higher than the control group at the same time point but not significantly different (probably due to the variability of BUN values within the FA group). At day 21, 28 and 42, FA group and control group did not show statistically different BUN values.

Body weight was registered before and after 2, 7, 14, 21, 28 and 42 days post FA injection (Figure 7-2 and Table 7-2). Animals within the FA group lost 2% of weight after 2 days from injection (22.53±0.77 g at day 2 compared with baseline 22.94±0.94 g) and continued to lose weight reaching -10% (compared with baseline body weight) at day 7 (20.87±0.91 g). Two animals in the FA treated group were euthanised as they lost ≥20% of body weight, percentage exceeding the value allowed by the Project Licence. Animals recovering after 7 days showed an increase in body weight. Vehicle treated mice increased consistently in weight over time. When compared with the control group, FA group did not show a statistically significant difference in the weight, probably due to the wide variability of body weight values within the group.

Tissue histology

By immunohistochemistry, striking changes were visible 2 days after FA administration in the renal cortex (Figure 7-3, B) where flattened cortical epithelia and dilated tubules were observed. Most of the proximal tubules showed partial loss or complete loss of the brush border. Casts were seen in some tubular lumina, likely composed of cellular debris detaching from the tubular basement membrane combined with proteins present in the lumen of tubules. Fourteen days after injection, most of cortical areas underwent

regeneration and kidneys showed reduced areas of injury with dilated tubules and protein casts (Figure 7-3, C). Most glomeruli were undamaged, although some showed a more prominent Bowman's space (Figure 7-3, C). By 21 days, most of the kidney cortical areas had regenerated, however some areas were unable to do so and showed a fibrotic appearance (Figure 7-3, D). These were also evident at 42 days post FA (Figure 7-3, E). Mice administered vehicle contained normal histology, with the renal corpuscle containing well-formed glomerular tufts and Bowman's space. The renal tubules showed normal histological architecture (Figure 7-3, A).

Macrophage infiltration following FA administration was detected using immunostaining for F4/80, a specific macrophage antigen (McKnight et al., 1996). Vehicle treated mice showed sparse macrophages, whereas F4/80-positive macrophages were observed in the interstitium around tubules and glomeruli in kidneys harvested 14, 21 and 42 days after FA administration (Figure 7-4). I also examined the presence of fibrosis-associated markers, collagen I and collagen III by immunohistochemistry. Both collagens increased in the kidneys of FA-injected mice versus the controls. Collagen I immunostaining was barely observed in sham controls (Figure 7-5, A), whereas its deposition increased in the interstitium around tubules and glomeruli in FA group starting from 14 days (Figure 7-5, B).

Collagen III was examined in vehicle group, where positive immunostaining was observed in the renal cortex (Figure 7-6, A and B). Fourteen days after FA, tubules showed signs of injury (Figure 7-6, C and D). After 21 days, large hypertrophic tubules that did not appear positive for collagen III were often observed surrounded by fibrotic areas with higher collagen deposition, this was even more evident 42 days after FA, where wide areas of collagen III accumulation/fibrosis could be observed. By immunostaining of collagens FA injured kidneys showed regenerated areas after injury alternated to areas with collagen deposition.

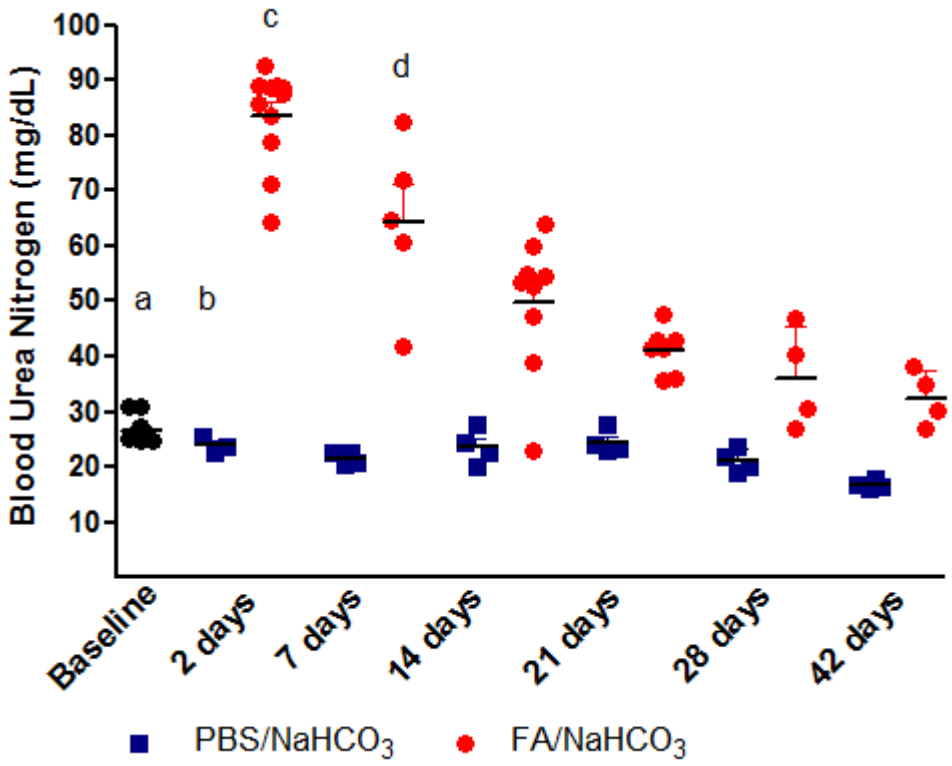

Figure 7-1 BUN measures at different times in control mice (vehicle, PBS/$NaHCO_3$) and in FA mice (FA/$NaHCO_3$).

BUN measures at different times in control mice (vehicle, PBS/NaHCO3) and in FA mice (FA/$NaHCO_3$). BUN values increased rapidly 48 hours post FA injection in FA/$NaHCO_3$ treated mice indicating that acute renal injury occurred within 2 days from FA injection. Injured kidneys recovered over time with BUN values slowly decreasing over time. Control mice did not show changes in BUN after PBS/$NaHCO_3$ injections. Values were analysed with non-parametric one-way ANOVA a= $P \leq 0.001$ compared to 2 days after FA. b= $P \leq 0.05$ compared to 2 days after FA. c= $P \leq 0.001$ compared to vehicle, d= $P \leq 0.05$ compared to control 7 days.

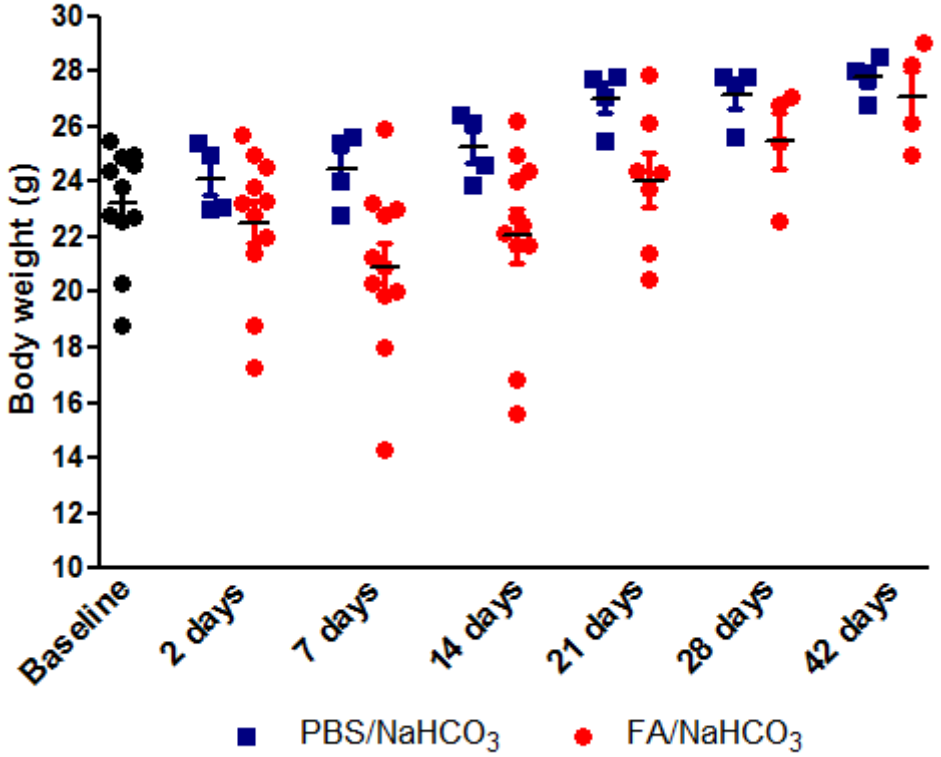

Figure 7-2 Body weight measurements at different time points in control group (vehicle, PBS/$NaHCO_3$) and FA group (FA/$NaHCO_3$).

Body weight loss of 2% of total body weight was measured in treated mice group at day 2, further increasing to minus 10% at day 7, indicaitng that acute kidney injury cause body weight loss in treated group. After 7 days, treated mice slowly recovered gaining weight, which values returned to baseline levels at day 42. In control mice group no significant body weight changes were recorded.

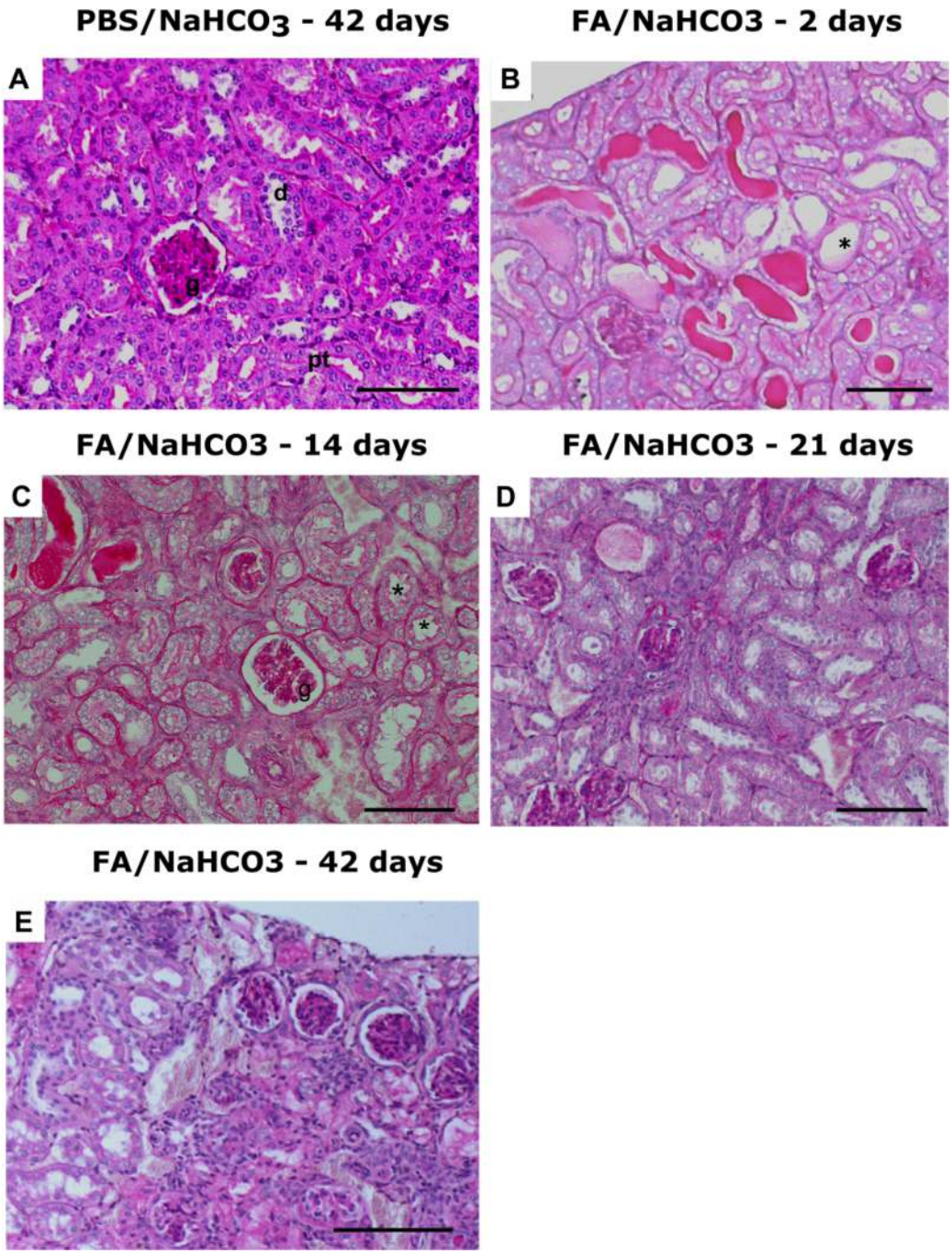

Figure 7-3 PAS staining in vehicle treated mice (PBS/$NaHCO_3$, 42 days post injection) and in folic acid treated mice at different time points (FA/$NaHCO_3$, 2, 14,21 and 42 days).

(A) PAS staining in vehicle animals after 42 days showed normal histology (representative of n=4 mice, 24 sections examined). Glomeruli (g) had normal appearance, as well as proximal (pt) and distal (d) tubules.(B) 2 days after FA, tubules in the renal cortex were dilated (*) with casts in the lumen (arrow). (Figure representative of n=4 mice, 40 sections examined). (C) 14 days after FA injection, areas with dilated tubules (*) and protein casts (arrow) although reduced in extension were still observable (figure representative of n=4 mice, 20 sections examined).(D) At 21 days and 42 days (E) most of the epithelia regenerated, however patchy fibrotic areas were observed in the renal cortex (arrows). Figures representative of n= 4 mice in 21 days group and 42 days group, respectively 12 and 21 sections examined). Scale bars = 100 µm.

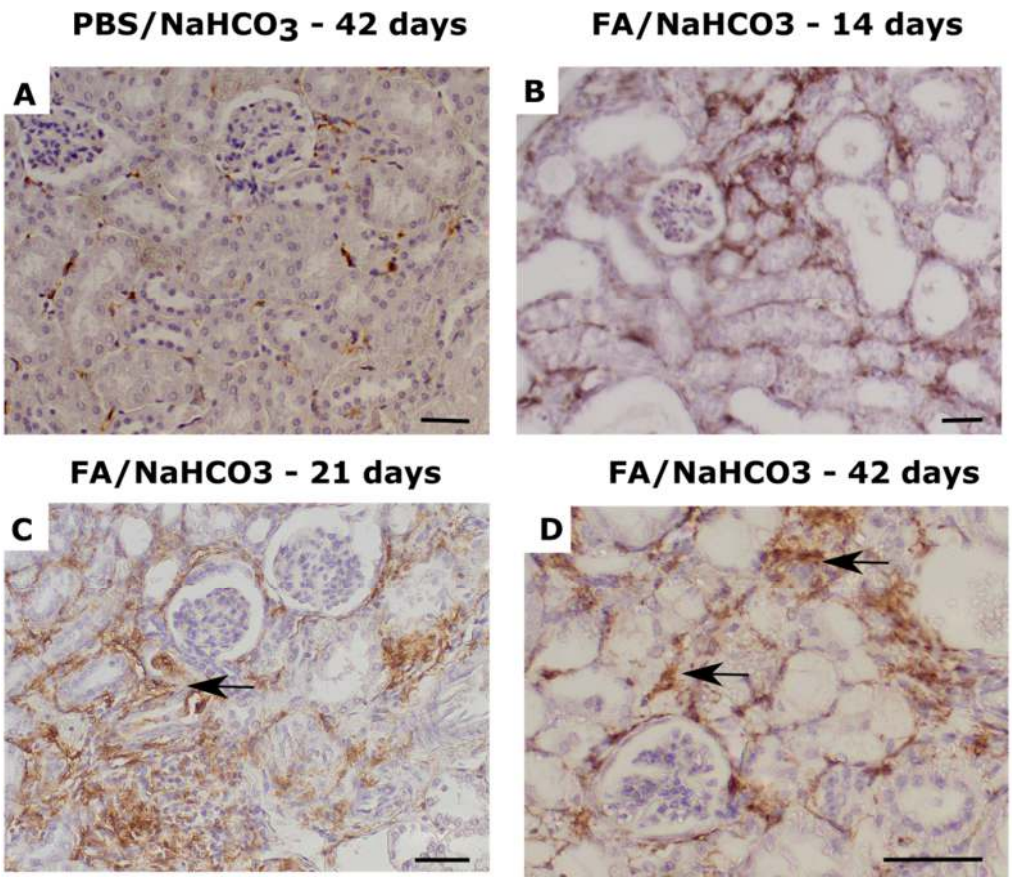

Figure 7-4 F4/80 immunostaining of macrophages in vehicle mice (PBS/$NaHCO_3$, 42 days post injection) and in FA mice at different time points (FA/$NaHCO_3$, 14, 21 and 42 days).

(A) Sparse macrophages (brown staining) were observed in interstitial areas of vehicle treated animals (arrow). Figure representative of n= 4 mice in 42 days group, 23 sections examined). (B) 14 days after FA injection, macrophages infiltrated in small areas. Figure representative of n= 4 mice, 12 sections examined (C) After 21 days and 42 days (D), when regeneration occurred, fibrotic areas still showed macrophage presence (arrows) Figures describing n= 4 mice in 21 and 42 days group, 20 and 28 sections examined). Scale bars = 50 μm.

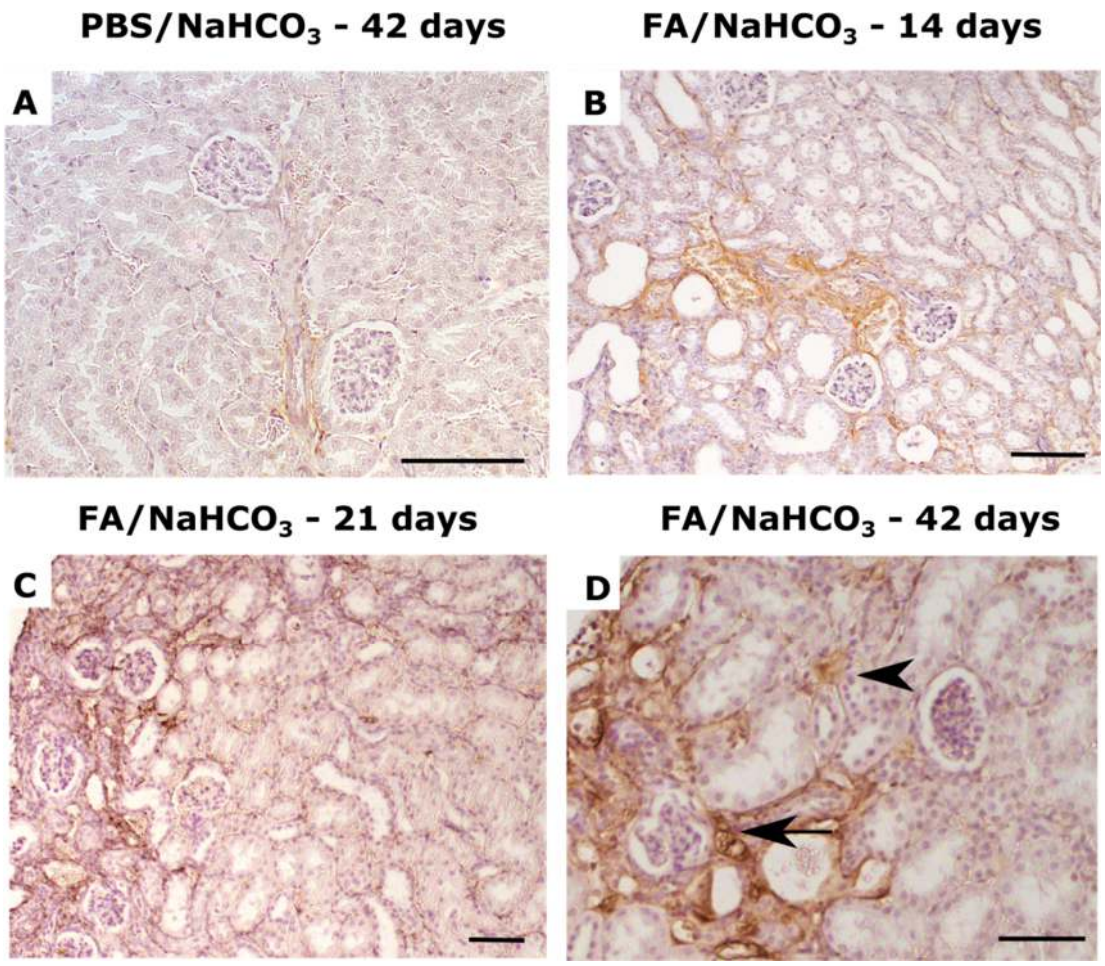

Figure 7-5 Collagen I immunostaining of fibrosis in vehicle mice (PBS/NaHCO3, 42 days post injection) and in FA mice at different time points (FA/NaHCO3, 14, 21 and 42 days).

(A) Collagen I staining in vehicle animals. Figure representative of n= 4 mice, 14 sections examined. (B) Fourteen days after FA injection, small areas with collagen I deposition were observed, whereas After 21 days (C) and 42 days (D) larger fibrotic areas showed increased collagen I presence (arrows) compared with the lack of it in regenerated areas (arrowhead) Figure representative of n= 4 mice in each group, 12 sections examined at 14 days, 16 sections at 21 days and 26 at 42 days. Scale bars = 50 □m.

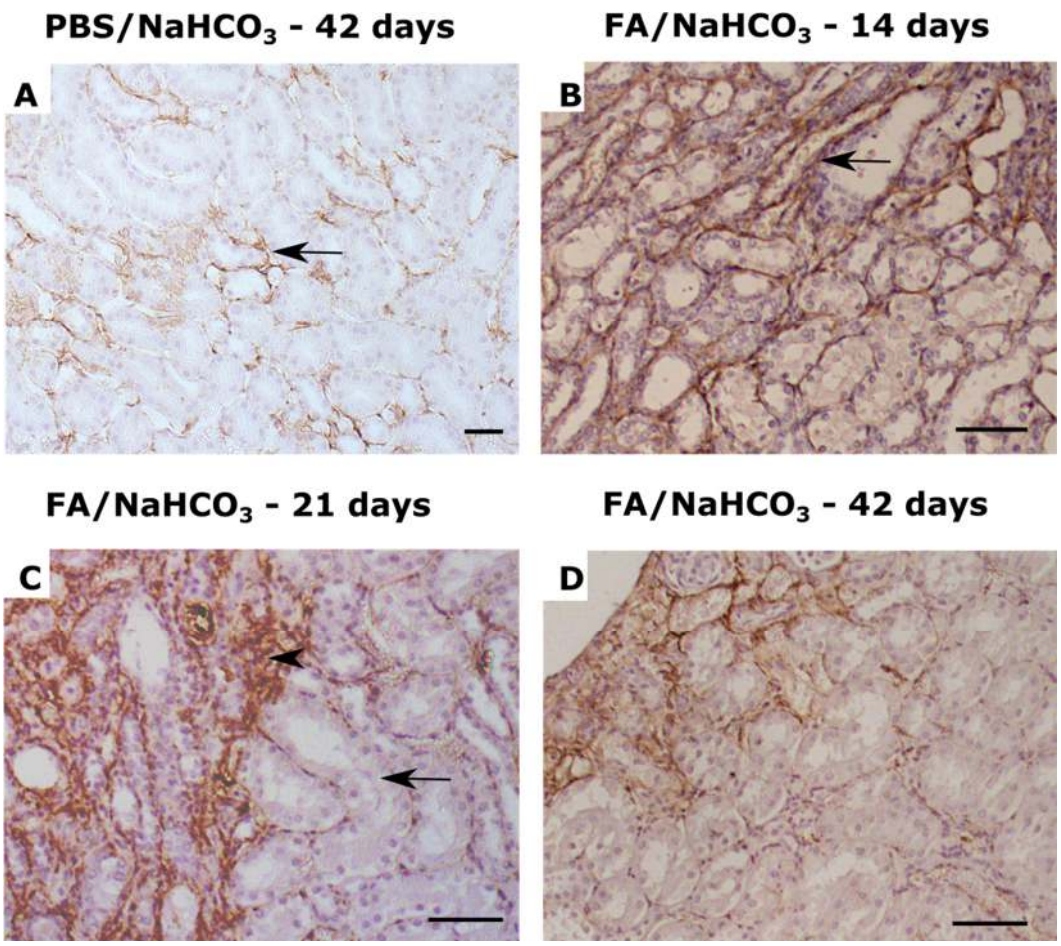

Figure 7-6 Collagen III immunostaining of fibrosis in vehicle mice (PBS/NaHCO3, 42 days post injection) and in FA mice at different time points (FA/NaHCO3, 14, 21 and 42 days).

(A) Low expression of collagen III around tubules (arrow) in sections from control group. Picture representative of n=4 mice, 12 kidney sections examined (B) At 14 days intense brown staining was observed. Figure representative of n=4 mice, 23 sections analysed. (C) At 21 days, regenerated areas (arrow) were alternated to fibrotic areas (arrowhead) with intense collagen III deposition. Figure representative of n=4 mice, 12 sections analysed. (D) After 42 days from FA injection, large regenerated areas with low collagen III deposition were surrounded by scarred areas characterised by intense collagen III. Figure representative of n=4 mice, 27 kidney sections examined. Scale bars were=100 µm.

7.1.2 *Evaluation and comparison of folic acid-induced renal injury in immunodeficient mice*

The development of the FA-induced renal injury was observed in immunodeficient 7 weeks old male BALB/c nude (BALB/c-Foxn1^{nu}),7 weeks old male BALB/c SCID (BALB/c-Prkdc^{scid}) and 7 weeks old male NOD-SCID (NOD.CB17-Prkdc^{scid}).

All the animals were injected with a single dose of FA of 240 μg/g body weight. Kidneys were initially planned to be collected at 21 days post FA injection.

After 2 days from FA, one mouse in the nude group (n=5) and one in the NOD-SCID (n=5) was sick and euthanised, showing that folic acid injection provoked an injury that resulted in the death of the animal.

The other FA treated animals in all groups started showing typical signs of illness, such as hunched posture, reduced alertness and lethargic behaviour. These appeared after 24 hours from FA injection.

BUN and Body weight

BUN and body weight were determined after 2,7,14 and 21. NOD-SCID were monitored up to 42 days after injury because of the lack of recovery of renal function.

Nude and SCID animals started showing signs of sickness after 24 hours from FA injection. BUN significantly increased of 2.8-fold in nude mice 2 days post FA injection compared with baseline ($P \leq 0.001$; 2 days, 65.58±7.42 mg/dl; baseline, 23.85±1.32 mg/dl). After 2 days they lost 5% of body weight ($P \leq 0.05$, 20.30±0.43 g compared with baseline 21.45±0.39 g), this progressively increased within a week after FA injection ($P \leq 0.05$, 21.58±0.25 g).

SCID mice FA-induced renal injury appeared milder than nude mice, with less than 2-fold increase in BUN 2 days after FA compared with the baseline ($P \leq 0.001$, 2 days, 51.93±6.61 mg/dl; baseline, 24.68±1.85 mg/dl). BUN decreased progressively over time reaching values not significantly different from the baseline (Figure 7-7, Table 7-3). Body weight decreased of 0.5% compared to baseline body weight within the first two days ($P \leq 0.05$, 23.13±0.35 g, baseline 23.25±0.37 g), increasing after this time (Figure 7-7, Table 7-3, Table 7-4).

In the NOD-SCID group, FA-induced injury appeared more severe than nude and SCID mice, with severe signs of sickness and a slower recovery phase.

BUN increase of 3 folds within two days from FA injection compared to baseline ($P \leq 0.001$, 70.57±12.66 mg/dl at day 2; baseline 22.86±2.09 mg/dl) and it stayed high for the whole duration of the experiment (42 days).

NOD-SCID mice lost almost 8% of their body weight within the first 2 days, which further increased to 9.5% at day 7 showing that the recovery phase was delayed in these mice, weight slowly increased over time (Figure 7-7, Table 7-3. Table 7-4).

Tissue histology

Kidney histology was examined by PAS staining 21 days post FA in treated nude and SCID, whereas treated NOD-SCID mice were euthanised at day 42 and histology performed at that time point.

NOD-SCID kidneys compared with nude and SCID sections, at day 42, showed extensive areas of fibrosis in the renal cortex and overall worse kidney histology. Inflammation and fibrosis was evaluated in these mice strains. Nude mice kidneys showed some areas of macrophages infiltration and patchy areas of collagen I and III deposition. Only few areas of collagens deposition were visible by histology. Whereas NOD-SCID kidney sections presented macrophages infiltration and extensive collagens deposition. Fibrotic areas were surrounded by hypertrophic tubules, possibly grown in size to overcome for the loss in function of fibrotic tissue.

To summarise the data and to have a clear idea of the features of FA-induced injury in different mice models, I compared the BUN measurements at the same time points within WT, nude, SCID and NOD-SCID animals. At 48 hours from FA-injection, BUN values raised in all the groups compared with baseline values, showing a clear decline in renal function. The degree of BUN increase after 2 days was statistically lower in SCID animals compared with the wild type at the same time point. Within 14 days from the injury, BUN in nude and SCID mice returned to levels not significantly different to the baseline value. WT and NOD-SCID mice, showed a delayed recovery: at day 21 NOD-SCID BUN had an average value of almost the double of the baseline value, which did not further decrease, even after 42 days from injection.

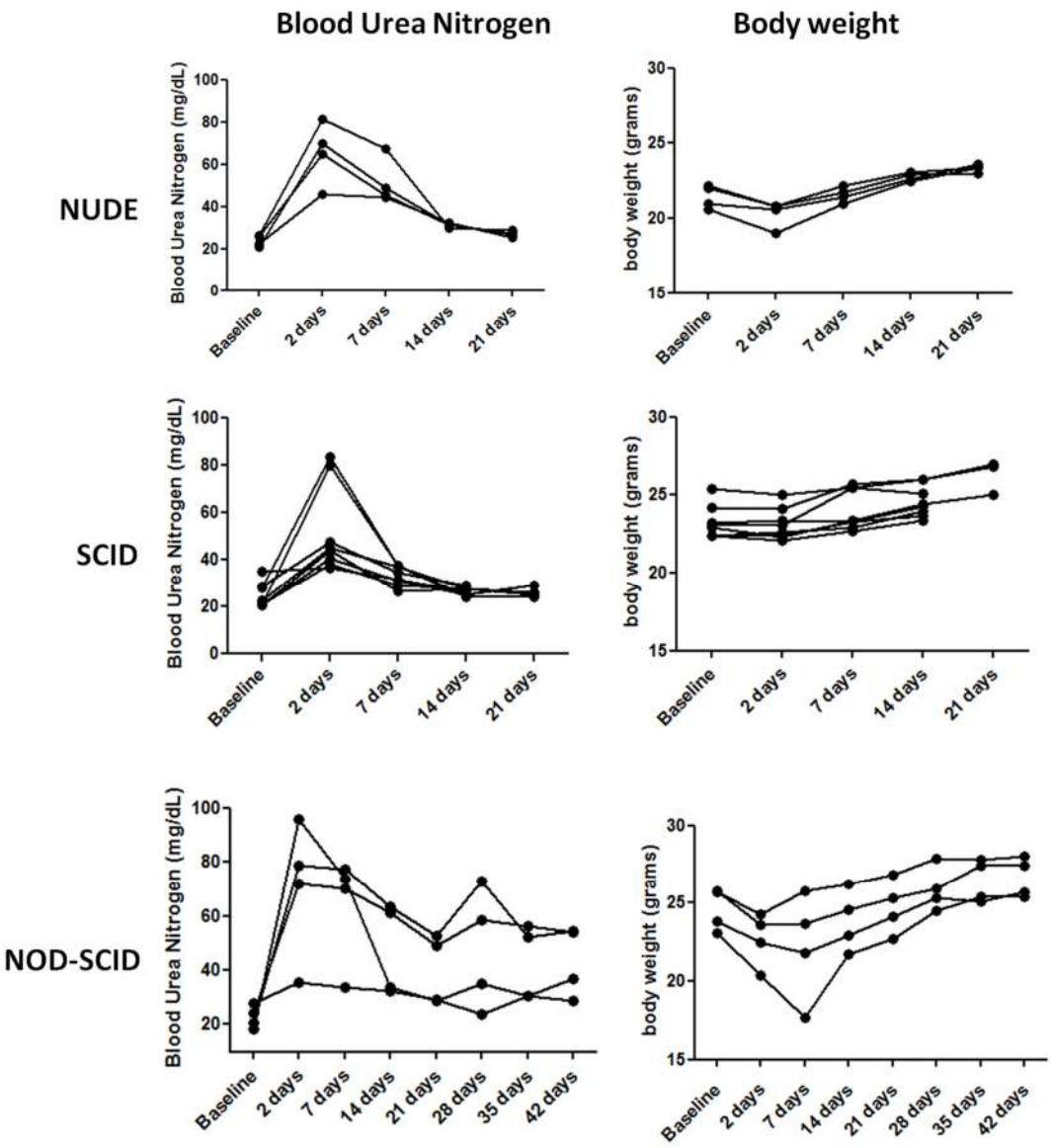

Figure 7-7 BUN and body weight measurements at different time points in nude, SCID (n=4 and n=8 respectively) and in NOD-SCID mice (n=4).

BUN values increased significantly in nude, SCID and NOD-SCID mice 48 hours post FA injection. Nude and SCID mice recovered from injury within 14 days, as observed by decreased BUN values and body weight increase. NOD-SCID mice-induced FA nephropathy appeared to be more severe with higher BUN values which did not significantly decrease over time possibly due to lack of full recovery from FA the injury.

Table 7-1 Blood urea nitrogen values in nude, SCID and NOD-SCID mice at different time points.

Blood Urea Nitrogen (mg/dl)			
	NUDE (Mean ± SEM)	SCID (Mean ± SEM)	NOD-SCID (Mean ± SEM)
Baseline	23.85±1.32	24.68±1.85	22.86±2.09
2 days	65.58±7.42[a]	51.93±6.61[a]	70.57±12.66[a]
7 days	51.44±5.42	33.15±1.48[b]	63.75±10.08
14 days	31.19±0.46	26.46±0.6	47.68±8.37
21 days	27.03±0.53	26.79±1.09	39.87±6.27
28 days			47.67±11.06
35 days			42.33±6.81
42 days			43.55±6.41

Values were analysed with repeated measures one-way ANOVA and Bonferroni's post test. NUDE: a=$P \leq 0.001$ 2 days compared to baseline. SCID: a=$P \leq 0.001$ 2 days compared to baseline, b=$P \leq 0.01$, 7 days compared to 2 days. NOD-SCID: a=$P \leq 0.001$ 2 days compared to baseline.

Table 7-2 Body weight measurements in nude, SCID and NOD-SCID mice at different time points.

	Body weight (g)		
	NUDE	SCID	NOD-SCID
	(Mean ± SEM)	(Mean ± SEM)	(Mean ± SEM)
Baseline	21.45±0.39	23.25±0.37	24.60±0.67
2 days	20.30±0.43[a]	23.13±0.35	22.70±0.85[a]
7 days	21.58±0.25[b]	24.04±0.45	22.25±1.72[b]
14 days	22.78±0.13	24.61±0.35	23.85±0.98
21 days	23.35±0.12	26.27±0.63	24.73±0.87
28 days			25.92±0.72
35 days			26.43±0.68
42 days			26.63±0.63

Values were analysed with repeated measures one-way ANOVA and Bonferroni's post test. NUDE: a=$P \leq 0.05$, 2 days compared to baseline. $P \leq 0.05$, 2 days compared to 7 days. SCID: a=$P \leq 0.01$, 2 days compared to baseline. NOD-SCID: a=$P \leq 0.05$ baseline compared 7 days.

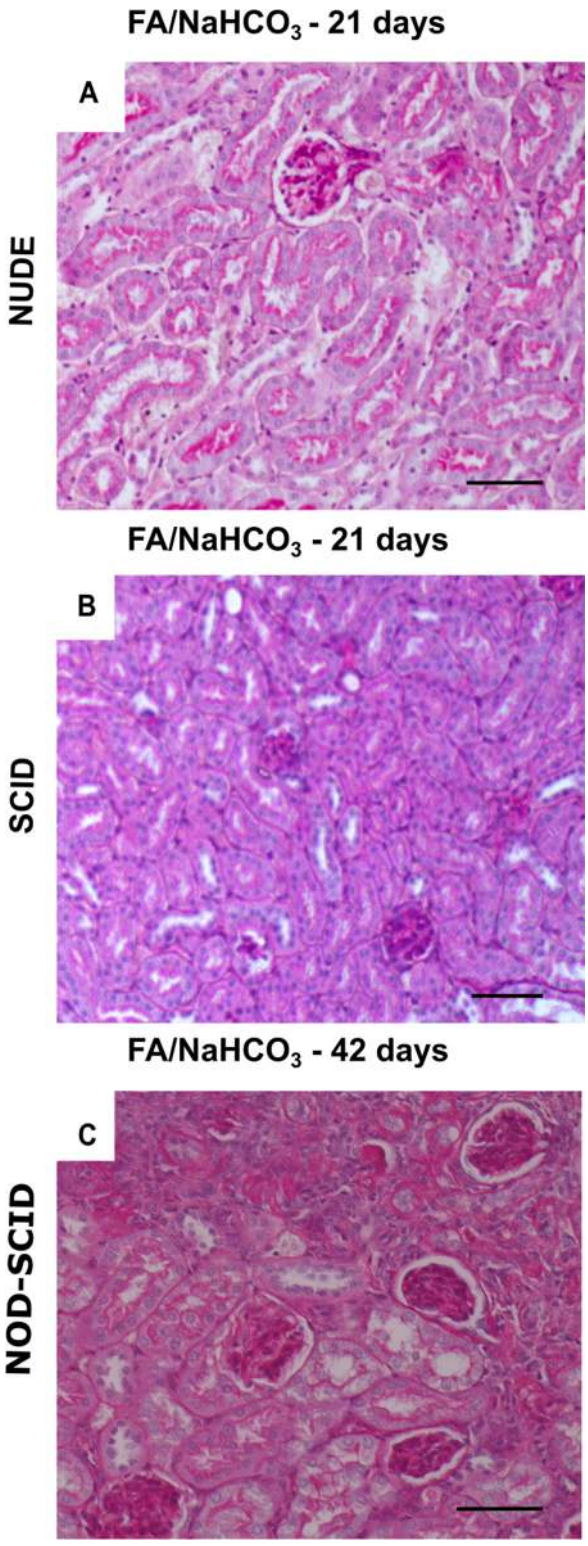

Figure 7-8 PAS staining performed on kidneys from nude, SCID and NOD-SCID after 21 days (nude, SCID) and 42 days (NOD-SCID).

(A) Nude and SCID (B) mice kidney histology at 21 days post FA injection appeared fairly normal compared to NOD-SCID (C), which showed extensive areas of fibrosis (arrow). Figures are representative of n=4 mice and 19, 11 and 22 PAS sections examined from nude, SCID and NOD-SCID animals. Unfortunately, NUDE, SCID and NOD-SCID kidney sections of untreated mice at the same time points were not available.Scale bars are 100 μm.

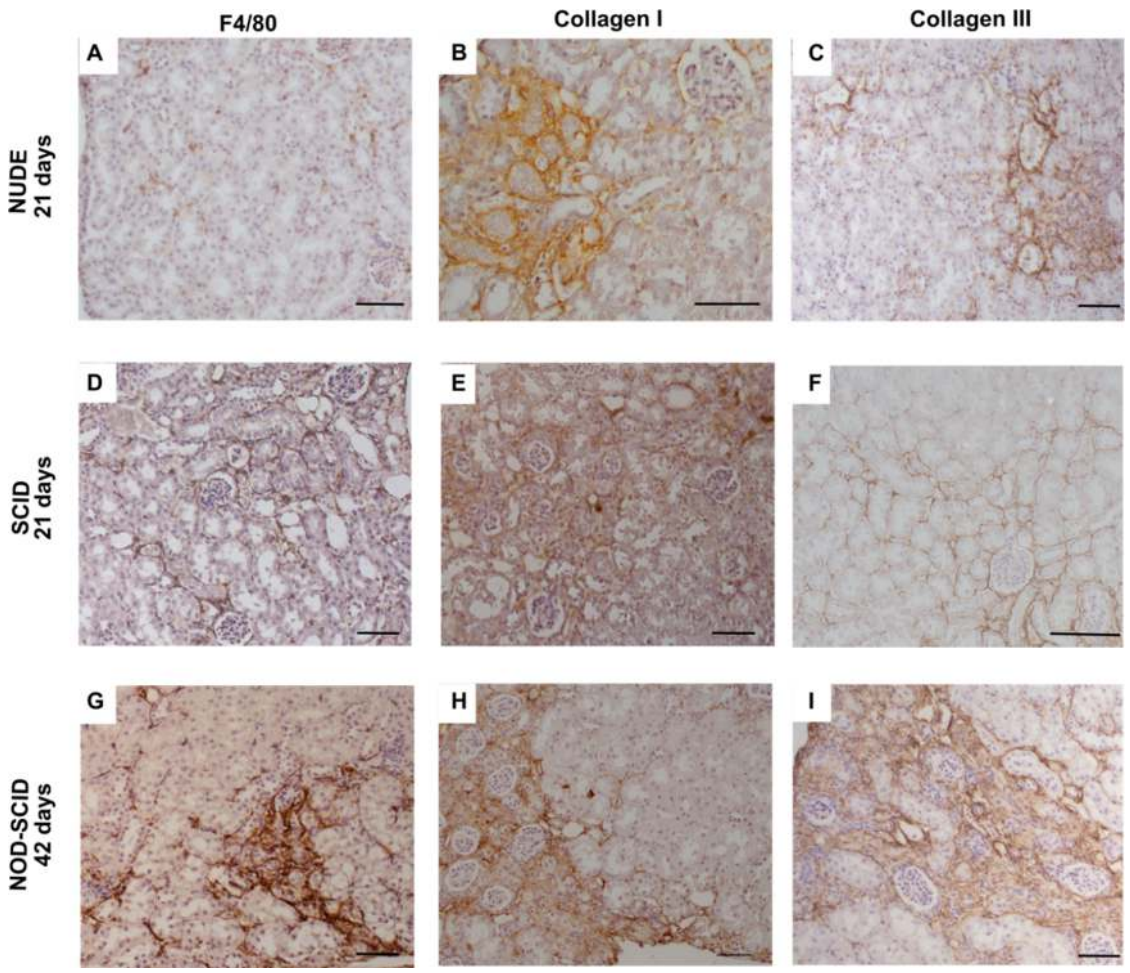

Figure 7-9 Macrophages (F4/80), collagen I and collagen III immunostaining on kidneys from nude, SCID and NOD-SCID mice after 21 days (nude, SCID) and 42 days (NOD-SCID).

(A) Nude mice kidneys showed sparse macrophages F480+, patchy areas of Collagen I and III deposition. Figure is representative of n=4 mice. 16 sections stained with anti-F4/80 antibody, 8 sections and 10 sections stained for anti-collagen I and anti-collagen III were examined. (B, C). In SCID mice, similarly to nude, few macrophages were visible in the kidney tissue (D). Very few areas were positive for collagen I and collagen III. Figure is representative of n=4 mice. 17 sections stained with anti-F4/80 antibody, 21 sections and 27 sections stained for anti-collagen I and anti-collagen III were examined. (E, F). NOD-SCID kidneys showed extensive F4/80 positivity around tubules (G). Moreover several areas of fibrosis, positively highlighted with collagen I and collagen III deposits alternated to areas of regenerated epithelia were positive staining was not visible (H, I). Figure is representative of n=4 mice. 27 sections stained with anti-F4/80 antibody, 40 sections and 18 sections stained for anti-collagen I and anti-collagen III were examined. Scale bars are 100 µm.

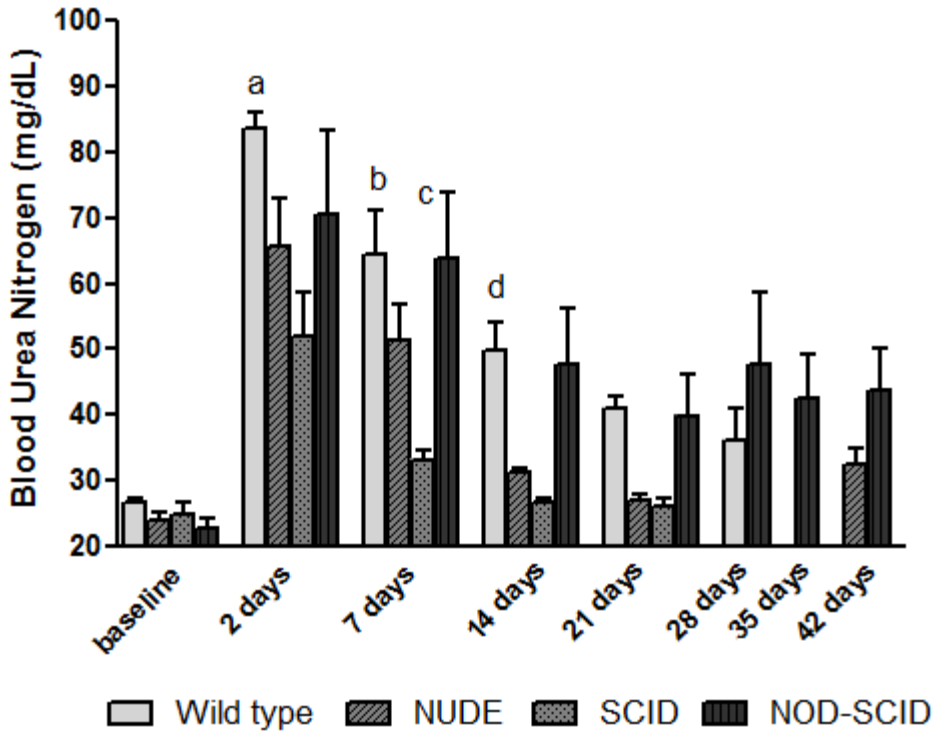

Figure 7-10 Comparison of BUN values among wild type, nude, SCID and NOD-SCID mice strains at different time points.

Values were analysed with non-parametric one-way ANOVA (Kruskall-Wallis test) and Dunns post-test. a=P≤0.01 wild type BUN compared to SCID at day 2, b=P≤0.001 wild type compared to SCID at day 7, c=P≤0.01 SCID compared to NOD-SCID at day 7, d=P≤0.05 wild type compared to SCID, 14 days. Wild type mice showed the highest peak of BUN after 2 days post FA-injection, suggesting that kidney injury was the most severe compared to the other mice groups. BUN values gradually decreased over time. On the contrary, NOD-SCID mice showed a BUN increase susceptible to extensive variation after 2 days post-FA, which did not return to levels similar to baseline indicating lack of kidney injury repair. NUDE and SCID mice kidney injury was milder compared to wild type and NOD-SCID, suggested by the lower BUN increase at day 2 and its quick decrease by day 21.

7.1.3 *Evaluation of therapeutic effects on Folic acid-induced injury by administration of $CD24^+CD133^+$ and $CD24^-CD133^-$ cells*

The aim of this part of the study was to evaluate whether FA- induced nephropathy could be modulated by injection of $CD24^-CD133^-$ or $CD24^+CD133^+$ cell lines.

NOD-SCID mice were chosen for the experiment as consequently to FA injection, they developed an acute renal injury that did not totally resolve, determining fibrotic areas in the kidneys. Therefore, the effects of human cells injection could be studied on such model of both acute and chronic renal injury. Moreover, NOD-SCID, being the most immunodeficient mice among the groups studied were also the most suitable to allow engraftment of exogenous human cells.

The tail vein was chosen as the route of administration of human cells. Intravenous cells injection was performed by an expert user in my research laboratory, Dr. Elisavet Vasilopoulou.

As we observed, the peak of injury manifested between two and seven days from FA administration in NOD-SCID mice. We reasoned that two days could be a good time point to inject the human cells and to observe whether the recovery from the initial FA insult was ameliorated along with the related kidney fibrosis.

In this part of the study, to increase the number of the mice treated, both female and male NOD-SCID mice were included. Sample size calculation was performed. Based on the pilot study on NOD-SCID mice and the variability in terms of kidney injury in response to FA (expressed in Standard Deviation), to observe a difference of the 20%-30% between groups with a power of 99%, at least 20 mice per group in each experiment should have been enrolled. However, for budget, time and human cell numbers limitations, the focus of this part of the study was to examine whether any evident difference in the FA-induced injury progression and resolution could be achieved with the injection of the two types of isolated human cell lines. If an effect of one or both cell lines injected in diseased animals would have been observed, the following experiment would have been performed with one or both cell lines determining the minimum number of mice needed for adequate study power.

NOD-SCID mice received IP injection of FA in $NaHCO_3$ (240 μg/g b.w.). Unpredictably, the expected mortality rate was exceeded within the first 2 days, as folic acid caused sickness resulting in the culling of seven males and two females, which as a result of more than 20% loss of body weight had to be euthanised.

In the remaining animals, BUN values and body weights were analysed and registered. BUN did not significantly change in one male mouse and two females after 48 hours compared to baseline levels; thus, these were excluded from the study as they appeared to not develop any renal injury. Consistent with their BUN values, animals were then homogenously divided in three groups. Groups were arranged as follow:

- Group I (n= 5, 2 males and 3 females) received IV injection in the tail vein of 80μl of PBS.
- Group II (n=5, 3 males and 2 females) received IV injection of $0.4x10^6$ of $CD24^-CD133^-$ in 80 μl of PBS.
- Group III (n=6, 3 males and 3 females) was IV injected with $0.4x10^6$ of $CD24^+CD133^+$ in 80 μl of PBS.

After PBS and cells injection, animals were constantly monitored until the end of the experiment (day 21 post FA) to assess any change in their response to renal injury. Briefly, out of five mice in group I, 2 were euthanised due to severe sickness. Out of 6 mice in group III, five had to be euthanised, whereas the group that received $CD24^-CD133^-$ cells injection appeared to have less severity, with only one mouse culled one day post-cells injection and the other four maintained for the whole length of the experiment.

Kaplan-Meier curve was used to plot the differences in survival between groups, the significance between groups was estimated by log-rank (Mantel-Cox) test. Although group II and group III had a clear difference in mortality the test appeared to be not significant (P=0.5).

Animals were monitored up to day 21 after FA injection when they were euthanised. At this time point, renal function values were compared.

At the end of the experiment (day 21), only one mouse survived within group III (NOD-SCID mice administered with $CD24^+CD133^+$ cells). Three mice survived in the control group I (PBS) and four in group II ($CD24^-CD133^-$).

When BUN at day 21 was measured and compared among control group and CD24-CD133- group, the BUN values of the PBS control group were significantly lower (P=0.0281). This suggested that IV injection of human cells might have worsened the renal function and probably the FA-induced injury.

Kidneys dissected out after euthanasia at day 21 were processed for RNA. mRNA expression of fibrosis markers, collagen I and collagen III, as well as macrophages marker CD68 were analysed. A significant increase of collagen I deposition was measured in

$CD24^{-}CD133^{-}$ treated mice compared with control. Overall the data suggested that injection of cell lines 2 days after folic acid administration aggravated the renal injury, measured with BUN, compared to the PBS control group.

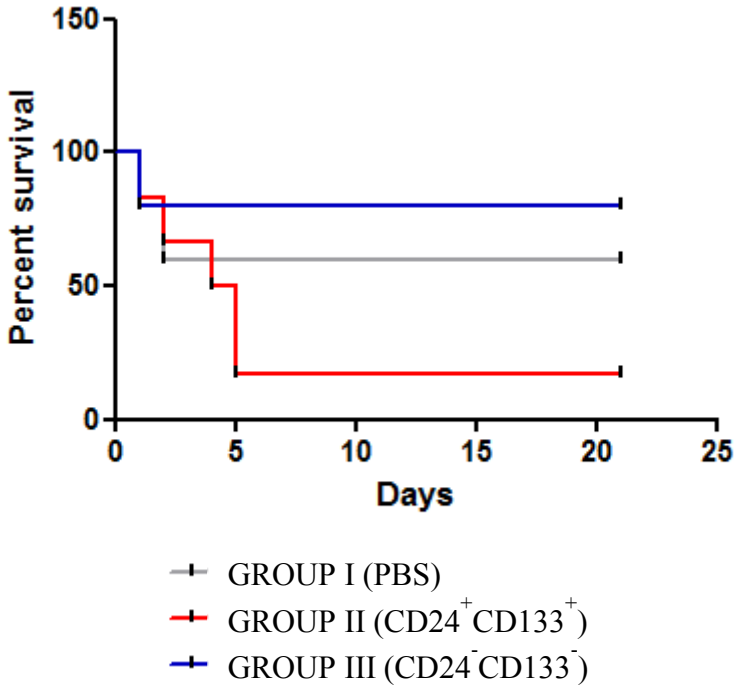

Figure 7-11 Association between PBS, CD24-CD133- or CD24+CD133+ administration and NOD-SCID mice overall survival.

Kaplan-Meier plot showed that administration of CD24-CD133- was associated with longer overall survival, however this trend was not statistically significant when analysed with log-rank test.

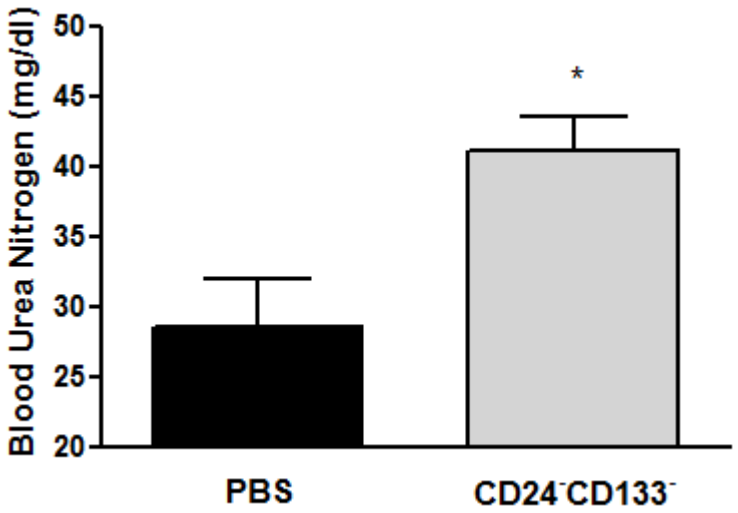

Figure 7-13 BUN values 21 days post FA of PBS control group (n=3) and group delivered with $CD24^{-}CD133^{-}$ cells (n=4). BUN in mice that received $CD24^{-}CD133^{-}$ cells injection was significantly higher than control when analysed with unpaired t test. *P=0.0281.

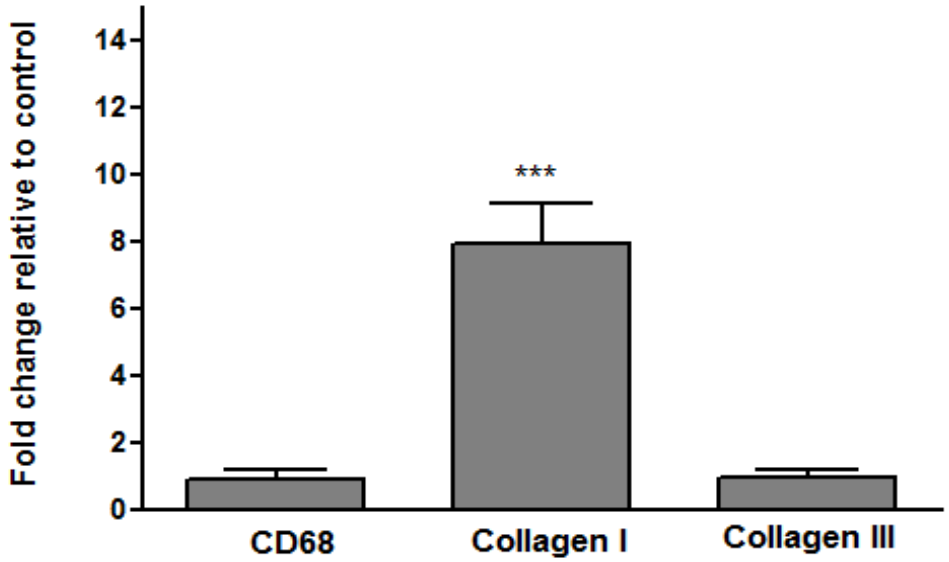

Figure 7-12 mRNA expression of macrophages gene CD68, collagen I and collagen III.

mRNA extracted from n=4 mice that received IV injection of CD24-CD133- cells and were euthanised at day 21. Gene expression was normalised to HPRT housekeeping gene and compared with n=3 mice from control group injected with PBS. Error bars= mean ± SEM. ***P≤0.001 when analysed with unpaired t test.

7.1.4 *Evaluation of biodistribution of CD24+CD133+ and CD24-CD133- cells upon administration in Folic acid-treated NOD-SCID mice*

Aim of this part of the study was to assess the body distribution, over time, of human renal cells upon IV injection in the mouse tail vein after FA injection.

Two methods were compared to determine the tracking system most suitable for *in vivo* studies:

- Transient expression of luciferase with a non-integrating vector (plasmid).
- Stable expression with integrating system (viral vector).

In the first case, $CD24^{-}CD133^{-}$ and $CD24^{+}CD133^{+}$ were transfected with pGL4.51 reporter vector expressing the luciferase gene *luc2* under the control of the cytomegalovirus promoter. Two transfection methods were compared, the Lipofectamine 3000 and the Genejuice. In the second case, a lentiviral system was used to insert the luciferase gene.

Light radiance was measured by drawing region of interests (ROI) around the wells and quantified by the AMIX software. After 24 hours, the highest luminescence intensity was registered in the wells infected with the lentivirus. It was estimated that the cells treated with the lentivirus were around 10X to 20X brighter than the cells treated with the GeneJuice (data measured at CABI). Moreover, light intensity decreased after 4 days in GeneJuice treated cells compared with the lentivirus. Lipofectamine 3000 was not measured further than 24 hours for contamination problems that affected the outcome of the experiment. $CD24^{-}CD133^{-}$ and $CD24^{+}CD133^{+}$ were not able to retain luciferase expression which decreased over days, when transfected with a non-integrating system, whereas lentiviral transduction appeared to successfully integrate the gene in the cells genome resulting in continuous expression over days. Hence, luciferase gene transfer was carried out with lentiviral vector given the promising bioluminescent signal.

Transduced cells were amplified for few passages before *in vivo* experiments. These were performed on male NOD-SCID mice following the same protocol as for the other *in vivo* experiments. Mice were treated with a single IP injection of folic acid. Two days after, were grouped according to body weight. Four received IV injection of $CD24^{-}CD133^{-}$ cells and four received $CD24^{+}CD133^{+}$ cells. Four hours after cells injection, animals were administered IP with luciferin, anesthetised and imaged. At this time point, bioluminescence signal was clearly visible in the lungs area of animals, thus suggesting that cells were transiting across lungs capillaries. At 24 hours post cells injection, one

mouse administered with $CD24^{+}CD133^{+}$ was euthanised due to excessive sickness. The others were imaged and cells were found to still reside in the lungs. Forty-eight hours after cells injection, four mice were euthanised because of illness, of these, two had been injected with $CD24^{+}CD133^{+}$ cells and two with $CD24^{-}CD133^{-}$ cells. Before euthanasia, mice were imaged. Two of them showed bioluminescence signal possibly originating from the kidney area, however when kidneys were dissected out from sacrificed animals, they did not show any signal. Whereas dim luminescence signal was observed from both kidneys taken from a mouse injected with $CD24^{-}CD133^{-}$ cells. Three mice were then further imaged at day 5 post cells injection. Cells appeared to have spread across the whole body and when kidneys were imaged upon dissection they did not show any cell signal.

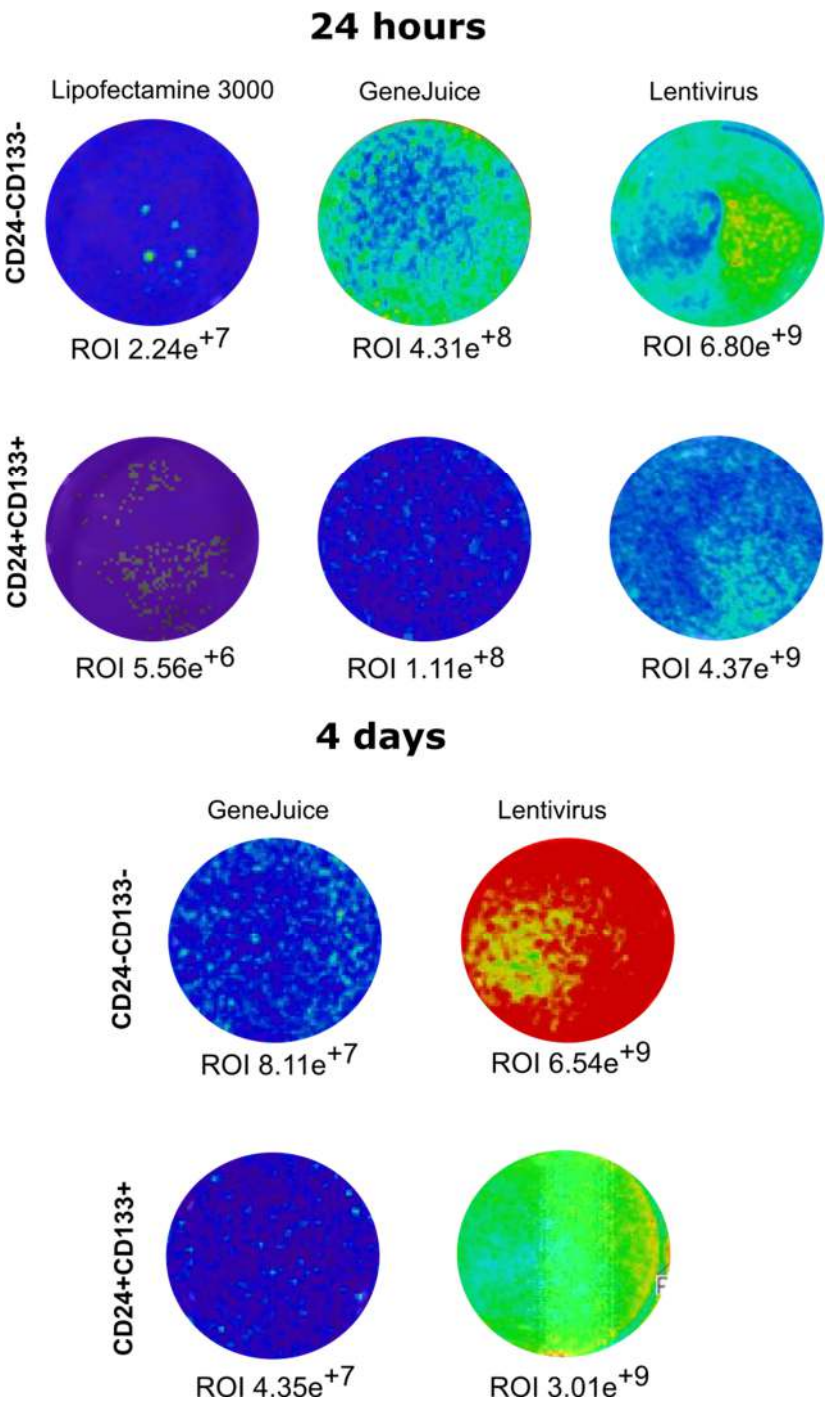

Figure 7-14 Bioluminescence imaging of CD24-CD133- and CD24+CD133+ cells transfected with pGL4.51 vector using Lipofectamine 3000 and GeneJuice or infected with the lentivirus vector encoding a Luciferase-GFP transgene.

Luminescence was measured after 24 hours and 4 days. Bioluminescence for each well was quantified with the ROI measurement tool and the radiance quantified by the AMIX software. The highest luminescence intensity was measured in the well plates infected with the lentivirus system compared to the GeneJuice wells, indicating that the most suitable system to detect luciferase expression over time was throug the lentiviral transduction.

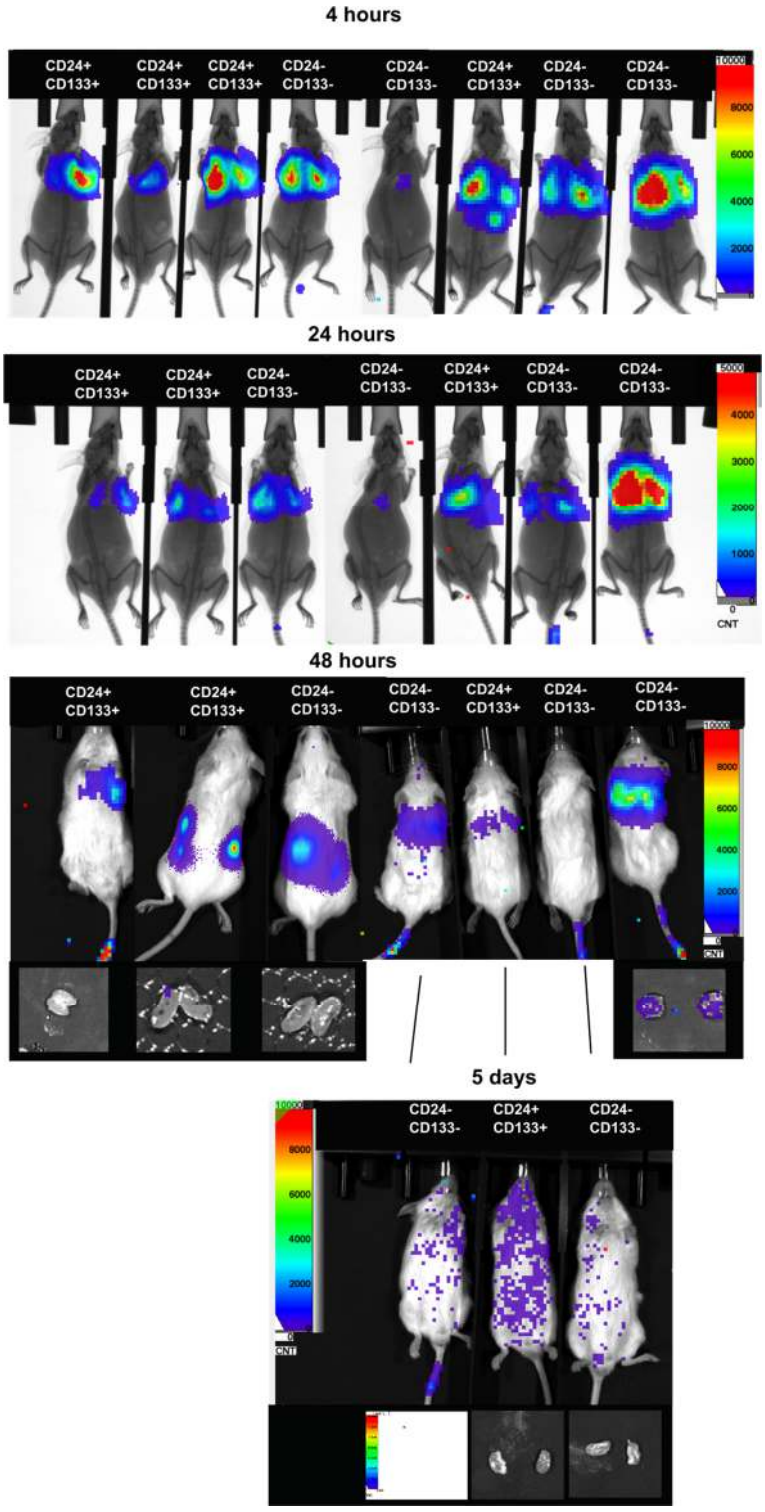

Figure 7-15 Bioluminescence imaging of mice injected with $CD24^{-}CD133^{-}$ and $CD24^{+}CD133^{+}$ cell lines two days after FA administration.

Mice were imaged 4 hours, 24 hours and 48 hours after cells injection. At 48 hours, kidneys were collected from 4 euthanised animals and imaged. Three animals were euthanised 5 days post cells injection and kidneys imaged. Within the first 24 hours cells were trapped in the lungs and few cells appeared to reach the kidneys in two mice injected with double positive and double negative cell lines. However these cells presence in the kidneys was not further confirmed after kidneys dissection.

7.2 SUMMARY

The first aim of this study was to evaluate folic acid (FA)-induce nephrotoxicity response in BALB/c Wild type mice. Intraperitoneal injections of FA, at the dose of 240 μg/g of body weight, induced severe changes in renal function (BUN) and body weight loss in wild type BALB/c adult male mice, with a peak of injury 2 days after FA administration. This resulted in architectural changes indicative of acute kidney injury, such as dilated kidney tubules with protein casts in the lumen. The kidney injury gradually resolved and BUN values returned to levels close to baseline before day 42. Although kidney function was re-established, histological changes were observed in FA-treated animals compared to $NaHCO_3$ controls, with wide scarred areas within the kidney and increased collagen I deposition.

The second aim was to examine FA-induced kidney injury among mice strains with increased levels of immunodeficiency and determine the most suitable model for the subsequent experiment with human renal cells. Nude mice (lacking T-cell response), SCID mice (lacking T- and B- cell response) and NOD-SCID mice (lacking T-, B- cell response as well as mature macrophages, natural killer cells and serum haemolytic complement) were treated with FA. The NOD-SCID mice showed the harshest injury among the mice strains. In these mice, BUN, did not return to baseline levels even after 42 days suggesting an impairment in the ability to restore physiological renal function after the injury. NOD-SCID mice strain was chosen as the most suitable mouse model in which to test human cell lines as such strain, having the most impaired immune system response, would best allow the engraftment of human cells. In addition, it was interesting to determine any effect of human cells injection upon FA-induced acute renal injury, as FA-induced nephropathy in this mice strain did not totally resolve, determining fibrotic areas in the kidneys.

The third aim was to test whether human renal cell lines administered in NOD-SCID mice at the peak of the FA-induced renal injury determined any amelioration of renal damage caused by folic acid.

$CD24^-CD133^-$ and $CD24^+CD133^+$ cells were injected intravenously in NOD-SCID males and females, 2 days post FA. The high severity of the injury caused high mortality within all the groups. In addition, the number of mice included in the experiment were not enough to show significant effects of cells injections in the FA-induced injury. For these reasons, data derived from this experiment were difficult to interpret. Overall the data

suggested that injection of the cell lines might have aggravated the renal injury, measured with BUN, compared to the PBS control group.

The fourth aim was to observe human renal cell lines body-distribution over time with *in vivo* bioluminescence imaging.

The body distribution, over time, of human renal cells upon injection in the mouse tail vein after folic acid injury was evaluated with luminescence bioimaging *in vivo*. Upon intravenous injection, human cells were transported to the lungs. At 48 hours after cells injection, two out of seven mice showed luminescence signal from the kidneys, sign of presence of human cells, however this was not further confirmed after kidneys were dissected. Five days after FA cells were spread across the whole body. Data suggested that injected human cells probably did not reach the kidneys, it is possible that because of this, injured mice did not show amelioration of FA-induced injury post cells injection.

8 GENERAL DISCUSSION

Kidney diseases are heterogeneous disorders altering the kidney architecture and function, these can be classified as acute (AKI) or chronic (CKD) depending on the duration (National Kidney Foundation, 2002). CKD is more frequent, affecting more than the 10% of the world's population (Levey and Coresh, 2012).

Kidney failure is often the most serious outcome of CKD. For patients with kidney failure the only treatment options are dialysis or kidney transplantation (Lazzeri et al., 2015). Dialysis is often accompanied with higher morbidity and mortality with a lower life expectancy due to cardiovascular diseases (Rayner et al., 2004). On the other hand, kidney transplant is limited by severe organ donor shortage, higher morbidity and premature death (Stoumpos et al., 2015).

Therefore, innovative methods to alleviate, cure or prevent kidney injury and progression to CKD are needed. The regenerative medicine approaches are now starting to satisfy this necessity.

Regenerative medicine is a general term indicative of any biomedical method used to replace and regenerate tissues or organs for therapeutic purposes. This has the potential to provide an innovative treatment for organ failure. However the more complex the organ is, the more difficult is to success with this approach; up to date there are no published clinical studies regarding the regeneration of a functional organ (Al-Awqati and Oliver, 2002).

The kidney is very complex as it maintains body homeostasis, it is responsible for the blood filtration and the production of urine and it also has endocrine functions such as the production of erythropoietin. The regenerative medicine approaches in renal disease are therefore aimed at regenerating all the cells constituting the kidney; although this is a great challenge that has not yet been overcome and it will be achieved in the next future only by gradual advances in stem cell research and bioengineering.

Regenerative medicine approaches have the potential to prevent the progression of kidney disease to end stage renal disease or CKD5 by increasing the kidney filtration function and to construct a healthy kidney *in vitro* with bioengineered scaffolds to replace defective kidneys.

Within the first approach, stem cells would be directly needed *in situ* to prevent the progression to end stage renal disease. This effect has been observed before with mesenchymal stem cells, which delayed interstitial fibrosis and the progression to chronic kidney disease in rat models of 5/6 nephrectomy. These results were mediated by induction of regulatory T cells anti-fibrotic and anti-inflammatory effects (Chang et al., 2012).

Another approach would be the generation of the entire kidney for renal transplant. In this case, the whole kidney can be used as extracellular matrix scaffold, supporting, with its three dimensional architecture, the differentiation to endothelial, mesenchymal and epithelial cells (Vacanti and Langer, 1999).Various studies demonstrated that kidneys from animals or humans can be decellularised removing their inhabiting cells and leaving the three dimensional extracellular bio-scaffold (Song et al., 2013) . The decellularisation process preserves the mechanical and biological properties of the extracellular matrix, generating a template that can promote cells engraftment. Putative renal stem cells can therefore be expanded in culture, seeded into a scaffold and placed into a bioreactor to induce cell acclimation, adhesion to the scaffold and maturation. Reached this process, the cells/scaffold can be implanted in the host (Zambon et al., 2014). Both approaches involve the use of stem cells able to differentiate towards different lineages and the ones constituting the nephron. The overall aim of my study was therefore to meet the need for primary human renal stem cell lines for both regenerative medicine purposes and drug testing applications with the identification, isolation and characterisation of this cell line.

8.1 Discussion

The human kidney ceases its development upon birth and the fetal kidney is the best tissue in which a renal stem-cell population can be examined.

To identify and isolate renal stem cells in the fetal kidney we would need proteins expressed on the cell membrane. However, these are not known, instead, their transcription factor signature and localisation in the developing kidney has been well-studied in mouse. Renal stem cells reside in the 'cap mesenchyme' and their organization has been studied along with the stem cell niche signals playing a role in their self-renewal and differentiation (please see Chapter 1.4). A specific gene, *Six2*, is recognised as the renal stem cells master gene, its expression with the transcription factor *Cited1* addresses the renal stem cells with the greatest capacity in terms of self-renewal and differentiation whereas CITED1$^-$SIX2$^-$ cells are less 'stem-' and more committed-cells, initiating the differentiation in pre-tubular aggregates and consequently the transition to epithelial cells.

With the aim to find markers expressed on cell surface through which the renal stem cells would be easily sortable by FACS or MACS, tow surface markers were found. These are CD24 and CD133 and the main hypothesis of my study has been to understand whether CD24 and CD133 identify a stem cell population in the human fetal kidney or they target a progenitor cell line with limited self-renewal capacity and potency, as well as, to evaluate whether these cells can be used as a 'cell-based therapy' to ameliorate kidney injury *in vivo*.

The first goal of my study was to assess CD24 and CD133 protein localisation in sections of human fetal kidneys. CD24 and CD133 analysed in sections of 9 weeks human fetal kidneys appeared to localise in early epithelial structures derived from cap mesenchyme, such as renal vesicles, comma and S-shaped bodies but also in forming epithelial tubules and the ureteric bud.

By addressing the first goal, I soon realised that CD24 and CD133 are not expressed in the cap mesenchyme. Therefore, the early stem cells SIX2$^+$ cannot be isolated with CD24 and CD133 markers. In addition, I performed double staining on human fetal kidney sections of CD133 with known renal stem cells transcription factors: *Six2*, *Pax2* and *Wt1* (please refer to Paragraph 3.1.3). It was clear that no cells were positive for both SIX2 and CD133. CD133 appeared to co-localise with PAX2 in the epithelium of the ureteric bud and in the epithelial derivatives of the cap mesenchyme. CD133 and WT1 co-

localised in the proximal side of the S-shaped body, which develops into podocytes but no co-localisation of CD133 and WT1 was observed in cap mesenchyme.
The conclusion of this part of the study was that cells co-expressing CD24 and CD133 could probably be considered as committed renal progenitor cells, possibly with a limited self-renewal capacity and potency.

The second goal of my study was to isolate and characterise the $CD24^+CD133^+$ cells.
FACS sorting was used for the isolation of $CD24^+CD133^+$ cells from kidneys of 9 weeks of gestation after culture. In addition, at the same time, the cell subpopulation negative for both markers was isolated. This cell fraction presumably included renal stem cells $SIX2^+$ as well as stromal, vascular, interstitial and tubular elements.
$CD24^+CD133^+$ and $CD24^-CD133^-$ cell populations generated from cultured fetal kidney cells of 8 to 9 weeks of gestation were characterised in terms of morphology and growth rate. The double positive proliferated slowly and showed morphological changes over passages, from epithelial- to mesenchymal-like cells. Double negative cells showed higher proliferation rate compared to double positive and were expanded for longer in culture, whereas $CD24^+CD133^+$ cells proliferation arrested within 6-7 passages from the isolation. $CD24^+CD133^+$ cells and double negative cells were evaluated in terms of mRNA expression at different passages in culture; differentiation potential was assessed towards renal epithelium and extra-renal lineages (osteocytes and adipocytes), as well as assessment of nephrogenic potential performed with the use of a novel *ex vivo* assay.
CD24 and CD133, when examined by mRNA expression in double positive cells, showed downregulation after few passages in culture thus suggesting changes in the composition of this cell line. Moreover, all the progenitor genes were downregulated upon culture. At early passages $CD24^-CD133^-$ appeared to express some progenitor genes, such as *EYA1, SIX2* and *OSR1* higher than $CD24^+CD133^+$, which in turn expressed higher *PAX2* and *OCT4* and the epithelial marker *E-cadherin*.
When extra-renal differentiation potential was tested on isolated cell lines, this had controversial results, as the double positive appeared to differentiate towards the osteo-lineage but not the adipocytes and the double negative cells to differentiate better towards adipocytes. Cells were also stimulated towards epithelial lineage with LiCl. $CD24^+CD133^+$ cell lines upregulated the epithelial differentiation marker *E-cadherin* and proximal tubule protein *Aminopeptidase A*, whereas $CD24^-CD133^-$ were capable of *E-cadherin* upregulation only if treated transiently (48 hours) with LiCl.

This part of the study showed that repeated passaging of both cell lines resulted in deep changes in morphology and progenitor gene expression. Moreover, differentiation experiments did not result in a conclusive or clear understanding of cell lines differentiation potential only suggesting that epithelial stimulation, induced by LiCl, is easier to be achieved in double positive cells. The induction of non-renal lineages was limited to the lack of proper controls, furthermore the cell lines were heterogeneous to start with, thus different cell types could have reacted differently resulting in a difficult interpretation of these experiments. Although the limitations were several, this set of data confirmed that in these culture conditions, $CD24^{+}CD133^{+}$ cells displayed a very limited proliferation capacity and to be epithelial-line committed cells.

To better address isolated cell potential and eventual applications in drug discovery, we started a collaboration with the group of Professor Roos Masereeuw of the University of Utrecht where we delivered $CD24^{-}CD133^{-}$ and $CD24^{+}CD133^{+}$ cell lines generated from a 9-week embryo. They induced differentiation of these cell populations by culturing in proximal tubule complete medium (PTCM). In order to study the potential of these cells to form tubules, these were arranged in 3-dimensional matrigel culture. In addition, their functional maturation was assessed using fluorescent tracers to investigate transport function. Presence and activity of renal markers was determined over passages. Preliminary data demonstrated that the cells acquired a proximal tubule-like phenotype, as determined by decreased expression of the mesenchymal marker *Snail1* and increased expression of the sodium-dependant glucose transporter - *SLGT1*. The key tubular transporters *P-glycoprotein* (P-gp) and *Multidrug resistance protein 4* (MRP4) expression and functional activity increased in both populations when cultured in PTCM. In addition, when grown in Matrigel, both populations formed tubule-like structures after two days in culture. These experiments showed that both cell lines had the potential to differentiate towards proximal tubule cells given the correct differentiation conditions.

The last goal of the study was to evaluate renal regenerative potential of isolated cells in a murine model of Folic acid-induced kidney failure, localising the intravenously-injected cell lines upon kidney injury with the use of bioluminescence imaging *in vivo.*

It has been shown before that the severity of renal injury models in mice is dependent on genetic background (Randles et al., 2015), however there have been no studies comparing the progression of renal injury in different mice strains. I tackled this issue by testing the murine model of acute tubular necrosis induced by FA in different mice with an increased degree of immunodeficiency on the same genetic background (BALB/c). Nude, SCID

and NOD-SCID strains of immunodeficient mice were injected IP with a single dose of FA (240 mg/kg of body weight) and responded differently to folic-acid nephrotoxicity. SCID and nude mice recovered within 14 days from the acute effects of folic acid injection. In contrast, NOD-SCID mice did not recover from the folic acid insult leading to an increased fibrotic response. The potential of generated cell lines to improve kidney injury was tested in NOD-SCID mice 48 hours after receiving FA dose. However, the renal injury provoked by FA was so severe to determine a higher illness than expected. When distribution of human cells upon FA-induced injury was evaluated, these were found to reside in the lungs for the first 48 hours after cells injection and then to home to other body districts. Cells administration did not ameliorate the injury. This could be due to the massive inflammatory micro-environment to which the cells were subjected or simply to the fact that these cells did not reach the kidneys and were trapped in the lungs vasculature first. These experiments therefore did not lead to any conclusive result on the effects of the administration of fetal renal cell lines after injury. A higher mortality of animals injected with double positive cells compared to the double negative was observed, however the low number of animals considered affected the statistical significance of the experiment. These *in vivo* experiments showed that the FA-induced injury was too severe and that animals could have been to ill and stressed upon cells injection.

8.2 Future directions

Data in this thesis might require more in-depth study in order to delineate a better strategy for the characterisation, maintenance and *in vivo* assessment of therapeutic effects of progenitor cells. I will address the different questions that I came along within the project and different ways on how these could be addressed.

8.2.1 *$CD24^+$ $CD133^+$ cells as source of progenitor cell lines*

CD24 and CD133 might be useful markers to target epithelial-committed cells in the developing kidney, however the opportunity to isolate and study the $SIX2^+$ population in humans is lost when using only these two markers.

The group of Prof. Dekel proposed to utilise a combination of surface markers in order to examine renal stem cells in developing kidneys. These markers, such as NCAM1, were found to be overexpressed in Wilms tumor, composed of cap mesenchymal cells and

differentiated elements resembling the nephrogenic zone of the developing kidney (Shukrun et al., 2014). The limitation of this approach was that some of the surface proteins proposed, such as NCAM1, not only specified cap mesenchyme $SIX2^+$ cells, but also stromal elements in the developing kidney, thus not being suitable to solely isolate this population.

The group of Prof. Oxburgh, followed a different approach: they enriched $CITED1^+$ cells from a mixed population of embryonic mouse metanephric mesenchyme, by depleting of 'unwanted' lineages ($Ter119^+CD140a^+$ and $CD105^+$ cells) (Brown et al., 2013). This could be another approach presumably limited due to the prolonged immunosort steps that cells undergo to and probably still not resulting in a pure $SIX2^+$ purification.

A promising new method was unfortunately developed towards the end of my PhD period. This utilises an innovative method that enables live-cells isolation by targeting the specific mRNA (McClellan et al., 2015). It is a commercially available technology (SmartFlare, Millipore), which makes use of designed probes, able to enter the cell by active endocytosis and to fluoresce when the mRNA of interest is detected. Hence, by using SIX2 mRNA as target, specifically SIX2+ cells might be isolated by FACS giving the opportunity to examine this cell population for the first time in human.

A limitation of my study consisted in basing the experiments on heterogeneous cell lines rather than a clonal cell population. However, it was considered that in the developing kidney, renal stem cells ($SIX2^+$ cells) need to interact and cross-talk with other cell types (such as stroma and ureteric bud) to survive and differentiate, therefore, by selecting clones of isolated cell population, this cross-talk would be missed probably leading to a premature epithelialisation of renal stem cells. This limitation could have been overcome only by selecting a growth medium supplemented with all the factors needed by renal stem cells to survive and self-renew. There have been progress in that direction, with studies suggesting that cap mesenchymal $SIX2^+$ cells need FGF factors (FGF9 and FGF20), low concentration of LIF, Rho kinase inhibitor, NOTCH inhibitor, low concentrations of BMP7 to survive and to differentiate (Brown et al., 2011a, Barak et al., 2012, Tanigawa et al., 2016). However, the right concentration and timing of such factors are still going to be elucidated in human $SIX2^+$ renal stem cells.

Moreover, culture conditions should be improved from bi-dimensional to three dimensional, as it has been observed that in 2D conditions, cells extended mainly in horizontal direction and as a result they become more flattened and undergo

dedifferentiation. A three-dimensional system approach could be constituted of cells embedded in an ECM matrix such as Matrigel (Desrochers et al., 2014).

In my culture conditions, I have shown deregulation of progenitor gene expression in cultured cell lines compared to the expression in the human fetal kidney, this suggests that 2D culture conditions affected stemness properties.

Conclusion and Future prospects

CD24 and CD133 appear to target epithelial-committed cells with a limited self-renewal and multi-differentiation capacity, the ideal cell source would be constituted by $SIX2^+$ cells, as a future plan I would:

- Isolate SIX2+ cells with the technologies now available
- Assess well defined culture conditions for the maintenance and differentiation of this cell population, including 3D culture approaches.

8.2.2 *Evaluation of immunodeficient mouse strains for pre-clinical studies*

The folic acid experiments in NOD-SCID animals suggested that this strain might be very sensitive to FA-induced nephropathy at the dose used. Moreover, the planning of the experiment should probably be improved. In first instance the cells, when delivered IV in the tail vein were seen to be trapped for at least 48 hours in the lungs. In order to avoid this, an injection under the kidney capsule could be considered, having the advantage of delivering the cells directly to the site of the injury. In this case, a lower cell number could be used thus limiting significantly the expansion steps prior to *in vivo* experiments.

Recent studies have shown that embryonic kidneys when transplanted under the renal capsule of healthy animals, were able to form new structures. On the other hand, when transplanted in rats with nephropathy, these not only developed glomeruli and tubules functionally active in filtering the blood but also appeared to ameliorate the injury, as increased cell proliferation and the expression of markers relevant to kidney regeneration were observed in the tissue adjacent to the transplant (Imberti et al., 2015).

Conclusion and future prospects

Progenitor cells therapeutic effects should be assessed in less severe acute renal injury mouse models: this could only be achieved by planning a well-defined experiments with different doses.

In situ transplantation of progenitor cell lines under the kidney capsule might offer the advantage of:

1. Examining differentiation potential *in vivo* when transplanted in healthy kidneys.
2. Examining regenerative potential when transplanted in injured kidneys.

8.3 Conclusions

The data presented in this thesis provide new insights into the significance of $CD24^+$ $CD133^+$ and $CD24^-CD133^-$ surface proteins in the human fetal kidneys. This study showed that the renal stem cells resident in the cap mesenchyme are not targeted with CD24 and CD133 markers. These markers appear to be expressed on more differentiated cells committed towards the epithelial lineage, which do not show stemness potential and are highly affected by *in vitro* culture.

In comparison to published literature in the field, the novelty of my work consists in a critical evaluation of $CD24^+CD133^+$ double positive cells isolated from human fetal kidneys. This analysis has involved a 360° approach for the evaluation of stemness capacity: starting from the study of the progenitor genes expression, through the potential for differentiation towards renal and non-renal lineages, and the integration capacity in developing kidney structures up to the *in vivo* effects on injured kidneys.

Because of the lack of the proper negative/positive controls or an insufficient number of samples analysed, the study did not show any advantage of a prospective use of $CD24^+CD133^+$ human fetal kidney cells in kidney injury.

Although the work in the project did not achieve its main hypothesis, nevertheless it provided a perception into the importance of the correct markers utilisation when addressing stem/progenitor cells, their maintenance *in vitro* and the pre-clinical studies to be performed in order to assess their therapeutic properties. In depth understanding underlying renal stem/progenitor cells properties and regenerative potential will enable translation of the laboratory researches into targeted renal cell replacement therapy.

9 REFERENCES

AGGARWAL, S., MOGGIO, A. & BUSSOLATI, B. 2013. Concise review: stem/progenitor cells for renal tissue repair: current knowledge and perspectives. Stem Cells Transl Med, 2, 1011-9.

AL-AWQATI, Q. & OLIVER, J. A. 2002. Stem cells in the kidney. Kidney Int, 61, 387-95.

ALLMAN, D. M., FERGUSON, S. E. & CANCRO, M. P. 1992. Peripheral B cell maturation. I. Immature peripheral B cells in adults are heat-stable antigenhi and exhibit unique signaling characteristics. J Immunol, 149, 2533-40.

ANGELOTTI, M. L., LAZZERI, E., LASAGNI, L. & ROMAGNANI, P. 2010. Only anti-CD133 antibodies recognizing the CD133/1 or the CD133/2 epitopes can identify human renal progenitors. Kidney Int, 78, 620-1; author reply 621.

ANGELOTTI, M. L., RONCONI, E., BALLERINI, L., PEIRED, A., MAZZINGHI, B., SAGRINATI, C., PARENTE, E., GACCI, M., CARINI, M., ROTONDI, M., FOGO, A. B., LAZZERI, E., LASAGNI, L. & ROMAGNANI, P. 2012. Characterization of renal progenitors committed toward tubular lineage and their regenerative potential in renal tubular injury. Stem Cells, 30, 1714-25.

APPEL, D., KERSHAW, D. B., SMEETS, B., YUAN, G., FUSS, A., FRYE, B., ELGER, M., KRIZ, W., FLOEGE, J. & MOELLER, M. J. 2009. Recruitment of podocytes from glomerular parietal epithelial cells. J Am Soc Nephrol, 20, 333-43.

ARMSTRONG, J. F., PRITCHARD-JONES, K., BICKMORE, W. A., HASTIE, N. D. & BARD, J. B. 1993. The expression of the Wilms' tumour gene, WT1, in the developing mammalian embryo. Mech Dev, 40, 85-97.

BARAK, H., HUH, S. H., CHEN, S., JEANPIERRE, C., MARTINOVIC, J., PARISOT, M., BOLE-FEYSOT, C., NITSCHKE, P., SALOMON, R., ANTIGNAC, C., ORNITZ, D. M. & KOPAN, R. 2012. FGF9 and FGF20 maintain the stemness of nephron progenitors in mice and man. Dev Cell, 22, 1191-207.

BARASCH, J., QIAO, J., MCWILLIAMS, G., CHEN, D., OLIVER, J. A. & HERZLINGER, D. 1997. Ureteric bud cells secrete multiple factors, including bFGF, which rescue renal progenitors from apoptosis. Am J Physiol, 273, F757-67.

BARASCH, J., YANG, J., WARE, C. B., TAGA, T., YOSHIDA, K., ERDJUMENT-BROMAGE, H., TEMPST, P., PARRAVICINI, E., MALACH, S., ARANOFF, T. & OLIVER, J. A. 1999. Mesenchymal to epithelial conversion in rat metanephros is induced by LIF. Cell, 99, 377-86.

BARBAUX, S., NIAUDET, P., GUBLER, M. C., GRUNFELD, J. P., JAUBERT, F., KUTTENN, F., FEKETE, C. N., SOULEYREAU-THERVILLE, N., THIBAUD, E., FELLOUS, M. & MCELREAVEY, K. 1997. Donor splice-site mutations in WT1 are responsible for Frasier syndrome. Nat Genet, 17, 467-70.

BASTA, J. M., ROBBINS, L., KIEFER, S. M., DORSETT, D. & RAUCHMAN, M. 2014. Sall1 balances self-renewal and differentiation of renal progenitor cells. Development, 141, 1047-58.

BATES, C. M. 2011. Role of fibroblast growth factor receptor signaling in kidney development. Pediatr Nephrol, 26, 1373-9.

BELLOMO, R., KELLUM, J. A. & RONCO, C. 2012. Acute kidney injury. Lancet, 380, 756-66.

BELLOMO, R., RONCO, C., KELLUM, J. A., MEHTA, R. L. & PALEVSKY, P. 2004. Acute renal failure - definition, outcome measures, animal models, fluid therapy and information technology needs: the Second International Consensus Conference of the Acute Dialysis Quality Initiative (ADQI) Group. Crit Care, 8, R204-12.

BENIGNI, A., MORIGI, M. & REMUZZI, G. 2010. Kidney regeneration. Lancet, 375, 1310-7.

BIASON-LAUBER, A., KONRAD, D., NAVRATIL, F. & SCHOENLE, E. J. 2004. A WNT4 mutation associated with Mullerian-duct regression and virilization in a 46,XX woman. N Engl J Med, 351, 792-8.

BLANK, U., BROWN, A., ADAMS, D. C., KAROLAK, M. J. & OXBURGH, L. 2009. BMP7 promotes proliferation of nephron progenitor cells via a JNK-dependent mechanism. Development, 136, 3557-66.

BLANTZ, R. C. 1998. Pathophysiology of pre-renal azotemia. Kidney Int, 53, 512-23.

BLAZEK, E. R., FOUTCH, J. L. & MAKI, G. 2007. Daoy medulloblastoma cells that express CD133 are radioresistant relative to CD133- cells, and the CD133+ sector is enlarged by hypoxia. Int J Radiat Oncol Biol Phys, 67, 1-5.

BLUNT, T., FINNIE, N. J., TACCIOLI, G. E., SMITH, G. C., DEMENGEOT, J., GOTTLIEB, T. M., MIZUTA, R., VARGHESE, A. J., ALT, F. W., JEGGO, P. A. & JACKSON, S. P. 1995. Defective DNA-dependent protein kinase activity is linked to V(D)J recombination and DNA repair defects associated with the murine scid mutation. Cell, 80, 813-23.

BOSCH, R. J., WOOLF, A. S. & FINE, L. G. 1993. Gene transfer into the mammalian kidney: direct retrovirus-transduction of regenerating tubular epithelial cells. Exp Nephrol, 1, 49-54.

BOWER, M., SALOMON, R., ALLANSON, J., ANTIGNAC, C., BENEDICENTI, F., BENETTI, E., BINENBAUM, G., JENSEN, U. B., COCHAT, P., DECRAMER, S., DIXON, J., DROUIN, R., FALK, M. J., FERET, H., GISE, R., HUNTER, A., JOHNSON, K., KUMAR, R., LAVOCAT, M. P., MARTIN, L., MORINIERE, V., MOWAT, D., MURER, L., NGUYEN, H. T., PERETZ-AMIT, G., PIERCE, E., PLACE, E., RODIG, N., SALERNO, A., SASTRY, S., SATO, T., SAYER, J. A., SCHAAFSMA, G. C., SHOEMAKER, L., STOCKTON, D. W., TAN, W. H., TENCONI, R.,

VANHILLE, P., VATS, A., WANG, X., WARMAN, B., WELEBER, R. G., WHITE, S. M., WILSON-BRACKETT, C., ZAND, D. J., ECCLES, M., SCHIMMENTI, L. A. & HEIDET, L. 2012. Update of PAX2 mutations in renal coloboma syndrome and establishment of a locus-specific database. Hum Mutat, 33, 457-66.

BOYLE, S., MISFELDT, A., CHANDLER, K. J., DEAL, K. K., SOUTHARD-SMITH, E. M., MORTLOCK, D. P., BALDWIN, H. S. & DE CAESTECKER, M. 2008. Fate mapping using Cited1-CreERT2 mice demonstrates that the cap mesenchyme contains self-renewing progenitor cells and gives rise exclusively to nephronic epithelia. Dev Biol, 313, 234-45.

BOYLE, S., SHIODA, T., PERANTONI, A. O. & DE CAESTECKER, M. 2007. Cited1 and Cited2 are differentially expressed in the developing kidney but are not required for nephrogenesis. Dev Dyn, 236, 2321-30.

BOYLE, S. C., KIM, M., VALERIUS, M. T., MCMAHON, A. P. & KOPAN, R. 2011. Notch pathway activation can replace the requirement for Wnt4 and Wnt9b in mesenchymal-to-epithelial transition of nephron stem cells. Development, 138, 4245-54.

BRADLEY, A., EVANS, M., KAUFMAN, M. H. & ROBERTSON, E. 1984. Formation of germ-line chimaeras from embryo-derived teratocarcinoma cell lines. Nature, 309, 255-256.

BRENNER, B. M., BOHRER, M. P., BAYLIS, C. & DEEN, W. M. 1977. Determinants of glomerular permselectivity: Insights derived from observations in vivo. Kidney Int, 12, 229-37.

BROWN, A. C., ADAMS, D., DE CAESTECKER, M., YANG, X., FRIESEL, R. & OXBURGH, L. 2011a. FGF/EGF signaling regulates the renewal of early nephron progenitors during embryonic development. Development, 138, 5099-112.

BROWN, A. C., BLANK, U., ADAMS, D. C., KAROLAK, M. J., FETTING, J. L., HILL, B. L. & OXBURGH, L. 2011b. Isolation and culture of cells from the nephrogenic zone of the embryonic mouse kidney. J Vis Exp.

BROWN, A. C., MUTHUKRISHNAN, S. D., GUAY, J. A., ADAMS, D. C., SCHAFER, D. A., FETTING, J. L. & OXBURGH, L. 2013. Role for compartmentalization in nephron progenitor differentiation. Proc Natl Acad Sci U S A, 110, 4640-5.

BROWN, A. C., MUTHUKRISHNAN, S. D. & OXBURGH, L. 2015. A synthetic niche for nephron progenitor cells. Dev Cell, 34, 229-41.

BRUNO, S., BUSSOLATI, B., GRANGE, C., COLLINO, F., GRAZIANO, M. E., FERRANDO, U. & CAMUSSI, G. 2006. CD133+ renal progenitor cells contribute to tumor angiogenesis. Am J Pathol, 169, 2223-35.

BURG MB. BRENNER BM, R. J. F., EDS. THE KIDNEY. 1986. Renal handling of sodium, chloride, water, amino acids and glucose. Philadelphia: WB Saunders.

BUSSOLATI, B., BRUNO, S., GRANGE, C., BUTTIGLIERI, S., DEREGIBUS, M. C., CANTINO, D. & CAMUSSI, G. 2005. Isolation of renal progenitor cells from adult human kidney. Am J Pathol, 166, 545-55.

BUSSOLATI, B., BRUNO, S., GRANGE, C., FERRANDO, U. & CAMUSSI, G. 2008. Identification of a tumor-initiating stem cell population in human renal carcinomas. Faseb j, 22, 3696-705.

BUSSOLATI, B., HAUSER, P. V., CARVALHOSA, R. & CAMUSSI, G. 2009. Contribution of stem cells to kidney repair. Curr Stem Cell Res Ther, 4, 2-8.

BUZHOR, E., OMER, D., HARARI-STEINBERG, O., DOTAN, Z., VAX, E., PRI-CHEN, S., METSUYANIM, S., PLENICEANU, O., GOLDSTEIN, R. S. & DEKEL, B. 2013. Reactivation of NCAM1 Defines a Subpopulation of Human Adult Kidney Epithelial Cells with Clonogenic and Stem/Progenitor Properties. Am J Pathol, 183, 1621-33.

BYRNES, K. A., GHIDONI, J. J. & MAYFIELD, E. D., JR. 1972. Response of the rat kidney to folic acid administration. I. Biochemical studies. Lab Invest, 26, 184-90.

CAMPEAN, V., KRICKE, J., ELLISON, D., LUFT, F. C. & BACHMANN, S. 2001. Localization of thiazide-sensitive Na(+)-Cl(-) cotransport and associated gene products in mouse DCT. Am J Physiol Renal Physiol, 281, F1028-35.

CAPEL, B., ALBRECHT, K. H., WASHBURN, L. L. & EICHER, E. M. 1999. Migration of mesonephric cells into the mammalian gonad depends on Sry. Mech Dev, 84, 127-31.

CARROLL, T. J., PARK, J. S., HAYASHI, S., MAJUMDAR, A. & MCMAHON, A. P. 2005. Wnt9b plays a central role in the regulation of mesenchymal to epithelial transitions underlying organogenesis of the mammalian urogenital system. Dev Cell, 9, 283-92.

CHANG, C. H. & DAVIES, J. A. 2012. An improved method of renal tissue engineering, by combining renal dissociation and reaggregation with a low-volume culture technique, results in development of engineered kidneys complete with loops of Henle. Nephron Exp Nephrol, 121, e79-85.

CHANG, J. W., TSAI, H. L., CHEN, C. W., YANG, H. W., YANG, A. H., YANG, L. Y., WANG, P. S., NG, Y. Y., LIN, T. L. & LEE, O. K. 2012. Conditioned mesenchymal stem cells attenuate progression of chronic kidney disease through inhibition of epithelial-to-mesenchymal transition and immune modulation. J Cell Mol Med, 16, 2935-49.

CHAU, Y. Y., BROWNSTEIN, D., MJOSENG, H., LEE, W. C., BUZA-VIDAS, N., NERLOV, C., JACOBSEN, S. E., PERRY, P., BERRY, R., THORNBURN, A., SEXTON, D., MORTON, N., HOHENSTEIN, P., FREYER, E., SAMUEL, K., VAN'T HOF, R. & HASTIE, N. 2011. Acute multiple organ failure in adult mice deleted for the developmental regulator Wt1. PLoS Genet, 7, e1002404.

CHAWLA, L. S., EGGERS, P. W., STAR, R. A. & KIMMEL, P. L. 2014. Acute kidney injury and chronic kidney disease as interconnected syndromes. N Engl J Med, 371, 58-66.

CHI, N. & EPSTEIN, J. A. 2002. Getting your Pax straight: Pax proteins in development and disease. Trends Genet, 18, 41-7.

CHUMAN, L., FINE, L. G., COHEN, A. H. & SAIER, M. H., JR. 1982. Continuous growth of proximal tubular kidney epithelial cells in hormone-supplemented serum-free medium. J Cell Biol, 94, 506-10.

COCA, S. G., YALAVARTHY, R., CONCATO, J. & PARIKH, C. R. 2008. Biomarkers for the diagnosis and risk stratification of acute kidney injury: a systematic review. Kidney Int, 73, 1008-16.

COLLINS, A. T., BERRY, P. A., HYDE, C., STOWER, M. J. & MAITLAND, N. J. 2005. Prospective identification of tumorigenic prostate cancer stem cells. Cancer Res, 65, 10946-51.

CORBEAUX, T., HESS, I., SWANN, J. B., KANZLER, B., HAAS-ASSENBAUM, A. & BOEHM, T. 2010. Thymopoiesis in mice depends on a Foxn1-positive thymic epithelial cell lineage. Proc Natl Acad Sci U S A, 107, 16613-8.

CORBEIL, D., ROPER, K., HELLWIG, A., TAVIAN, M., MIRAGLIA, S., WATT, S. M., SIMMONS, P. J., PEAULT, B., BUCK, D. W. & HUTTNER, W. B. 2000. The human AC133 hematopoietic stem cell antigen is also expressed in epithelial cells and targeted to plasma membrane protrusions. J Biol Chem, 275, 5512-20.

CRIBBS, A. P., KENNEDY, A., GREGORY, B. & BRENNAN, F. M. 2013. Simplified production and concentration of lentiviral vectors to achieve high transduction in primary human T cells. BMC Biotechnol, 13, 98.

DAAR, A. S. 2006. The case for a regulated system of living kidney sales. Nat Clin Pract Nephrol, 2, 600-1.

DAS, A., TANIGAWA, S., KARNER, C. M., XIN, M., LUM, L., CHEN, C., OLSON, E. N., PERANTONI, A. O. & CARROLL, T. J. 2013. Stromal-epithelial crosstalk regulates kidney progenitor cell differentiation. Nat Cell Biol, 15, 1035-44.

DAVIES, J. A. & BARD, J. B. 1998. The development of the kidney. Curr Top Dev Biol, 39, 245-301.

DAVIES, J. A., LADOMERY, M., HOHENSTEIN, P., MICHAEL, L., SHAFE, A., SPRAGGON, L. & HASTIE, N. 2004. Development of an siRNA-based method for repressing specific genes in renal organ culture and its use to show that the Wt1 tumour suppressor is required for nephron differentiation. Hum Mol Genet, 13, 235-46.

DAVIES, J. A., UNBEKANDT, M., INESON, J., LUSIS, M. & LITTLE, M. H. 2012. Dissociation of embryonic kidney followed by re-aggregation as a method for chimeric analysis. Methods Mol Biol, 886, 135-46.

DESROCHERS, T. M., PALMA, E. & KAPLAN, D. L. 2014. Tissue-engineered kidney disease models. Adv Drug Deliv Rev, 69-70, 67-80.

DIETERICH, H. J., BARRETT, J. M., KRIZ, W. & BULHOFF, J. P. 1975. The ultrastructure of the thin loop limbs of the mouse kidney. Anat Embryol (Berl), 147, 1-18.

DIJKMAN, H. B., ASSMANN, K. J., STEENBERGEN, E. J. & WETZELS, J. F. 2006. Expression and effect of inhibition of aminopeptidase-A during nephrogenesis. J Histochem Cytochem, 54, 253-62.

DOI, K., OKAMOTO, K., NEGISHI, K., SUZUKI, Y., NAKAO, A., FUJITA, T., TODA, A., YOKOMIZO, T., KITA, Y., KIHARA, Y., ISHII, S., SHIMIZU, T. & NOIRI, E. 2006. Attenuation of folic acid-induced renal inflammatory injury in platelet-activating factor receptor-deficient mice. Am J Pathol, 168, 1413-24.

DONO, R., TEXIDO, G., DUSSEL, R., EHMKE, H. & ZELLER, R. 1998. Impaired cerebral cortex development and blood pressure regulation in FGF-2-deficient mice. EMBO J, 17, 4213-25.

DRESSLER, G. R. 2006. The cellular basis of kidney development. Annu Rev Cell Dev Biol, 22, 509-29.

DRESSLER, G. R. 2011. Patterning and early cell lineage decisions in the developing kidney: the role of Pax genes. Pediatr Nephrol, 26, 1387-94.

DRESSLER, G. R., DEUTSCH, U., CHOWDHURY, K., NORNES, H. O. & GRUSS, P. 1990. Pax2, a new murine paired-box-containing gene and its expression in the developing excretory system. Development, 109, 787-95.

DRESSLER, G. R. & DOUGLASS, E. C. 1992. Pax-2 is a DNA-binding protein expressed in embryonic kidney and Wilms tumor. Proc Natl Acad Sci U S A, 89, 1179-83.

DRESSLER, G. R., WILKINSON, J. E., ROTHENPIELER, U. W., PATTERSON, L. T., WILLIAMS-SIMONS, L. & WESTPHAL, H. 1993. Deregulation of Pax-2 expression in transgenic mice generates severe kidney abnormalities. Nature, 362, 65-7.

DUDLEY, A. T., GODIN, R. E. & ROBERTSON, E. J. 1999. Interaction between FGF and BMP signaling pathways regulates development of metanephric mesenchyme. Genes Dev, 13, 1601-13.

DUDLEY, A. T., LYONS, K. M. & ROBERTSON, E. J. 1995. A requirement for bone morphogenetic protein-7 during development of the mammalian kidney and eye. Genes Dev, 9, 2795-807.

ECCLES, M. R. 1998. The role of PAX2 in normal and abnormal development of the urinary tract. Pediatr Nephrol, 12, 712-20.

ECCLES, M. R., WALLIS, L. J., FIDLER, A. E., SPURR, N. K., GOODFELLOW, P. J. & REEVE, A. E. 1992. Expression of the PAX2 gene in human fetal kidney and Wilms' tumor. Cell Growth Differ, 3, 279-89.

EVANS, M. J. & KAUFMAN, M. H. 1981. Establishment in culture of pluripotential cells from mouse embryos. Nature, 292, 154-6.

FAA, G., GEROSA, C., FANNI, D., MONGA, G., ZAFFANELLO, M., VAN EYKEN, P. & FANOS, V. 2012. Morphogenesis and molecular mechanisms involved in human kidney development. J Cell Physiol, 227, 1257-68.

FANG, T. C., PANG, C. Y., CHIU, S. C., DING, D. C. & TSAI, R. K. 2012. Renoprotective effect of human umbilical cord-derived mesenchymal stem cells in immunodeficient mice suffering from acute kidney injury. PLoS One, 7, e46504.

FANNI, D., FANOS, V., MONGA, G., GEROSA, C., LOCCI, A., NEMOLATO, S., VAN EYKEN, P. & FAA, G. 2011. Expression of WT1 during normal human kidney development. J Matern Fetal Neonatal Med, 24 Suppl 2, 44-7.

FINK, M., HENRY, M. & TANGE, J. D. 1987. Experimental folic acid nephropathy. Pathology, 19, 143-9.

FISCHER, G. F., MAJDIC, O., GADD, S. & KNAPP, W. 1990. Signal transduction in lymphocytic and myeloid cells via CD24, a new member of phosphoinositol-anchored membrane molecules. J Immunol, 144, 638-41.

FLOREK, M., HAASE, M., MARZESCO, A. M., FREUND, D., EHNINGER, G., HUTTNER, W. B. & CORBEIL, D. 2005. Prominin-1/CD133, a neural and hematopoietic stem cell marker, is expressed in adult human differentiated cells and certain types of kidney cancer. Cell Tissue Res, 319, 15-26.

FOUNDATION, N. K. 2002. K/DOQI clinical practice guidelines for chronic kidney disease: evaluation, classification, and stratification. Am J Kidney Dis, 39, S1-266.

FRIEDMAN, P. A. 1999. Calcium transport in the kidney. Curr Opin Nephrol Hypertens, 8, 589-95.

GAGE, F. H. 2000. Mammalian neural stem cells. Science, 287, 1433-8.

GAO, M. Q., CHOI, Y. P., KANG, S., YOUN, J. H. & CHO, N. H. 2010. CD24+ cells from hierarchically organized ovarian cancer are enriched in cancer stem cells. Oncogene, 29, 2672-80.

GEORGAS, K., RUMBALLE, B., VALERIUS, M. T., CHIU, H. S., THIAGARAJAN, R. D., LESIEUR, E., ARONOW, B. J., BRUNSKILL, E. W., COMBES, A. N., TANG, D., TAYLOR, D., GRIMMOND, S. M., POTTER, S. S., MCMAHON, A. P. & LITTLE, M. H. 2009. Analysis of early nephron patterning reveals a role for distal RV proliferation in fusion to the ureteric tip via a cap mesenchyme-derived connecting segment. Dev Biol, 332, 273-86.

GNARRA, J. R. & DRESSLER, G. R. 1995. Expression of Pax-2 in human renal cell carcinoma and growth inhibition by antisense oligonucleotides. Cancer Res, 55, 4092-8.

GONG, K. Q., YALLOWITZ, A. R., SUN, H., DRESSLER, G. R. & WELLIK, D. M. 2007. A Hox-Eya-Pax complex regulates early kidney developmental gene expression. Mol Cell Biol, 27, 7661-8.

GOOD, D. W. & BURG, M. B. 1984. Ammonia production by individual segments of the rat nephron. J Clin Invest, 73, 602-10.

GREGER, R., SCHLATTER, E. & HEBERT, S. C. 2001. Milestones in nephrology: Presence of luminal K+, a prerequisite for active NaCl transport in the cortical thick ascending limb of Henle's loop of rabbit kidney. J Am Soc Nephrol, 12, 1788-93.

GRIESHAMMER, U., CEBRIAN, C., ILAGAN, R., MEYERS, E., HERZLINGER, D. & MARTIN, G. R. 2005. FGF8 is required for cell survival at distinct stages of nephrogenesis and for regulation of gene expression in nascent nephrons. Development, 132, 3847-57.

HAGER, H., KWON, T. H., VINNIKOVA, A. K., MASILAMANI, S., BROOKS, H. L., FROKIAER, J., KNEPPER, M. A. & NIELSEN, S. 2001. Immunocytochemical and immunoelectron microscopic localization of alpha-, beta-, and gamma-ENaC in rat kidney. Am J Physiol Renal Physiol, 280, F1093-106.

HARARI-STEINBERG, O., METSUYANIM, S., OMER, D., GNATEK, Y., GERSHON, R., PRI-CHEN, S., OZDEMIR, D. D., LERENTHAL, Y., NOIMAN, T., BEN-HUR, H., VAKNIN, Z., SCHNEIDER, D. F., ARONOW, B. J., GOLDSTEIN, R. S., HOHENSTEIN, P. & DEKEL, B. 2013. Identification of human nephron progenitors capable of generation of kidney structures and functional repair of chronic renal disease. EMBO Mol Med, 5, 1556-68.

HARTMAN, H. A., LAI, H. L. & PATTERSON, L. T. 2007. Cessation of renal morphogenesis in mice. Dev Biol, 310, 379-87.

HARVEY, K. F. & HARIHARAN, I. K. 2012. The hippo pathway. Cold Spring Harb Perspect Biol, 4, a011288.

HATINI, V., HUH, S. O., HERZLINGER, D., SOARES, V. C. & LAI, E. 1996. Essential role of stromal mesenchyme in kidney morphogenesis revealed by targeted disruption of Winged Helix transcription factor BF-2. Genes Dev, 10, 1467-78.

HAYFLICK, L., KRUSE, P.F. & PATTERSON, M.K. 1973. Tissue Culture Methods and Applications. Academic Press, 220.

HE, S., LIU, N., BAYLISS, G. & ZHUANG, S. 2013. EGFR activity is required for renal tubular cell dedifferentiation and proliferation in a murine model of folic acid-induced acute kidney injury. Am J Physiol Renal Physiol, 304, F356-66.

HENDRY, C., RUMBALLE, B., MORITZ, K. & LITTLE, M. H. 2011. Defining and redefining the nephron progenitor population. Pediatr Nephrol, 26, 1395-406.

HENDRY, C. E., VANSLAMBROUCK, J. M., INESON, J., SUHAIMI, N., TAKASATO, M., RAE, F. & LITTLE, M. H. 2013. Direct transcriptional reprogramming of adult cells to embryonic nephron progenitors. J Am Soc Nephrol, 24, 1424-34.

HERMAN, M. B., RAJKHOWA, T., CUTULI, F., SPRINGATE, J. E. & TAUB, M. 2010. Regulation of renal proximal tubule Na-K-ATPase by prostaglandins. Am J Physiol Renal Physiol, 298, F1222-34.

HERZER, U., CROCOLL, A., BARTON, D., HOWELLS, N. & ENGLERT, C. 1999. The Wilms tumor suppressor gene wt1 is required for development of the spleen. Curr Biol, 9, 837-40.

HERZLINGER, D., QIAO, J., COHEN, D., RAMAKRISHNA, N. & BROWN, A. M. 1994. Induction of kidney epithelial morphogenesis by cells expressing Wnt-1. Dev Biol, 166, 815-8.

HOFMEISTER, M. V., FENTON, R. A. & PRAETORIUS, J. 2009. Fluorescence isolation of mouse late distal convoluted tubules and connecting tubules: effects of vasopressin and vitamin D3 on Ca2+ signaling. Am J Physiol Renal Physiol, 296, F194-203.

HU, J., ZHANG, L., WANG, N., DING, R., CUI, S., ZHU, F., XIE, Y., SUN, X., WU, D., HONG, Q., LI, Q., SHI, S., LIU, X. & CHEN, X. 2013. Mesenchymal stem cells attenuate ischemic acute kidney injury by inducing regulatory T cells through splenocyte interactions. Kidney Int, 84, 521-31.

HUGHSON, M., FARRIS, A. B., 3RD, DOUGLAS-DENTON, R., HOY, W. E. & BERTRAM, J. F. 2003. Glomerular number and size in autopsy kidneys: the relationship to birth weight. Kidney Int, 63, 2113-22.

HUMPHREYS, B. D., VALERIUS, M. T., KOBAYASHI, A., MUGFORD, J. W., SOEUNG, S., DUFFIELD, J. S., MCMAHON, A. P. & BONVENTRE, J. V. 2008. Intrinsic epithelial cells repair the kidney after injury. Cell Stem Cell, 2, 284-91.

IMBERTI, B., CORNA, D., RIZZO, P., XINARIS, C., ABBATE, M., LONGARETTI, L., CASSIS, P., BENEDETTI, V., BENIGNI, A., ZOJA, C., REMUZZI, G. & MORIGI, M. 2015. Renal primordia activate kidney regenerative events in a rat model of progressive renal disease. PLoS One, 10, e0120235.

IMGRUND, M., GRONE, E., GRONE, H. J., KRETZLER, M., HOLZMAN, L., SCHLONDORFF, D. & ROTHENPIELER, U. W. 1999. Re-expression of the developmental gene Pax-2 during experimental acute tubular necrosis in mice 1. Kidney Int, 56, 1423-31.

ISCOVE, N. N. & NAWA, K. 1997. Hematopoietic stem cells expand during serial transplantation in vivo without apparent exhaustion. Curr.Biol., 7, 805-8.

ITO, Y., HAMAZAKI, T. S., OHNUMA, K., TAMAKI, K., ASASHIMA, M. & OKOCHI, H. 2007. Isolation of murine hair-inducing cells using the cell surface marker prominin-1/CD133. J Invest Dermatol, 127, 1052-60.

ITOH, N. 2007. The Fgf families in humans, mice, and zebrafish: their evolutional processes and roles in development, metabolism, and disease. Biol Pharm Bull, 30, 1819-25.

IVANOVA, L., HIATT, M. J., YODER, M. C., TARANTAL, A. F. & MATSELL, D. G. 2010. Ontogeny of CD24 in the human kidney. Kidney Int, 77, 1123-31.

JAMES, R. G., KAMEI, C. N., WANG, Q., JIANG, R. & SCHULTHEISS, T. M. 2006. Odd-skipped related 1 is required for development of the metanephric kidney and regulates formation and differentiation of kidney precursor cells. Development, 133, 2995-3004.

JUNG, D., BIGGS, H., ERIKSON, J. & LEDYARD, P. U. 1975. New Colorimetric reaction for end-point, continuous-flow, and kinetic measurement of urea. Clin Chem, 21, 1136-40.

KALATZIS, V., SAHLY, I., EL-AMRAOUI, A. & PETIT, C. 1998. Eya1 expression in the developing ear and kidney: towards the understanding of the pathogenesis of Branchio-Oto-Renal (BOR) syndrome. Dev Dyn, 213, 486-99.

KANOJIA, D., GARG, M., SAINI, S., AGARWAL, S., PARASHAR, D., JAGADISH, N., SETH, A., BHATNAGAR, A., GUPTA, A., KUMAR, R., LOHIYA, N. K. & SURI, A. 2013. Sperm associated antigen 9 plays an important role in bladder transitional cell carcinoma. PLoS One, 8, e81348.

KARNER, C. M., DAS, A., MA, Z., SELF, M., CHEN, C., LUM, L., OLIVER, G. & CARROLL, T. J. 2011. Canonical Wnt9b signaling balances progenitor cell expansion and differentiation during kidney development. Development, 138, 1247-57.

KELLER, S., RUPP, C., STOECK, A., RUNZ, S., FOGEL, M., LUGERT, S., HAGER, H. D., ABDEL-BAKKY, M. S., GUTWEIN, P. & ALTEVOGT, P. 2007. CD24 is a marker of exosomes secreted into urine and amniotic fluid. Kidney Int, 72, 1095-102.

KEMPER, K., SPRICK, M. R., DE BREE, M., SCOPELLITI, A., VERMEULEN, L., HOEK, M., ZEILSTRA, J., PALS, S. T., MEHMET, H., STASSI, G. & MEDEMA, J. P. 2010. The AC133 epitope, but not the CD133 protein, is lost upon cancer stem cell differentiation. Cancer Res, 70, 719-29.

KIHIRA, Y., MIYAKE, M., HIRATA, M., HOSHINA, Y., KATO, K., SHIRAKAWA, H., SAKAUE, H., YAMANO, N., IZAWA-ISHIZAWA, Y., ISHIZAWA, K., IKEDA, Y., TSUCHIYA, K., TAMAKI, T. & TOMITA, S. 2014. Deletion of hypoxia-inducible factor-1alpha in adipocytes enhances glucagon-like peptide-1 secretion and reduces adipose tissue inflammation. PLoS One, 9, e93856.

KIM, J., TISHER, C. C., LINSER, P. J. & MADSEN, K. M. 1990. Ultrastructural localization of carbonic anhydrase II in subpopulations of intercalated cells of the rat kidney. J Am Soc Nephrol, 1, 245-56.

KLINGLER, E. L., JR., EVAN, A. P. & ANDERSON, R. E. 1980. Folic acid-induced renal injury and repair. Correlation of structural and functional abnormalities. Arch Pathol Lab Med, 104, 87-93.

KNOBLICH, J. A. 2010. Asymmetric cell division: recent developments and their implications for tumour biology. Nat Rev Mol Cell Biol, 11, 849-60.

KOBAYASHI, A., VALERIUS, M. T., MUGFORD, J. W., CARROLL, T. J., SELF, M., OLIVER, G. & MCMAHON, A. P. 2008. Six2 defines and regulates a multipotent self-renewing nephron progenitor population throughout mammalian kidney development. Cell Stem Cell, 3, 169-81.

KOHLHASE, J., WISCHERMANN, A., REICHENBACH, H., FROSTER, U. & ENGEL, W. 1998. Mutations in the SALL1 putative transcription factor gene cause Townes-Brocks syndrome. Nat Genet, 18, 81-3.

KOLATSI-JOANNOU, M., PRICE, K. L., WINYARD, P. J. & LONG, D. A. 2011. Modified citrus pectin reduces galectin-3 expression and disease severity in experimental acute kidney injury. PLoS One, 6, e18683.

KREIDBERG, J. A. 2010. WT1 and kidney progenitor cells. Organogenesis, 6, 61-70.

KREIDBERG, J. A., SARIOLA H FAU - LORING, J. M., LORING JM FAU - MAEDA, M., MAEDA M FAU - PELLETIER, J., PELLETIER J FAU - HOUSMAN, D., HOUSMAN D FAU - JAENISCH, R. & JAENISCH, R. 1993. WT-1 is required for early kidney development. Cell, 74.

KRISTIANSEN, G., PILARSKY, C., PERVAN, J., STURZEBECHER, B., STEPHAN, C., JUNG, K., LOENING, S., ROSENTHAL, A. & DIETEL, M. 2004. CD24 expression is a significant predictor of PSA relapse and poor prognosis in low grade or organ confined prostate cancer. Prostate, 58, 183-92.

KRISTIANSEN, G., SCHLUNS, K., YONGWEI, Y., DENKERT, C., DIETEL, M. & PETERSEN, I. 2003a. CD24 is an independent prognostic marker of survival in nonsmall cell lung cancer patients. Br J Cancer, 88, 231-6.

KRISTIANSEN, G., WINZER, K. J., MAYORDOMO, E., BELLACH, J., SCHLUNS, K., DENKERT, C., DAHL, E., PILARSKY, C., ALTEVOGT, P., GUSKI, H. & DIETEL, M. 2003b. CD24 expression is a new prognostic marker in breast cancer. Clin Cancer Res, 9, 4906-13.

KUSABA, T., LALLI, M., KRAMANN, R., KOBAYASHI, A. & HUMPHREYS, B. D. 2014. Differentiated kidney epithelial cells repair injured proximal tubule. Proc Natl Acad Sci U S A, 111, 1527-32.

KUURE, S., POPSUEVA, A., JAKOBSON, M., SAINIO, K. & SARIOLA, H. 2007. Glycogen synthase kinase-3 inactivation and stabilization of beta-catenin induce nephron differentiation in isolated mouse and rat kidney mesenchymes. J Am Soc Nephrol, 18, 1130-9.

LAN, Y., KINGSLEY, P. D., CHO, E. S. & JIANG, R. 2001. Osr2, a new mouse gene related to Drosophila odd-skipped, exhibits dynamic expression patterns during craniofacial, limb, and kidney development. Mech Dev, 107, 175-9.

LANDSVERK, O. J., OTTESEN, A. H., BERG-LARSEN, A., APPEL, S. & BAKKE, O. 2012. Differential regulation of MHC II and invariant chain expression during maturation of monocyte-derived dendritic cells. J Leukoc Biol, 91, 729-37.

LAOUARI, D., BURTIN, M., PHELEP, A., BIENAIME, F., NOEL, L. H., LEE, D. C., LEGENDRE, C., FRIEDLANDER, G., PONTOGLIO, M. & TERZI, F. 2012. A transcriptional network underlies susceptibility to kidney disease progression. EMBO Mol Med, 4, 825-39.

LASAGNI, L., BALLERINI, L., ANGELOTTI, M. L., PARENTE, E., SAGRINATI, C., MAZZINGHI, B., PEIRED, A., RONCONI, E., BECHERUCCI, F., BANI, D., GACCI, M., CARINI, M., LAZZERI, E. & ROMAGNANI, P. 2010. Notch activation differentially regulates renal progenitors proliferation and differentiation toward the podocyte lineage in glomerular disorders. Stem Cells, 28, 1674-85.

LAZZERI, E., CRESCIOLI, C., RONCONI, E., MAZZINGHI, B., SAGRINATI, C., NETTI, G. S., ANGELOTTI, M. L., PARENTE, E., BALLERINI, L., COSMI, L., MAGGI, L., GESUALDO, L., ROTONDI, M., ANNUNZIATO, F., MAGGI, E., LASAGNI, L., SERIO, M., ROMAGNANI, S., VANNELLI, G. B. & ROMAGNANI, P.

2007. Regenerative potential of embryonic renal multipotent progenitors in acute renal failure. J Am Soc Nephrol, 18, 3128-38.

LAZZERI, E., ROMAGNANI, P. & LASAGNI, L. 2015. Stem cell therapy for kidney disease. Expert Opin Biol Ther, 15, 1455-68.

LEE, H. J., KIM, D. I., KWAK, C., KU, J. H. & MOON, K. C. 2008. Expression of CD24 in clear cell renal cell carcinoma and its prognostic significance. Urology, 72, 603-7.

LEMLEY, K. V. & KRIZ, W. 1991. Anatomy of the renal interstitium. Kidney Int, 39, 370-81.

LEVEY, A. S. & CORESH, J. 2012. Chronic kidney disease. Lancet, 379, 165-80.

LEVINSON, R. S., BATOURINA, E., CHOI, C., VORONTCHIKHINA, M., KITAJEWSKI, J. & MENDELSOHN, C. L. 2005. Foxd1-dependent signals control cellularity in the renal capsule, a structure required for normal renal development. Development, 132, 529-39.

LINDGREN, D., BOSTROM, A. K., NILSSON, K., HANSSON, J., SJOLUND, J., MOLLER, C., JIRSTROM, K., NILSSON, E., LANDBERG, G., AXELSON, H. & JOHANSSON, M. E. 2011. Isolation and characterization of progenitor-like cells from human renal proximal tubules. Am J Pathol, 178, 828-37.

LITTLE, M. H. 2006. Regrow or repair: potential regenerative therapies for the kidney. J Am Soc Nephrol, 17, 2390-401.

LIU, K. D. & BRAKEMAN, P. R. 2008. Renal repair and recovery. Crit Care Med, 36, S187-92.

LIVAK, K. J. & SCHMITTGEN, T. D. 2001. Analysis of relative gene expression data using real-time quantitative PCR and the 2(-Delta Delta C(T)) Method. Methods, 25, 402-8.

LODISH, H., FLYGARE J FAU - CHOU, S. & CHOU, S. 2010. From stem cell to erythroblast: regulation of red cell production at multiple levels by multiple hormones. IUBMB Life, 62.

LOMBARD, W. E., KOKKO, J. P. & JACOBSON, H. R. 1983. Bicarbonate transport in cortical and outer medullary collecting tubules. Am J Physiol, 244, F289-96.

LONG, D. A., KOLATSI-JOANNOU, M., PRICE, K. L., DESSAPT-BARADEZ, C., HUANG, J. L., PAPAKRIVOPOULOU, E., HUBANK, M., KORSTANJE, R., GNUDI, L. & WOOLF, A. S. 2013. Albuminuria is associated with too few glomeruli and too much testosterone. Kidney Int, 83, 1118-29.

LONG, D. A., PRICE, K. L., IOFFE, E., GANNON, C. M., GNUDI, L., WHITE, K. E., YANCOPOULOS, G. D., RUDGE, J. S. & WOOLF, A. S. 2008. Angiopoietin-1 therapy enhances fibrosis and inflammation following folic acid-induced acute renal injury. Kidney Int, 74, 300-9.

LONG, D. A., WOOLF, A. S., SUDA, T. & YUAN, H. T. 2001. Increased renal angiopoietin-1 expression in folic acid-induced nephrotoxicity in mice. J Am Soc Nephrol, 12, 2721-31.

MAARTEN W. TAAL, G. M. C., PHILIP A. MARSDEN, KARL SKORECKI, ALAN S. L. YU, AND BARRY M. BRENNER 2012. Brenner and Rector's The Kidney 9th edition, Saunders Elsevier.

MADJDPOUR, C., BACIC, D., KAISSLING, B., MURER, H. & BIBER, J. 2004. Segment-specific expression of sodium-phosphate cotransporters NaPi-IIa and -IIc and interacting proteins in mouse renal proximal tubules. Pflugers Arch, 448, 402-10.

MADSEN, K. M., CLAPP, W. L. & VERLANDER, J. W. 1988a. Structure and function of the inner medullary collecting duct. Kidney Int, 34, 441-54.

MADSEN, K. M., VERLANDER, J. W. & TISHER, C. C. 1988b. Relationship between structure and function in distal tubule and collecting duct. J Electron Microsc Tech, 9, 187-208.

MANDEL, H., SHEMER, R., BOROCHOWITZ, Z. U., OKOPNIK, M., KNOPF, C., INDELMAN, M., DRUGAN, A., TIOSANO, D., GERSHONI-BARUCH, R., CHODER, M. & SPRECHER, E. 2008. SERKAL syndrome: an autosomal-recessive disorder caused by a loss-of-function mutation in WNT4. Am J Hum Genet, 82, 39-47.

MANSOURI, A., CHOWDHURY, K. & GRUSS, P. 1998. Follicular cells of the thyroid gland require Pax8 gene function. Nat Genet, 19, 87-90.

MCCLELLAN, S., SLAMECKA, J., HOWZE, P., THOMPSON, L., FINAN, M., ROCCONI, R. & OWEN, L. 2015. mRNA detection in living cells: A next generation cancer stem cell identification technique. Methods, 82, 47-54.

MCKNIGHT, A. J., MACFARLANE, A. J., DRI, P., TURLEY, L., WILLIS, A. C. & GORDON, S. 1996. Molecular cloning of F4/80, a murine macrophage-restricted cell surface glycoprotein with homology to the G-protein-linked transmembrane 7 hormone receptor family. J Biol Chem, 271, 486-9.

MEHTA, R. L., KELLUM, J. A., SHAH, S. V., MOLITORIS, B. A., RONCO, C., WARNOCK, D. G. & LEVIN, A. 2007. Acute Kidney Injury Network: report of an initiative to improve outcomes in acute kidney injury. Crit Care, 11, R31.

MELTON, D. 2014. Chapter 2 - 'Stemness': Definitions, Criteria, and Standards. Essentials of Stem Cell Biology (Third Edition). Boston: Academic Press.

MENKE, A. L., A, I. J., FLEMING, S., ROSS, A., MEDINE, C. N., PATEK, C. E., SPRAGGON, L., HUGHES, J., CLARKE, A. R. & HASTIE, N. D. 2003. The wt1-heterozygous mouse; a model to study the development of glomerular sclerosis. J Pathol, 200, 667-74.

METSUYANIM, S., HARARI-STEINBERG, O., BUZHOR, E., OMER, D., PODE-SHAKKED, N., BEN-HUR, H., HALPERIN, R., SCHNEIDER, D. & DEKEL, B. 2009. Expression of stem cell markers in the human fetal kidney. PLoS One, 4, e6709.

MILWID, J. M., ICHIMURA, T., LI, M., JIAO, Y., LEE, J., YARMUSH, J. S., PAREKKADAN, B., TILLES, A. W., BONVENTRE, J. V. & YARMUSH, M. L. 2012. Secreted factors from bone marrow stromal cells upregulate IL-10 and reverse acute kidney injury. Stem Cells Int, 2012, 392050.

MIRAGLIA, S., GODFREY, W., YIN, A. H., ATKINS, K., WARNKE, R., HOLDEN, J. T., BRAY, R. A., WALLER, E. K. & BUCK, D. W. 1997. A novel five-transmembrane hematopoietic stem cell antigen: isolation, characterization, and molecular cloning. Blood, 90, 5013-21.

MONTSERRAT, N., RAMIREZ-BAJO, M. J., XIA, Y., SANCHO-MARTINEZ, I., MOYA-RULL, D., MIQUEL-SERRA, L., YANG, S., NIVET, E., CORTINA, C., GONZALEZ, F., IZPISUA BELMONTE, J. C. & CAMPISTOL, J. M. 2012. Generation of induced pluripotent stem cells from human renal proximal tubular cells with only two transcription factors, OCT4 and SOX2. J Biol Chem, 287, 24131-8.

MOON, K. H., KO, I. K., YOO, J. J. & ATALA, A. 2016. Kidney diseases and tissue engineering. Methods, 99, 112-9.

MORALES, E. E. & WINGERT, R. A. 2014. Renal stem cell reprogramming: Prospects in regenerative medicine. World J Stem Cells, 6, 458-66.

MORIZANE, R., LAM, A. Q., FREEDMAN, B. S., KISHI, S., VALERIUS, M. T. & BONVENTRE, J. V. 2015. Nephron organoids derived from human pluripotent stem cells model kidney development and injury. Nat Biotechnol.

MORRISON, S. J. & KIMBLE, J. 2006. Asymmetric and symmetric stem-cell divisions in development and cancer. Nature, 441, 1068-74.

MUGFORD, J. W., SIPILA, P., MCMAHON, J. A. & MCMAHON, A. P. 2008. Osr1 expression demarcates a multi-potent population of intermediate mesoderm that undergoes progressive restriction to an Osr1-dependent nephron progenitor compartment within the mammalian kidney. Dev Biol, 324, 88-98.

MUGFORD, J. W., YU, J., KOBAYASHI, A. & MCMAHON, A. P. 2009. High-resolution gene expression analysis of the developing mouse kidney defines novel cellular compartments within the nephron progenitor population. Dev Biol, 333, 312-23.

MURPHY, A. J., PIERCE, J., DE CAESTECKER, C., TAYLOR, C., ANDERSON, J. R., PERANTONI, A. O., DE CAESTECKER, M. P. & LOVVORN, H. N., 3RD 2012. SIX2 and CITED1, markers of nephronic progenitor self-renewal, remain active in primitive elements of Wilms' tumor. J Pediatr Surg, 47, 1239-49.

MUSTONEN, S., ALA-HOUHALA, I. O. & TAMMELA, T. L. 2001. Long-term renal dysfunction in patients with acute urinary retention. Scand J Urol Nephrol, 35, 44-8.

NAZKI, F. H., SAMEER, A. S. & GANAIE, B. A. 2014. Folate: metabolism, genes, polymorphisms and the associated diseases. Gene, 533, 11-20.

NISHINAKAMURA, R., MATSUMOTO, Y., NAKAO, K., NAKAMURA, K., SATO, A., COPELAND, N. G., GILBERT, D. J., JENKINS, N. A., SCULLY, S., LACEY, D. L., KATSUKI, M., ASASHIMA, M. & YOKOTA, T. 2001. Murine homolog of SALL1 is essential for ureteric bud invasion in kidney development. Development, 128, 3105-15.

NISHINAKAMURA, R. & OSAFUNE, K. 2006. Essential roles of Sall family genes in kidney development. J Physiol Sci, 56, 131-6.

NYENGAARD, J. R. 1993. The quantitative development of glomerular capillaries in rats with special reference to unbiased stereological estimates of their number and sizes. Microvasc Res, 45, 243-61.

O'NEIL, R. G. & HELMAN, S. I. 1977. Transport characteristics of renal collecting tubules: influences of DOCA and diet. Am J Physiol, 233, F544-58.

OLIVER, G., WEHR, R., JENKINS, N. A., COPELAND, N. G., CHEYETTE, B. N., HARTENSTEIN, V., ZIPURSKY, S. L. & GRUSS, P. 1995. Homeobox genes and connective tissue patterning. Development, 121, 693-705.

OLIVER, J. A., BARASCH, J., YANG, J., HERZLINGER, D. & AL-AWQATI, Q. 2002. Metanephric mesenchyme contains embryonic renal stem cells. Am J Physiol Renal Physiol, 283, F799-809.

ORTEGA, S., ITTMANN, M., TSANG, S. H., EHRLICH, M. & BASILICO, C. 1998. Neuronal defects and delayed wound healing in mice lacking fibroblast growth factor 2. Proc Natl Acad Sci U S A, 95, 5672-7.

ORTIZ, A., LORZ, C., CATALAN, M. P., DANOFF, T. M., YAMASAKI, Y., EGIDO, J. & NEILSON, E. G. 2000. Expression of apoptosis regulatory proteins in tubular epithelium stressed in culture or following acute renal failure. Kidney Int, 57, 969-81.

OWEN, M. E., CAVE, J. & JOYNER, C. J. 1987. Clonal analysis in vitro of osteogenic differentiation of marrow CFU-F. J Cell Sci, 87 (Pt 5), 731-8.

PANNABECKER, T. L. 2012. Structure and function of the thin limbs of the loop of Henle. Compr Physiol, 2, 2063-86.

PARK, J. S., MA, W., O'BRIEN, L. L., CHUNG, E., GUO, J. J., CHENG, J. G., VALERIUS, M. T., MCMAHON, J. A., WONG, W. H. & MCMAHON, A. P. 2012. Six2 and Wnt regulate self-renewal and commitment of nephron progenitors through shared gene regulatory networks. Dev Cell, 23, 637-51.

PARK, J. S., VALERIUS, M. T. & MCMAHON, A. P. 2007. Wnt/beta-catenin signaling regulates nephron induction during mouse kidney development. Development, 134, 2533-9.

PATEL, S. R., RANGHINI, E. & DRESSLER, G. R. 2014. Mechanisms of gene activation and repression by Pax proteins in the developing kidney. Pediatr Nephrol, 29, 589-95.

PELEKANOS, R. A., LI, J., GONGORA, M., CHANDRAKANTHAN, V., SCOWN, J., SUHAIMI, N., BROOKE, G., CHRISTENSEN, M. E., DOAN, T., RICE, A. M., OSBORNE, G. W., GRIMMOND, S. M., HARVEY, R. P., ATKINSON, K. & LITTLE, M. H. 2012. Comprehensive transcriptome and immunophenotype analysis of renal and cardiac MSC-like populations supports strong congruence with bone marrow MSC despite maintenance of distinct identities. Stem Cell Res, 8, 58-73.

PELLETIER, J., BRUENING, W., KASHTAN, C. E., MAUER, S. M., MANIVEL, J. C., STRIEGEL, J. E., HOUGHTON, D. C., JUNIEN, C., HABIB, R., FOUSER, L. & ET AL. 1991. Germline mutations in the Wilms' tumor suppressor gene are associated with abnormal urogenital development in Denys-Drash syndrome. Cell, 67, 437-47.

PERANTONI, A. O., DOVE, L. F. & KARAVANOVA, I. 1995. Basic fibroblast growth factor can mediate the early inductive events in renal development. Proc Natl Acad Sci U S A, 92, 4696-700.

PERANTONI, A. O., TIMOFEEVA, O., NAILLAT, F., RICHMAN, C., PAJNI-UNDERWOOD, S., WILSON, C., VAINIO, S., DOVE, L. F. & LEWANDOSKI, M. 2005. Inactivation of FGF8 in early mesoderm reveals an essential role in kidney development. Development, 132, 3859-71.

PERIN, L., GIULIANI, S., JIN, D., SEDRAKYAN, S., CARRARO, G., HABIBIAN, R., WARBURTON, D., ATALA, A. & DE FILIPPO, R. E. 2007. Renal differentiation of amniotic fluid stem cells. Cell Prolif, 40, 936-48.

PITTENGER, M. F., MACKAY, A. M., BECK, S. C., JAISWAL, R. K., DOUGLAS, R., MOSCA, J. D., MOORMAN, M. A., SIMONETTI, D. W., CRAIG, S. & MARSHAK, D. R. 1999. Multilineage potential of adult human mesenchymal stem cells. Science, 284, 143-7.

PLENICEANU, O., HARARI-STEINBERG, O. & DEKEL, B. 2010. Concise review: Kidney stem/progenitor cells: differentiate, sort out, or reprogram? Stem Cells, 28, 1649-60.

PLISOV, S., TSANG, M., SHI, G., BOYLE, S., YOSHINO, K., DUNWOODIE, S. L., DAWID, I. B., SHIODA, T., PERANTONI, A. O. & DE CAESTECKER, M. P. 2005. Cited1 is a bifunctional transcriptional cofactor that regulates early nephronic patterning. J Am Soc Nephrol, 16, 1632-44.

PLISOV, S. Y., YOSHINO, K., DOVE, L. F., HIGINBOTHAM, K. G., RUBIN, J. S. & PERANTONI, A. O. 2001. TGF beta 2, LIF and FGF2 cooperate to induce nephrogenesis. Development, 128, 1045-57.

PODE-SHAKKED, N., METSUYANIM, S., ROM-GROSS, E., MOR, Y., FRIDMAN, E., GOLDSTEIN, I., AMARIGLIO, N., RECHAVI, G., KESHET, G. & DEKEL, B. 2009. Developmental tumourigenesis: NCAM as a putative marker for the malignant renal stem/progenitor cell population. J Cell Mol Med, 13, 1792-808.

PODE-SHAKKED, N., PLENICEANU, O., GERSHON, R., SHUKRUN, R., KANTER, I., BUCRIS, E., PODE-SHAKKED, B., TAM, G., TAM, H., CASPI, R., PRI-CHEN, S., VAX, E., KATZ, G., OMER, D., HARARI-STEINBERG, O., KALISKY, T. & DEKEL, B. 2016. Dissecting Stages of Human Kidney Development and Tumorigenesis with Surface Markers Affords Simple Prospective Purification of Nephron Stem Cells. Sci Rep, 6, 23562.

POLADIA, D. P., KISH, K., KUTAY, B., HAINS, D., KEGG, H., ZHAO, H. & BATES, C. M. 2006. Role of fibroblast growth factor receptors 1 and 2 in the metanephric mesenchyme. Dev Biol, 291, 325-39.

POTTEN, C. S. & LOEFFLER, M. 1990. Stem cells: attributes, cycles, spirals, pitfalls and uncertainties. Lessons for and from the crypt. Development, 110, 1001-20.

PRICE, K. L., LONG, D. A., JINA, N., LIAPIS, H., HUBANK, M., WOOLF, A. S. & WINYARD, P. J. 2007. Microarray interrogation of human metanephric mesenchymal cells highlights potentially important molecules in vivo. Physiol Genomics, 28, 193-202.

PRITCHARD-JONES, K., FLEMING, S., DAVIDSON, D., BICKMORE, W., PORTEOUS, D., GOSDEN, C., BARD, J., BUCKLER, A., PELLETIER, J., HOUSMAN, D. & ET AL. 1990. The candidate Wilms' tumour gene is involved in genitourinary development. Nature, 346, 194-7.

ALISON, MR. 2017. Stem Cell Plasticity. In: SCHWAB, M. (ed.) Encyclopedia of Cancer. Springer Berlin Heidelberg.

RAHMAN, M. S., AKHTAR, N., JAMIL, H. M., BANIK, R. S. & ASADUZZAMAN, S. M. 2015. TGF-beta/BMP signaling and other molecular events: regulation of osteoblastogenesis and bone formation. Bone Res, 3, 15005.

RANDLES, M. J., WOOLF, A. S., HUANG, J. L., BYRON, A., HUMPHRIES, J. D., PRICE, K. L., KOLATSI-JOANNOU, M., COLLINSON, S., DENNY, T., KNIGHT, D., MIRONOV, A., STARBORG, T., KORSTANJE, R., HUMPHRIES, M. J., LONG, D. A. & LENNON, R. 2015. Genetic Background is a Key Determinant of Glomerular Extracellular Matrix Composition and Organization. J Am Soc Nephrol, 26, 3021-34.

RAYNER, H. C., PISONI, R. L., BOMMER, J., CANAUD, B., HECKING, E., LOCATELLI, F., PIERA, L., BRAGG-GRESHAM, J. L., FELDMAN, H. I., GOODKIN, D. A., GILLESPIE, B., WOLFE, R. A., HELD, P. J. & PORT, F. K. 2004. Mortality and hospitalization in haemodialysis patients in five European countries: results from the Dialysis Outcomes and Practice Patterns Study (DOPPS). Nephrol Dial Transplant, 19, 108-20.

REIDY, K. J. & ROSENBLUM, N. D. 2009. Cell and molecular biology of kidney development. Semin Nephrol, 29, 321-37.

REILLY, R. F. & ELLISON, D. H. 2000. Mammalian distal tubule: physiology, pathophysiology, and molecular anatomy. Physiol Rev, 80, 277-313.

REWA, O. & BAGSHAW, S. M. 2014. Acute kidney injury-epidemiology, outcomes and economics. Nat Rev Nephrol, 10, 193-207.

RICCI-VITIANI, L., LOMBARDI, D. G., PILOZZI, E., BIFFONI, M., TODARO, M., PESCHLE, C. & DE MARIA, R. 2007. Identification and expansion of human colon-cancer-initiating cells. Nature, 445, 111-5.

RICHARDSON, G. D., ROBSON, C. N., LANG, S. H., NEAL, D. E., MAITLAND, N. J. & COLLINS, A. T. 2004. CD133, a novel marker for human prostatic epithelial stem cells. J Cell Sci, 117, 3539-45.

ROBSON, E. J., HE, S. J. & ECCLES, M. R. 2006. A PANorama of PAX genes in cancer and development. Nat Rev Cancer, 6, 52-62.

RONCONI, E., MAZZINGHI, B., SAGRINATI, C., ANGELOTTI, M. L., BALLERINI, L., PARENTE, E., ROMAGNANI, P., LAZZERI, E. & LASAGNI, L. 2009a. [The role of podocyte damage in the pathogenesis of glomerulosclerosis and possible repair mechanisms]. G Ital Nefrol, 26, 660-9.

RONCONI, E., SAGRINATI, C., ANGELOTTI, M. L., LAZZERI, E., MAZZINGHI, B., BALLERINI, L., PARENTE, E., BECHERUCCI, F., GACCI, M., CARINI, M., MAGGI, E., SERIO, M., VANNELLI, G. B., LASAGNI, L., ROMAGNANI, S. & ROMAGNANI, P. 2009b. Regeneration of glomerular podocytes by human renal progenitors. J Am Soc Nephrol, 20, 322-32.

ROY, S., GASCARD, P., DUMONT, N., ZHAO, J., PAN, D., PETRIE, S., MARGETA, M. & TLSTY, T. D. 2013. Rare somatic cells from human breast tissue exhibit extensive lineage plasticity. Proc Natl Acad Sci U S A, 110, 4598-603.

RUMBALLE, B. A., GEORGAS, K. M., COMBES, A. N., JU, A. L., GILBERT, T. & LITTLE, M. H. 2011. Nephron formation adopts a novel spatial topology at cessation of nephrogenesis. Dev Biol, 360, 110-22.

RUNZ, S., MIERKE, C. T., JOUMAA, S., BEHRENS, J., FABRY, B. & ALTEVOGT, P. 2008. CD24 induces localization of beta1 integrin to lipid raft domains. Biochem Biophys Res Commun, 365, 35-41.

RYAN, G., STEELE-PERKINS, V., MORRIS, J. F., RAUSCHER, F. J., 3RD & DRESSLER, G. R. 1995. Repression of Pax-2 by WT1 during normal kidney development. Development, 121, 867-75.

SAGRINATI, C., NETTI, G. S., MAZZINGHI, B., LAZZERI, E., LIOTTA, F., FROSALI, F., RONCONI, E., MEINI, C., GACCI, M., SQUECCO, R., CARINI, M., GESUALDO, L., FRANCINI, F., MAGGI, E., ANNUNZIATO, F., LASAGNI, L., SERIO, M., ROMAGNANI, S. & ROMAGNANI, P. 2006. Isolation and characterization of multipotent progenitor cells from the Bowman's capsule of adult human kidneys. J Am Soc Nephrol, 17, 2443-56.

SAJITHLAL, G., ZOU, D., SILVIUS, D. & XU, P. X. 2005. Eya 1 acts as a critical regulator for specifying the metanephric mesenchyme. Dev Biol, 284, 323-36.

SANDS, J. M. & KNEPPER, M. A. 1987. Urea permeability of mammalian inner medullary collecting duct system and papillary surface epithelium. J Clin Invest, 79, 138-47.

SAXEN, L. & SARIOLA, H. 1987. Early organogenesis of the kidney. Pediatr Nephrol, 1, 385-92.

SCHMIDT-OTT, K. M. & BARASCH, J. 2008. WNT/beta-catenin signaling in nephron progenitors and their epithelial progeny. Kidney Int, 74, 1004-8.

SCHMIDT, T., BIERHALS, T., KORTUM, F., BARTELS, I., LIEHR, T., BURFEIND, P., SHOUKIER, M., FRANK, V., BERGMANN, C. & KUTSCHE, K. 2014. Branchio-otic syndrome caused by a genomic rearrangement: clinical findings and molecular cytogenetic studies in a patient with a pericentric inversion of chromosome 8. Cytogenet Genome Res, 142, 1-6.

SCHMIDT, U., TORHORST, J., HUGUENIN, M. & DUBACH, U. C. 1973. Acute renal failure after folate: NaK ATPase in isolated rat renal tubule. Ultramicrochemical and clinical studies. Eur J Clin Invest, 3, 169-78.

SCHOLER, HR., BALLING, R., HATZOPOULOS, AK., SUZUKI, N., GRUSS, P., Octamer binding proteins confer transcriptional activity in early mouse embryogenesis. EMBO J. 1989; 8:2551–7.

SEABERG, R. M. & VAN DER KOOY, D. 2002. Adult rodent neurogenic regions: the ventricular subependyma contains neural stem cells, but the dentate gyrus contains restricted progenitors.

SEDRAKYAN, S., DA SACCO, S., MILANESI, A., SHIRI, L., PETROSYAN, A., VARIMEZOVA, R., WARBURTON, D., LEMLEY, K. V., DE FILIPPO, R. E. & PERIN, L. 2012. Injection of amniotic fluid stem cells delays progression of renal fibrosis. J Am Soc Nephrol, 23, 661-73.

SELF, M., LAGUTIN, O. V., BOWLING, B., HENDRIX, J., CAI, Y., DRESSLER, G. R. & OLIVER, G. 2006. Six2 is required for suppression of nephrogenesis and progenitor renewal in the developing kidney. EMBO J, 25, 5214-28.

SHI, Y. & MASSAGUE, J. 2003. Mechanisms of TGF-beta signaling from cell membrane to the nucleus. Cell, 113, 685-700.

SHIRASAWA, T., AKASHI, T., SAKAMOTO, K., TAKAHASHI, H., MARUYAMA, N. & HIROKAWA, K. 1993. Gene expression of CD24 core peptide molecule in developing brain and developing non-neural tissues. Dev Dyn, 198, 1-13.

SHMELKOV, S. V., BUTLER, J. M., HOOPER, A. T., HORMIGO, A., KUSHNER, J., MILDE, T., ST CLAIR, R., BALJEVIC, M., WHITE, I., JIN, D. K., CHADBURN, A., MURPHY, A. J., VALENZUELA, D. M., GALE, N. W., THURSTON, G., YANCOPOULOS, G. D., D'ANGELICA, M., KEMENY, N., LYDEN, D. & RAFII, S. 2008. CD133 expression is not restricted to stem cells, and both CD133+ and CD133- metastatic colon cancer cells initiate tumors. J Clin Invest, 118, 2111-20.

SHUKRUN, R., PODE-SHAKKED, N., PLENICEANU, O., OMER, D., VAX, E., PEER, E., PRI-CHEN, S., JACOB, J., HU, Q., HARARI-STEINBERG, O., HUFF, V. & DEKEL, B. 2014. Wilms' tumor blastemal stem cells dedifferentiate to propagate the tumor bulk. Stem Cell Reports, 3, 24-33.

SHULEWITZ, M., SOLOVIEV, I., WU, T., KOEPPEN, H., POLAKIS, P. & SAKANAKA, C. 2006. Repressor roles for TCF-4 and Sfrp1 in Wnt signaling in breast cancer. Oncogene, 25, 4361-9.

SHULTZ, L. D., SCHWEITZER, P. A., CHRISTIANSON, S. W., GOTT, B., SCHWEITZER, I. B., TENNENT, B., MCKENNA, S., MOBRAATEN, L., RAJAN, T. V., GREINER, D. L. & ET AL. 1995. Multiple defects in innate and adaptive immunologic function in NOD/LtSz-scid mice. J Immunol, 154, 180-91.

SIEGEL, N., ROSNER, M., UNBEKANDT, M., FUCHS, C., SLABINA, N., DOLZNIG, H., DAVIES, J. A., LUBEC, G. & HENGSTSCHLAGER, M. 2010. Contribution of human amniotic fluid stem cells to renal tissue formation depends on mTOR. Hum Mol Genet, 19, 3320-31.

SILVER, S. A., CARDINAL, H., COLWELL, K., BURGER, D. & DICKHOUT, J. G. 2015. Acute kidney injury: preclinical innovations, challenges, and opportunities for translation. Can J Kidney Health Dis, 2, 30.

SIM, E. U., SMITH, A., SZILAGI, E., RAE, F., IOANNOU, P., LINDSAY, M. H. & LITTLE, M. H. 2002. Wnt-4 regulation by the Wilms' tumour suppressor gene, WT1. Oncogene, 21, 2948-60.

SIMS-LUCAS, S., CUSACK, B., BAUST, J., ESWARAKUMAR, V. P., MASATOSHI, H., TAKEUCHI, A. & BATES, C. M. 2011. Fgfr1 and the IIIc isoform of Fgfr2 play critical roles in the metanephric mesenchyme mediating early inductive events in kidney development. Dev Dyn, 240, 240-9.

SINGH, V. K., SAINI, A., KALSAN, M., KUMAR, N. & CHANDRA, R. 2016. Describing the Stem Cell Potency: The Various Methods of Functional Assessment and In silico Diagnostics. Front Cell Dev Biol, 4.

SLACK, J. M. 2008. Origin of stem cells in organogenesis. Science, 322, 1498-501.

SMEETS, B., BOOR, P., DIJKMAN, H., SHARMA, S. V., JIRAK, P., MOOREN, F., BERGER, K., BORNEMANN, J., GELMAN, I. H., FLOEGE, J., VAN DER VLAG, J., WETZELS, J. F. & MOELLER, M. J. 2013. Proximal tubular cells contain a phenotypically distinct, scattered cell population involved in tubular regeneration. J Pathol, 229, 645-59.

SMITH, S. C., OXFORD, G., WU, Z., NITZ, M. D., CONAWAY, M., FRIERSON, H. F., HAMPTON, G. & THEODORESCU, D. 2006. The metastasis-associated gene CD24 is regulated by Ral GTPase and is a mediator of cell proliferation and survival in human cancer. Cancer Res, 66, 1917-22.

SO, P. L. & DANIELIAN, P. S. 1999. Cloning and expression analysis of a mouse gene related to Drosophila odd-skipped. Mech Dev, 84, 157-60.

SONG, J. J., GUYETTE, J. P., GILPIN, S. E., GONZALEZ, G., VACANTI, J. P. & OTT, H. C. 2013. Regeneration and experimental orthotopic transplantation of a bioengineered kidney. Nat Med, 19, 646-51.

SONG, R., PRESTON, G., KIDD, L., BUSHNELL, D., SIMS-LUCAS, S., BATES, C. M. & YOSYPIV, I. V. 2016. Prorenin receptor is critical for nephron progenitors. Dev Biol, 409, 382-91.

SPANGRUDE, G. J., HEIMFELD S FAU - WEISSMAN, I. L. & WEISSMAN, I. L. 1989. Purification and characterization of mouse hematopoietic stem cells. Science, 58-62.

STALLONS, L. J., WHITAKER, R. M. & SCHNELLMANN, R. G. 2014. Suppressed mitochondrial biogenesis in folic acid-induced acute kidney injury and early fibrosis. Toxicol Lett, 224, 326-32.

STARK, K., VAINIO, S., VASSILEVA, G. & MCMAHON, A. P. 1994. Epithelial transformation of metanephric mesenchyme in the developing kidney regulated by Wnt-4. Nature, 372, 679-83.

STEIN, J. H. & FADEM, S. Z. 1978. The renal circulation. Jama, 239, 1308-12.

STOUMPOS, S., JARDINE, A. G. & MARK, P. B. 2015. Cardiovascular morbidity and mortality after kidney transplantation. Transpl Int, 28, 10-21.

STRINGER, K. D., KOMERS, R., OSMAN, S. A., OYAMA, T. T., LINDSLEY, J. N. & ANDERSON, S. 2005. Gender hormones and the progression of experimental polycystic kidney disease. Kidney Int, 68, 1729-39.

SURENDRAN, K., BOYLE, S., BARAK, H., KIM, M., STOMBERSKI, C., MCCRIGHT, B. & KOPAN, R. 2010. The contribution of Notch1 to nephron segmentation in the developing kidney is revealed in a sensitized Notch2 background and can be augmented by reducing Mint dosage. Dev Biol, 337, 386-95.

SUZUKI, T., KIYOKAWA, N., TAGUCHI, T., SEKINO, T., KATAGIRI, Y. U. & FUJIMOTO, J. 2001. CD24 induces apoptosis in human B cells via the glycolipid-enriched membrane domains/rafts-mediated signaling system. J Immunol, 166, 5567-77.

SZCZECH, L. A. & LAZAR, I. L. 2004. Projecting the United States ESRD population: issues regarding treatment of patients with ESRD. Kidney Int Suppl, S3-7.

TAGUCHI, A. & NISHINAKAMURA, R. 2014. Nephron reconstitution from pluripotent stem cells. Kidney Int.

TAKAHASHI, K., TANABE, K., OHNUKI, M., NARITA, M., ICHISAKA, T., TOMODA, K. & YAMANAKA, S. 2007. Induction of pluripotent stem cells from adult human fibroblasts by defined factors. Cell, 131, 861-72.

TAKAHASHI, K. & YAMANAKA, S. 2006. Induction of pluripotent stem cells from mouse embryonic and adult fibroblast cultures by defined factors. Cell, 126, 663-76.

TAKASATO, M., ER, P. X., BECROFT, M., VANSLAMBROUCK, J. M., STANLEY, E. G., ELEFANTY, A. G. & LITTLE, M. H. 2014. Directing human embryonic stem cell differentiation towards a renal lineage generates a self-organizing kidney. Nat Cell Biol, 16, 118-26.

TAKASATO, M., ER, P. X., CHIU, H. S., MAIER, B., BAILLIE, G. J., FERGUSON, C., PARTON, R. G., WOLVETANG, E. J., ROOST, M. S., CHUVA DE SOUSA LOPES, S. M. & LITTLE, M. H. 2015. Kidney organoids from human iPS cells contain multiple lineages and model human nephrogenesis. Nature.

TAN, J., WU, W., XU, X., LIAO, L., ZHENG, F., MESSINGER, S., SUN, X., CHEN, J., YANG, S., CAI, J., GAO, X., PILEGGI, A. & RICORDI, C. 2012. Induction therapy with autologous mesenchymal stem cells in living-related kidney transplants: a randomized controlled trial. Jama, 307, 1169-77.

TANG, J., YAN, Y., ZHAO, T. C., GONG, R., BAYLISS, G., YAN, H. & ZHUANG, S. 2014. Class I HDAC activity is required for renal protection and regeneration after acute kidney injury. Am J Physiol Renal Physiol.

TANIGAWA, S. & PERANTONI, A. O. 2016. Modeling renal progenitors - defining the niche. Differentiation.

TANIGAWA, S., SHARMA, N., HALL, M. D., NISHINAKAMURA, R. & PERANTONI, A. O. 2015. Preferential Propagation of Competent SIX2+ Nephronic Progenitors by LIF/ROCKi Treatment of the Metanephric Mesenchyme. Stem Cell Reports, 5, 435-47.

TANIGAWA, S., TAGUCHI, A., SHARMA, N., PERANTONI, A. O. & NISHINAKAMURA, R. 2016. Selective In Vitro Propagation of Nephron Progenitors Derived from Embryos and Pluripotent Stem Cells. Cell Rep.

TANK, K. C., SAIYAD, S.S., PANDYA, A.M., AKBARI, V.J., AND DANGAR, K.P. 2012. A study of histogenesis of human fetal kidney. Int. J. Biol. Med. Res. , 3.

TISCORNIA, G., SINGER, O. & VERMA, I. M. 2006. Production and purification of lentiviral vectors. Nat Protoc, 1, 241-5.

TOGEL, F., HU, Z., WEISS, K., ISAAC, J., LANGE, C. & WESTENFELDER, C. 2005. Administered mesenchymal stem cells protect against ischemic acute renal failure through differentiation-independent mechanisms. Am J Physiol Renal Physiol, 289, F31-42.

TORRENTE, Y., BELICCHI, M., SAMPAOLESI, M., PISATI, F., MEREGALLI, M., D'ANTONA, G., TONLORENZI, R., PORRETTI, L., GAVINA, M., MAMCHAOUI, K., PELLEGRINO, M. A., FURLING, D., MOULY, V., BUTLER-BROWNE, G. S., BOTTINELLI, R., COSSU, G. & BRESOLIN, N. 2004. Human circulating AC133(+) stem cells restore dystrophin expression and ameliorate function in dystrophic skeletal muscle. J Clin Invest, 114, 182-95.

TORRES, M., GOMEZ-PARDO, E., DRESSLER, G. R. & GRUSS, P. 1995. Pax-2 controls multiple steps of urogenital development. Development, 121, 4057-65.

TREISMAN, J., HARRIS, E. & DESPLAN, C. 1991. The paired box encodes a second DNA-binding domain in the paired homeo domain protein. Genes Dev, 5, 594-604.

TRZPIS, M., MCLAUGHLIN, P. M., VAN GOOR, H., BRINKER, M. G., VAN DAM, G. M., DE LEIJ, L. M., POPA, E. R. & HARMSEN, M. C. 2008. Expression of EpCAM is up-regulated during regeneration of renal epithelia. J Pathol, 216, 201-8.

UCHIDA, N., BUCK, D. W., HE, D., REITSMA, M. J., MASEK, M., PHAN, T. V., TSUKAMOTO, A. S., GAGE, F. H. & WEISSMAN, I. L. 2000. Direct isolation of human central nervous system stem cells. Proc Natl Acad Sci U S A, 97, 14720-5.

UNBEKANDT, M. & DAVIES, J. A. 2010. Dissociation of embryonic kidneys followed by reaggregation allows the formation of renal tissues. Kidney Int, 77, 407-16.

VACANTI, J. P. & LANGER, R. 1999. Tissue engineering: the design and fabrication of living replacement devices for surgical reconstruction and transplantation. Lancet, 354 Suppl 1, Si32-4.

WAGNER, K. D., WAGNER, N., VIDAL, V. P., SCHLEY, G., WILHELM, D., SCHEDL, A., ENGLERT, C. & SCHOLZ, H. 2002. The Wilms' tumor gene Wt1 is required for normal development of the retina. Embo j, 21, 1398-405.

WANG, Y., HE, J., PEI, X. & ZHAO, W. 2013. Systematic review and meta-analysis of mesenchymal stem/stromal cells therapy for impaired renal function in small animal models. Nephrology (Carlton), 18, 201-8.

WEIGMANN, A., CORBEIL, D., HELLWIG, A. & HUTTNER, W. B. 1997. Prominin, a novel microvilli-specific polytopic membrane protein of the apical surface of epithelial cells, is targeted to plasmalemmal protrusions of non-epithelial cells. Proc Natl Acad Sci U S A, 94, 12425-30.

WELLIK, D. M., HAWKES, P. J. & CAPECCHI, M. R. 2002. Hox11 paralogous genes are essential for metanephric kidney induction. Genes Dev, 16, 1423-32.

WELLING, L. W. & WELLING, D. J. 1975. Surface areas of brush border and lateral cell walls in the rabbit proximal nephron. Kidney Int, 8, 343-8.

WENG, Z., XIN, M., PABLO, L., GRUENEBERG, D., HAGEL, M., BAIN, G., MULLER, T. & PAPKOFF, J. 2002. Protection against anoikis and down-regulation of cadherin expression by a regulatable beta-catenin protein. J Biol Chem, 277, 18677-86.

WINKLER, A., ZIGEUNER, R., REHAK, P., HUTTERER, G., CHROMECKI, T. & LANGNER, C. 2007. CD24 expression in urothelial carcinoma of the upper urinary tract correlates with tumour progression. Virchows Arch, 450, 59-64.

WINYARD, P. J. & PRICE, K. L. 2013. Experimental renal progenitor cells: Repairing and recreating kidneys? Pediatr Nephrol.

WINYARD, P. J., RISDON, R. A., SAMS, V. R., DRESSLER, G. R. & WOOLF, A. S. 1996. The PAX2 tanscription factor is expressed in cystic and hyperproliferative dysplastic epithelia in human kidney malformations. J Clin Invest, 98, 451-9.

WITZGALL, R., BROWN, D., SCHWARZ, C. & BONVENTRE, J. V. 1994. Localization of proliferating cell nuclear antigen, vimentin, c-Fos, and clusterin in the postischemic kidney. Evidence for a heterogenous genetic response among nephron segments, and a large pool of mitotically active and dedifferentiated cells. J Clin Invest, 93, 2175-88.

XIA, Y., NIVET, E., SANCHO-MARTINEZ, I., GALLEGOS, T., SUZUKI, K., OKAMURA, D., WU, M. Z., DUBOVA, I., ESTEBAN, C. R., MONTSERRAT, N., CAMPISTOL, J. M. & IZPISUA BELMONTE, J. C. 2013. Directed differentiation of human pluripotent cells to ureteric bud kidney progenitor-like cells. Nat Cell Biol, 15, 1507-15.

XINARIS, C., BENEDETTI, V., RIZZO, P., ABBATE, M., CORNA, D., AZZOLLINI, N., CONTI, S., UNBEKANDT, M., DAVIES, J. A., MORIGI, M., BENIGNI, A. & REMUZZI, G. 2012. In vivo maturation of functional renal organoids formed from embryonic cell suspensions. J Am Soc Nephrol, 23, 1857-68.

XU, J., LIU, H., PARK, J. S., LAN, Y. & JIANG, R. 2014. Osr1 acts downstream of and interacts synergistically with Six2 to maintain nephron progenitor cells during kidney organogenesis. Development, 141, 1442-52.

XU, P. X., ADAMS, J., PETERS, H., BROWN, M. C., HEANEY, S. & MAAS, R. 1999. Eya1-deficient mice lack ears and kidneys and show abnormal apoptosis of organ primordia. Nat Genet, 23, 113-7.

YATES, L. L., PAPAKRIVOPOULOU, J., LONG, D. A., GOGGOLIDOU, P., CONNOLLY, J. O., WOOLF, A. S. & DEAN, C. H. 2010. The planar cell polarity gene Vangl2 is required for mammalian kidney-branching morphogenesis and glomerular maturation. Hum Mol Genet, 19, 4663-76.

YAYON, A., KLAGSBRUN, M., ESKO, J. D., LEDER, P. & ORNITZ, D. M. 1991. Cell surface, heparin-like molecules are required for binding of basic fibroblast growth factor to its high affinity receptor. Cell, 64, 841-8.

YE, P., NADKARNI, M. A. & HUNTER, N. 2006. Regulation of E-cadherin and TGF-beta3 expression by CD24 in cultured oral epithelial cells. Biochem Biophys Res Commun, 349, 229-35.

YIN, A. H., MIRAGLIA, S., ZANJANI, E. D., ALMEIDA-PORADA, G., OGAWA, M., LEARY, A. G., OLWEUS, J., KEARNEY, J. & BUCK, D. W. 1997. AC133, a novel marker for human hematopoietic stem and progenitor cells. Blood, 90, 5002-12.

YIN, S., LI, J., HU, C., CHEN, X., YAO, M., YAN, M., JIANG, G., GE, C., XIE, H., WAN, D., YANG, S., ZHENG, S. & GU, J. 2007. CD133 positive hepatocellular carcinoma cells possess high capacity for tumorigenicity. Int J Cancer, 120, 1444-50.

YOSHIDA, K., TAGA, T., SAITO, M., SUEMATSU, S., KUMANOGOH, A., TANAKA, T., FUJIWARA, H., HIRATA, M., YAMAGAMI, T., NAKAHATA, T., HIRABAYASHI, T., YONEDA, Y., TANAKA, K., WANG, W. Z., MORI, C., SHIOTA, K., YOSHIDA, N. & KISHIMOTO, T. 1996. Targeted disruption of gp130, a common signal transducer for the interleukin 6 family of cytokines, leads to myocardial and hematological disorders. Proc Natl Acad Sci U S A, 93, 407-11.

YU, Y., FLINT, A., DVORIN, E. L. & BISCHOFF, J. 2002. AC133-2, a novel isoform of human AC133 stem cell antigen. J Biol Chem, 277, 20711-6.

ZAMBON, J. P., MAGALHAES, R. S., KO, I., ROSS, C. L., ORLANDO, G., PELOSO, A., ATALA, A. & YOO, J. J. 2014. Kidney regeneration: Where we are and future perspectives. World J Nephrol, 3, 24-30.

ZHAI, X. Y., BIRN, H., JENSEN, K. B., THOMSEN, J. S., ANDREASEN, A. & CHRISTENSEN, E. I. 2003. Digital three-dimensional reconstruction and ultrastructure of the mouse proximal tubule. J Am Soc Nephrol, 14, 611-9.

ZHANG, X., IBRAHIMI, O. A., OLSEN, S. K., UMEMORI, H., MOHAMMADI, M. & ORNITZ, D. M. 2006. Receptor specificity of the fibroblast growth factor family. The complete mammalian FGF family. J Biol Chem, 281, 15694-700.

ZHOU, T., BENDA, C., DUNZINGER, S., HUANG, Y., HO, J. C., YANG, J., WANG, Y., ZHANG, Y., ZHUANG, Q., LI, Y., BAO, X., TSE, H. F., GRILLARI, J., GRILLARI-VOGLAUER, R., PEI, D. & ESTEBAN, M. A. 2012. Generation of human induced pluripotent stem cells from urine samples. Nat Protoc, 7, 2080-9.

ZHOU, Y., XU, H., XU, W., WANG, B., WU, H., TAO, Y., ZHANG, B., WANG, M., MAO, F., YAN, Y., GAO, S., GU, H., ZHU, W. & QIAN, H. 2013. Exosomes released by human umbilical cord mesenchymal stem cells protect against cisplatin-induced renal oxidative stress and apoptosis in vivo and in vitro. Stem Cell Res Ther, 4, 34.

ZITO, G., RICHIUSA, P., BOMMARITO, A., CARISSIMI, E., RUSSO, L., COPPOLA, A., ZERILLI, M., RODOLICO, V., CRISCIMANNA, A., AMATO, M., PIZZOLANTI, G., GALLUZZO, A. & GIORDANO, C. 2008. In vitro identification and characterization of CD133(pos) cancer stem-like cells in anaplastic thyroid carcinoma cell lines. PLoS One, 3, e3544.

ZOU, D., ERICKSON, C., KIM, E. H., JIN, D., FRITZSCH, B. & XU, P. X. 2008. Eya1 gene dosage critically affects the development of sensory epithelia in the mammalian inner ear. Hum Mol Genet, 17, 3340-56.